Polycationic and Oxo-Functionalized Cyclophosphazenes

Thesis Submitted in Accordance with The University of Liverpool Requirements for the Degree of Doctor of Philosophy

Joanne Rachel Ledger

October 2009

Contents:

Abstract:

This thesis investigates both the synthesis of polycationic phosphazene ring systems, supported by N-donor ligands and the functionalization of the ring phosphorus atoms with oxo-functions. Such systems promise interesting applications as polycationic materials, surfactants and supramolecular building blocks.

The reaction of hexachlorocyclotriphosphazene with the neutral donor ligand DMAP gives $[N_3P_3(DMAP)_6]Cl_6$, which contains the hexacation $[N_3P_3(DMAP)_6]^{6+}$. Complete reaction is achieved either in superheated chloroform using microwave irradiation or by slow diffusion techniques. Hydrochlorocarbon solvents are best suited, since they effectively coordinate the chloride ions via CH...Cl bonds. The crystal structures of the solvates $[N_3P_3(DMAP)_6]Cl_6 \cdot 19CHCl_3$, and $[N_3P_3(DMAP)_6]Cl_6 \cdot 11CH_2Cl_2$, show that the solvent has a strong structure directing role leading to different arrangements of ions in the salt lattices. Chloroform binds in a monodentate fashion and dichloromethane can engage itself in a bridging manner. Oxo-functions can be added to the hexacation, when the syntheses are carried with controlled amounts of water. This yields the tetracations $[N_3P_3(DMAP)_5O]^{4+}$ and $[N_4P_4(DMAP)_6O_2]^{4+}$, respectively. The tetracation $[N_3P_3(DMAP)_5O]^{4+}$ forms a centrosymmetric dimer in the solid state, where the oxo function of one cation is located directly above the phosphazene ring of the other.

Synthetic routes to cyclotriphosphazenes that feature oxo-functions at one ring phosphorus centre were developed. Starting from geminal dichlorides $Z_4N_3P_3Cl_2$ (Z = NHR, NR_2) (**C**), phosphate (**D**), pyrophosphate (**E**), phosphamide (**F**) and phosphite (**G**) derivatives were prepared. The zwitterionic phosphate $Z_4N_3P_3H_2O_2$ **D** is obtained via the DMAP-catalyzed hydrolysis of **C** in a biphasic mixture of aqueous KOH and THF. **D** contains a PO_2 unit and two protonated NH ring sites. It crystallizes in form of the tetrahydrate $Z_4N_3P_3H_2O_2.4H_2O$. The tetrahydrate dehydrates at 160°C in vacuum to the pyrophosphate $(Z_4N_3P_3HO)_2O$ **E**, in which two phosphazene

rings are linked via an oxo-bridge. When heated in a mixture of aqueous KOH, primary amine and THF, **C** undergoes a concurrent aminolysis-hydrolysis reaction, which gives the phosphamide $Z_4P_3N_3H(O)NHR$ **F** featuring a P(=O)NHR unit. The corresponding reaction of **C** with *p*- and *m*-xylylenediamine, respectively, in a 2:1 ratio in the presence of aqueous KOH leads to the formation of $(Z_4P_3N_3H(O)NHCH_2)_2C_6H_4$, in which two phosphamides are linked by a xylylene bridge. Phosphites **G** containing PHO units are obtained via reduction of **C** with potassium and subsequent treatment with KOH. The initial product consists of a hexameric potassium phosphate complex, which features a central K_6O_6 double cube arrangement. Addition of NH_4Cl yields the neutral phosphite $((EtN)_2C_3H_6)_2P_3N_3HOH$.

Acknowledgments:

I would first like to thank The University of Liverpool and the EPSRC for allowing me to carry out my PhD and providing the funding, without which, this work would not have been possible.

There are many people who have helped me during the course of this research. I would like to thank Dr Yaroslav Khimyak, Dr James Jones and Dr Jean-Baptiste Guilbaud who recorded the solid state NMR spectra of our compounds; Dr Neil Campbell and The Centre for Materials Discovery for training and use of their microwave facilities; Dr Hongjun Niu for carrying out TGA on our behalf; Dr Richard Bonar-Law for the theoretical studies he did on our compounds; Dr John Basca for his help with X-ray crystallography along with all of the technical staff in the Department of Chemistry who keep analytical services running on behalf of researchers, in particular Steve Apter for carrying out microanalysis and Allan Mills for running Mass Spectrometry.

In addition to this I owe most thanks to my supervisor Dr Alexander Steiner and Dr BoomiShanker Ramamoorthy, who was a postdoctoral researcher in our group when I began my PhD. Boomi has helped me with many lab techniques and to extend my knowledge within this area of chemistry. Aggi has allowed me to work on this research project and given me all the help and support I require during this time. His extensive knowledge of phosphazene chemistry and X-ray crystallography has proved invaluable while pursuing this research.

I would also like to thank all my friends and family for the love and support, which they give me in everything I do, especially my grandparents and my brother and sister, Dan and Vicky.

To Lisa, Kerri, Helen, Gill, Shane, Fliss, James, Ray and Lee thank you for all the fun and distractions through out the eight years I've spent at Liverpool University.

To Michael thank you for sticking with me, when I left to come to Liverpool and then for up rooting and moving here, so I could do my PhD. All the support you have given me through out this has meant the world.

Last but definitely not least to my parents, Karen and Bruce. Thank you for everything, for making me believe there is nothing I can't achieve and for always being there anytime day or night whenever I need you. I never would have made it this far without you both.

Abbreviations:

°C	-	Degrees Celsius
Å	-	Angstroms
Aq	-	Aqueous
Av.	-	Averaged
2,2'-BiPy	-	2,2'-Bipyridine
4,4'-BiPy	-	4,4'-Bipyridine
Bu	-	Butyl
Bz	-	Benzyl
Cat.	-	Catalyst
Calcd	-	Calculated
CB	-	Conjugate base
Conc	-	Concentrated
CP	-	Cross polarizaion
CSD	-	Cambridge Structural Database
Cy	-	Cyclohexyl
d	-	Doublet
Da	-	Daltons
DABCO	-	1,4-Diazabicyclo[2.2.2]octane
DBN	-	1,5-diazabicyclo[4.3.0]non-5-ene
DCM	-	Dichloromethane
Decomp	-	Decomposed
Deg	-	Degrees
DHTP	-	1,4-Dihydroxy terephtalic acid
DMAP	-	4-Dimethylamino pyridine
DMF	-	Dimethylformamide
DMP	-	2,6-Dimethylphenyl
Eq	-	Equivalents
ESI	-	Electrospray Ionization
Et	-	Ethyl
FT/IR	-	Fourier Transform Infrared Spectroscopy

g	-	grams
Hdht	-	1,4-dihydroxy terephthalic acid
H	-	Hours
Hz	-	Hertz
K	-	Kelvin
KHz	-	Kilo Hertz
m	-	Multiplet
M	-	Molar
MAS	-	Magic Angle Spinning
Me	-	Methyl
*Mes	-	2,4,6-Tri-tert-butylphenyl
MHz	-	Mega Hertz
Min	-	Minutes
ml	-	Millilitres
mm	-	Millimetre
mmol	-	Millimoles
M. P.	-	Melting point
MS	-	Mass Spectrometry
MW	-	Molecular weight
NMR	-	Nuclear Magnetic Resonance
Ph	-	Phenyl
ppm	-	Parts per million
ppt	-	Precipitate
Pr	-	Propyl
Py	-	Pyridine
Pyz	-	Pyrazine
Pz	-	Pyrazole
Rt	-	Room temperature
t	-	Triplet
T	-	Temperature
TCE	-	Tetrachloroethane
THF	-	Tetrahydrofuran

TGA	-	Thermogravametric analysis
Tf	-	Triflate
TPPM	-	Two phase pulse modulation
V	-	Volume
V_{sol}	-	Solvent accessible volume
V/Z	-	Volume per formula unit
W	-	Watts
Xs	-	Excess
Xy	-	Xylyl

Chapter 1:

Project Aims

Over recent years our research group has developed polyanionic ligand systems of type **A** that are based on the chemically robust cyclophosphazene ring structure. The high anionic charge and the large number of potential donor sites offer versatile ligand systems that can accommodate multinuclear metal arrays.[1-3] Thus we were curious if cyclophosphazene rings would also support polycationic structures such as **B**. Neutral donor ligands L are needed to saturate the phosphorus centres of such systems. Considering **B** being a somewhat electronically inverse to structure to **A**, it would be interesting to see how the anionic counter ions are accommodated within the polycations. In addition, there is an interesting analogy to cationic metal complexes $[M^{(n)}L_6]^{n+}$. While these exhibit an octahedral arrangement of ligands, the $[N_3P_3L_6]^{6+}$ cation features a unique trigonal prismatic ligand environment due to the D_{3h} symmetry of the N_3P_3 ring. This offers exciting possibilities in supramolecular chemistry and framework structures, in particular when L constitutes a linearly bridging ligand such as 4,4'-bipyridyl. Another incentive for the research is that cyclotriphosphazene cations have been proposed as intermediates in the ring opening polymerisation of $N_3P_3Cl_6$,[4] but they, as well as their adducts with neutral donor ligands, have remained elusive and so far evaded structural characterisation.

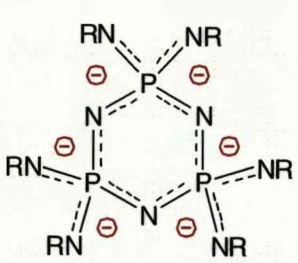

A

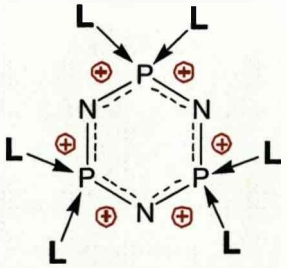

B

Cyclotriphosphazenes with oxo-functionalities at specific phosphorus sites offer interesting possibilities as building blocks in supramolecular chemistry. The only structurally characterized phosphorus nitrogen ring system that contains dioxo phosphate centres $[=PO_2]^-$ is the trimetaphosphimate ion $[(NHPO_2)_3]^{3-}$.[5-7] This trianionic ligand is a versatile building block for solid state compounds.[6] However, the direct functionalization of phosphazene rings is a relatively under developed area of phosphazene chemistry. In particular, when compared to the modification of the molecular periphery of cyclophosphazenes. We were therefore interested in developing synthetic routes to cyclotriphosphazenes that feature oxo-functions, such as zwitterionic phosphate **D**, pyrophosphate **E**, phosphamide **F** and phosphite **G** at one ring phosphorus centre while the others are protected by amino groups.

Previous work in our group has shown that amino phosphazene derivatives form a range of supramolecular structures.[8-10] The combination of hydrogen donor sites (NH) and acceptor sites (PO) and the possibility of generating cationic and anionic species promises applications as ligand systems for metal coordination and anion binding.

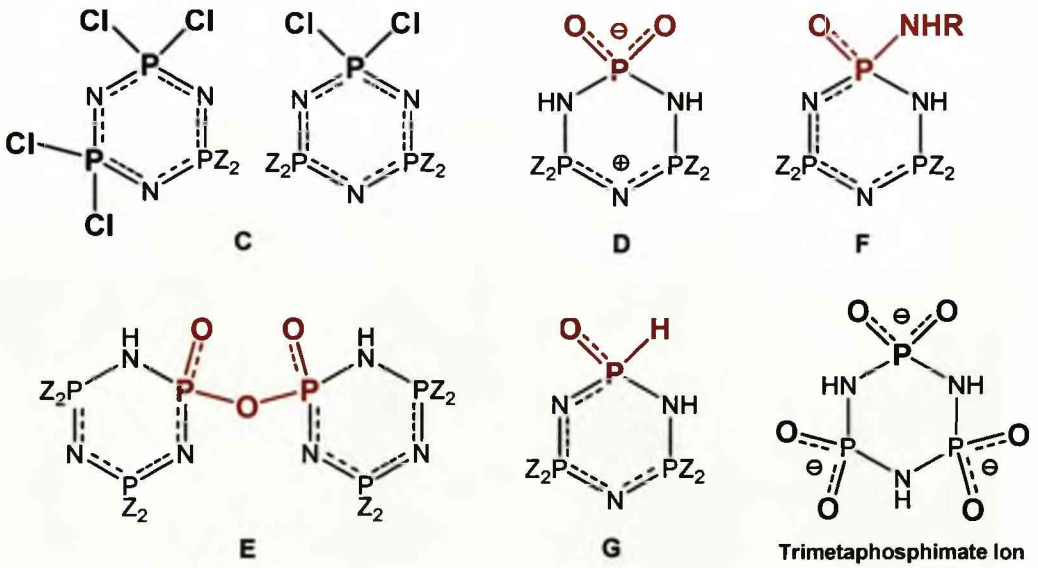

References

(1) Boomishankar, R., Richards, P. I.; Steiner, A. *Angew. Chem., Int. Ed.* **2006**, *45*, 4632.

(2) Steiner, A., Zacchini, S.; Richards, P. I. *Coord. Chem. Rev.* **2002**, *227*, 193.

(3) Rivals, F.; Steiner, A. *Chem. Commun.* **2001**, 1426.

(4) Sulkowski, W. W. in Phosphazenes: A Worldwide Insight, (M. Gleria and R. De Jaeger), Nova Science Publishers, Inc., **2004**, 69.

(5) Chandrasekhar, V.; Krishnan, V. *Adv. Inorg. Chem.* **2002**, *53*, 159.

(6) Marchand, R., Schnick, W.; Stock, N. *Adv. Inorg. Chem.* **2000**, *50*, 193.

(7) Allcock, H. R. *Chem. Rev.* **1972**, *72*, 315.

(8) Benson, M. A., Zacchini, S., Boomishankar, R., Chan, Y.; Steiner, A. *Inorg. Chem.* **2007**, *46*, 7097.

(9) Richards, P. I., Benson, M. A.; Steiner, A. *Chem. Commun.* **2003**, 1392.

(10) Bickley, J. F., Bonar-Law, R., Lawson, G. T., Richards, P. I., Rivals, F., Steiner, A.; Zacchini, S. *Dalton Trans.* **2003**, 1235.

Chapter 2:

Introduction

The literature covering phosphazene chemistry can be described as both vast and extensive and can be traced as far back as the mid 1800s. Phosphazene derivatives are generally classified as either inorganic ring systems or inorganic polymers and are one of the most well studied members of both categories. Phosphazene chemistry crosses the boundaries of many chemistry sub-divisions; as formally unsaturated P-N species they are of interest to inorganic and theoretical chemists, their coordination chemistry has been widely investigated,[1-3] they undergo many fundamental organic reactions such as acylation and alkylation,[4,5] in terms of materials chemistry they form a vast array of polymers[6,7] and last but not least they show a rich supramolecular chemistry.[8] The versatility of phosphazene species arises from the great stability of the phosphorus nitrogen backbone and their ability to carry out reactions at both phosphorus and nitrogen centres.

Here we will focus the discussion on the structure and bonding of phosphazenes, reactions of cyclotriphosphazenes, multianionic phosphazenate ligands and the supramolecular chemistry of phosphazenes.

2.1. Structure and Bonding of Phosphazenes

Phosphazenes can be considered as aza-phosphorus(V) species as they contain formally bridging P-N=P units within the formula $[-N{=}PX_2-]_n$.[2,9] They exhibit an extensive range of structures, including cyclic species with ring sizes from 4 to 34 and both linear and cross linked polymeric compounds.[5,9,10] The substituent X can range from halogens to organic

groups such as alkyl, aryl, alkoxy, aryloxy, mercapto, alkylamino or arylamino.[9] Figure 2.1 shows the most widely studied phosphazene species, which are the cyclic trimer and tetramer and the linear polymer, although interest is increasing in cross-linked polymeric materials.[5,11,12]

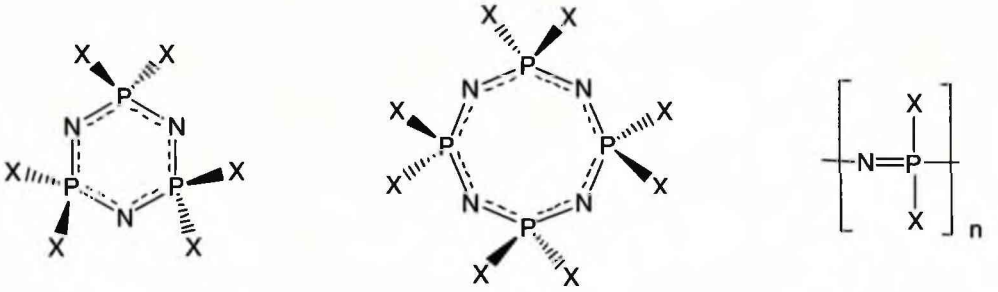

Figure 2.1.

The properties of phosphazenes are as varied as their structures. Cyclic trimers and tetramers are generally stable, white crystalline solids showing "organic" physical properties and solubilities, while high molecular weight polymers phosphazenes range from rubbery elastomers to thermoplasts depending on the nature of the substuents.[9] Despite varying physical properties cyclo- and polyphosphazenes are closely related,[5] this is highlighted by the use of cyclophosphazenes as molecular models for the corresponding polyphosphazenes.[5]

2.1.1. Structural Features of Cyclophosphazene Rings

Extensive studies have been carried out on the structural properties of cyclophosphazenes. These include crystallographic studies and theoretical calculations. Such investigations have given insight not only to the molecular geometry of cyclophosphazenes but also to the complex nature of P-N bonding.[2,13,14]

Phosphazene tetramers and higher oligomers tend to adopt a puckered ring structure.[2,8,9] However, this moderate puckering does not appear to affect the molecular stability.[9] In contrast to this cyclotriphosphazenes almost always adopt a planar ring structure with a tetrahedral geometry around P causing the substituents to adopt positions above and below the plane of the ring.[8,10,15,16] This makes them excellent candidates for supramolecular building blocks.[8,16] They also act as hexa-functional dendrimer cores as they contain six growth sites, see Figure 2.2. In contrast, benzene and related systems tend to grow from just three sites.[8,16-19]

G = Dendrimer growth site

Figure 2.2.[16]

Ring nitrogen atoms are best considered as divalent centres with lone pairs of electrons. They are basic sites but, their basicities are heavily dependent on the substituent X. Below Table 2.1 gives pK_a' values for several cyclotriphosphazenes.[1,8,20,21] Amino-cyclophosphazenes contain the most basic ring nitrogen atoms and can act as moderately strong nucleophiles and readily engage in hydrogen bonding.[1,2,8,22,23] In contrast to this the chloro-derivative $N_3P_3Cl_6$ is a weak base and only interacts with strong Lewis acids, as shown in Figure 2.3.[8,24]

X	pK_{a1}'	pK_{a2}'
Cl	< -6.0	
OEt	0.2	
Ph	1.5	
Et	6.4	
NHEt	8.2	-1.3

Table 2.1. pK_a' Values of Nitrogen Atoms in Cyclotriphosphazenes $N_3P_3X_6$.[8]

-in nitrobenzene at 25 °C

-pK_{a1}' corresponds to the ring nitrogen, pK_{a2}' corresponds to nitrogen on X group

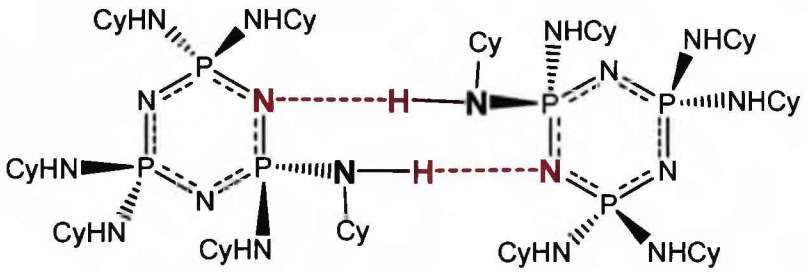

Dimesrisation of Amino-Cycltriphosphazenes
- illustrating hydrogen bonding involving basic ring nitrogens

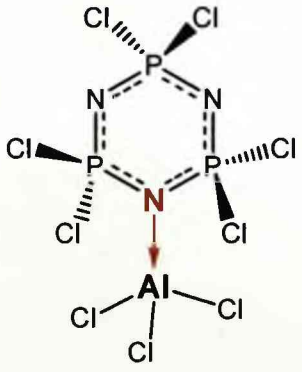

$N_3P_3Cl_6$ Donating to a Lewis Acid

Figure 2.3. Basic Behaviour of Phosphazene Ring Nitrogens

The geometry of the phosphazene ring is also affected to a degree by the X substituent of phosphorus. Here we see that shorter PN bonds are observed when X is a more electronegative substituent as this causes electron density to be drawn away from P thus increasing its partial positive charge and strengthening the PN bond. However, it must be noted here that homo-substituted cyclophosphazene trimers actually exhibit only a slight variation in their PN ring bond angles and distances, as shown in Table 2.2. In contrast to this it has been found that hetero- cyclotriphosphazene derivatives (containing substituents $-X^1$ and $-X^2$) have unequal bond lengths around the ring (again this is due to the varying electronegativity of the different substituents).[9] For example, Figure 2.4 and Table 2.3 show that the germinal dichloride $N_3P_3(NHCy)_4Cl_2$, contains three inequivalent $P\text{-}N_{(ring)}$ distances, where as the fully substituted $N_3P_3(NHCy)_6$, has equal distances of 1.60 Å[22,25]

	P - N (Å)	P-N-P (deg)	N-P-N (deg)
$N_3P_3H_6$*	1.606	121.3	118.7
$N_3P_3F_6$[26]	1.570(6)	121.0(4)	119.0(2)
$N_3P_3Cl_6$[27]	1.575(5)	121.4(4)	118.4(3)
$N_3P_3Br_6$[28]	1.576(12)	121(2)	118.6(11)
$N_3P_3(CH_3)_6$**[29]	1.61(2)	124.0(6)	114.7(9)
$N_3P_3(CF_3)_6$[26]	1.581(5)	120.2(4)	119.8(3)
$N_3P_3(NC_2H_4)_6$[30]	1.5869(7)	122.93(4)	116.99(4)
$N_3P_3(O_2C_6H_4)_3$[31]	1.56(2)	123(2)	116.5(10)

Table 2.2. Geometrical Parameters of Homo-Substituted Neutral Cyclotriphosphazene Rings.[13]

(Values are averaged, *values theoretically calculated, **I_2 adduct)

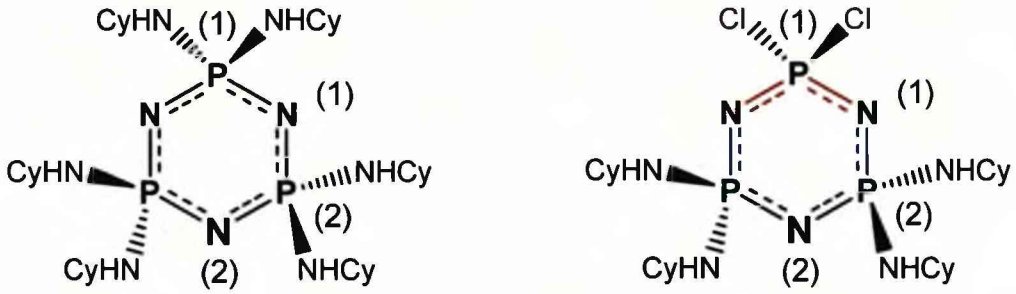

Figure 2.4.

	P(1) – N(1) (Å)	P(2) – N(1) (Å)	P(2) – N(2) (Å)
$N_3P_3(NHC_6H_{11})_6$[22]	1.60*	1.60*	1.60*
$N_3P_3(NHC_6H_{11})_4Cl_2$[25]	1.553(5), 1.561(5)	1.622(5), 1.611(5)	1.589(5), 1.581(5)

Table 2.3. P-N Ring Bond Distances of Homo- and Hetero- Substituted Cyclotriphosphazenes[22,25]

(*Averaged values standard deviations not given in paper)

This clearly illustrates that the electronic properties of phosphazene rings can be altered by varying X. In addition to this, the steric effects imposed by X allow a wide variety of functional groups to be added to the periphery of the molecule. These include metal coordination sites, hydrogen bond donors and acceptors and ionic end groups.[4,5,8,32,33] Furthermore, the substituent effects control solubility and physical properties. Hence, these can be "fine tuned" to enable desired characteristics and behaviour.[8,15] Table 2.4 shows varying melting points for different X substituents of $N_3P_3X_6$.[15]

X	M. P. (°C)
Cl	113
C_6H_5	115
Cl and C_6H_5	70
CH_2CF_3	49
CH_2CF_3 and C_6H_5	oil
$4\text{-}C_2H_5\text{-}C_6H_4$	75
$4\text{-}C_2H_5\text{-}C_6H_4$ and C_6H_5	oil
$CH_2(CF_2)_2H$	41
NHC_5H_{11}[22]	159
NHC_5H_{11} and Cl*	181

Table 2.4. Melting points of various cyclotriphosphazenes.[15]

* Reported in this work.

2.1.2. Phosphorus – Nitrogen Bonding

Cyclotriphosphazenes exhibit relatively short phosphorus-nitrogen bond distances of equal length (1.55-1.62 Å)[14]. This clearly shows that the P-N ring bond contains some multiple bond character, being significantly longer than a formal P-N single bond (~1.77 Å in saturated phosphazanes[14]).[2,13,14] The shortening of the P-N bond arises from ionic interactions of partial positive and negative charges on phosphorus and nitrogen, respectively, which result in an ylidic bond, see Figure 2.5.

Recent theoretical studies by Luaña et al. and Chaplin et al. do agree that the P-N bond is best described as a highly polarised σ bond contracted by electrostatic interactions.[13,14] However, they also show that there is some degree of delocalisation within the ring.[13,14] Natural bond order analysis has indicated that ~15 % of the P and N valence electrons, which are not involved in σ bonding, take part in negative hyperconjugation.[13] This occurs

via the interaction of nitrogen lone pair orbitals with σ^*_{PN} and σ^*_{PX} orbitals.[13] It is also worth noting here that electronegative substituents were found to increase the role of negative hyperconjugation.[13]

Figure 2.5. Ylidic structure containing positively charged P and negatively charged N-centres.
On the right hand side the covalent bond part is depicted as a solid line and the electrostatic contribution as a dashed line.

2.2. Synthesis of Cyclophosphazenes

Chloro- and fluoro- derivatives constitute an important class of cyclophosphazene precursors. They undergo facile reactions with many nucleophiles to produce homo- and hetero- substituted derivatives.[5,8,33] Fluorocyclophosphazenes are more stable, volatile and less reactive than their chloro- counterparts, however the reduced basicity of their ring nitrogens leads to cleaner reactions with organometallic compounds.[33] There are several accounts for the synthesis of perfluorinated cyclophosphazenes, however these all involve fluorinating the chloro-analogues, see Figure 2.6.[33-37] NaF is reported as the most effective fluorinating agent for $N_3P_3F_6$ and $N_4P_4F_8$.[33]

The chloro- trimer and tetramer derivatives are most commonly synthesised from the reaction of ammonium chloride with phosphorus pentachloride, see Figure 2.7. This reaction also produces higher phosphazene oligomers and requires careful separation by fractional crystallisation and sublimation.[5,9,10,38]

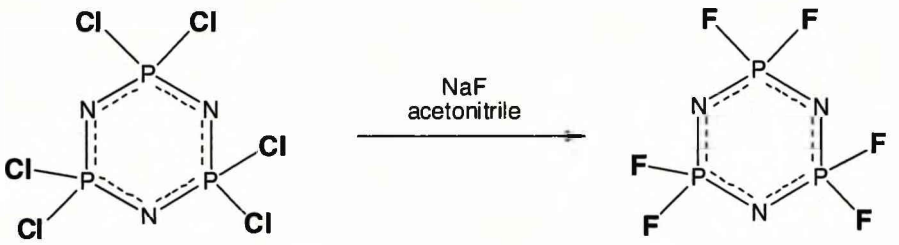

Figure 2.6. Formation of Hexafluorotriphosphazene

$$nNH_4Cl + nPCl_5 \xrightarrow[\text{heat}]{\text{TCE}} (NPCl_2)_{3\text{-}10} + HCl\uparrow$$

$$nN(SiMe_3)_3 + nPCl_5 \xrightarrow[40\ ^{o}C]{\text{DCM}} (NPCl_2)_{3\text{-}10} + Me_3SiCl$$

Figure 2.7. Reactions Producing Chlorophosphazenes

Another route involves the reaction of tris(trimethylsilyl)amide with phosphorus pentachloride in DCM.[39] This method requires a lower temperature and produces higher yields of trimer than the synthesis from ammonium chloride.[5,39] However, it has not been adapted for large scale preparations.

This reaction proceeds via the intermediate $Cl_3P{=}NSiMe_3$, which is also an important species for the synthesis of polyphosphazenes. Mechanistically, both of the above reactions are thought to be similar, with the main differences occurring in the termination step. The latter is thought to terminate via an intermolecular process assisted by $N(SiMe_3)_3$, in contrast to intramolecular ring closure with the ammonium chloride synthesis, see Figure 2.8.[5,38,39]

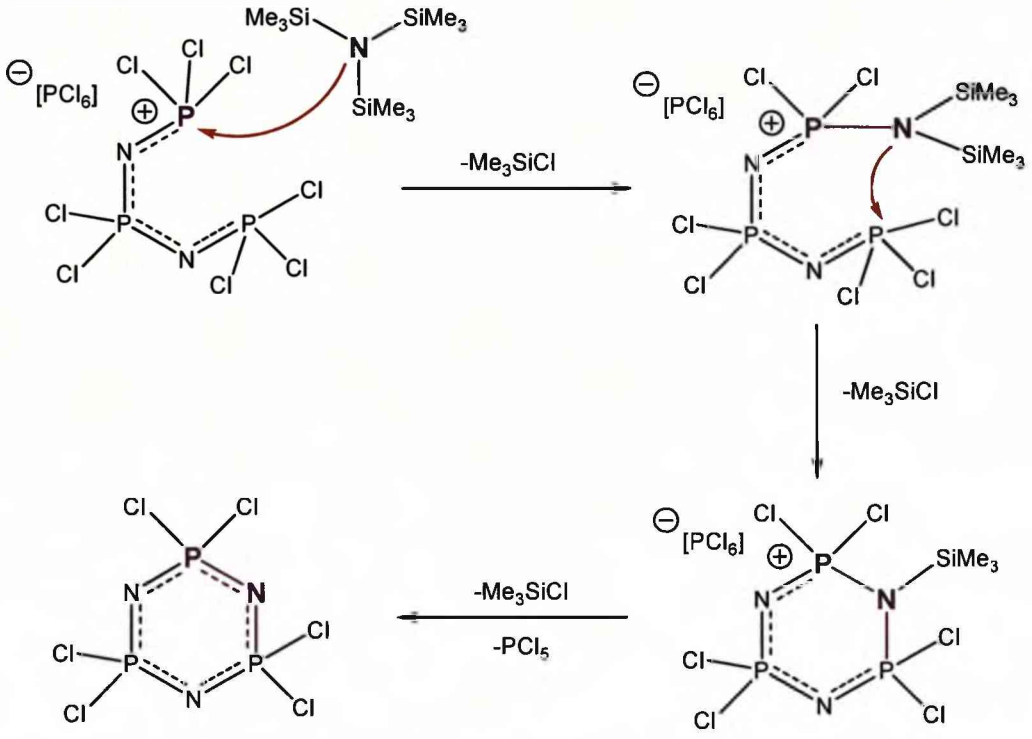

Termination Step for $N_3P_3Cl_6$ Synthesis from $N(SiMe_3)_3$

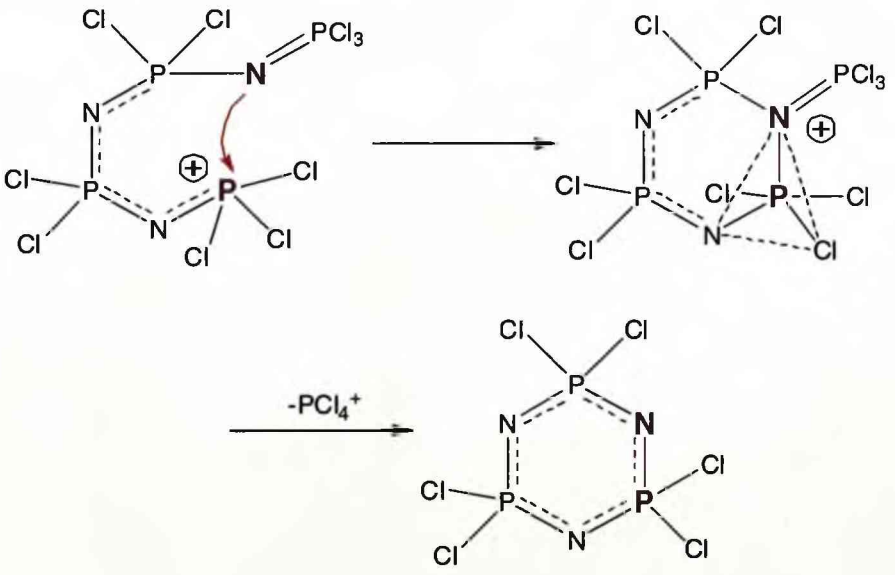

Termination Step for Sythesis of $N_3P_3Cl_6$ from NH_4Cl

Figure 2.8. Termination Step for $N_3P_3Cl_6$ Formation.[5,38]

2.3. Nucleophilic Substitution of Cyclophosphazenes

The nucleophilic substitution of chloro- and fluoro- phosphazenes is one of the most important and well studied reactions in phosphazene chemistry. It is regularly used to synthesise both homo- and hetero- substituted phosphazenes containing RNH, NR_2, RO and R substituents.[8] This chapter will focus predominately on the synthesis of amino cyclophosphazenes. The incoming nucleophile attacks the electrophilic phosphorus centre to displace a leaving group. The reaction is considered to proceed by either S_N1- or S_N2 -type pathways, as shown in Figure 2.9.[5,9]

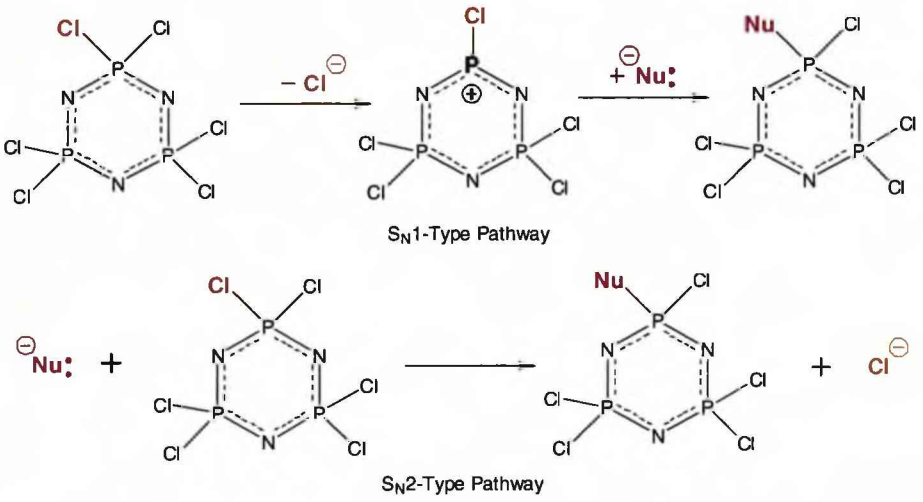

Figure 2.9. Nucleophilic Substitution Pathways.[5,9]

However, the finer mechanistic details of these reactions are rather more complicated and depend heavily on the electronic and steric properties of the incoming nucleophile.[5] They can produce a variety of homo- and hetero-substituted products and these often form as a number of regio- and stereo-isomers, see Figure 2.10. Regio-isomers are geminal and non-geminal substitution products, where as stereo-isomers are non-geminal species with cis- and trans- arrangements above and below the plane of the cyclotriphosphazene ring.[5,9,40]

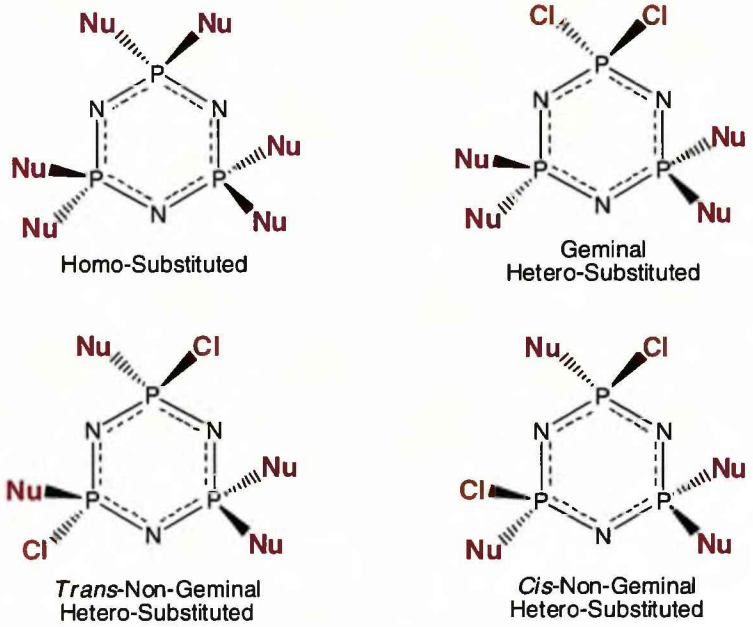

Figure 2.10.

2.3.1. Mechanistic Details

Together with alkoxide derivatives the amino- derivatives are the most well studied cyclophosphazenes. In particular the amino substitution of chloro-cyclophosphazenes has been the subject of detailed kinetic studies.[5,40] We shall therefore illustrate the mechanistic details of the nucleophilic substitution with amines as the attacking nucleophile.

The variation of isomers observed when hetero- (or incomplete) substitution occurs in cyclotriphosphazenes can be attributed to four mechanistic pathways; two of S_N1-type and two of S_N2-type, see Figure 2.11.[5,40]

(I) a standard dissociative S_N1 mechanism, involving the formation of a three coordinate cationic intermediate.

(II) an $S_N1(CB)$ (CB = conjugate base) pathway. It involves the loss of HCl from a P(NHR)Cl unit to produce an intermediate containing an electrophilic, sterically strained, three coordinate phosphorus centre. This pathway is associated with the formation of geminal products.

(III) a concerted S_N2 mechanism, involving a polar transition state (this transition state tends to require stabilisation by polar solvents such as acetonitrile).[5]

(IV) a non-polar S_N2 pathway, which forms a five-coordinate (non-polar) phosphorus intermediate. Kinetic studies have shown that a $\Delta H^{\ddagger}$ term associated with the ease of formation of the five coordinate intermediate characterises S_N2 reactions.[5]

It is worth mentioning here that, detailed kinetic studies by Krishnamurthy et al. have indicated that mechanistic changes tend to occur as the degree of substitution progresses. In other words, the initial chlorine replacement may occur via an S_N2-non-polar pathway, where as the later stage could follow a concerted S_N2 path (if promoted by a polar solvent such as acetonitrile).[5,41]

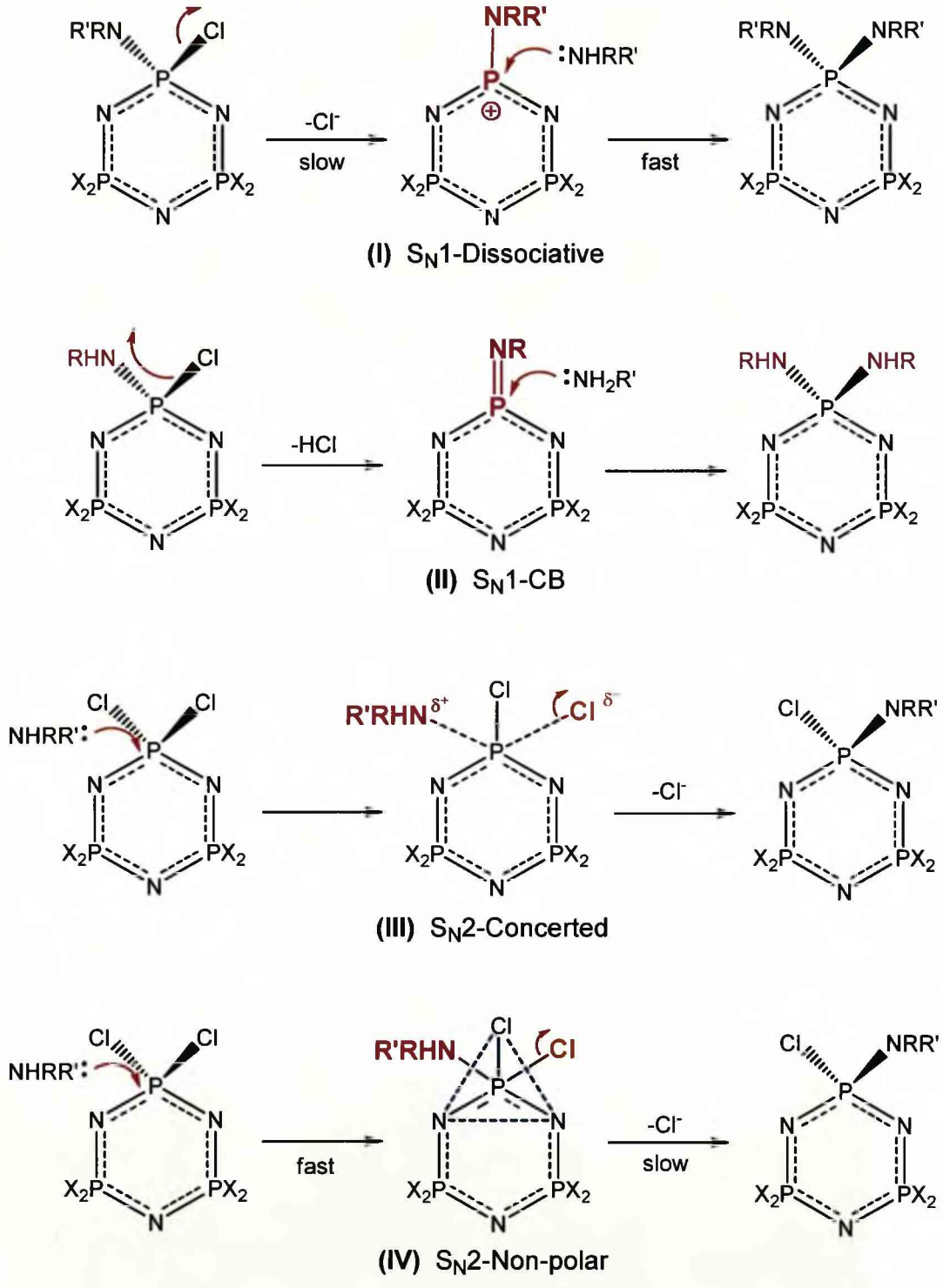

Figure 2.11. Mechanistic Pathways for Nucleophilic Substitution.[5,41]

2.3.2. Amino-Cyclophosphazenes

Amino-cyclophosphazenes can be synthesised from a variety of primary and secondary amines; including simple alky, vinyl and aryl amines[22,25,42] and chelating or bridging diamines.[43-45] Synthesis generally occurs by refluxing $N_3P_3Cl_6$ with stoichiometric amounts of the desired amine and an auxiliary base under standard conditions. However, the degree of substitution is largely depends on the steric effects of the amine. Bulky amines generally do not go to full substitution under standard conditions. For example, Figure 2.12 shows that *tert*-butyl amine does not react beyond the tetra-substituted derivative under standard conditions (although full substitution can be induced under pressure).[22] Hetero- substituted products can be obtained for many amino-phosphazenes using stoichiometric amounts of the amine. This can lead to the formation of various regio- and stereo-isomers.[5,40]

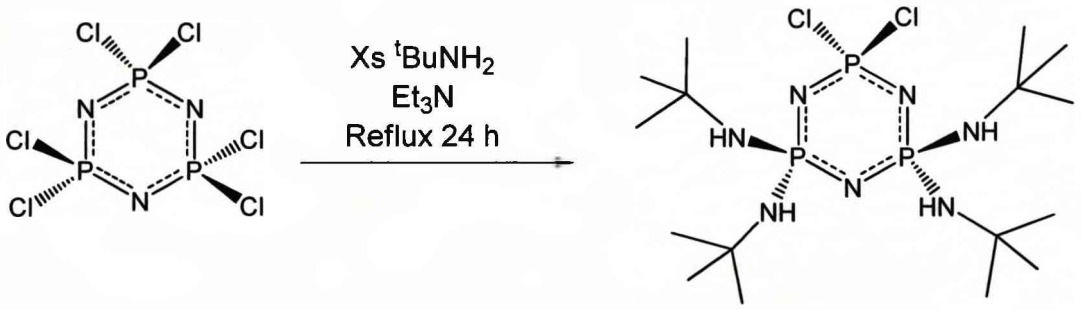

Figure 2.12.

The majority of primary amines give geminally substituted hetero-phosphazenes, this can be attributed to chlorine replacement proceeding via the $S_N1(CB)$ mechanism. The main variation to this rule occurs for the smaller methyl- and ethyl amine, which form non-geminal phosphazene derivatives. This can be explained in terms of competing rates for proton abstraction ($S_N1(CB)$) and formation of the bimolecular intermediate (S_N2(non-polar). The latter of these two is likely to be slow for bulky amines making S_N1 reactions more favourable.[5]

In contrast to this, secondary amines tend to form *trans*-non-geminal substitution products. Proton abstraction can not occur with secondary amines, while the electron donating and steric properties of secondary amines direct the incoming nucleophile to non-geminal sites for both S_N2(non-polar) and S_N1(dissociative) pathways.[5] Figure 2.13 shows the intramolecular stabilised five coordinate transition state, proposed by Allen, to account for the preferential trans-substitution.[40] This transition state forces the attacking amine into a position trans to the residing amine (the proton involved can come from proton transfer of the incoming amine or solvating effects).[5,40,46]

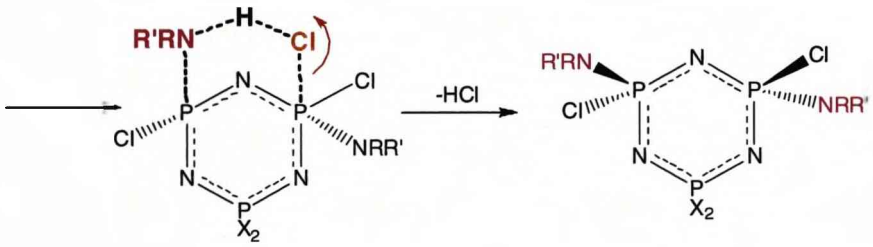

Figure 2.13.[40]

It should also be noted that penta- and tris- substituted amino derivatives have rarely been observed and that chelating diamines tend to react in a geminal fashion to give spirocyclic products.[5,43]

The tetramer $N_4P_4Cl_8$ reacts, predominantly in a non-geminal fashion and faster than the corresponding trimer. This is due to more flexibility within the puckered ring, which lowers the enthalpy of the five coordinate intermediate of the S_N2(non-polar) pathway.[5]

2.3.3. Alkoxy- and Alkyl-Cyclophosphazenes

Alkoxy- and aryloxy- substituted cyclophosphazenes are generally synthesised by the reaction of the alcohol or phenol salts with the parent

chlorophosphazene, see Figure 2.14. These reactions give homo-substituted products via a non-geminal substitution pattern.[5,40,47-50]

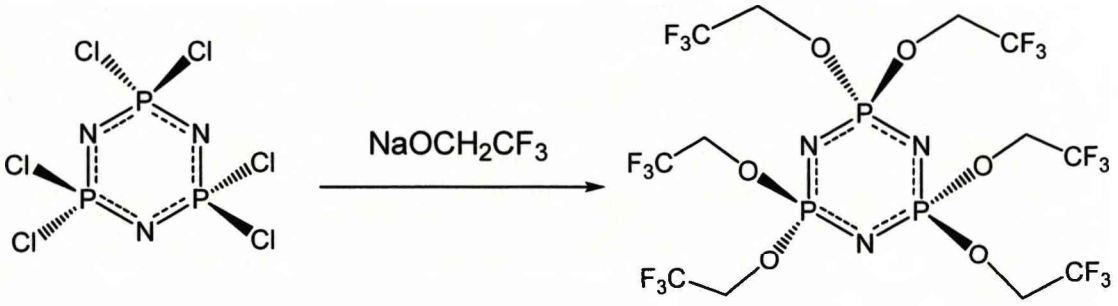

Figure 2.14.

In contrast to this, there are various methods for the synthesis of alkyl- and aryl- substituted cyclophosphazenes. The most prominent route involves the reaction of fluoro phosphazenes with organolithium compounds. Chloro phosphazenes tend to ring-open in the presence of organolithium and Grignard reagents.

2.4. Polyanionic Cyclotriphosphazenate Ligands

Multianionic phosphazenate ligands can be synthesised by the deprotonation of amino-cyclotriphosphazenes using strong organometallic bases.[2,51,52] Hexa- and tri- anionic ligands have been isolated and structurally and characterised using stoichiometric amounts of metalating agents, see Figure 2.15.[51-53] The resulting anionic ligands often adopt a puckered ring geometry in a chair conformation, with similar P-N(ring) and P-N$^-$(amino) bond distances.[2] The trianion forms by the deprotonation of amino groups on only one side of the phosphazene ring. This allows the formation of a hexadentate ligand surface, consisting of three ring nitrogens and three amino nitrogens, as the deprotonated nitrogen centres all occupy equatorial positions of the P_3N_3 chair, see Figure 2.16.[8]

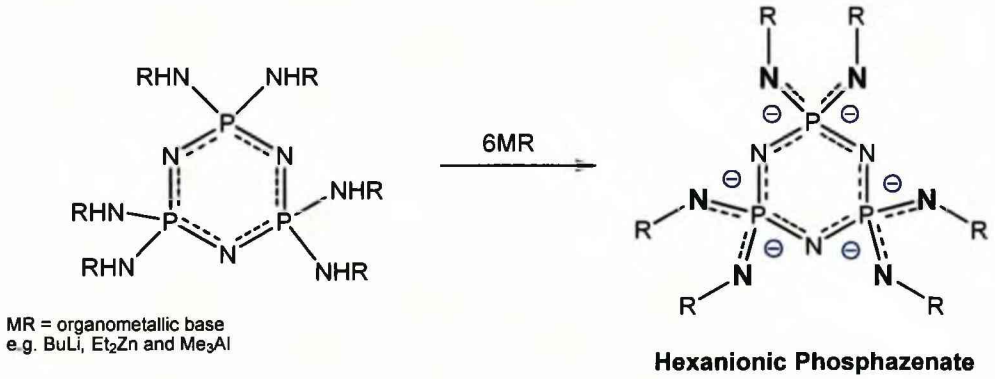

Figure 2.15. Schematic of Hexanionic Phosphazenate Formation

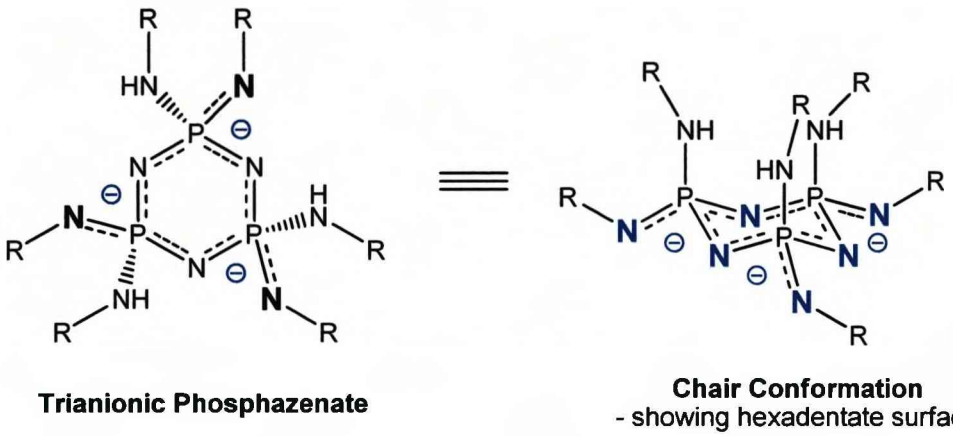

Figure 2.16. Trianionic Phosphazenate with Deprotonation in Equatorial Positions.[8]

These ligand systems can behave as templates for well defined multinuclear arrays.[8,51,52,54] An example of this is the anisidyl derivative, **2.1**, which can complex with twelve lithium ions in bidentate chelation sites and is prepared by the reaction of twelve equivalents of butyl lithium in THF to form **[2.1]**$Li_{12}[CH_2{=}CHO]_6(THF)_6$, see Figure 2.17.[54] This complex is shown in Figure 2.18 and contains six enolate anions along with the hexa-anion $[\mathbf{2.1}]^{6-}$, which accommodates the lithium ions in two types of bidentate chelation sites. These consist of an inner site, N(exo)-P-N(ring) and an outer site, N(exo)-C_6H_4-O, both sites coordinate to six lithium ions each. The six enolate anions can be considered to cap the complex from either side.

Enolate anions form by the ring cleavage of THF, which is usually a slow reaction. However **[2.1]**$Li_{12}[CH_2{=}CHO]_6(THF)_6$ forms instantaneously, suggesting that here enolate formation occurs by a concerted mechanism aided by the multianionic ligand and the lithium ions.[8,54] It should also be noted that the P_3N_3 ring adopts a planar conformation in this complex[2]

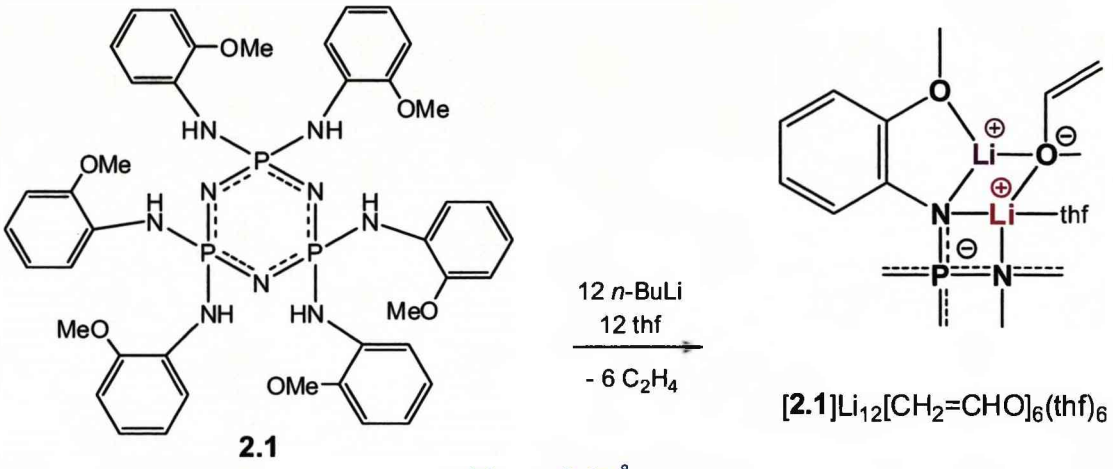

Figure 2.17.[8]

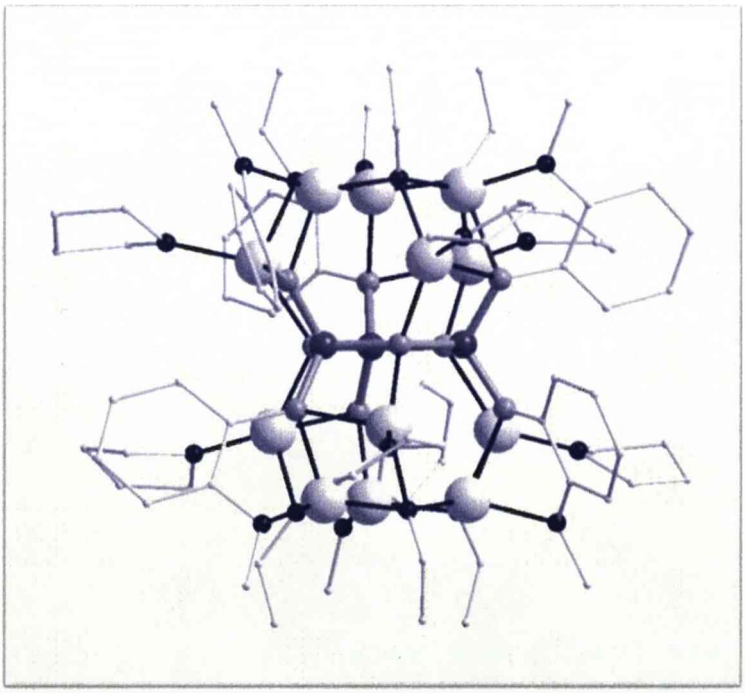

Figure 2.18. Crystal Structure of [2.1]$Li_{12}[CH_2CHO](THF)$.[7,22,54]

-Li shown as large light gray spheres, O small dark gray spheres, P medium dark spheres, N medium light spheres, C small light spheres and H atoms omitted.

Polyanionic phosphazenate ligands have also been shown to template zinc oxide clusters.[8,51] The trianionic phosphazenate species $[N_3P_3(HN^nPr)_3(N^nPr)_3]^{3-}$, $[\mathbf{2.2}]^{3-}$ (shown in Figure 2.19) is generated when the *n*-propylamino derivative $N_3P_3(NH^nPr)_6$, **2.2** is treated with three equivalents of diethyl zinc.[51] This trianion forms as a dimeric complex $([\mathbf{2.2}]3(ZnEt))_2$ and contains six ethyl zinc units sandwiched between two phosphazenate ligands, see Figure 2.20. This structure can also be viewed as a dimer of two "bowl" shaped tris(ethylzinc) phosphazenate segments, which each contain a coordinating surface of three Lewis acidic zinc sites and three Lewis basic N(exo) sites.[8] In this respect it acts as a template for trimeric and hexameric zinc oxide clusters, in the form of planar $(ZnO)_3$ rings and hexagonal $(ZnO)_6$ prisms, respectively.[51] Zinc oxide clusters can be obtained when phosphazene hydrates are treated with appropriate amounts of diethyl zinc.[51] The clusters are generated *in-situ* and encapsulated by the, above mentioned, "bowl" shaped coordination surface. Cluster size can be controlled by varying the R group of the amino substituent. The n-propyl- derived hydrate $\mathbf{2.2}\cdot 1.5H_2O$ forms the complex $([\mathbf{2.2}]3(ZnEt))_2(Zn_3O_3)$,[51] which hosts the planar $(ZnO)_3$ cluster, see Figure 2.21. Where as, the cyclohexyl- derived hydrate, $N_3P_3(NHCy)_6\cdot 5H_2O$, $\mathbf{2.3}\cdot 5H_2O$ gives the complex $([\mathbf{2.3}]3(ZnEt))_2(Zn_6O_6)$,[51] which encapsulates the $(ZnO)_6$ prism, as shown in Figure 2.22.[8,51]

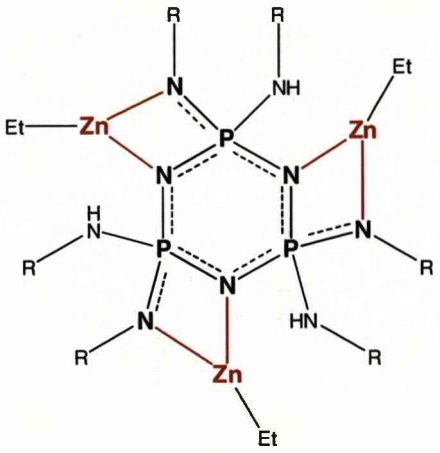

Coordination of Ethyl Zinc within Trianionic Phospazenate Ligands
R = ^{n}Pr and Cy

Figure 2.19.[51]

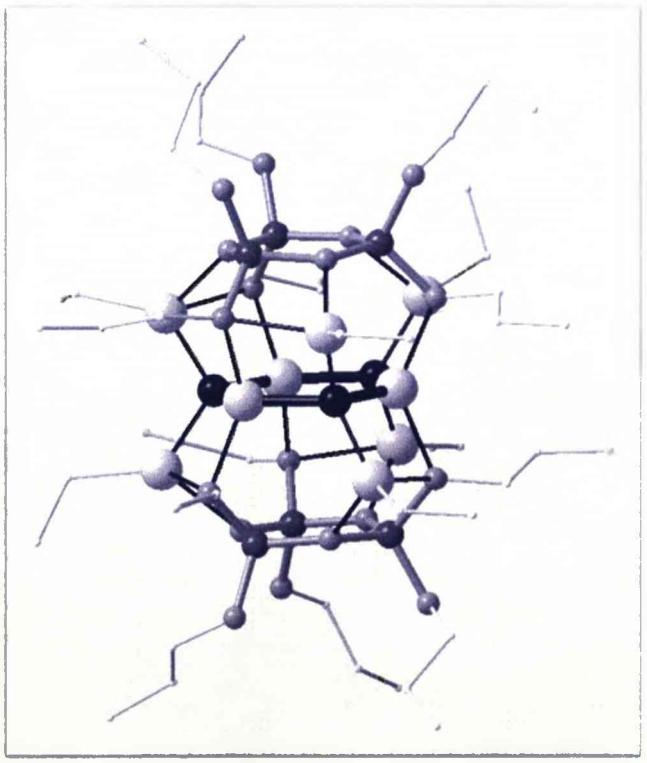

Figure 2.20. Crystal Structure of $([2.2]3(ZnEt))_2(Zn_3O_3)$[7,51]

-Zn shown as large light gray spheres, O medium very dark gray spheres, P medium dark spheres, N medium light spheres, C small light spheres and H atoms omitted.

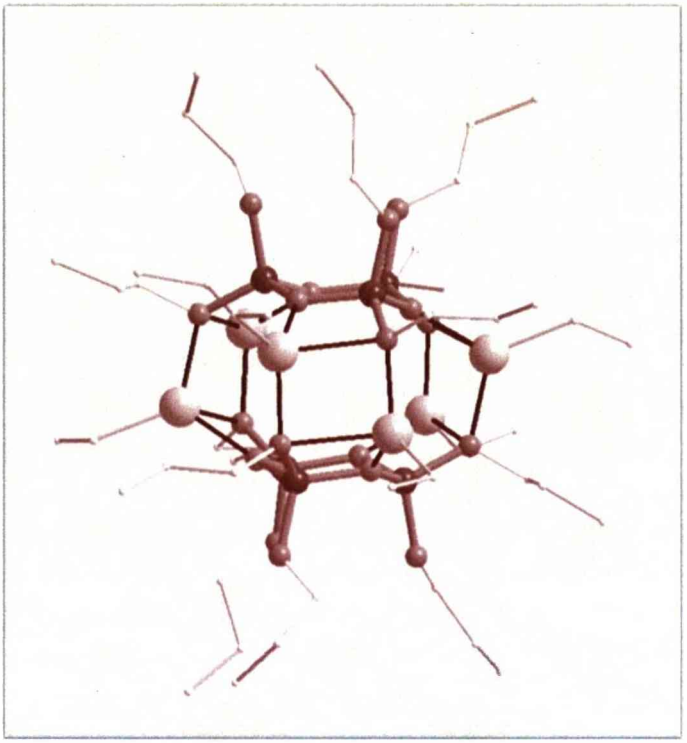

Figure 2.21. Crystal Structure of $([2.2]3(ZnEt))_2$[7,51]

-Zn shown as large light spheres, P medium dark spheres, N medium light spheres, C small light spheres and H atoms omitted.

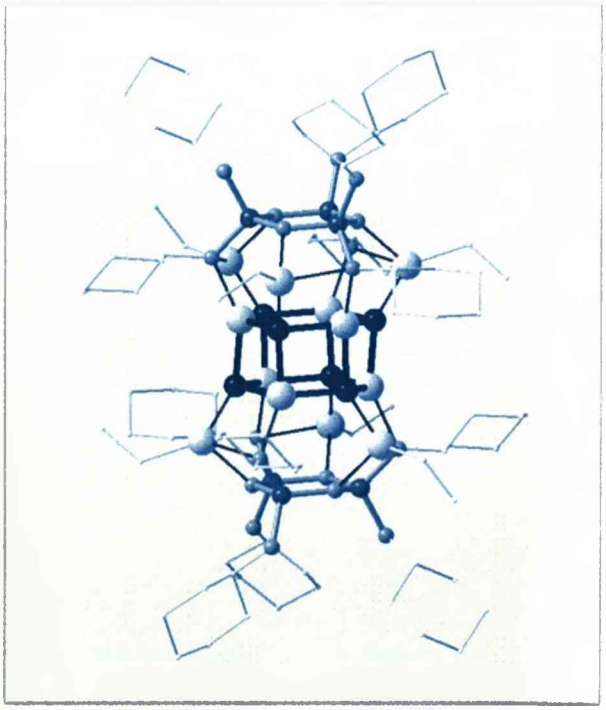

Figure 2.22. Crystal Structure of $([2.3]3(ZnEt))_2(Zn_6O_6)$[7,51]

-Zn shown as large light spheres, O large dark spheres, P medium dark spheres, N medium light spheres, C small light spheres and H atoms omitted.

2.5. Supramolecular Chemistry of Cyclophosphazenes

Numerous supramolecular structures based on cyclotriphosphazenes have been reported.[8] These can be split into two groups described as "form" and "function" .[8] This notation arises from the structural role of the phosphazene ring within these materials; "form" indicates that the supramolecular structure is dictated by the geometrical arrangement of substituents around the ring, while "function", on the other hand, arise from direct interaction of the phosphazene ring in non-covalent intermolecular bonds.[8]

2.5.1. "Form"

This includes host-guest systems and dendrimers. Within these materials the phosphazene ring is considered a molecular support, which is not actively involved in supramolecular interactions.[8] We have already mentioned that cyclotriphosphazenes form planar geometries containing three tetrahedral sites, this offers three substituent binding sites above and below the plane of the phosphazene ring.[8] Dendrimers arise by the attachment of branched substituents to these sites, allowing the assembly of distinct supramolecular architectures, where as a more rigid sphere of substituents can create clathrate structures.[8]

2.5.1.1. Host-Guest Compounds

These are known as clathrates or inclusion compounds. They consist of guest molecules in closed cavities, channels or between layers of a lattice of host molecules.[8,55] The most prominent examples are spirocyclic hosts, which contain three chelating substituent. Other examples include basket shaped molecules, see Figure 2.23.[8]

Trispirocyclic phosphazenes, such as $N_3P_3(O_2C_6H_4)_3$, **2.4** and $N_3P_3(O_2C_{10}H_8)_3$, **2.5** form inclusion compounds with solvent molecules and were first reported by Allcock in the 1960s, see Figure 2.24.[8,56-58] The quest

to find porous materials for applications in gas storage devices and fuel cells is the driving force behind much of today's research in materials chemistry and it has indeed sparked recently renewed attention towards spirocyclic phosphazenes.[8,59]

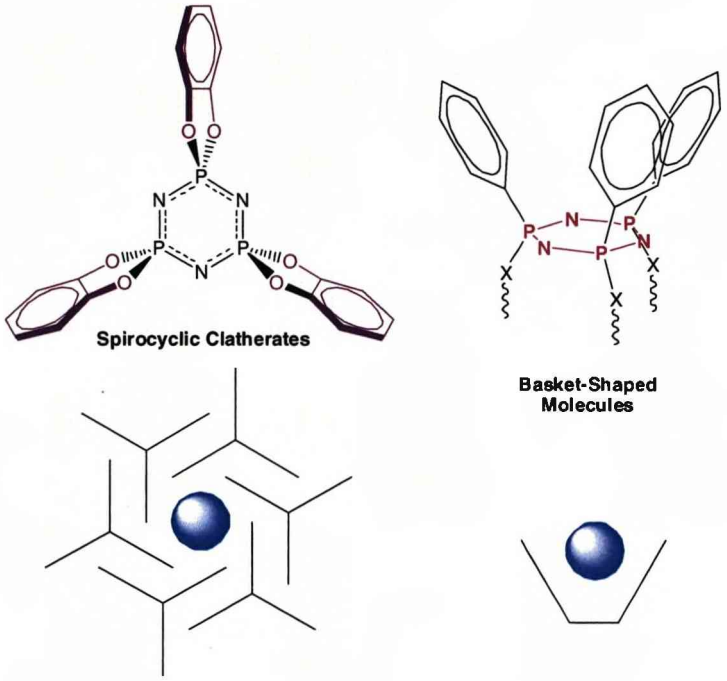

Figure 2.23[8]

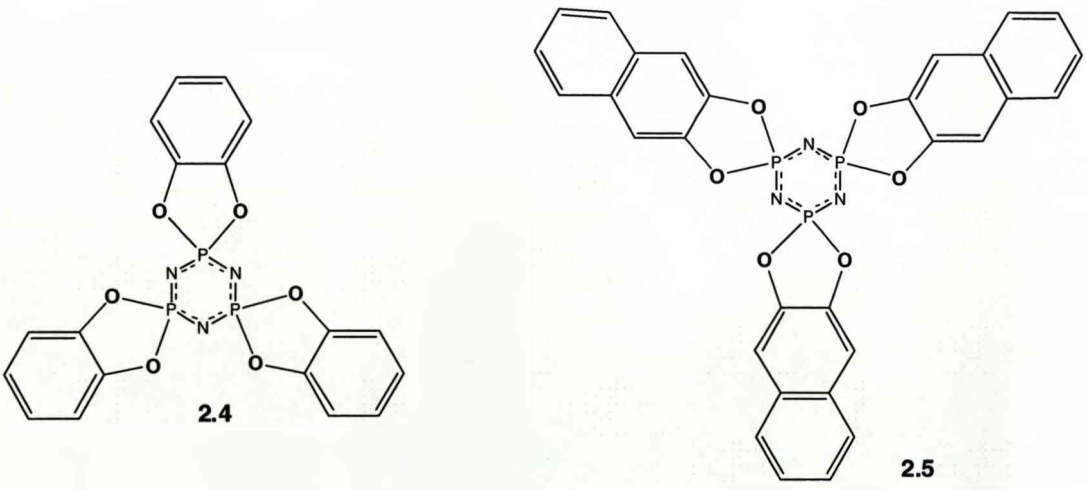

Figure 2.24. Examples of Cyclotriphosphazenes which form Inclusion Compounds with Guest Molecules.[8,58]

The crystal structure of **2.4** contains hexagonal channels of 4.5-5.0 Å in diameter along the crystallographic z-axis, these channels form as **2.4** arranges itself into alternating layers of interlocking "paddle-wheels", see Figure 2.25.[8,58,60] The guest molecule can be removed by either vacuum sublimation or heating above 170 °C.[60] However this causes a collapse of the hexagonal open channel structure to give a monoclinic phase of pure **2.4**, which does not contain channels or large voids.[8,60] This is due to a distortion of the "paddle-wheel" shape away from three-fold symmetry, leading to more efficient packing.[8] Although, the hexagonal structure does reform when exposed to guest molecules.[8] The loss of the open structure in the absence of the guest is clearly not ideal in the search for porous materials. However, pure **2.4** can retain the porous hexagonal structure when volatile guests are removed below the exothermic transition temperature (-75 °C) under reduced pressure.[8]

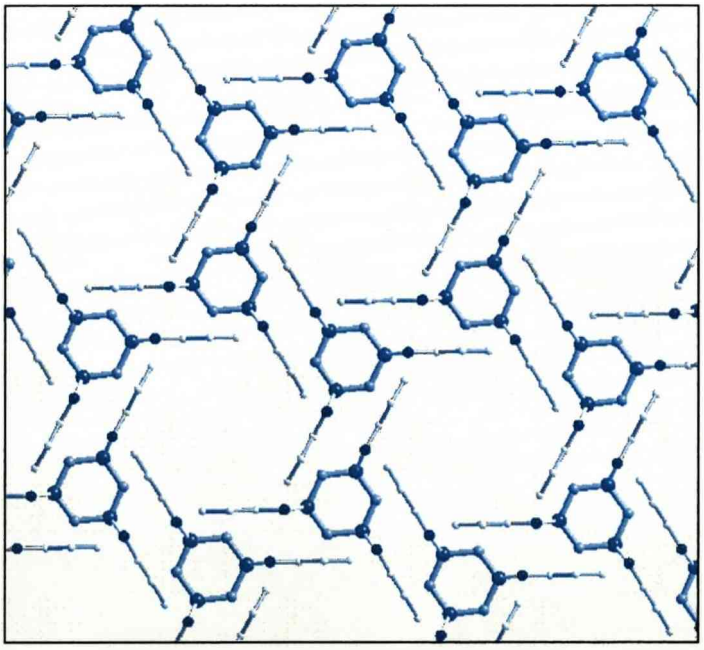

Figure 2.25. Crystal Structure of 2.4[7,8]

-O shown as dark spheres, P medium blue spheres, N lighter spheres, C very small spheres and H atoms omitted

The hexagonal host structure of **2.4** can accommodate a variety of guests from gaseous compounds to linear polymers.[8] These types of clathrates are ideal candidates for gas storage and purification devices as **2.4** exhibits high storage capacities with CO_2 and CH_4, although it does poorly absorb N_2 and O_2.[61] Iodine has been shown to readily diffuse into the channels of **2.4**, this process can be observed by the development of a purple colour into the colourless rod-like crystals.[62] These iodine-saturated crystals show no significant weight loss of I_2 under vacuum at room temperature.[8] The iodine chains within **2.4** have a similar conductivity to pure iodine, this is significant as iodine is a 2D semiconductor and one of the best characterised n-type molecular donors for the formation of $n \rightarrow \sigma^*$ charge transfer complexes.[62] The channels of **2.4** can also incorporate linear polymers, such as polyethyleneoxide and polyethylene, resulting in materials with melting points elevated above those of both pure **2.4** and pure polymer.[8,63-66] **2.4** favours the inclusion of long chain polymers over those with shorter chains and monomers, thus offering interesting applications in polymer purification.[67] Clathrates containing poly conjugated molecules have also been reported.[68] Furthermore, polymerisations of vinylic and acrylic monomers can be carried out within the channels, by initiation by γ-irradiation,.[8,69,70] Clathrate systems provide an environment that facilitates exclusive formation of 1,4-trans-polydienes from 1,3-dienes.[71]

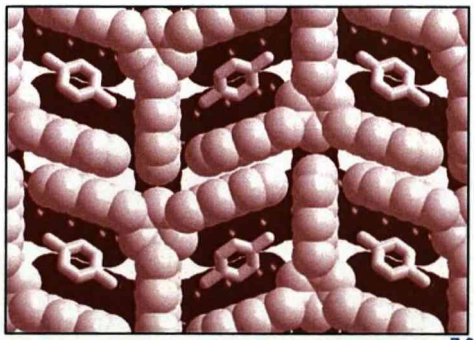

Figure 2.26. Crystal Structure of 2.5[7,8]

The clathrate properties of **2.5** differ somewhat from those of **2.4**, despite the fact that **2.5** also forms as a hexagonal host structure when accommodating

benzene as a guest.[72] Here the channel diameter is 9-10 Å, as the naphthalene groups have more extended π-stacking interactions.[72] In contrast to **2.4** the structure of **2.5** is altered with different guest molecules. In the presence of p-xylene and p-chlorotoluene **2.5** forms closed cavities rather than open channels, see Figure 2.26.[73,74] These cavities have a defined shape therefore, **2.5** can effectively separate para-isomers from a mixture of disubstituted benzenes.[70,74,75]

Basket-type structures can be formed from arrays of three aryl groups on one face of the phosphazene ring.[8] These systems surround cavities with an electron rich wall in a similar fashion to calixarenes.[76] However they exhibit free rotation around the P-C(aryl) bonds, allowing conformational flexibility of the aromatic groups that is not observed for calixarenes.[8] Figure 2.27 shows hexaphenyl cyclotriphosphazene, which adopts this "basket" arrangement when it crystallises from THF.[8] It forms a 1:1 complex with one molecule of THF occupying the guest site within the basket. The three phenyl groups, on the opposite side of the ring to THF, arrange themselves in a manner which allows them to interlock with the phenyl rings of a neighbouring phosphazene.[8] Solvent free crystals are obtained if suitable guest molecules are not present.[8]

Wisan-Neilson et al. have recently developed cyclotriphosphazenes of the form $N_3P_3Ph_3E_3$, which contain three phenyl groups on one side of the phosphazene ring plane and three alky (or functionalized alky groups) on the other. These compounds offer interesting possibilities for self assembly applications, however their supramolecular structures have not been studied.[8,77-80]

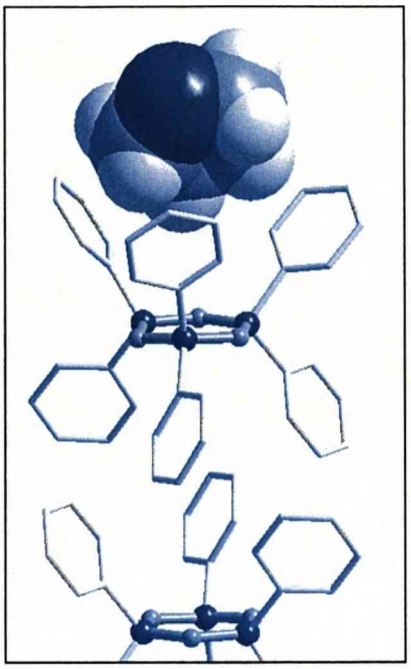

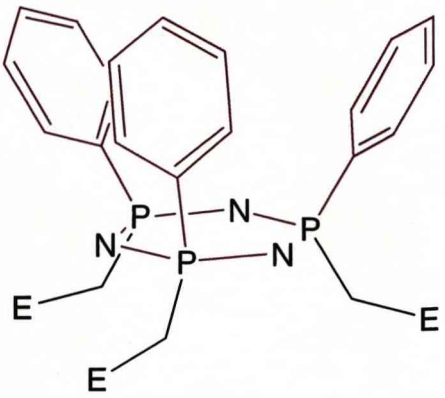

E = Me, SR, SO_2R, Cl, Br, I

Figure 2.27. Crystal Structure of $N_3P_3Ph_6$·THF.[7,8]

2.5.1.2. Dendritic Cyclophosphazenes

Phosphazene rings offer a unique platform for dendritic molecules. Their ability to anchor six substituents around the ring, with three above and three below the ring plane, offers interesting applications in supramolecular assemblies.[8] Supramolecular cyclophosphazene dendritic systems have been investigated with regard to liquid crystal behaviour, hydrogels and self-assembled nano-structures.[8]

2.5.1.2.1. Liquid Crystal Applications

There is an increasing interest in specifically functionalised mesogens owing to the important role of liquid crystals in display technology.[81] Phosphazene derivatives offer promising candidates for liquid crystals due to their synthetic versatility, chemical stability, low flammability and optical transparency from near infra-red to 210-190 nm in the ultraviolet spectrum.[8,82] Two important arrangements in liquid crystals are rod-like and disk-like structures, as shown in Figure 2.28.[81,82] Cyclophosphazenes can adopt both of these arrangements depending on their substituents. Rod-like (calamitic) systems

are observed with linear mesogenic substituents, which tend to bundle either side of the phosphazene ring. Smectic phases have been obtained with linear Schiff's base and biphenoxy substiuents.[8,83-85] On the other hand, disk-like (discotic) conformations can form when phosphazenes are substituted with branching mesogens. These result in columnar mesophases, which are stable at room temperature.[8,86,87]

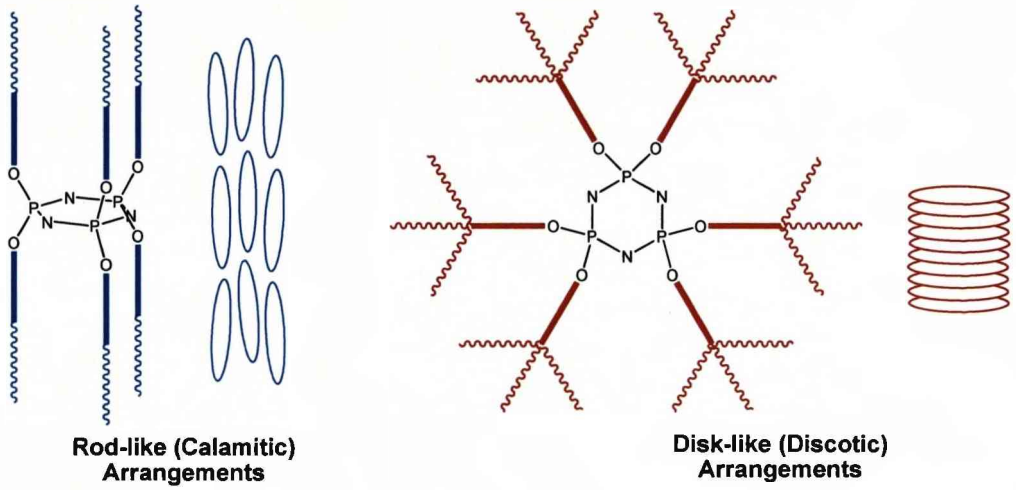

Figure 2.28.[8]

2.5.1.2.2. Self-Assembly Applications

Cyclotriphosphazenes can be equipped with intermolecular binding sites at terminal substituent positions. This facilitates supramolecular self-assembly, in particular to form nano-rods with cylindrical phosphazenes.[8,32] This type of assembly may be achieved in three ways, shown below in Figure 2.29: (i) Phosphazenes can co-crystallise with compatible difunctional molecules. For example phosphazenes containing 4-pyridyl end groups can form hydrogen bond with linear dicarboxylic acids.[8,88] (ii) Two phosphazene derivatives, with compatible substituent end groups (X and Y) may co-crystallise. This type of co-crystallisation has been reported when X = 4-pyridyl and Y = COOH.[8,89] (iii) Via the formation of coordination polymers using metal ions as linkers. This has been achieved using silver ions to coordinatively link phosphazenes with 4-pyridyl end groups.[8,90]

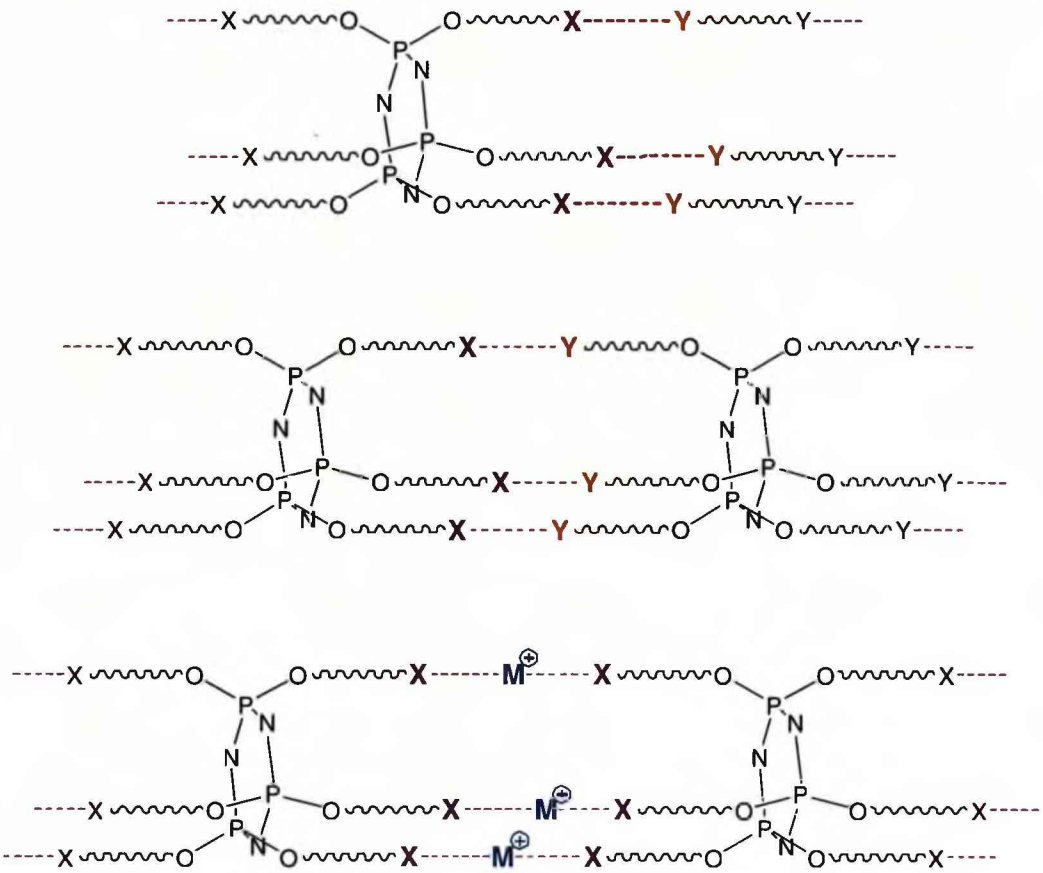

Figure 2.29. Examples of Cyclophosphazene Self-Assembly to form Nano-Rods.[8]

2.5.2. "Function"

This section will discuss supramolecular structures, in which the phosphazene ring is directly involved in non-covalent intermolecular bonds. As we have already mentioned the ring nitrogens of phosphazenes are basic sites, which can interact with Lewis acids such as metal ions and hydrogen bond donor molecules.[8] Here we will provide examples of hydrogen bonded structures as well as those involving metal ion coordination.

2.5.2.1. Hydrogen Bonding in Cyclotriphosphazenes

Supramolecular solids assembled by hydrogen bonds are extremely important in the field of crystal engineering.[8] The most commonly used building blocks to date are polycarboxylic acids, ureas and nitrogen heterocycles, as they are molecularly rigid, thus allowing highly directional interactions. This allows the rational design of supramolecular architectures.[8,91-93] Cyclotriphosphazenes display a unique arrangement of potential hydrogen bonding sites, however they have been studied to a lesser degree than the above mentioned materials.[8]

In previous years our research group has investigated the hydrogen bonding properties of polyamino phosphazenes, in particular $N_3P_3(NHR)_6$.[22] These compounds are very robust and can resist extreme conditions, including exposure to strongly acidic and basic media as well as hydrothermal treatment.[8] In addition to this they contain a mixture of hydrogen bond acceptor sites (ring nitrogens) and hydrogen bond donor sites (exocyclic nitrogens), thus they can be considered as promising supramolecular building blocks.[8] We should also note that polyamine based compounds are of interest within anion detection and separation along with supramolecular assembled nano- materials.[8,94]

The crystal structures of a series of polyamino phosphazenes, $N_3P_3(NHR)_6$ have shown an unprecedented variety of supramolecular hydrogen bonded networks that is controlled by the slightest variation in the size or shape of R.[8,22] These molecules are arranged so that they contain an equatorial chain of three ring nitrogens and six NH functions, which is sandwiched between layers of the lipophilic substituents R. This causes phosphazene molecules to interact in a "side-by-side" fashion rather than "face-to-face", thus forming a type of lipid-bilayer, see Figure 2.30.[8,22]

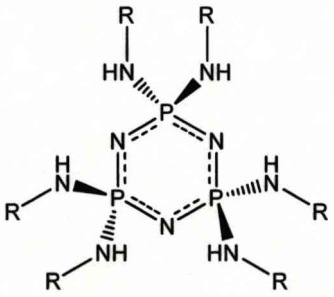

Polyamino Cyclophosphazene

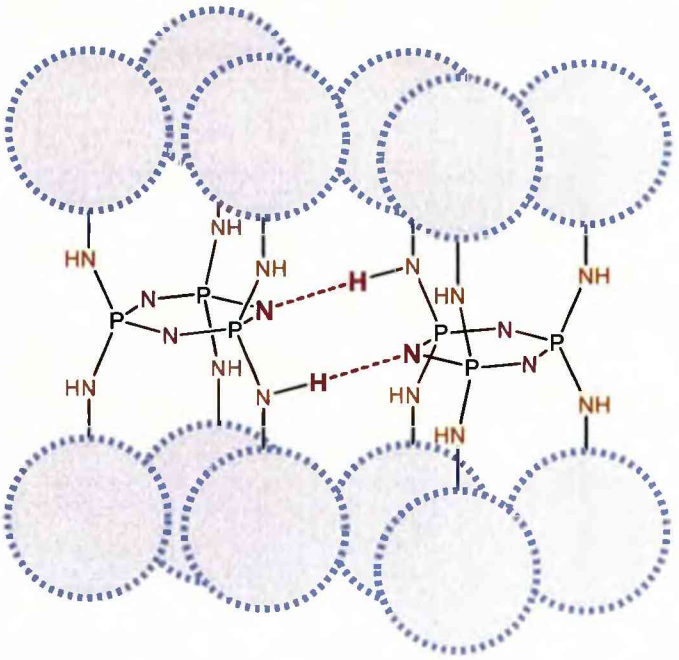

Lipid-Bilayer of Hydrogen Bonded Phosphazenes $N_3P_3(NHR)_6$

Figure 2.30[22]

The hydrogen bonding between these molecules is extremely diverse, due to free rotation around the exocyclic P-N bond. All together ten principal types of intermolecular hydrogen bridges were observed, as shown in Figure 2.31.[8,22] These include single (**a**), double (**b**, **c** and **d**), triple (**e**, **f**, **g** and **h**), quadruple (**j**) and sextuple (**k**) bridges exhibited over compounds where R = methyl, *n*-propyl, *iso*-propyl, *iso*-butyl, *tert*-butyl, cyclohexyl, allyl, benzyl, phenyl, *para*-tolyl, 2-phenyl-ethyl and propargyl.[22]

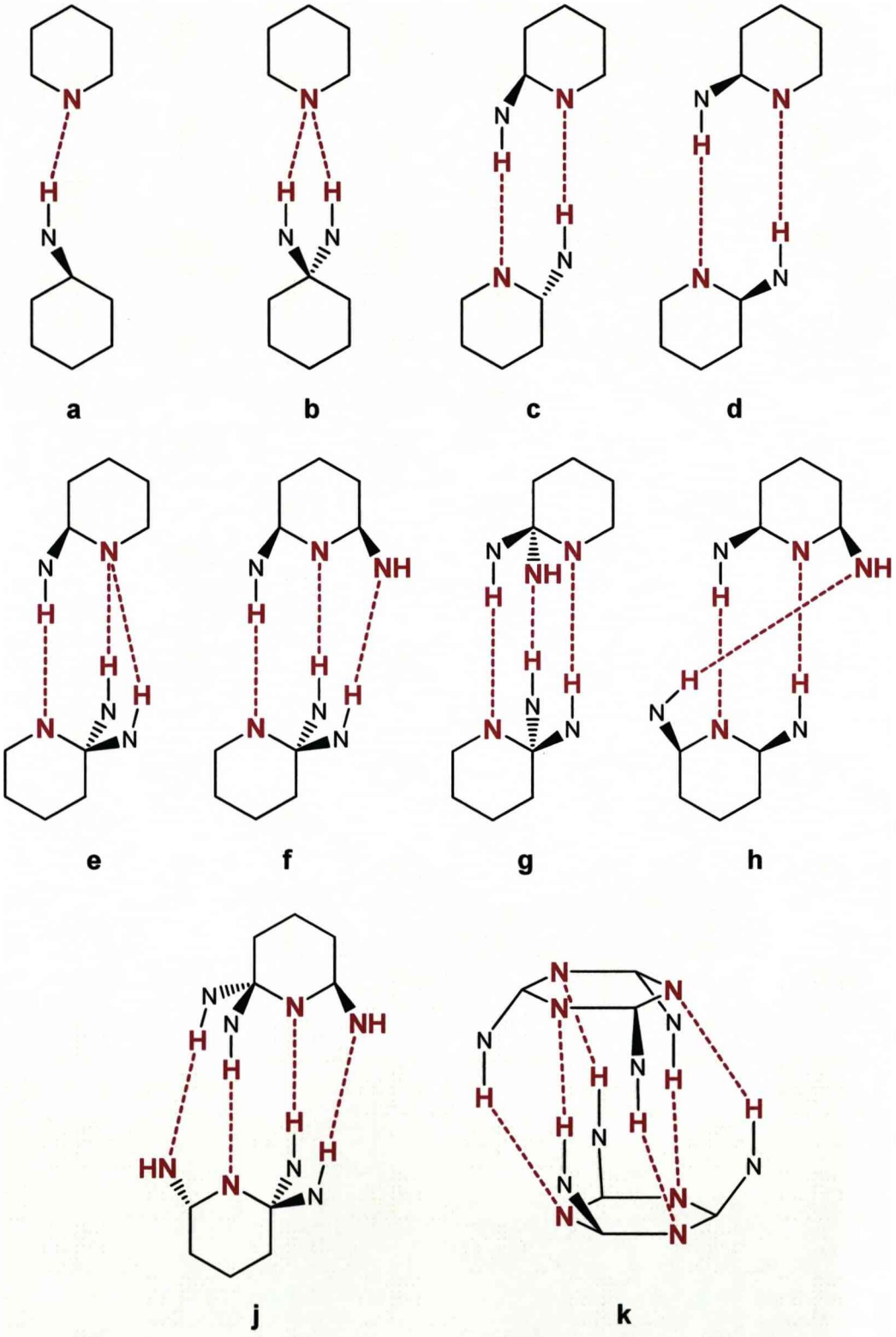

Figure 2.31. Hydrogen Bonding Modes of $N_3P_3(NHR)_6$ and $N_3P_3(NH_2)_6$[22]

Crystal structures to illustrate the diversity of supramolecular networks exhibited by polyamino phosphazenes are shown below in Figure 2.32.[22]

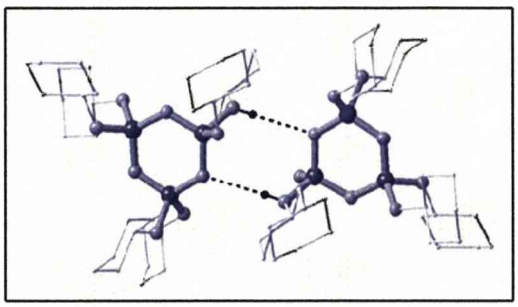

R = Cyclohexyl

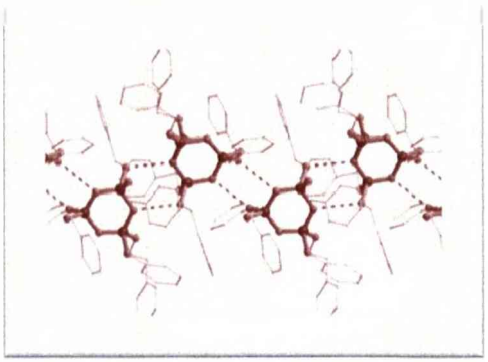

R = Benzyl

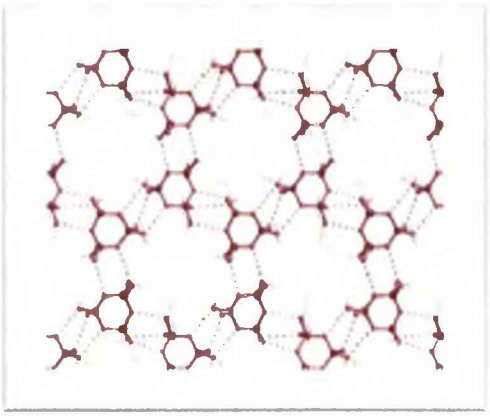

R = Allyl

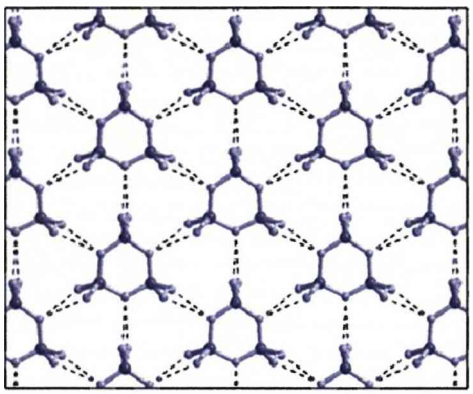

R = Methyl

Figure 2.32. Crystal Structures of Selected $N_3P_3(NHR)_6$ Compounds[7,22]

-P shown as darkest spheres, N lighter spheres, C very small light spheres, H atoms omitted and dashed line illustrates H-bond.

It is worth noting here that the *tert*-butyl derivative (not shown here) does not show any NH...N intermolecular interactions in its crystal structure, because of the steric bulk of the *tert*-butyl groups. The cyclohexyl and benzyl derivatives exhibit **c**-type linkers in just one dimension. More extended structures are achieved for the smaller methyl and allyl derivatives, with the allyl compound giving "honeycomb" sheets of molecules linked by both **c** and **g** bridges. The methyl derivative forms hexagonal close packed sheets, in which each phosphazene molecule interacts with its six neighbours via **b**-bridges. Here all of the NH functions are acting as hydrogen donors, while all of the N(ring) sites are behaving as hydrogen acceptors.[8,22] As we have already mentioned, the directionality of the hydrogen bonds is dependent on

the steric factors of the R groups. This can be attributed to the fact that both the H atom and the R group are hinged on a freely rotating nitrogen centre. Thus, a correlation between R group interactions and N-H bond directionality, must be adhered to.[8,22] The majority of N....N distances in these structures range between 2.9 and 3.3 Å, indicating the hydrogen-bonds are moderately strong.[8,22]

In contrast to the structures we have just discussed $N_3P_3(NH_2)_6$ contains twelve hydrogen donor sites but lacks a lipophilic periphery. It therefore forms a complex three-dimensional structure in the sold state. Here each molecule interacts with eight neighbours, utilising all NH and N sites.[8,95]

The above mentioned hydrogen bonds have also been observed in a variety of other amino-substituted phosphazene trimers[42,96-98] and tetramers.[25,99,100] It should be pointed out that the centrosymmetric **c** bridge occurs most often.[8] Further to this $N_3P_3(NHR)_6$ compounds have been shown to form a number of solvate structures, involving the above mentioned hydrogen bonding motifs.[8] An example of this is shown below, in Figure 2.33. The structure consists of the 2-phenylethyl derivative, solvated with THF. This contains **f** bonded chains and one molecule of THF per phosphazene, which is situated in a cavity formed by four 2-phenylethyl groups.[8,22]

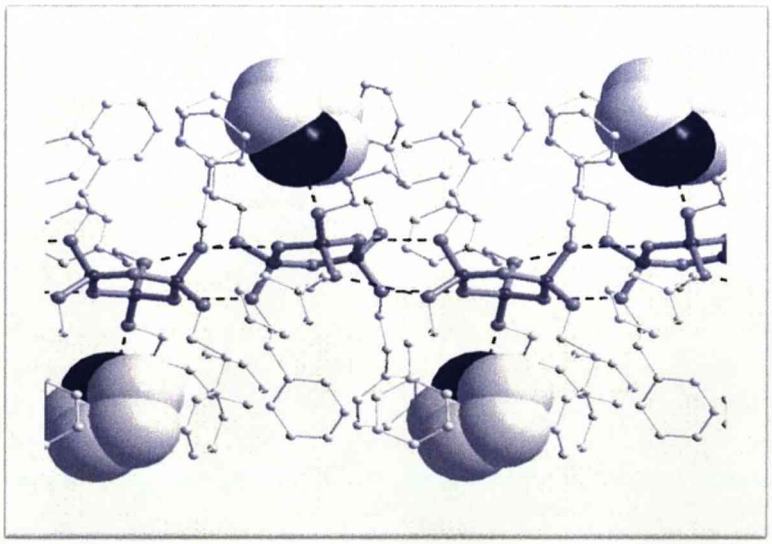

Figure 2.33. Crystal Structure of the 2-Phenylethyl Derivative Solvated by THF.[7,8]

-THF shown in space filling format, P shown as darkest spheres, N lighter spheres, C very light spheres, H atoms omitted and dashed line illustrates H-bond.

In addition to this, these hexa-amino phosphazenes of the form $N_3P_3(NHR)_6$ can form distinct hydrates, in which water binds to the phosphazene via NH...O and OH...N hydrogen bonds.[8] Figure 2.34 below shows several examples of this, in which structures display a variety of aggregation patterns, again controlled by the steric factors of R.[8,101]

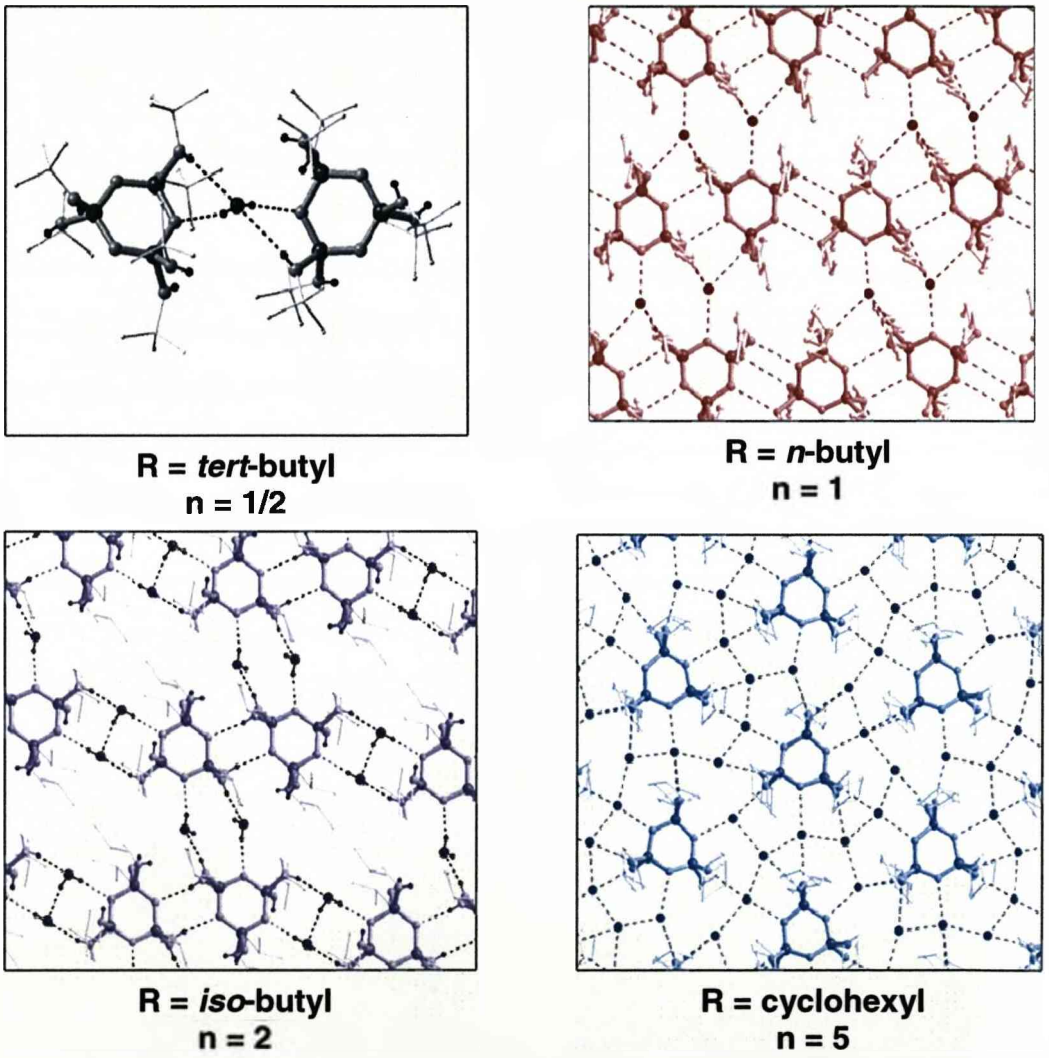

Figure 2.34. Crystal Structures of Hydrates, $N_3P_3(NHR)_6 \cdot nH_2O$[7,8]

-O shown as darkest spheres, P dark spheres, N lighter spheres, C very small light spheres, H atoms omitted and dashed line illustrates H-bond.

The bulky *tert*-butyl derivative encapsulates one molecule of water in a dimeric fashion. The *n*-butylamino phosphazene contains one water per ring to form hydrogen bonded sheets, where chains of phosphazene rings are created via **c** and **g** bridges and then interconnected by water molecules. The *iso*-butyl derivative forms hydrogen bonded dimers that are connected via water molecules, while the cyclohexyl derivative is completely surrounded by water molecules in an extended two-dimensional network.[8]

The water molecules within these hydrates are effectively contained by a hydrophobic layer of R groups. In fact the two dimensional structures of the *iso*-butyl, *n*-butyl and cyclohexyl hydrates still retain the lipid-bilayer arrangement, that is observed in the structures of solvent free polyamino phosphazenes $N_3P_3(NHR)_6$. It should however also be noted that certain of these amino derivatives (*iso*-propyl, allyl, methyl) have so far resisted the formation of solvates or hydrates. This may be due to more effective crystal packing as all three exhibit hexagonal type structures. This illustrates that the properties of polyamino phosphazene can be tailored by modification of their lipophilic periphery.[8]

2.5.2.2. Supramolecular Structures Involving Metal Coordination

The connection of metal centres via multiprotic ligands can lead to the formation of coordination polymers, in which the coordination geometry of both the ligand and metal control the topology of the system.[8,102] Current ligands in coordination polymers include organo nitrogen heterocycles, which contain a stereorigid arrangement of nitrogen donor sites.[8,103]

The stable arrangement of trigonal planar ring nitrogens, coupled with the positioning of phosphorus substituents above and below the plane of the ring, provides ideal conditions for metal coordination to phosphazene rings, see Figure 2.35.[8]

Polyamino cyclophosphazenes $N_3P_3(NHR)_6$ have been reported to form coordination polymers with various silver salts via linear N-Ag-N connections.[23] The topology of these networks is controlled by the steric demands of the amino groups combined with the donor properties of the counter anion.[8]

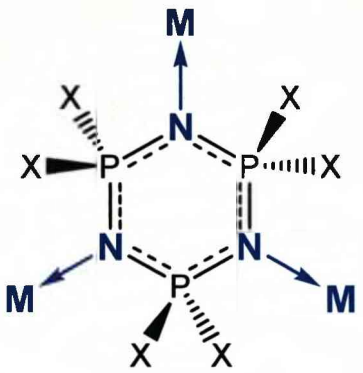

Figure 2.35. Schematic of Metal Coordination to Phosphazene Rings.[8]

For example the *n*-propyl derivative forms a graphite type network with silver perchlorate, $(N_3P_3(NH^nPr)_6)_2(AgClO_4)_3$, with each silver ion bridging two phosphazenes in such a way that all three ring nitrogens coordinate to silver, where as, a zig-zag arrangement occurs on coordination to silver nitrate forming $(N_3P_3(NH^nPr)_6)(AgNO_3)_2$. Here each phosphazene molecule coordinates to one bridging silver ion and one terminal silver ion. A two dimensional network is then created as terminal silver ions connect to the silver ions of neighbouring chains via nitrate ions.[8,23] In contrast to this the more sterically demanding cyclohexyl derivative forms a one dimensional zig-zag chain when coordinated to silver perchlorate. In this example only two phosphazene ring nitrogens bind to silver ions, leaving one site vacent.[8,23] Both examples are shown in Figure 2.36.

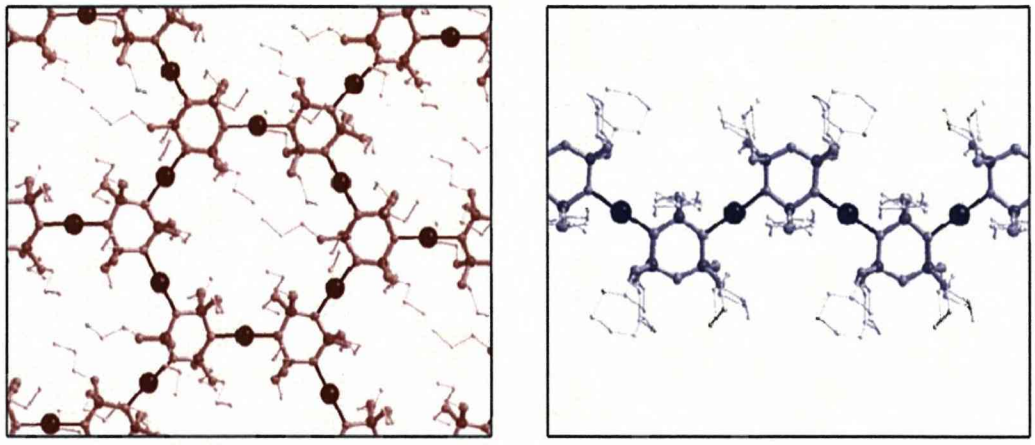

Figure 2.36. Crystal Structures of Amino Phosphazenes Coordinating to metal ions.[7,104]

-Ag shown as darkest spheres, P dark small spheres, N lighter small spheres, C very small light spheres, H atoms and counter ions omitted.

Incorporating functionality into the R groups of the amine substituents further increases the array of supramolecular structures which can be generated. This is due to the introduction of additional cation binding sites. For example silver salt networks with benzyl- and allyl- amino phosphazene derivatives both show Ag-π(aryl) interactions as well as Ag-N(ring) and Ag-anion interactions, see Figure 2.37.[8,23,104]

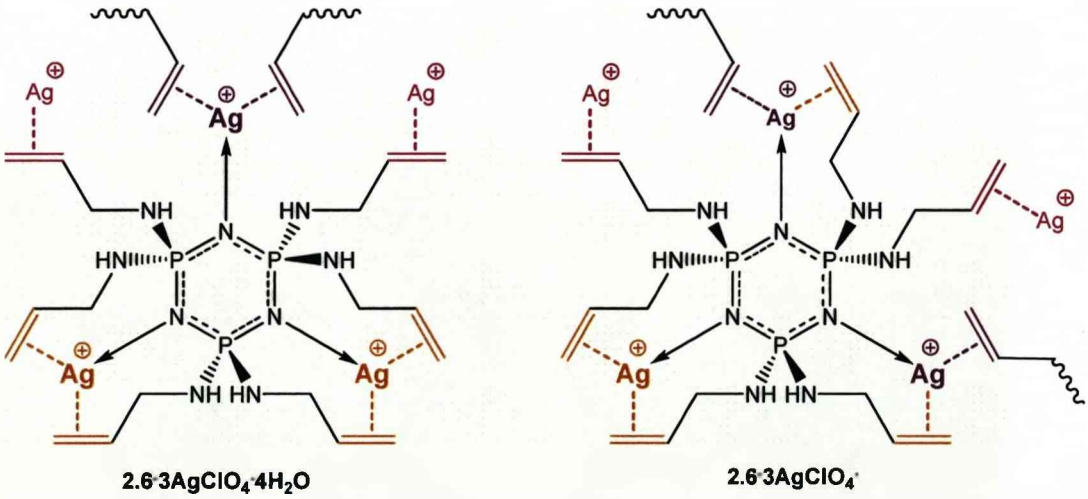

Figure 2.37. Schematic Showing Ag-P Binding Sites in the Two Isomers of $[N_3P_3(NHCH_2CHCH_2)_6Ag_3]^{3+}$.[8]

Two coordination polymers of the allylamino derived phosphazene **2.6** with silver perchlorate have been reported.[104] The hydrate **2.6**·3$AgClO_4$·4H_2O contains a one dimensional chain of [**2.6**Ag_3]$^{3+}$ units, in which two silver ions act as intramolecular bridges between neighbouring allyl functions on the same phosphazene ring. The third silver ion then intermolecularly connects the phosphazene ring with two neighbouring [**2.6**Ag_3]$^{3+}$ units via Ag—olefin bonds. In contrast to this the non-hydrated **2.6**·3$AgClO_4$ forms a three dimensional isomer of the hydrate. This network also involves [**2.6**Ag_3]$^{3+}$ units connected by silver ions coordinated to two allyl groups. However, here the phosphazene is only connected to one intramolecular silver bridge. The other two silver ions both coordinate to one intra- and one intermolecular olefin function. Thus, connecting each [**2.6**Ag_3]$^{3+}$ to four neighbours creating a diamondoid network topology.[8,104] We should also mention that **2.6**·3$AgClO_4$ forms by spontaneous recrystallisation of the solid hydrate in methanol.[104] This is attributed to the diffusion of [**2.6**Ag_3]$^{3+}$ units through the methanol facilitated by the flexible coordination behaviour of [**2.6**Ag_3]$^{3+}$.[8,104] The allylamino groups within this structure are also involved in hydrogen bonding to perchlorate ions and solvent molecules. Hydrogen bonding and metal coordination are thought to be correlated to some extent as NH functions and allyl groups are coordinated to the same P-N bond.[8,104]

In addition to these coordination polymers numerous metal complexes of cyclotriphosphazenes have been reported.[1,8,105,106] These involve cyclophosphazene species, which have been substituted with a variety of functional side arms and display various coordination modes.[8]

References

(1) Chandrasekhar, V., Thilagar, P.; Pandian, B. M. *Coord. Chem. Rev.* **2007**, *251*, 1045.

(2) Steiner, A., Zacchini, S.; Richards, P. I. *Coord. Chem. Rev.* **2002**, *227*, 193.

(3) Lawson, G. T., Jacob, C.; Steiner, A. *Eur. J. Inorg. Chem.* **1999**, 1881.

(4) Benson, M. A., Zacchini, S., Boomishankar, R., Chan, Y.; Steiner, A. *Inorg. Chem.* **2007**, *46*, 7097.

(5) Chandrasekhar, V.; Krishnan, V. *Adv. Inorg. Chem.* **2002**, *53*, 159.

(6) Gleria, M.; De Jaeger, R., *Phosphazenes: A Worldwide Insight*, Nova Science Publishers, Inc., **2004**.

(7) *Crystal structure included with authors permission*

(8) Steiner, A. in Polyphosphazenes for Biomedical Applications, (A. K. Andrianov), Wiley, **2009**, 411.

(9) Allcock, H. R. *Chem. Rev.* **1972**, *72*, 315.

(10) Chandrasekhar, V.; Thomas, K. R. J. *Struct. Bond.* **1993**, *81*, 42.

(11) Allcock, H. R. in Phosphazenes: A Worldwide Insight, (M. Gleria and R. De Jaeger), Nova Science Publishers, Inc., **2004**, 1.

(12) Zhu, L., Zhu, Y., Pan, Y., Huang, Y. W., Huang, X. B.; Tang, X. Z. *Macromol. React. Eng.* **2007**, *1*, 45.

(13) Chaplin, A. B., Harrison, J. A.; Dyson, P. J. *Inorg. Chem.* **2005**, *44*, 8407.

(14) Luana, V., Pendas, A. M., Costales, A., Carriedo, G. A.; Garcia-Alonso, F. J. *J. Phys. Chem. A* **2001**, *105*, 5280.

(15) Tonei, D. M., Bertani, R., De Jaeger, R.; Gleria, M. in Phosphazenes: A Worldwide Insight, (M. Gleria and R. De Jaeger), Nova Sience Publishers, Inc., **2004**, 669.

(16) Chang, J. Y. in Phosphazenes: A Worldwide Insight, (M. Gleria and R. De Jaeger), Nova science Publishers, Inc., **2004**, 669.

(17) Haridas, V., Sharma, Y. K.; Naik, S. *Eur. J. Org. Chem.* **2009**, 1570.

(18) Caminade, A. M.; Majoral, J. P. in Phosphazenes: A Worldwide Insight, (M. Gleria and R. De Jaeger), Nova Science Publishers, Inc., **2004**, 713.

(19) Zhao, Y. L., Chen, Y. M., Chen, C. F.; Xi, F. *Polymer* **2005**, *46*, 5808.

(20) Feakins, D., Last, W. A., Neemuchw.N; Shaw, R. A. *J. Chem. Soc.* **1965**, 2804.

(21) Feakins, D., Shaw, R. A.; Last, W. A. *J. Chem. Soc.* **1964**, 4464.

(22) Bickley, J. F., Bonar-Law, R., Lawson, G. T., Richards, P. I., Rivals, F., Steiner, A.; Zacchini, S. *Dalton Trans.* **2003**, 1235.

(23) Richards, P. I.; Steiner, A. *Inorg. Chem.* **2004**, *43*, 2810.

(24) Heston, A. J., Panzner, M. J., Youngs, W. J.; Tessier, C. A. *Inorg. Chem.* **2005**, *44*, 6518.

(25) Chandrasekhar, V., Vivekanandan, K., Nagendran, S., Andavan, G. T. S., Weathers, N. R., Yarbrough, J. C.; Cordes, A. W. *Inorg. Chem.* **1998**, *37*, 6192.

(26) Singh, R. P., Vij, A., Kirchmeier, R. L.; Shreeve, J. M. *Inorg. Chem.* **2000**, *39*, 375.

(27) Bullen, G. J. *J. Chem. Soc. a Inorg. Phys. Theo.* **1971**, 1450.

(28) Zoer, H.; Wagner, A. J. *Acta Crystallogr., Sect. B: Struct. Sci.* **1970**, *B26*, 1812.

(29) Markila, P. L.; Trotter, J. *Can. J. Chem.* **1974**, *52*, 2197.

(30) Cameron, T. S., Borecka, B.; Kwiatkowski, W. *J. Am. Chem. Soc.* **1994**, *116*, 1211.

(31) Allcock, H. A., Levin, M. L.; Whittle, R. R. *Inorg. Chem.* **1986**, *25*, 41.

(32) Inoue, K.; Itaya, T. *Bull. Chem. Soc. Jpn.* **2001**, *74*, 1381.

(33) Elias, A. J.; Shreeve, J. M. *Adv. Inorg. Chem.* **2001**, *52*, 335.

(34) Bamgboye, T. T.; Sowerby, D. B. *J. Inorg. Nucl. Chem.* **1981**, *43*, 2253.

(35) Paddock, N. L.; Patmore, D. J. *J. Chem. Soc., Dalton Trans.* **1976**, 1029.

(36) Emsley, J.; Paddock, N. L. *J. Chem. Soc. a Inorg. Phys. Theo.* **1968**, 2590.

(37) Ratz, R.; Grundmann, C. *J. Inorg. Nucl. Chem.* **1960**, *16*, 60.

(38) Emsley, J.; Udy, P. B. *J. Chem. Soc. a Inorg. Phys. Theo.* **1970**, 3025.

(39) Allcock, H. R., Crane, C. A., Morrissey, C. T.; Olshavsky, M. A. *Inorg. Chem.* **1999**, *38*, 280.

(40) Allen, C. W. *Chem. Rev.* **1991**, *91*, 119.

(41) Katti, K. V.; Krishnamurthy, S. S. *J. Chem. Soc., Dalton Trans.* **1985**, 285.

(42) Bartlett, S. W., Coles, S. J., Davies, D. B., Hursthouse, M. B., Ibisoglu, H., Kilic, A., Shaw, R. A.; Un, I. *Acta Crystallogr. Sect. B-Struct. Commun.* **2006**, *62*, 321.

(43) Chandrasekhar, V., Muralidhara, M. G. K.; Reddy, N. S. *Heterocycles* **1992**, *33*, 111.

(44) Kumar, E. S., Muralidhara, M. G.; Chandrasekhar, V. *Polyhedron* **1995**, *14*, 1571.

(45) Chivers, T.; Hedgelan.R *Can. J. Chem.* **1972**, *50*, 1017.

(46) Goldschmidt, J. M. E.; Licht, E. *J. Chem. Soc., Dalton Trans.* **1981**, 107.

(47) Ferrar, W. T., Distefano, F. V.; Allcock, H. R. *Macromolecules* **1980**, *13*, 1345.

(48) Schmutz, J. L.; Allcock, H. R. *Inorg. Chem.* **1975**, *14*, 2433.

(49) Dhathathreyan, K. S., Krishnamurthy, S. S.; Woods, M. *J. Chem. Soc., Dalton Trans.* **1982**, 2151.

(50) Allcock, H. R., AlShali, S., Ngo, D. C., Visscher, K. B.; Parvez, M. *J. Chem. Soc., Dalton Trans.* **1996**, 3549.

(51) Boomishankar, R., Richards, P. I.; Steiner, A. *Angew. Chem., Int. Ed.* **2006**, *45*, 4632.

(52) Steiner, A.; Wright, D. S. *Angew. Chem., Int. Ed. Engl.* **1996**, *35*, 636.

(53) Lawson, G. T., Rivals, F., Tascher, M., Jacob, C., Bickley, J. F.; Steiner, A. *Chem. Commun.* **2000**, 341.

(54) Rivals, F.; Steiner, A. *Chem. Commun.* **2001**, 1426.

(55) Macnicol, D. D., McKendrick, J. J.; Wilson, D. R. *Chem. Soc. Rev.* **1978**, *7*, 65.

(56) Allcock, H. R.; Siegel, L. A. *J. Am. Chem. Soc.* **1964**, *86*, 5140.

(57) Allcock, H. R. *J. Am. Chem. Soc.* **1964**, *86*, 2591.

(58) Inoue, K.; Itaya, T. in Phosphazenes: A Worldwide Insight, (M. Gleria and R. De Jaeger), Nova Sciences Publishers, Inc., **2004**, 739.

(59) Davis, M. E. *Nature* **2002**, *417*, 813.

(60) Allcock, H. R. *Acc. Chem. Res.* **1978**, *11*, 81.

(61) Sozzani, P., Bracco, S., Comotti, A., Ferretti, L.; Simonutti, R. *Angew. Chem., Int. Ed.* **2005**, *44*, 1816.

(62) Hertzsch, T., Budde, F., Weber, E.; Hulliger, J. *Angew. Chem., Int. Ed.* **2002**, *41*, 2281.

(63) Sozzani, P., Comotti, A., Bracco, S.; Simonutti, R. *Chem. Commun.* **2004**, 768.

(64) Comotti, A., Simonutti, R., Catel, G.; Sozzani, P. *Chem. Mater.* **1999**, *11*, 1476.

(65) Allcock, H. R., Primrose, A. P., Sunderland, N. J., Rheingold, A. L., Guzei, I. A.; Parvez, M. *Chem. Mater.* **1999**, *11*, 1243.

(66) Primrose, A. P., Parvez, M.; Allcock, H. R. *Macromolecules* **1997**, *30*, 670.

(67) Allcock, H. R.; Sunderland, N. J. *Macromolecules* **2001**, *34*, 3069.

(68) Sozzani, P., Comotti, A., Bracco, S.; Simonutti, R. *Angew. Chem., Int. Ed.* **2004**, *43*, 2792.

(69) Allcock, H. R., Ferrar, W. T.; Levin, M. L. *Macromolecules* **1982**, *15*, 697.

(70) Allcock, H. R., Silverberg, E. N.; Dudley, G. K. *Macromolecules* **1994**, *27*, 1033.

(71) Allcock, H. R., Dudley, G. K.; Silverberg, E. N. *Macromolecules* **1994**, *27*, 1039.

(72) Allcock, H. R.; Stein, M. T. *J. Am. Chem. Soc.* **1974**, *96*, 49.

(73) Kubono, K., Asaka, N., Taga, T., Isoda, S.; Kobayashi, T. *J. Mater. Chem.* **1994**, *4*, 291.

(74) Kubono, K., Asaka, N., Isoda, S., Kobayashi, T.; Taga, T. *Acta Crystallogr., Sect. C: Cryst. Struct. Commun.* **1993**, *49*, 404.

(75) Kubono, K., Asaka, N., Isoda, S., Kobayashi, T.; Taga, T. *Acta Crystallogr., Sect. C: Cryst. Struct. Commun.* **1994**, *50*, 324.

(76) Bohmer, V. *Angew. Chem., Int. Ed. Engl.* **1995**, *34*, 713.

(77) Jung, J. H., Kmecko, T., Claypool, C. L., Zhang, H. M.; Wisian-Neilson, P. *Macromolecules* **2005**, *38*, 2122.

(78) Jung, J. H., Potluri, S. K., Zhang, H. M.; Wisian-Neilson, P. *Inorg. Chem.* **2004**, *43*, 7784.

(79) Wisian-Neilson, P., Johnson, R. S., Zhang, H. M., Jung, J. H., Neilson, R. H., Ji, J. M., Watson, W. H.; Krawiec, M. *Inorg. Chem.* **2002**, *41*, 4775.

(80) Jung, J. H., Zhang, H. M.; Wislan-Neilson, P. *Inorg. Chem.* **2002**, *41*, 6720.

(81) Kato, T., Mizoshita, N.; Kishimoto, K. *Angew. Chem., Int. Ed.* **2006**, *45*, 38.

(82) Laschat, S., Baro, A., Steinke, N., Giesselmann, F., Hagele, C., Scalia, G., Judele, R., Kapatsina, E., Sauer, S., Schreivogel, A.; Tosoni, M. *Angew. Chem., Int. Ed.* **2007**, *46*, 4832.

(83) Moriya, K., Suzuki, T., Yano, S.; Miyajima, S. *J. Phys. Chem. B* **2001**, *105*, 7920.

(84) Moriya, K., Suzuki, T., Kawanishi, Y., Masuda, T., Mizusaki, H., Nakagawa, S., Ikematsu, H., Mizuno, K., Yano, S.; Kajiwara, M. *Appl. Organomet. Chem.* **1998**, *12*, 771.

(85) Moriya, K., Mizusaki, H., Kato, M., Suzuki, T., Yano, S., Kajiwara, M.; Tashiro, K. *Chem. Mater.* **1997**, *9*, 255.

(86) Barbera, J., Jimenez, J., Laguna, A., Oriol, L., Perez, S.; Serrano, J. L. *Chem. Mater.* **2006**, *18*, 5437.

(87) Barbera, J., Bardaji, M., Jimenez, J., Laguna, A., Martinez, M. P., Oriol, L., Serrano, J. L.; Zaragozano, I. *J. Am. Chem. Soc.* **2005**, *127*, 8994.

(88) Itaya, T., Azuma, N.; Inoue, K. *Bull. Chem. Soc. Jpn.* **2002**, *75*, 2275.

(89) Inoue, K.; Itaya, T. *Supramolecular Science* **1998**, *5*, 163.

(90) Itaya, T.; Inoue, K. *Bull. Chem. Soc. Jpn.* **2000**, *73*, 2615.

(91) Zaworotko, M. J. *Chem. Commun.* **2001**, 1.

(92) Desiraju, G. R. *Chem. Commun.* **1997**, 1475.

(93) Desiraju, G. R. *Angew. Chem., Int. Ed. Engl.* **1995**, *34*, 2311.

(94) Wichmann, K., Antonioli, B., Sohnel, T., Wenzel, M., Gloe, K., Price, J. R., Lindoy, L. F., Blake, A. J.; Schroder, M. *Coord. Chem. Rev.* **2006**, *250*, 2987.

(95) Golinski, F.; Jacobs, H. *Z. Naturforsch.* **1994**, *620*, 965.

(96) Kumar, N. S.; Swamy, K. C. K. *Polyhedron* **2004**, *23*, 979.

(97) Rivals, F.; Steiner, A. *Z. Naturforsch.* **2003**, *629*, 139.

(98) Fincham, J. K., Parkes, H. G., Shaw, L. S., Shaw, R. A.; Hursthouse, M. B. *J. Chem. Soc., Dalton Trans.* **1988**, 1169.

(99) Muralidharan, K., Omotowa, B. A., Twamley, B., Piekarski, C.; Shreeve, J. M. *Chem. Commun.* **2005**, 5193.

(100) Cameron, T. S., Cordes, R. E.; Jackman, F. A. *Acta Crystallogr. Sect. B-Struct. Commun.* **1979**, *35*, 980.

(101) Lawson, G. T., Richards, P. I., Zacchini, S.; Steiner, A. Unpublished Work.

(102) Steel, P. J. *Acc. Chem. Res.* **2005**, *38*, 243.

(103) Khlobystov, A. N., Blake, A. J., Champness, N. R., Lemenovskii, D. A., Majouga, A. G., Zyk, N. V.; Schroder, M. *Coord. Chem. Rev.* **2001**, *222*, 155.

(104) Richards, P. I., Bickley, J. F., Boomishankar, R.; Steiner, A. *Chem. Commun.* **2008**, 1656.

(105) Chandrasekhar, V.; Nagendran, S. *Chem. Soc. Rev.* **2001**, *30*, 193.

(106) Allcock, H. R., Desorcie, J. L.; Riding, G. H. *Polyhedron* **1987**, *6*, 119.

Chapter 3:

Nitrogen Donor Stabilised Cyclophosphazene Polycations

3.1. Introduction

Over the recent years our research group has developed polyanionic ligand systems of type **A** that are based on the chemically robust cyclophosphazene ring structure. The high charge and the large number of potential donor sites offer versatile ligands that accommodate multinuclear metal arrays. Thus we were curious if cyclophosphazene rings would also support polycationic structures such as **B**.[1-3] The synthesis of **B** requires neutral donor ligands L to saturate the phosphorus centres. **B** can be considered as an electronically inverse structure to **A**. It is a potential ligand for the accommodation of larger arrays of anions. An additional interesting analogy arises on comparison with cationic metal complexes $[M^{(n)}L_6]^{n+}$. These exhibit an octahedral arrangement of ligands, where as the $[N_3P_3L_6]^{6+}$ cation features a unique trigonal prismatic ligand environment due to the D_{3h} symmetry of the P_3N_3 ring. This offers exciting possibilities in supramolecular chemistry and framework structures, in particular when L constitutes a linearly bridging ligand such as 4,4'bipyridyl.

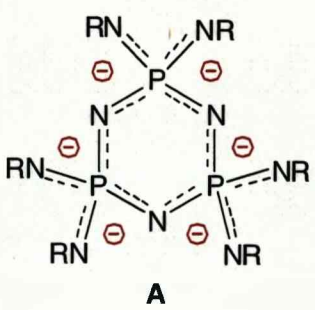

A

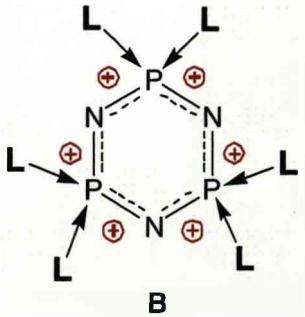

B

Another incentive for this research is that cyclotriphosphazene cations have been proposed as intermediates in the ring opening polymerisation of $P_3N_3Cl_6$,[4] but they, as well as their adducts with neutral donor ligands, have remained elusive and so far evaded structural characterisation. Despite the sparse reports of N-donor complexes with cyclophosphazenes, there are many examples of non-metal centres stabilised by N-donors.[5-10] Here we discuss some of these examples, focusing mainly on P- and C-complexes.

3.1.1. Nitrogen Donors as Ligands

Nitrogen centres are softer and more nucleophilic than oxygen centres, therefore, N-donor ligands (ammonia, amines and pyridines) are widely applied in the coordination chemistry of late transition metals. Pyridine derivatives are also regarded as π-acids, because their LUMO π* orbitals can accept electron density from the metal centre.[11] Furthermore, Lewis-acidic non-metal centres have been shown to interact with neutral ligands.

Prime examples are boranes that can interact with donor molecules such as amines to form adduct complexes of the form $R_3B{\leftarrow}NR'_3$, in which the formerly electron-deficient boron atom gains a filled octet of electrons in its valence shell.[12] The larger silicon can bind neutral ligands to form hypervalent species with five- or six-coordinated Si(IV) centres.

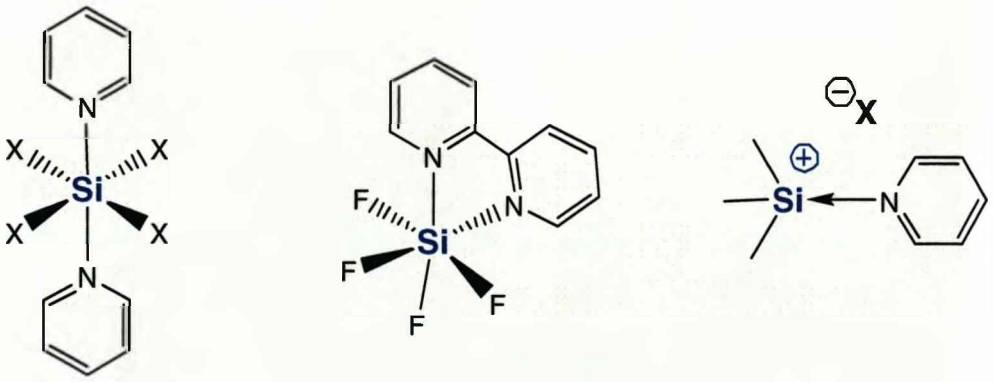

Figure 3.1. Examples of Silicon Species with Neutral Donor Ligands.

Examples are shown in Figure 3.1 and include the octahedral complexes $SiX_4(py)_2$ (X = F[7], Cl[13]), in which pyridine ligands occupy trans positions and the distorted octahedral complex $SiF_4(bipy)_2$, which contains the bidentate chelating ligand 2,2'-bipyridine.[14] In contrast the reactions of trimethylsilyl halides Me_3SiX (X = Br, I) with pyridine generate the cationic complex $[Me_3Si(py)]^+$, rather than forming hypervalent compounds.[15]

When considering N-donor species, particular attention must be paid to 4-dimethylamino pyridine (DMAP). DMAP shows a powerful donating ability towards many species, including phosphorus and carbon centres. It is a much stronger nucleophile than pyridine and so reacts readily with electrophilic phosphorus compounds.[16] In organic chemistry the strong nucleophilicty of DMAP has long been exploited to catalyse acylation reactions.[16-20] The high reactivity of DMAP arises from the electron releasing dimethyl amino group in the *para*-position of the pyridine ring. This introduces a strong mesomeric effect when forming adduct complexes with electrophilic centres E, enabling delocalisation of the positive charge onto the amino group, see Figure 3.2.[16]

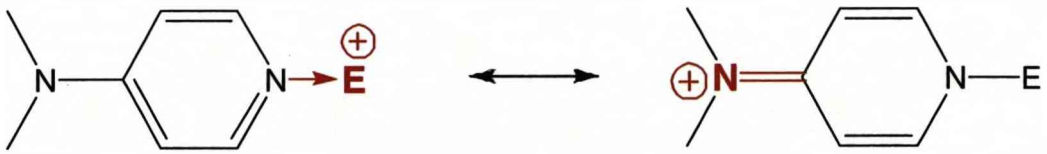

Figure 3.2.

3.1.2. Donor Stabilised Phosphorus Complexes

Phosphorus exhibits a rich coordination chemistry amongst the non-metals. Complex formation with neutral ligands has been widely reported. It mainly occurs by replacement of an anionic leaving group, such as halides and triflate, with nucleophiles, such as pyridine and phosphine ligands, to yield cationic complexes.[21] However, reports of stabilised cyclophosphazene cations are limited to the DMAP coordinated hexacation we report here.[22]

Reported examples mainly focus on organo-phosphorus compounds. In particular, Manners et al. have extensively investigated DMAP stabilised iminophosphorane derivatives, as precursors to phosphazene polymers,[23] while Burford et al. have investigated many phosphorus (III) stabilised complexes.[24] In addition to these there are also examples of N-donor stabilised cations of P-O, P-S and P-halide species.[5,6,25]

3.1.2.1. Phosphorus Halide Complexes

DMAP reacts with phosphorus halides to replace one or more halide ions and generate cationic complexes. For example, Figure 3.3 shows that two chloride ions of PCl_3 are replaced by DMAP ligands when reacted at room temperature to yield the dicationic P(III) complex $[PCl(DMAP)]^{2+}$.[25] Elimination of Cl_2 then forms the monocationic P(I) complex $[P(DMAP)_2]^+$, this occurs either rapidly with heating or slowly at room temperature.[25]

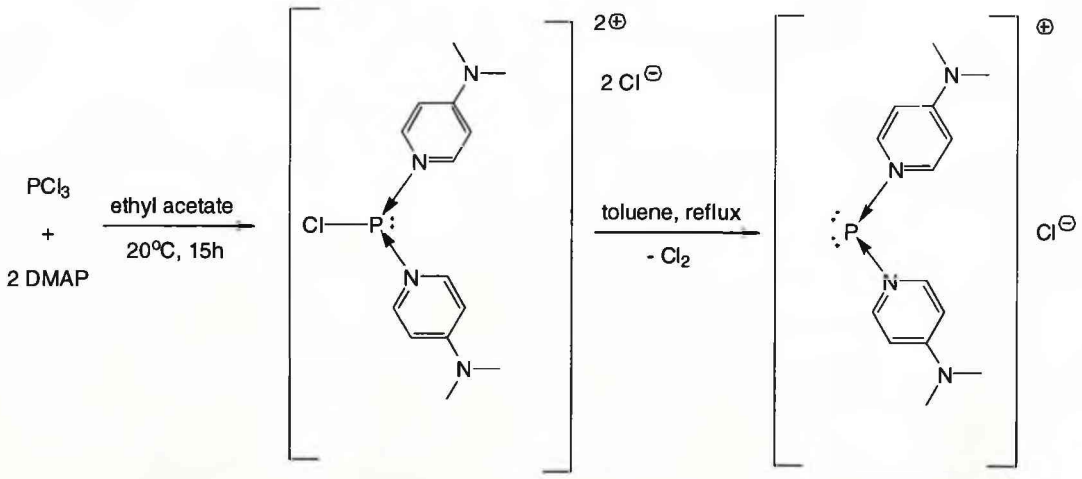

Figure 3.3. Formation of Cationic Complexes from PCl_3 and DMAP.

All three chlorides of PCl_3 can be replaced by the N-donor ligand 1,5-diazabicyclo[4.3.0]non-5-ene (= DBN), see Figure 3.4. However this requires the use of a "transfer agent"; when PCl_3 is reacted with the trimethylsilyl adduct $[DBN{\rightarrow}SiMe_3]OTf$, the tricationic complex $[P(DBN)_3]^{3+}$

is formed. This trication is not observed on the direct reaction of PCl_3 and DBN.[26,27]

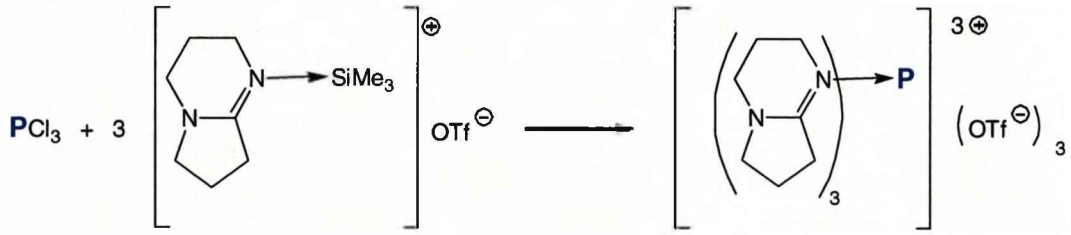

Figure 3.4

Phosphorus pentahalides, PF_5 and PCl_5 generate neutral octahedral complexes of the form py→PX_5 in the presence of pyridine derivatives, as shown in Figure 3.5.[28-31] Reported complexes include those of PF_5 with pyridine[29,31] and of PCl_5 with pyridine[30] and pyrazine,[28] py→PF_5 and pyz→PCl_5 have been characterised by X-ray crystallography.[28,29]

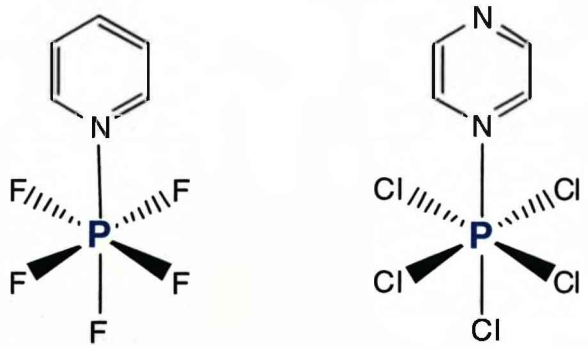

Figure 3.5. Phosphorus Pentahalides with Neutral Donor Ligands.

The phosphoryl halides $POCl_3$ and $POBr_3$ form monocationic dioxophosphonium complexes of the form $[(DMAP)_2PO_2]^+$ with nitrogen donating ligands.[5] $POBr_3$ forms complexes with both pyridine and DMAP, while $POCl_3$ is unreactive to pyridine but forms complexes with DMAP, as shown in Figure 3.6.[5] Monitoring this reaction by ^{31}P NMR revealed that initially the dichloro- monocationic complex $[(DMAP)POCl_2]^+$ forms, this then

reacts further with $POCl_3$ under halogen-oxygen-exchange to yield $[(DMAP)_2PO_2]^+$ and PCl_5 ($POBr_3$ proceeds in an analogous fashion).[5]

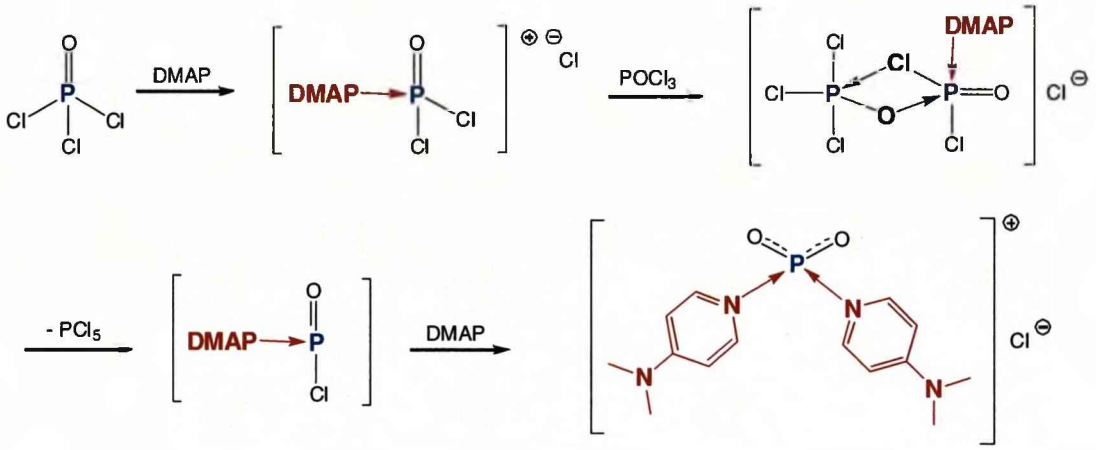

Figure 3.6. $POCl_3$ and DMAP Complex Formation.

The corresponding dithiophosphonium ions $[(py)_2PS_2]^+$ have also been reported. These form by refluxing mixtures of phosphorus halides and P_4S_{10} in pyridine.[6] In the solid state the compounds form salts $[(py)_2PS_2]X$ (X = Cl, Br, I), while in solutions of acetonitrile one pyridine ligand is replaced by a halide counter ion yielding the neutral compound $(py)PS_2X$, see Figure 3.7.[6] The equilibrium between $[(py)_2PS_2]X$ and $(py)PS_2X$ + py shifts progressively to the right for the series I, Br, Cl, which has been attributed to the decreasing basicity of the larger halide ions.[6]

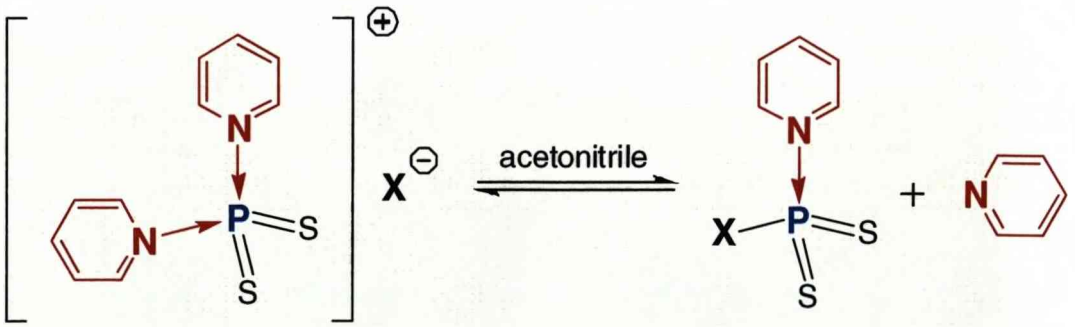

Figure 3.7.

3.1.2.2. Organo-Phosphorus Complexes

3.1.2.2.1. Phosphorus (III)

Coles et al have described bis-guanidine complexes of phosphorus cations. For example, dichlorophenyl phosphine reacts with the bidentate bis-guanidine ligand to give a dicationic chelate complex, as shown in Figure 3.8. The two chloride ions are located directly above the guanidine moieties and are bridged by a dichloromethane molecule via CH...Cl interactions. This shows that polycationic complexes of this kind promise interesting supramolecular structures, in which both anions and solvent molecules play an important structure-directing role. Remarkably, the dicationic complex can act as a ligand towards metal centres via its lone pair at phosphorus. Reaction with dimeric $[PtCl_2PEt_3]_2$ yields the square planar dicationic platinum complex, in which the Pt(II) centre is coordinated by the formally dicationic P(III) centre.[10]

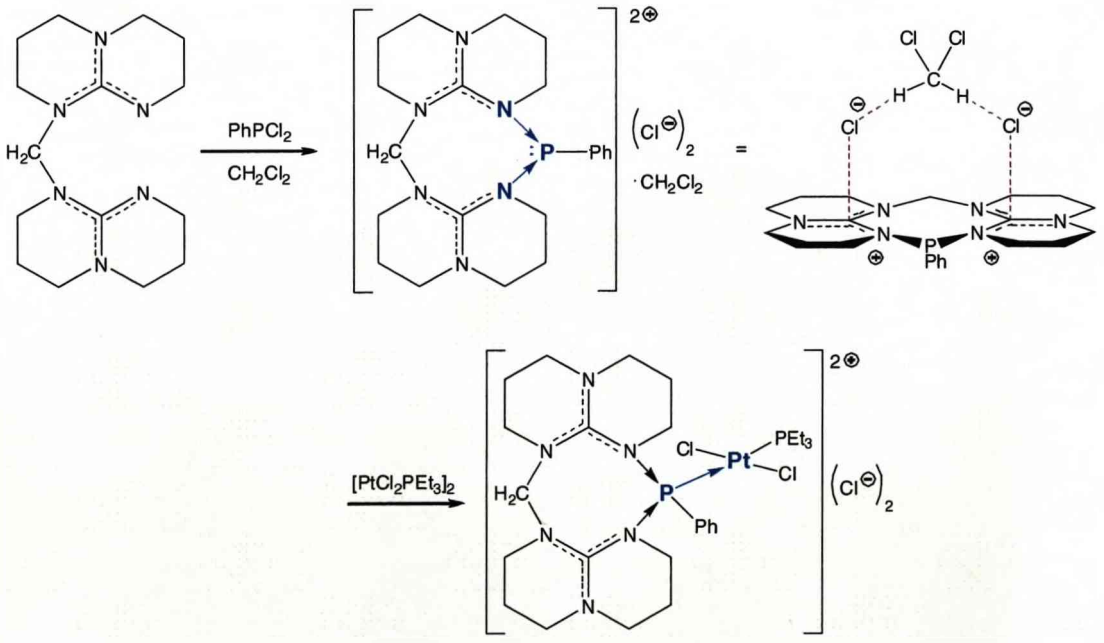

Figure 3.8. Formation of a Phosphine Cation Complexed with bis-Gaunidine.[10]

A number of cations containing organo-phosphorus (III) units, which can be considered as Lewis acid-base adducts have been reported by Burford et

al.[24,32,33] These adducts contain phosphorus (III) as a Lewis acceptor site, to neutral donating ligands and as a three coordinate hypervalent electron rich (lone-pair bearing) centre.[24,32] Various routes have been employed to synthesise these systems, depending on the nature of the parent phosphorus compound.

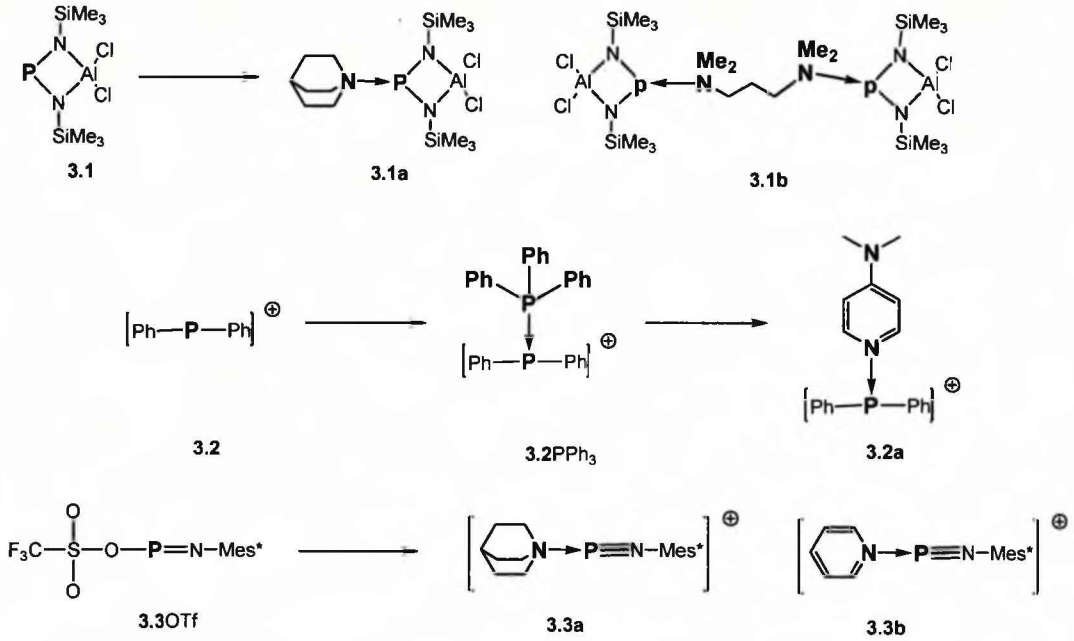

Figure 3.9. Synthetic Routes to Lewis Acid-Base Adducts Containing Organo-Phosphorus (III) Cations.[32]

Species **3.1a – 3.3b** are synthesised by three different methods as shown in Figure 3.9.[32] **3.1a** and **3.1b** form rapidly at room temperature directly from **3.1** and quinuclidine or tetramethylethylene diamaine.[32] **3.2a** forms via the ligand exchange of **3.2**PPh_3 with DMAP, while **3.3a** and **3.3b** form through anion displacement of **3.3**OTf with quinuclidine or pyridine.[32]

The displacement of triflate anions from the imino phosphine, **3.3**OTf, has been used to synthesise a variety of phosphadiazonium cations [R-N≡P]$^+$.[24,32,33] These are shown in Figure 3.10 and include the 1:1 adducts **3.3a-3.3c** and species with two DMAP ligands (**3.3d**), a chelating 2,2'-bipryidine (**3.3e**), a tetramethyl ethylene diamine, (**3.3f**) or a tridentate pentamethyl (**3.3g**) ligand and a bridging 4, 4'- bipyridine (**3.3h**) ligand.[24,32-34]

X-ray crystal structures of these species confirm that the pyridine ligand is coordinated to phosphorus and triflate is merely a counter ion (**3.3c** was observed by ^{31}P NMR and structural parameters were not provided).[24,32]

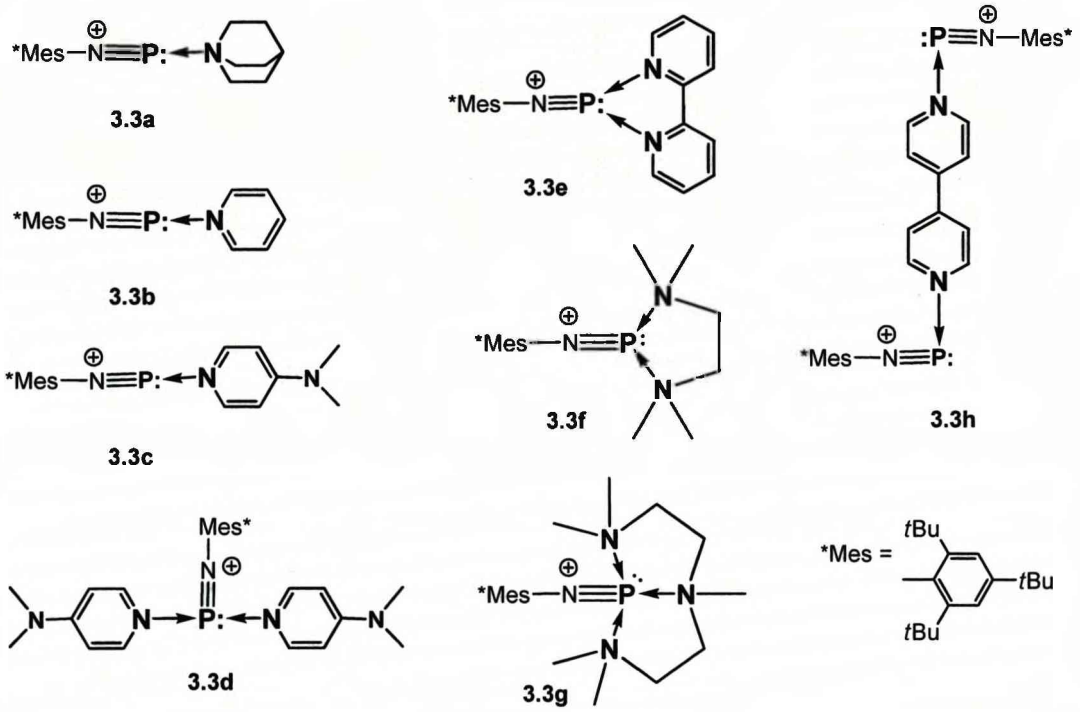

Figure 3.10. Examples of Phosphadiazonium Cations [R-N≡P]$^+$ Stabilised by Nitrogen Donors.

In addition to nitrogen donor systems, **3.3** has also been reported to form adducts with carbenes and phosphines yielding **3.3i**Cl, **3.3i**OTf and **3.3j**, as shown in Figure 3.11.[33,35]

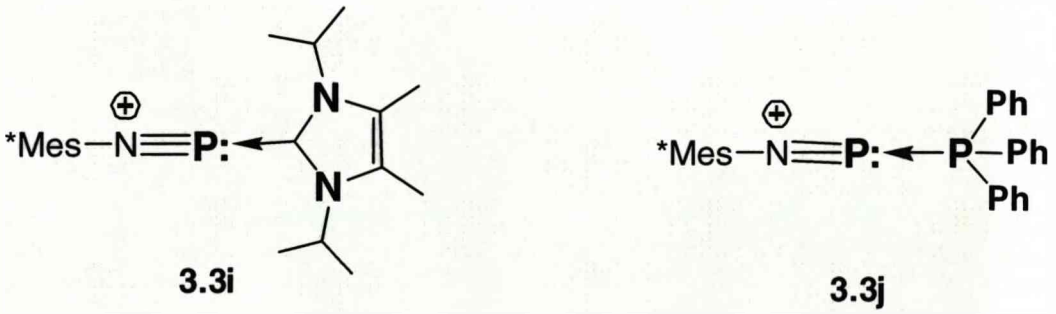

Figure 3.11. Phosphadiazonium Cations [R-N≡P]$^+$ Stabilised by Carbenes and Phosphines.

Cyclodiphosphazanes featuring four-membered P_2N_2 ring systems can be regarded as dimerised iminophosphines R-N=P-X. Large R groups support the monomeric iminophosphine form, where as less bulky R groups maintain the formally dimeric cyclodiphosphazane structure. Burford et al. have carried out anionic displacement of triflate on cyclodiphosphazanes to synthesise mono and dicationic cyclophosphonium adducts of DMAP and PMe_3, **3.4a – 3.4c**, structures shown in Figure 3.12.[36] These compounds could not be synthesised with the Mes* substituent on nitrogen, instead the less sterically demanding DMP (DMP = 2,6-dimethyl phenyl) was required.[36] The dicationic complexes are considered formal dimers of the N-donor-stabilised phosphadiazonium cation, **3.3**, $[R\text{-}N{\equiv}P]^+$.[36]

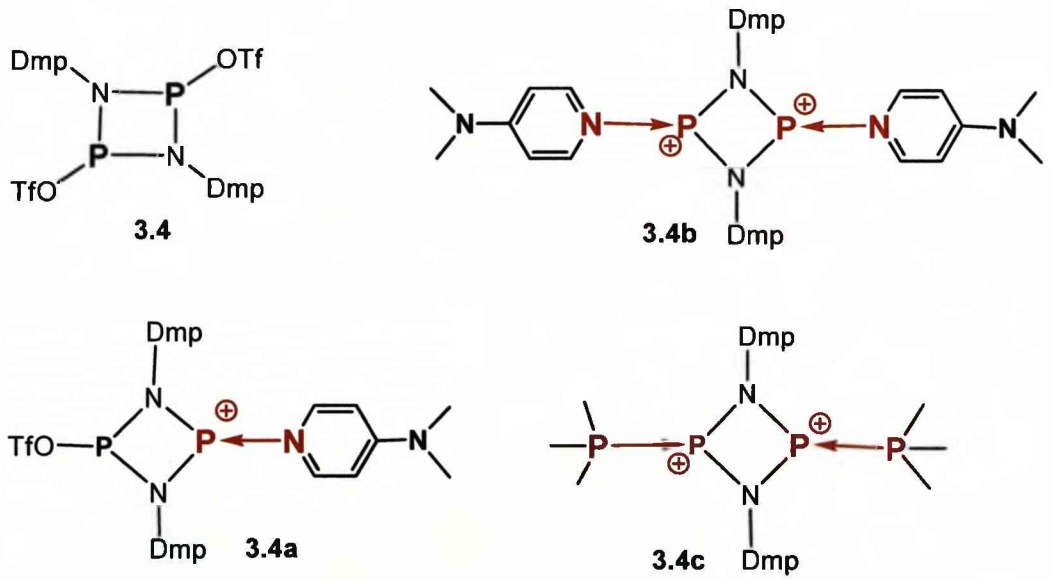

Figure 3.12. Structures of Neutral and Cationic Cyclodiphosphazanes.

3.1.2.2.2. Phosphorus (V)

The monocationic P(III) complex **3.5a**, $[Me_2P{\leftarrow}DMAP]^+$ is obtained by reacting chlorodimethylphosphine with MeOTf in the presence of DMAP.[37] Subsequent quaternisation of **3.5a** with methyl triflate yields the dicationic P(V) complex **3.6a**, $[R_3P{\leftarrow}DMAP]^{2+}$ which exhibits a tetrahedral coordination geometry at phosphorus, see Figure 3.13.[37] This is in contrast to the

phosphorus(III) centre of **3.5a**, which features a trigonal pyramidal environment due to its stereoactive lone pair.[37] An alternative synthetic route to **3.6a** is the chloride ion displacement or ligand exchange of the chlorotrimethylphosphonium ion **3.6** $[Me_3PCl]^+$, by reaction with Me_3SiOTf and DMAP.[37]

The reaction of **3.6a** with excess PMe_3 yields the diphosphonium dication, **3.6b** as DMAP is displaced by a PMe_3 ligand, as shown in Figure 3.13.[37] This illustrates the labile behaviour of DMAP indicative of the coordinating P-N(DMAP) bond.[37]

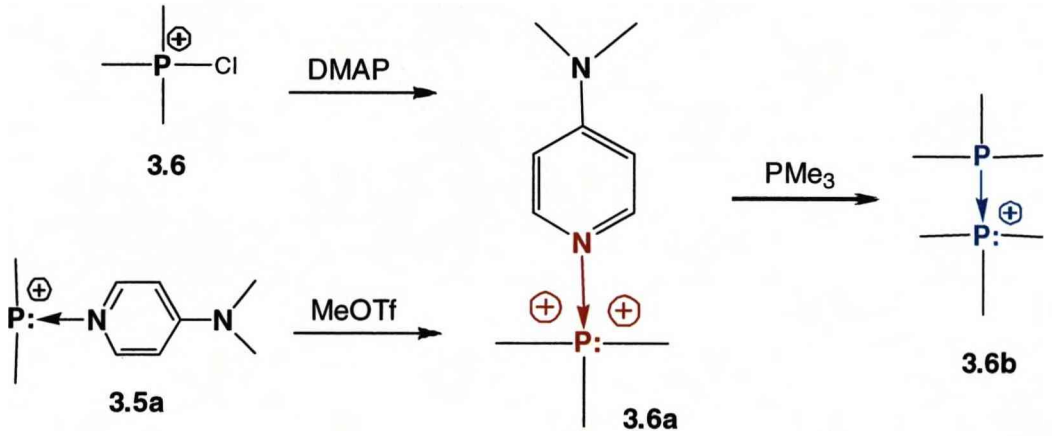

Figure 3.13. Formation of a DMAP Stabilised P(V) Dication and its Reaction with PMe_3.[37]

Niecke et al reported the synthesis and characterisation of DMAP stabilised bis(imino)phosphorus (V) complexes **3.7a** and **3.7b**, shown in Figure 3.14.[38] These adducts formed from the trigonal planar complex **3.7**, $BrP(=NR)_2$, which is stabilised by the bulky R groups 2,4,6-$tBu_3C_6H_2$.[38] The addition of one equivalent of DMAP to **3.7** initially leads to the neutral adduct **3.7a**, $DMAP(Br)P(=NR)_2$.[38] The monocationic bis(imino)phosphorane complex **3.7b**, $[(DMAP)_2P(=NR)_2]^+$, then forms on addition of a second equivalent of DMAP. **3.7b** is isovalent to $[(DMAP)_2PO_2]^+$.[38]

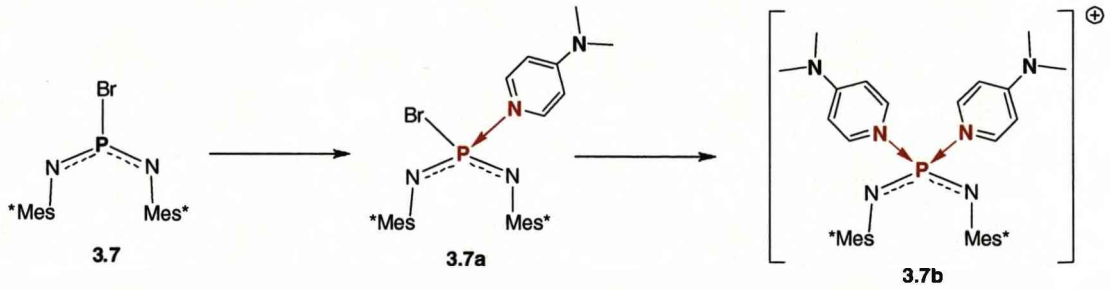

Figure 3.14. Formation of DMAP stabilised bis(imino)phosphorus (V) complexes.[38]

Manners et al have studied the reaction of DMAP with N-silylphosphoanimines, **3.8** in great detail.[23,39,40] Interest in this area arose from investigating alternate routes to polyphosphazenes.

The original method for synthesising polyphosphazenes involves the ring opening polymerization of $N_3P_3Cl_6$.[41] This method, although still investigated and used, has several limitations, in particular inconsistency in the quality of polymer produced.[42] More recently developed methods involve the thermal, fluoride-initiated and living cationic chain growth condensation polymerisation of N-silyliminophosphoranes, **3.8**, $R'_3P{=}NSiR_3$.[23,39,40] Cationic species are thought to be important intermediates in these condensations (see Figure 3.15), for example, $[Cl_3P{=}N{=}PCl_3]^+$ is a cationic initiator in the polymerisation of **3.8a**, $Cl_3P{=}NSiR_3$, catalysed by PCl_5.[23] Cations of the type $[R'_2P{=}NSiR_3]^+$, **3.8**, are proposed as intermediates in the thermal condensation polymerisation of monomers such as **3.8b**, $(CF_3CH_2O)R_2P{=}NSiMe_3$ (where R = alkyl/aryl).[23,39,40]

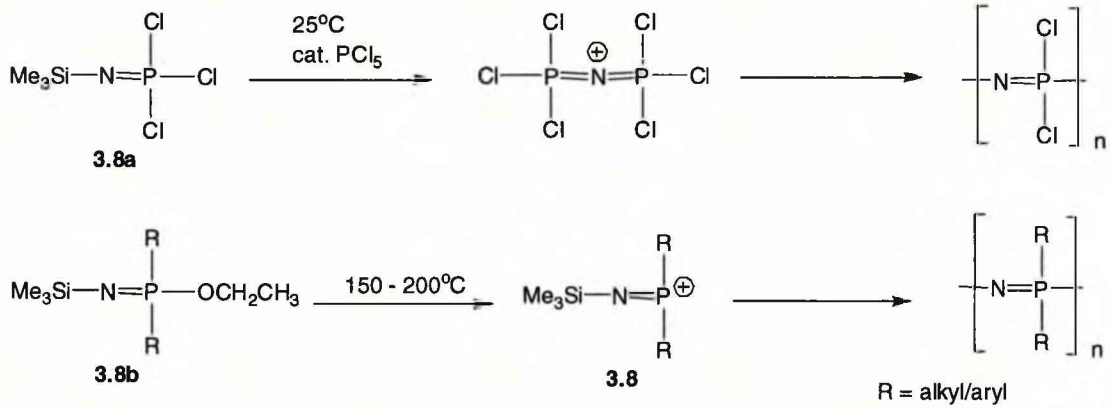

Figure 3.15. Examples of Proposed Cationic Intermediates in Condensation Polymerisations of N-Silyliminophosphoranes.

The cation $[\mathbf{3.8}]^+$ cannot be isolated without a donating ligand; attempts to synthesise the triflate salt [**3.8**]OTf yield only $[NPCl_2]_n$ and Me_3SiOTf.[39] Several salts of the DMAP stabilised cation $[\mathbf{3.8a(DMAP)}]^+$ can be synthesised by dissolving **3.8a** and DMAP in dichloromethane, either with or without a halide abstractor (in the form of the relevant silver salt), as shown below in Figure 3.16.[39]

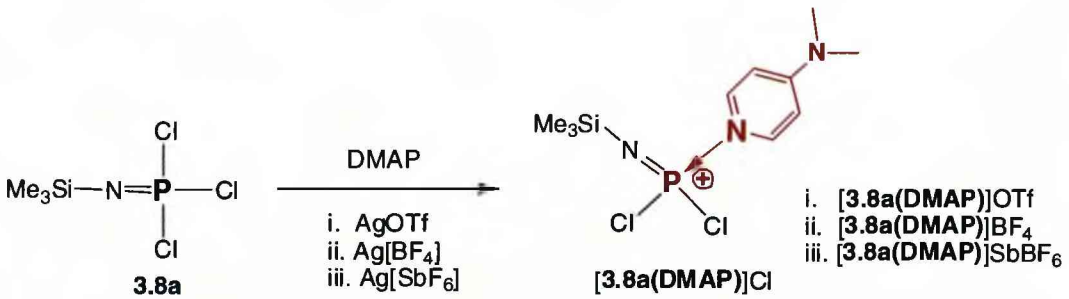

Figure 3.16. Formation of a DMAP Stabilised N-Silyliminophosphorane Cation.

The formation of the chloride salt is reversible, in the solid state [**3.8a(DMAP)**]Cl reverts slowly back to **3.8a**, however on re-addition of solvent the equilibrium shifts back to the cation.[39] The tetrafluoroborate salt, [**3.8a(DMAP)**]BF_4, is also unstable and decomposes to $N_3P_3Cl_6$.[39] Considering that [**3.8a(DMAP)**]SbF_6 is stable, this was attributed to fluoride ion transfer from BF_4^- to $[\mathbf{3.8a(DMAP)}]^+$ leading to the condensation of species such as $FCl_2P{=}NSiMe_3$ (SbF_6^- is relatively stable to fluoride ion transfer[43]).[39]

DMAP stabilised cations of a variety of mono-halide N-silyliminophosphoranes, **3.8c** - **3.8f** (where halide, X = Cl/Br) can also be synthesised, as shown in Figure 3.17.[23] Triflate and halide salts of **[3.8c(DMAP)]**$^+$ - **[3.8f(DMAP)]**$^+$ form by the reaction of their parent mono-halide derivative with DMAP and silver triflate.[23]

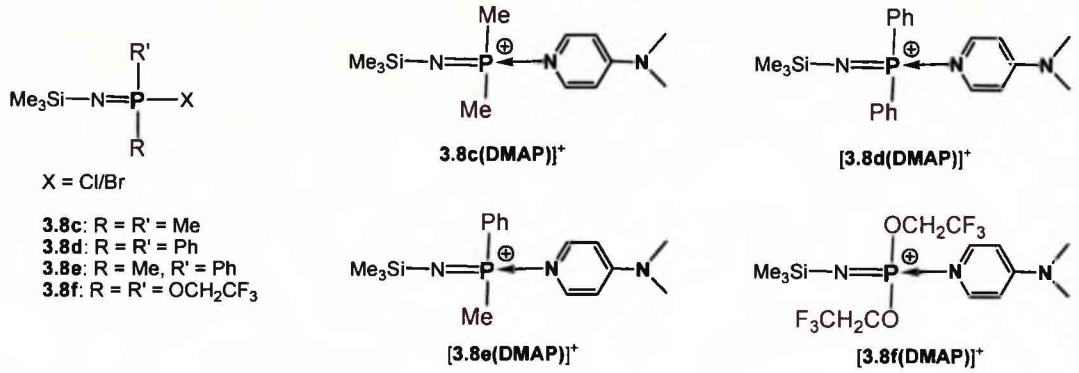

Figure 3.17. Examples of DMAP Stabilised Cations Synthesised from mono-Halide N-Silyliminophosphoranes.

The methyl derivative **[3.8c(DMAP)]**$^+$ forms from both chloro- and bromo-derivatives of **3.8c**.[23] The chloride salt forms reversibly, however conversion back to **3.8c** and DMAP is slow in comparison to **[3.8a(DMAP)]**Cl.[23] The bromide salt does not show any reversabilty.[23] This indicates that the counter ion is key to the stability of the complex.[23] Further evidence for this is that **3.8d** and **3.8e** only undergo partial conversion to the chloride salts **[3.8d(DMAP)]**Cl and **[3.8e(DMAP)]**Cl, whereas the triflate and bromide salts form readily (bromide salt **[3.8e(DMAP)]**Br was not formed due to instability of bromo-**3.8e**)[23] The triflouroethoxy derivative forms stable salts with triflate, bromide and BF_4^- as counter ions **[3.8f(DMAP)]**$^+$.[23] Attempts to synthesise the chloride salt actually yielded a complex with $SO_2 \cdot Cl^-$ as the counter ion, this was attributed to SO_2 as a dissolved byproduct in the preparation of **3.8f**.[23] This complex partially dissociated in solution to give **3.8f** and SO_2·DMAP.[23]

X-ray analysis of **[3.8a(DMAP)]**OTf showed a very short P=N($SiMe_3$) bond distance of 1.490 Å, this is comparable to the distances observed for P≡N

triple bonds in stabilised iminophosphinium cations (1.46 – 1.49 Å)[44,45] and suggests that bonding within the cation has two resonance forms, see Figure 3.18.[39]

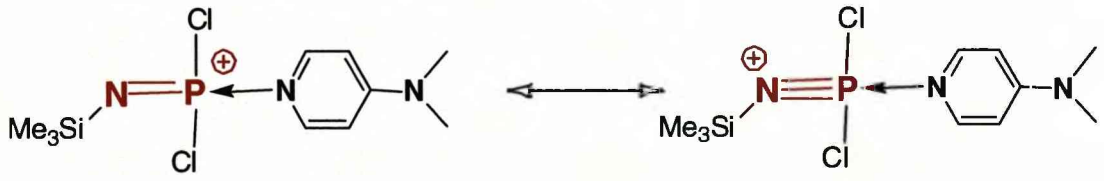

Figure 3.18. Resonance Forms of [3.8a(DMAP)]OTf.[39]

Attempts have also been made to synthesise phosphine stabilised cations **[3.8a(PR$_3$)]$^+$**, [R$_3$P→P(Cl$_2$)=NSiMe$_3$]$^+$.[39] However, these reactions instead produced R$_3$PCl$_2$, R$_3$P=N-PCl$_2$ and Me$_3$SiCl via a series of dechlorination/chlorination condensation steps (R = Ph, ^{n}Bu).[46] Phosphine stabilised N-silylphosphoranimines, can however be synthesised from the mono-halogen species. Figure 3.19 shows the formation of phosphine stabilised methyl derivative, **[3.8c(PR$_3$)]$^+$** and the trifluoroethoxy derivative, **[3.8f(PR$_3$)]$^+$**, as reported by Manners et al.[40,47] Structurally, the phosphine adducts are analogous to the DMAP species. **[3.8c(PMe$_3$)]**Br contains P→P distances (2.2229(11) Å) slightly longer than those of P-P single bonds (2.20 Å) and the P-N bonds (1.533(3) Å) are slightly longer than in the DMAP adduct.[40]

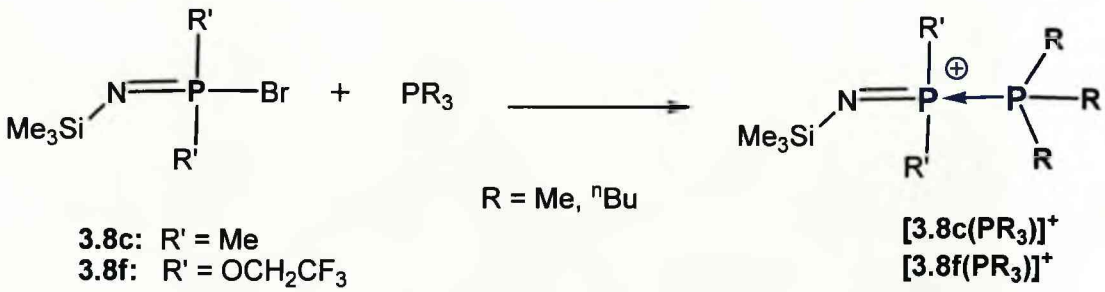

3.8c: R' = Me
3.8f: R' = OCH$_2$CF$_3$

[3.8c(PR$_3$)]$^+$
[3.8f(PR$_3$)]$^+$

Figure 3.19. Formation of Phosphine Stabilised N-Silylphosphoranimine Cations.[47]

3.1.2.2.3. Structural Variations

N-donor complexes of organo-phosphorus (III) compounds have a pyramidal geometry at the phosphorus centre; this is significant as it indicates the presence of a stereochemically active lone pair.[24,32] In contrast to this, phosphorus (V) adducts tend to show a distorted tetrahedral geometry around phosphorus.[37,38]

Donor-complexes of organo-phosphorus cations have P-N(ligand) distances that are somewhat longer than that of P-N single bonds in aminophosphines.[24,32,48] However, amino phosphines are considered to contain a degree of π bonding, as they contain short P-N bonds and often display a planar geometry at nitrogen.[32] There is a slight variation in the P-N(ligand) distances of donor complexes, this is generally dependant on the basicity of the ligand.[24] More basic ligands, such as DMAP give slightly shorter P-N(ligand) distances, see Table 3.1.[24]

A further variation occurs with the mono-DMAP dicationic complex **3.6a**. Here we can clearly see that the P-N distance of **3.6a** is much shorter than the corresponding distance in either, the mono-DMAP cations, **3.2a** and **3.5a**, or the bis-DMAP dication **3.3d**.[37] This can be attributed to the increased positive charge of **3.6a**.[37]

Compound	P-N(ligand) / Å
3.1a[32]	2.038(9)[32]
3.1b[32]	2.110(6)[32]
3.2a[32]	1.789(1)[32]
3.3a[33]	1.933(2)[33]
3.3b[33]	1.958(8)[33]
3.3e[33]	2.065(4); 2.066(4)[33]
3.3d[24]	1.873(2); 1.879(2)[24]
3.3h[24]	1.984(2); 2.025(2)[24]
3.4a[36]	1.774(2)[36]
3.4b[36]	1.775(3)[36]
3.5a[37]	1.801(2)[37]
3.6a[37]	1.720(3)[37]
3.7a[38]	1.815(5)[38]
3.7b[38]	1.830(4); 1.812(4)[38]
[3.8a(DMAP)]OTf[39]	1.713(2)[39]

Table 3.1. P-N(ligand) bond lengths for a variety of donor stabilised complexes
(Values in black and purple are P-DMAP complexes)

3.1.3. DMAP Stabilised Organic Ring Systems

Another p-block element that forms a wide variety of formal N-donor complexes is carbon. Classic examples are alkyl ammonium and pyridinium ions. These compounds are not regarded as N-donor complexes due to the strong covalent character of the resulting carbon-nitrogen bond and their historic classification as organic compounds. However they do show many parallels with the corresponding N-donor stabilised phosphorus compounds.

This is no surprise considering the diagonal relationship of carbon and phosphorus in the periodic Table. Thus in the following, we are reviewing a few characteristic N-donor complexes of carbon that are relevant to this work.

The classic reactions involve the formation of quaternary ammonium and pyridinium salts by treating tertiary amines and pyridines with alkyl halides RX, as shown in Figure 3.20. Quarternization is particularly effective when X is a good leaving group, such as bromide or iodide. Alkyl triflates are even more reactive due to the weakly binding properties of the triflate ion.[49]

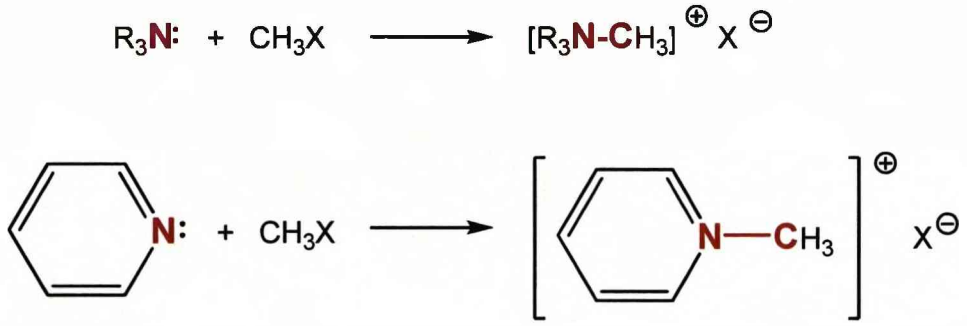

Figure 3.20. Quarternization of Tertiary Amines and Pyridines with Alkylating Agents.

In addition to this, a variety of acyl pyridinium ions have been described. These play an important role as intermediates in acylation reactions of alcohols and amines, which are catalysed by strong nucleophilic pyridines, such as DMAP, see Figure 3.21.[17-20] The initial step is formation of the reactive acyl pyridinium ion, which then reacts with the alcohol to form the ester. An auxiliary base such as triethylamine or sodium carbonate binds the resulting acid HX and removes it from the equilibrium.

Figure 3.21. DMAP Catalysed Acylation of Alcohols.

Poly-N-pyridinium cations form when poly-organohalides are reacted with DMAP. Streitwieser et al. have shown that tetrachloro cyclopropene readily reacts with four equivalents of DMAP under the formation of the corresponding tetra-cation, see Figure 3.22.[50] Further addition of DMAP causes ring opening of cyclopropene to form an open chain tetra-cation with an allylide structure and five DMAP ligands. Heating this compound to 190°C under vacuum gives a tri-cationic indolizine derivative via internal condensation between the allyl moiety and the ortho position of a DMAP ligand.[50-53]

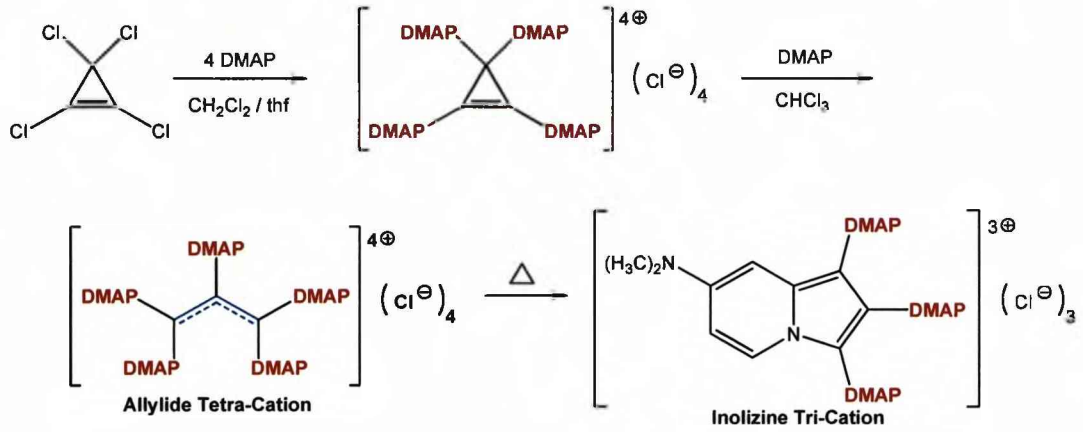

Figure 3.22. The Reaction of Tetrachloro Cyclopropene with DMAP.[50]

Hexachloro cyclopentadiene also reacts with DMAP to form poly-N-pyridinium cations, as shown in Figure 3.23.[54] However, it is less reactive than the cyclopropene derivative. After 4 days refluxing in acetonitrile, hexachloro cyclopentadiene yields a mixture of the fully substituted $[C_5(DMAP)_5]^{4+}$ and the tetra substituted $[C_5Cl(DMAP)_4]^{3+}$. These are obtained in a distribution of 25% and 12%, respectively.[55]

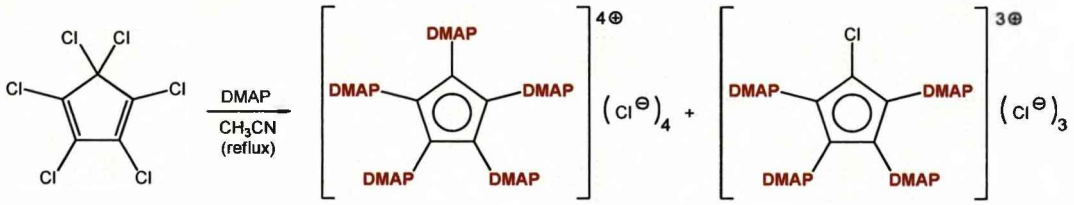

Figure 3.23. The Reaction of Cyclopentadiene with DMAP.[54]

Weiss et al have shown that the C_6 benzene ring can be equipped with six DMAP ligands, when hexafluoro benzene is refluxed with Me_3SiOTf and DMAP in THF for a week, see Figure 3.24.[54] The X-ray structure shows that the pyridine rings of the DMAP ligands are twisted by 80° with respect to the central C_6 ring plane. The salt $[C_6(DMAP)_6](OTf)_6$ is inert towards aqueous bases at room temperature, but hydrolyses when refluxed 0.1M $NaHCO_3$ solution to form the tetracation $[(DMAP)_5C_6O]^{4+}$ in which one DMAP ligand has been replaced by an oxo group, as shown in Figure 3.24.[54]

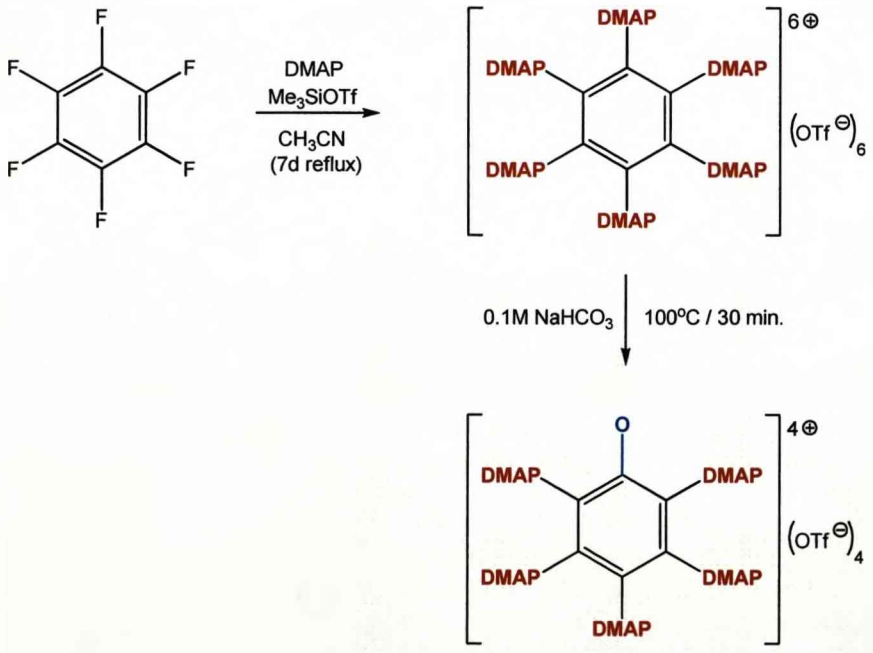

Figure 3.24.[54]

Using a similar synthetic protocol, the corresponding naphthalene and *p*-benzoquinone cations $[C_{10}(DMAP)_8]^{8+}$ and $[C_6O_2(DMAP)_4]^{4+}$ were prepared, see Figure 3.25.[56,57] The largest molecular cation of this type is the

tetraphenyl porphyrin which carries 20 DMAP ligands and has a charge of +20, see Figure 3.26.[58] The four phenyl groups are twisted by 70-80° relative to the porphyrin ring and the DMAP ligands by a similar angle relative to the phenyl groups. As a result, two large cavities are formed above and below the porphyrin ring structure. Both are filled with a triflate ion. The other triflate ions reside in peripheral cavities between DMAP ligands.

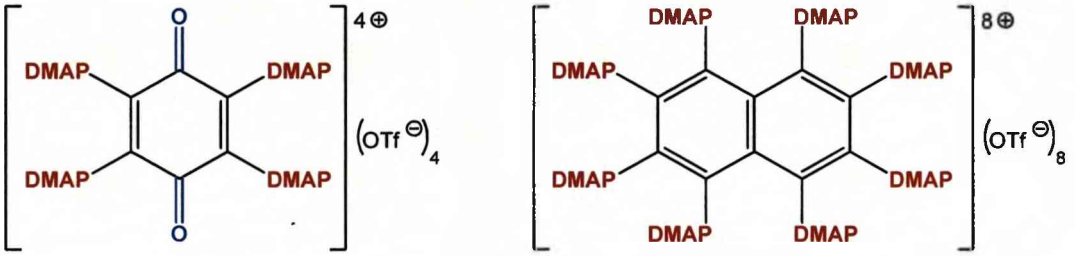

Figure 3.25.

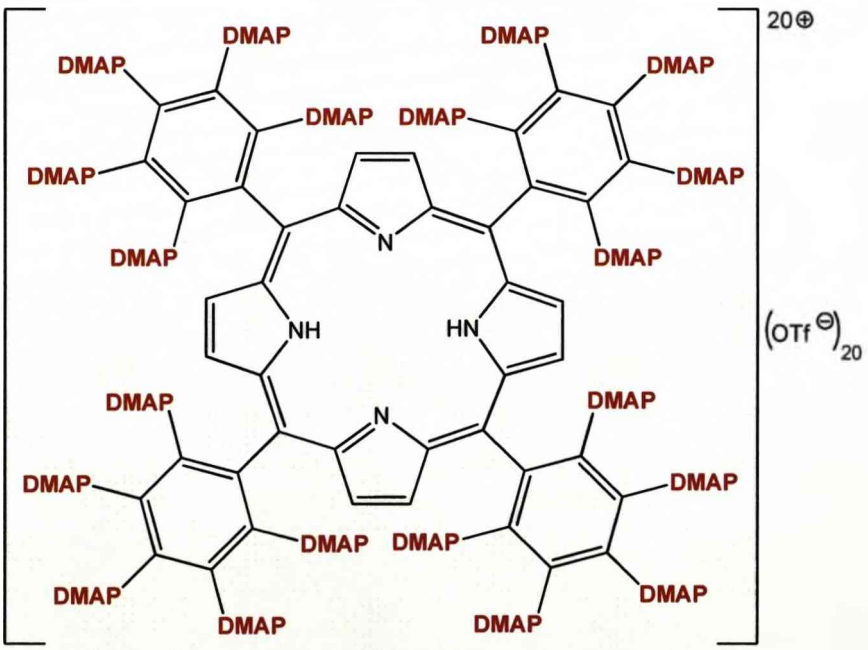

Figure 3.26.

The similar chemical behaviour of 1,3,5-cyclotriazenes, $C_3N_3X_3$ and cyclotriphosphazenes $P_3N_3X_6$ nicely illustrates the diagonal relationship of carbon and phosphorus in the periodic Table.[59] Cyanuric trichloride $C_3N_3Cl_3$

resembles in many ways $P_3N_3Cl_6$. Its chlorines can be substituted with a variety of other groups with retention of the ring structure. Also the basicity of the ring nitrogens of $C_3N_3X_3$ is very similar to those in the corresponding phosphazenes $P_3N_3X_6$. However, while the P_3N_3 ring of cyclophosphazenes is non-aromatic due to the tetrahedral phosphorus centres, the C_3N_3 ring of triazenes is aromatic owing to the planar character of the ring carbon atoms.

A number of star-shaped N-donor complexes of the 1,3,5-cyclotriazene have been described, see Figure 2.27.[60,61] These were prepared by reaction of the trichloride $C_3N_3Cl_3$ with a variety of pyridine derivatives. These complexes show high optical nonlinearities together with an excellent transparency, which make these compounds of promising interest for nonlinear optical applications whereby the multipolar character of the chromophores is of particular importance.[60,61]

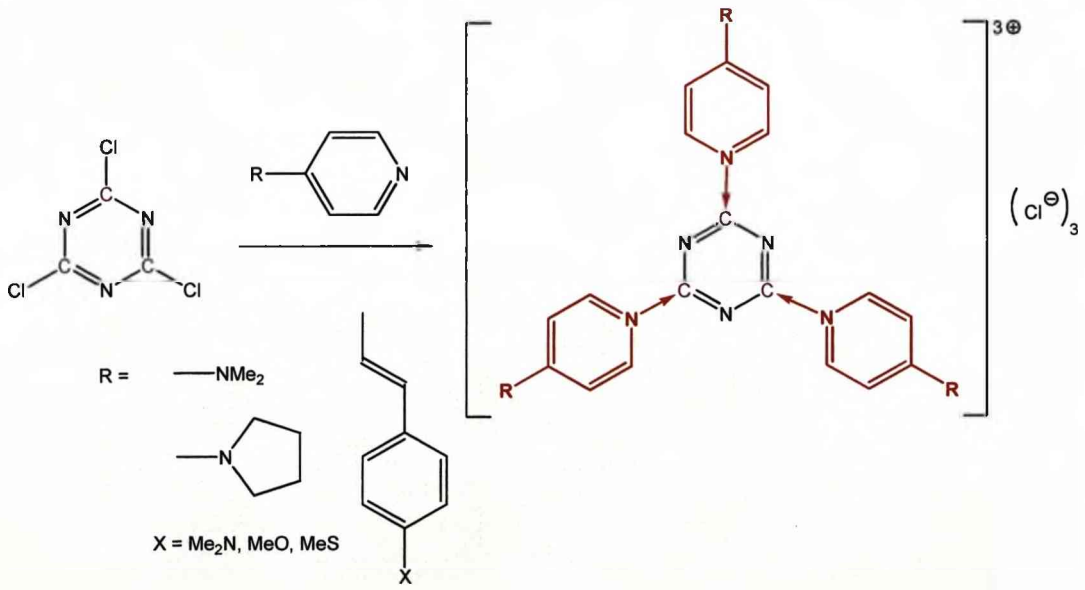

Figure 3.27. Nitrogen Donor Complexes of 1,3,5-Cyclotriazene.

3.2. Results and Discussion

3.2.1. The Hexacation $[N_3P_3(DMAP)_6]^{6+}$ (3.9)[22]

As outlined above, the strongly nucleophilic DMAP has been shown to stabilise a variety of phosphorus complexes. Thus we have chosen DMAP as the prime candidate for the generation of cyclophosphazene based polycations. The proposed synthesis of the hexa-cationic $[N_3P_3(DMAP)_6]^{6+}$ is shown below in Figure 3.28.

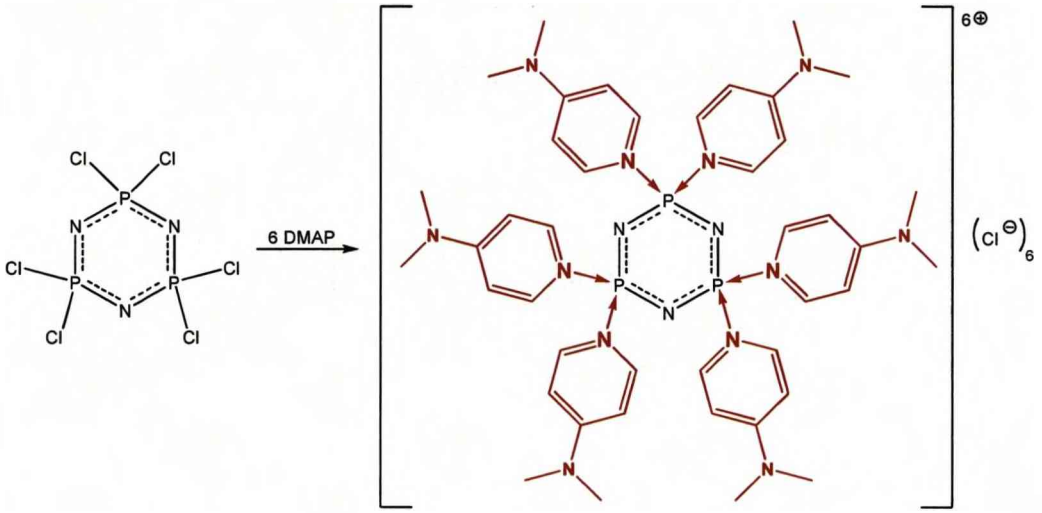

Figure 3.28. Proposed Synthesis for the Hexa-Cationic $[N_3P_3(DMAP)_6]^{6+}$.

In an earlier report Vapirov et al. claimed they had produced $[N_3P_3(DMAP)_6]^{6+}$ simply by mixing solutions of $N_3P_3Cl_6$ and DMAP in toluene. They analysed the resulting precipitate by IR and elemental analysis as well as argentometric titrations of the hydrolysed product. The authors concluded from the data that they had obtained a salt of composition $[N_3P_3(DMAP)_6]Cl_6$.[62] We repeated the procedure using the same protocol as outlined by Vapirov and found that the combined toluene solution becomes turbid instantaneously producing a colourless precipitate. The precipitate was filtered, washed with toluene and dried under vacuum. The elemental analysis of the resulting powdery material did not match the proposed structure (and also not the analysis given in the report). The solid state $^{31}P\{^1H\}$ MAS-NMR spectrum of the product is shown below in Figure 3.29

and consists of a number of broad undefined signals that cover a wide range of chemical shifts. The sharp signal at 19.6 ppm is due to unreacted $N_3P_3Cl_6$. Evidently under the conditions described it can be assumed that the reaction is leading to premature precipitation of partially substituted products of composition $[N_3P_3Cl_{6-x}(DMAP)_x]Cl_x$. In a separate paper, Vapirov and co-workers also claimed to have prepared the hexapyridine adduct $[N_3P_3(py)_6]^{6+}$. This was apparently achieved by adding an excess of pyridine to $N_3P_3Cl_6$. However, when we repeated the reaction we could not find any evidence of adduct formation. We found that $N_3P_3Cl_6$ simply dissolves in pyridine without reaction. The $^{31}P\{^1H\}$ NMR of this solution shows a single resonance at $\delta = 21.3$ due to unreacted $N_3P_3Cl_6$.

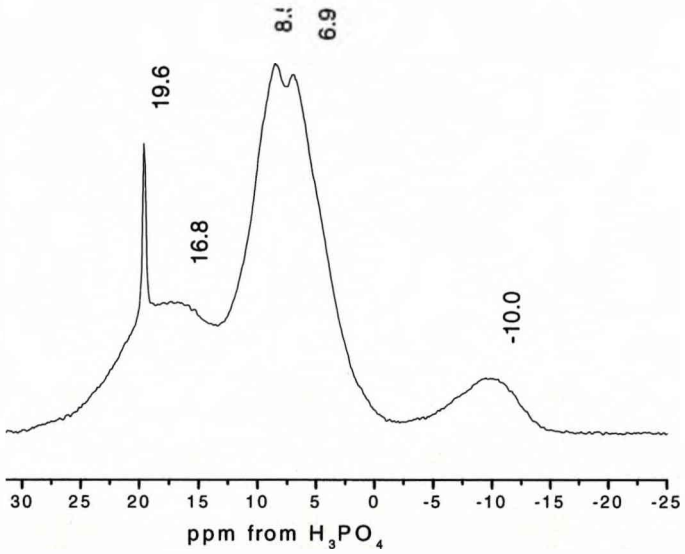

Figure 3.29. $^{31}P\{^1H\}$ MAS-NMR of the Product Obtained from the Reaction of $N_3P_3Cl_6$ and DMAP in Toluene.

3.2.1.1. The Solvate $[N_3P_3(DMAP)_6]Cl_6 \cdot 19\ CHCl_3$[22]

The reaction between hexachlorocyclotriphosphazene, $N_3P_3Cl_6$ and DMAP proceeds rapidly in chloroform as well as other common non-protic solvents yielding colourless precipitates that proved to be insoluble in common solvents and showed similarly indistinct $^{31}P\{^1H\}$ MAS-NMR spectra. The progressive substitution with DMAP ligands increases the charge of the ion,

which eventually becomes too polar to remain soluble in a non-protic solvent. On the other hand, more polar protic solvents, such as water and alcohols, are reactive towards $P_3N_3Cl_6$ forming hydroxides and alkoxides, respectively, and thus cannot be used in the synthesis of the desired complexes

The premature precipitation in chloroform can be circumvented in two ways: (1) the entire reaction mixture must be kept in solution until the reaction has reached completion, (2) the concentration of reactants must be kept at a minimum throughout the duration of the reaction. Method (1) involves superheating a solution of $N_3P_3Cl_6$ in chloroform to 100°C for 20 min. in a microwave reactor. The crystalline product consists of thin plates, which rapidly degrade in the absence of mother liquor due to loss of solvent. In method (2) crystals of $N_3P_3Cl_6$ and DMAP are carefully covered with chloroform. Leaving the mixture undisturbed for 24 h, yields large colourless prisms, see Figure 3.30.

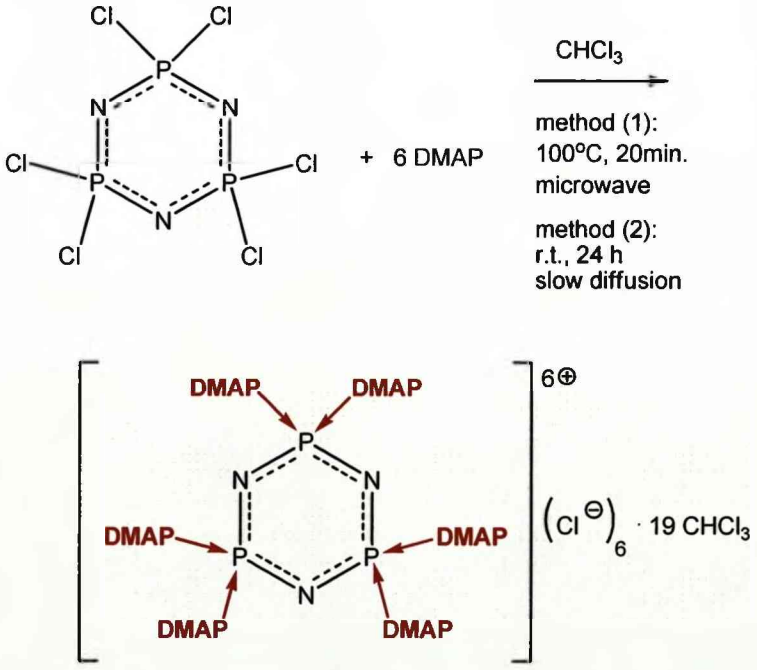

Figure 3.30. Formation of $[N_3P_3(DMAP)_6]6Cl^-\cdot 19CHCl_3$.

The crystals obtained from methods (1) and (2) were both suitable for single crystal X-ray diffraction and showed the same crystal structure with an overall composition of $[N_3P_3(DMAP)_6]Cl_6 \cdot 19\ CHCl_3$. In the crystal structure (space group $P2_1/n$) the hexacation $[N_3P_3(DMAP)_6]^{6+}$ occupies a general position in the asymmetric unit and has approximate D_{3h} symmetry. The planar phosphazene ring is equipped with six DMAP ligands, which are bound to the phosphorus centres. The $DMAP_3$ arrangements at either side of the P_3N_3 ring form basket type cavities. The hexacation provides suitable binding pockets for five chloride ions (Figure 3.31), which are held in close proximity due to strong ion pairing interactions. Each basket composed of three DMAP ligands accommodates one chloride ion. The shortest contacts between the basket-contained chloride ions and the hexacation are towards the P-bonded nitrogen centres of the DMAP ligands with an average N...Cl distance of 3.31 Å. Three chloride ions occupy the equatorial positions around the ring. Each of the three chlorides is held by a tetradentate binding site consisting of four *ortho*-H atoms of the DMAP ligands. The sixth chloride ion in [**3.9**]$Cl_6 \cdot 19CHCl_3$ connects the methyl groups of two DMAP ligands resulting in a networked structure (Figure 3.32). The C-H...Cl interactions between the DMAP ligands and the chloride ions range between 2.6 and 3.1 Å (for H...Cl distances) and 3.5 and 4.0 Å (for C...Cl distances).

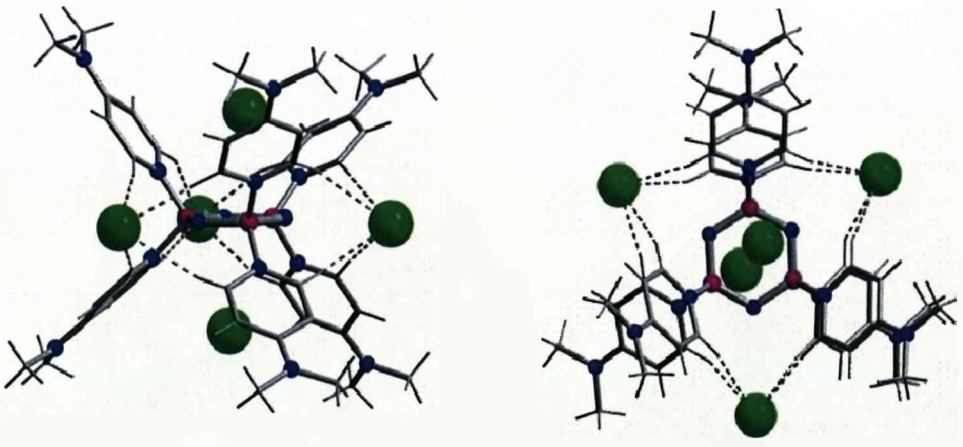

Figure 3.31. Crystal Structure of $[N_3P_3(DMAP)_6]Cl_6 \cdot 19CHCl_3$
- showing two views of the $([N_3P_3(DMAP)_6]Cl_5)^+$ unit.

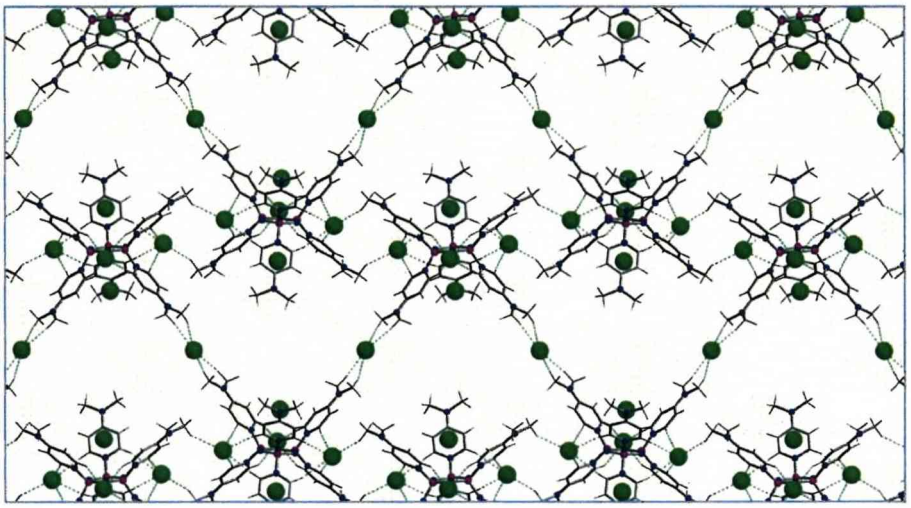

Figure 3.32. Crystal Structure of $[N_3P_3(DMAP)_6]Cl_6 \cdot 19CHCl_3$
- showing the network of ions.

The solvent accessible volume of **[3.9]**$Cl_6 \cdot 19CHCl_3$ amounts to 71%. It is occupied by nineteen molecules of chloroform per $[P_3N_3(DMAP)_6]Cl_6$ unit, seventeen of which are engaged in coordinating the six chloride ions. Figure 3.33 shows that the $([P_3N_3(DMAP)_6]Cl_5)^+$ assembly is effectively complexed by thirteen chloroform molecules; the two chlorides hosted in the baskets bind three $CHCl_3$ molecules each, while the equatorially located chlorides bind two and three solvent molecules, respectively. The sixth, bridging chloride ion is coordinated by four chloroform molecules. Some chloroform molecules are affected by disorder. However, the disorder could be resolved and a suitable model with rational $Cl_3CH...Cl^-$ contacts obtained. The C-H...Cl interactions between the chloroform molecules and chloride ions are somewhat shorter that the chloride-DMAP C-H...Cl contacts. They cover a range of 2.4 to 2.7 Å (for H...Cl distances) and of 3.3 to 3.6 Å (for C...Cl distances). In addition, there are two lattice bound chloroform molecules per formula unit that are not coordinated to chloride ions.

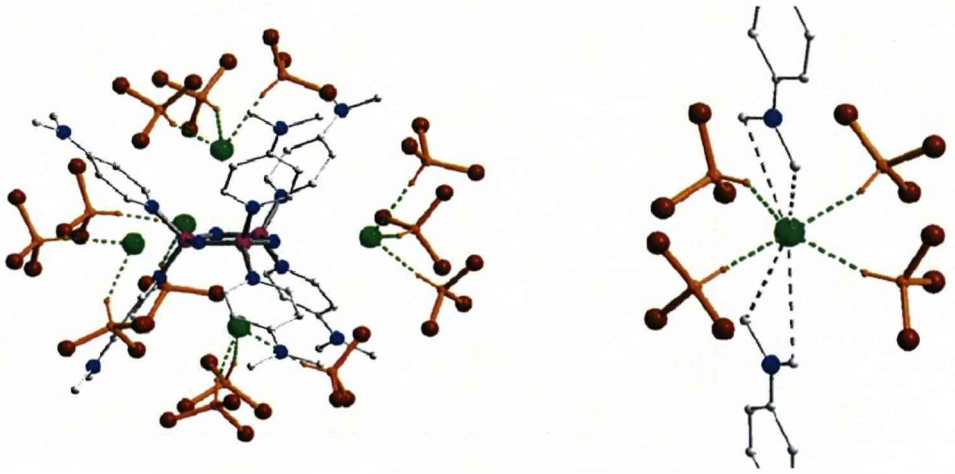

Figure 3.33. Crystal Structure of $[N_3P_3(DMAP)_6]Cl_6 \cdot 19CHCl_3$
- illustrating the coordination of chloroform molecules.

Filtration and vacuum treatment of [**3.9**]$Cl_6 \cdot 19CHCl_3$ produces a colourless powder that decomposes at 200°C.‡ It dissolves in 1,1,2,2-tetrachloroethane exhibiting a single resonance at δ = 10.3 ppm in the ^{31}P NMR spectrum. The ^{1}H NMR of the solution shows around five equivalents of chloroform per formula unit, which gives an overall composition of $[P_3N_3(DMAP)_6]Cl_6 \cdot 5CHCl_3$. The $^{31}P\{^{1}H\}$ MAS NMR of the solid consists of a sharp signal at δ = 6.7 ppm, while the ^{1}H-^{13}C CP/MAS NMR spectrum verifies the presence of chloroform and mirrors the ^{13}C resonances of the DMAP ligands observed in solution, see Figure 3.34. The thermogravimetric analysis (TGA), sown in Figure 3.35, correlates well with the loss of five chloroform and six DMAP molecules from $[P_3N_3(DMAP)_6]Cl_6 \cdot 5CHCl_3$ when heated above 260°C, leaving a residual weight that corresponds to $PNCl_2$. Below 260°C the TGA trace displays a gradual weight loss. It lacks distinct steps suggesting the absence of the pure desolvated $[P_3N_3(DMAP)_6]Cl_6$ at any given temperature during the heating process. The weight loss accelerates at around 200°C, at which point the sample weight corresponds to $[P_3N_3(DMAP)_6]Cl_6 \cdot CHCl_3$.

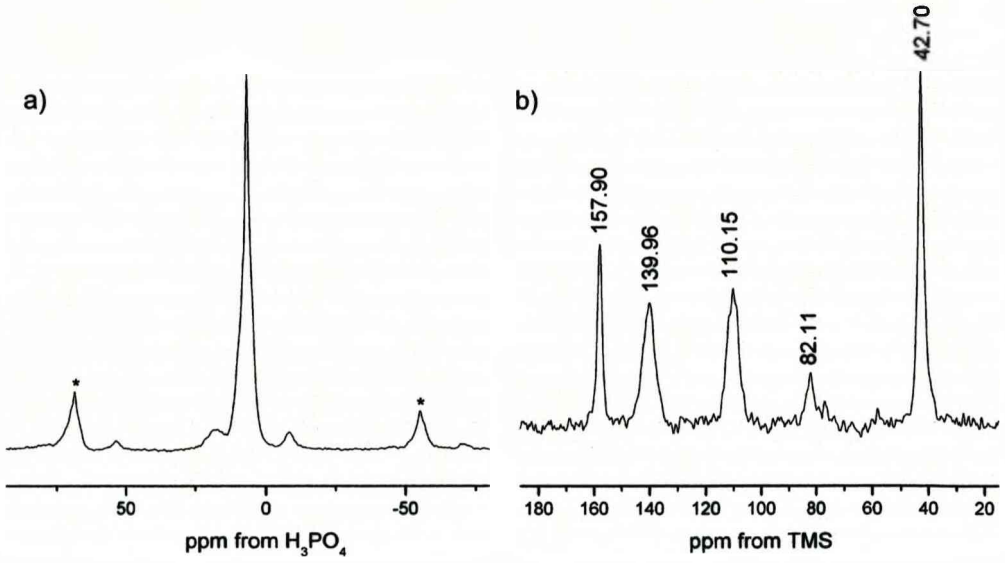

Figure 3.34. Solid State NMR Spectra of $[N_3P_3(DMAP)_6]Cl_6 \cdot 5CHCl_3$

(a) 31P{1H} MAS NMR (6.7 ppm), (b) 1H-13C CP/MAS NMR (CH3 42.70, CHCl3 82.11, meta-C 110.15, ortho-C 139.90, para-C 157.90 ppm). Both spectra were recorded at a spinning rate of 10 kHz. * Denotes spinning side bands.

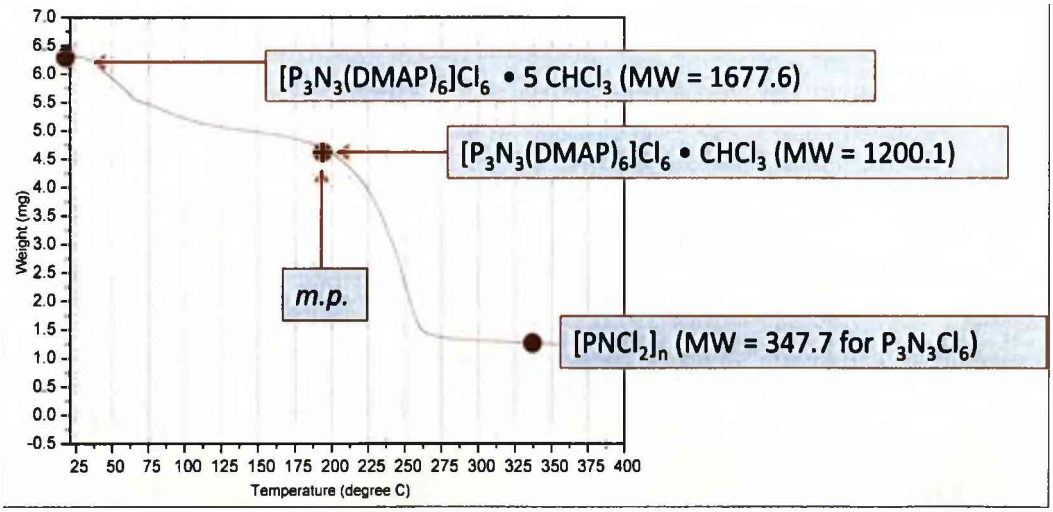

Figure 3.35. Thermogravimetrical Analysis of $[N_3P_3(DAMP)_6]Cl_6 \cdot 5CHCl_3$

3.2.1.2. The Solvate $[N_3P_3(DMAP)_6]Cl_6 \cdot 11\ CH_2Cl_2$

The slow diffusion experiment was repeated with dichloromethane in order to establish the role of the solvent in the assembly of salt networks of $[N_3P_3(DMAP)_6]Cl_6$. Crystals of $N_3P_3Cl_6$ and DMAP were carefully covered with dichloromethane. DMAP dissolves faster in dichloromethane than in

chloroform, thus crystal growth commences instantly. Colourless crystals were obtained, which also loose solvent rapidly when exposed to air. The X-ray crystal structure revealed that the compound crystallises in space group $P2_1/m$ with eleven molecules of dichloromethane per formula unit.

The solvate $[N_3P_3(DMAP)_6]Cl_6 \cdot 11\ CH_2Cl_2$ contains less solvent than the chloroform solvate, with a solvent accessible volume of 54.5%. As a result the ions form a denser lattice, which is now networked in 3 dimensions via CH...Cl contacts, as shown in Figure 3.36. In contrast to the $CHCl_3$ solvate, only one of the $DMAP_3$ baskets is occupied by a chloride ion. Three chloride ions reside in the tetradentate coordination sites of the ortho-CH positions as observed in the chloroform solvate. The remaining two chloride ions are bound to the periphery of the hexacation, binding to both meta-CH positions and methyl groups. Together with the equatorially located chloride ions, they connect neighbouring hexacations resulting in a 3D network structure. It should be noted that the basket-hosted chloride ion is closer to the P_3N_3 ring (Cl...ring centroid = 3.113 Å) than it is in the chloroform solvate, in which both $DMAP_3$ baskets accommodate a chloride ion (Cl...ring centroid = 3.307 and 3.239 Å).

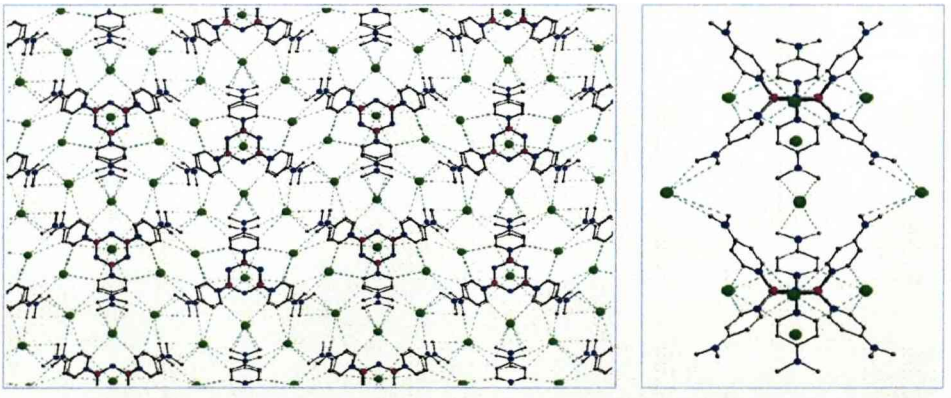

Figure 3.36. Network of Ions in the Crystal Structure of $[N_3P_3(DMAP)_6]\cdot 11CH_2Cl_2$

One interesting feature of the solvate structure of $[N_3P_3(DMAP)_6]Cl_6\cdot 11\ CH_2Cl_2$ is that the hexacations are stacked upon each other in eclipsed fashion. As a result two $DMAP_3$ baskets are facing each other connected via three chloride ions, see Figure 3.37. This arrangement generates a large

spherical void with a diameter of 8 Å (taking into account the Vander Waals radii of bordering atoms). The void is filled with the basket-hosted chloride ion and four dichloromethane molecules. While three CH_2Cl_2 molecules are bound to the chloride ion via CH...Cl contacts, the fourth molecule occupies the other $DMAP_3$ basket. It should be noted that this arrangement of solvent molecules is disordered across the crystallographic mirror plane. However, it was possible to model the disorder by splitting atoms over two positions.

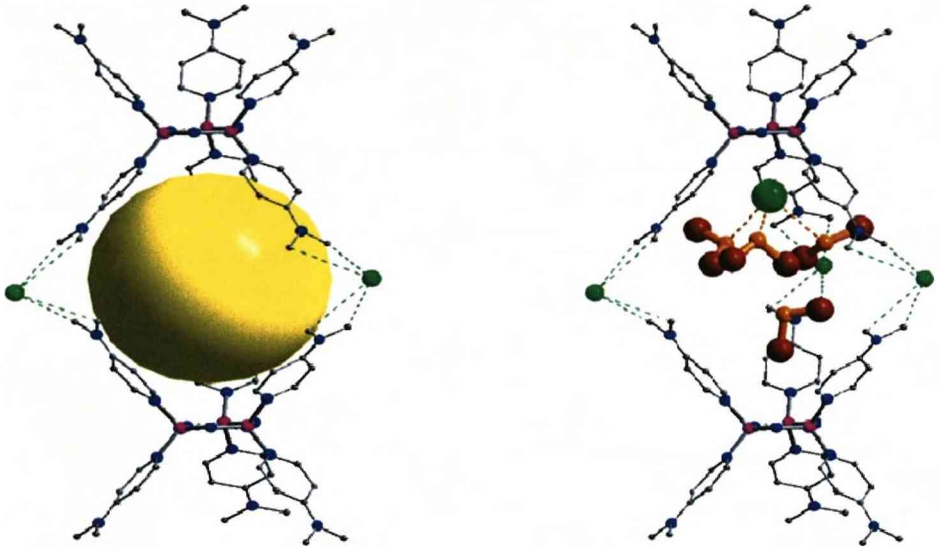

Figure 3.37. Crystal Structure of $[N_3P_3(DMAP)_6]Cl_6 \cdot 11CH_2CH_2$

- showing the large void encompassed by two $DMAP_3$ baskets (left) and the arrangement of one chloride ion and four dichloromethane molecules inside the void.

While four dichloromethane molecules occupy the "inner sphere" as described above, the seven remaining solvent molecules reside in the "outer sphere" of $[N_3P_3(DMAP)_6]Cl_6 \cdot 11CH_2Cl_2$. All seven molecules act as bridging ligands, each coordinating two chloride ions (Figure 3.38). The result is a coordination chain of composition $[(CH_2Cl_2)_7(Cl^-)_5]_\infty$ which consists of four-membered $[(CH_2Cl_2)_2(Cl^-)_2]$ and six-membered $[(CH_2Cl_2)_3(Cl^-)_3]$ ring structures that are connected via CH_2Cl_2 molecules to form the chain structure. The atom positions of the seven bridging dichloromethane molecules are well defined showing no disorder.

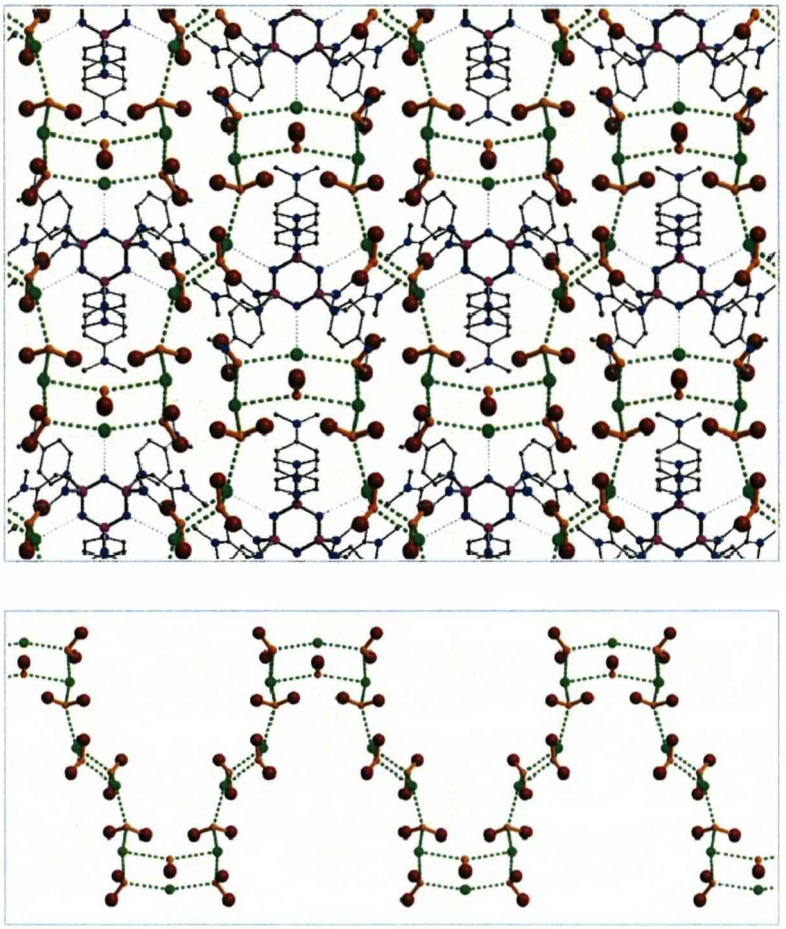

Figure 3.38. Crystal Structure of $[N_3P_3(DMAP)_6]Cl_6 \cdot 11CH_2Cl_2$

-exhibiting the coordination polymer of chloride ions and dichloromethane molecules.

3.2.1.3. Mixed Solvates of $[N_3P_3(DMAP)_6]Cl_6$

The diversity of the solvate structures of $[N_3P_3(DMAP)_6]Cl_6$ suggests that the solvent plays a structure-directing role. Chloroform possesses one electropositive proton and thus acts as a monodentate ligand in the presence of chloride ions, whereas dichloromethane features two protons and is able to bind two chloride ions in a bridging fashion.

Figure 3.339.

In both the solvate structures chloroform and dichloromethane form mostly well-defined non-disordered C-H...Cl interactions and C-H...Cl angles that are fairly linear (< 150°), see Figure 3.39. An earlier survey of C-H...anion contacts gives average values of 2.39(3) Å for the H...Cl distance and 3.42(2) Å for C(H)...Cl distance for chloroform and 2.53(3) Å and 3.57(3) Å for dichloromethane.[63] These values compare well with those measured in the solvate structures of $[N_3P_3(DMAP)_6]Cl_6$.

The topic of anion binding has received great attention, particularly in the field of ion sensors.[64-68] However, the coordination chemistry of anions with solvent molecules has been largely neglected. In general, chloroform and dichloromethane are being regarded as non-polar solvents. On the other hand, both solvents dissolve many salts containing organic cations and halide ions and a range of solvate structures featuring CH...anion contacts have been described. For example, a survey of the Cambridge Structure Database (CSD)[69,70] revealed that there are 161 crystal structures that contain chloride ions that are coordinated by chloroform.[71] They show various coordination modes with one chloride ion coordinated to 1 (70 structures), 2 (47 structures), 3 (30 structures), 4 (8 structures), 5 (1 structure) and 6 (5 structures) $CHCl_3$ molecules. In the case of 6-fold coordination the chloride ions are effectively shielded in an octahedral coordination environment, while the counter ions consist of large spherical cations with a non-polar surface.[72] The structures with lower coordination numbers show additional ion pairing as observed in $[N_3P_3(DMAP)_6]Cl_6 \cdot 19\ CHCl_3$ where the chloride ions bind to the hexacation and in addition to either two, three or four chloroform molecules. Thus the chloroform molecules are effectively shielding an otherwise exposed chloride anion. Another CSD

search showed that there are 239 crystal structures with interactions between chloride ions and dichloromethane molecules, 60 of these show the bridging mode.

In order to probe the structure directing factor of the solvent, the preparation of mixed solvates was attempted. Crystals of $P_3N_3Cl_6$ and DMAP (6 equivalents) were covered with a 1:1 mixture of chloroform and dichloromethane. Single crystals were obtained from two batches. One was kept at room temperature (A), while the other was stored at 4°C (B). Table 3.2 lists the crystal data together with the data of the single solvent systems $[N_3P_3(DMAP)_6]Cl_6 \cdot 19\ CHCl_3$ and $[N_3P_3(DMAP)_6]Cl_6 \cdot 11\ CH_2Cl_2$. The crystal data of (A) are very similar to those of $[N_3P_3(DMAP)_6]Cl_6 \cdot 11\ CH_2Cl_2$, while those of (B) closely resemble those of $[N_3P_3(DMAP)_6]Cl_6 \cdot 19\ CHCl_3$.

A careful assessment of the crystal structure of (A) revealed the same spatial arrangement of ions as $[N_3P_3(DMAP)_6]Cl_6 \cdot 11CH_2Cl_2$. The only difference between the two structures is the replacement of one dichloromethane molecule that is bound to the basket-hosted chloride ion by a chloroform molecule (Figure 3.40), which gives (A) the formula $[N_3P_3(DMAP)_6]Cl_6 \cdot 10CH_2Cl_2 \cdot CHCl_3$. As a result the volume per formula unit (V/Z) increases by 20 $Å^3$, which equates to the difference in volume of chloroform and dichloromethane (the molecular volumes of crystalline chloroform[73] and DCM[74] are 82.1 and 103.8 $Å^3$, respectively, this gives a difference of about 20 $Å^3$)

The chloride bound array of one chloroform and two dichloromethane molecules is disordered across the crystallographic mirror plane. However, an adequate model was obtained by splitting atom positions, see Figure 3.40b. The overall coordination of solvent molecules is not affected by the substitution, since the "inner sphere" solvent molecules are bound in monodentate fashion. The "outer sphere" of (A) shows the same bridging coordination as in $[N_3P_3(DMAP)_6]Cl_6 \cdot 11CH_2Cl_2$.

	[3.6]Cl_6·19$CHCl_3$	[3.6]Cl_6·11CH_2Cl_2	Crystals (A) (r.t.)	Crystals (B) (4°C)
a (Å)	19.961(5)	14.033(3)	13.972(4)	20.306(5)
b (Å)	26.652(7)	23.091(5)	23.207(7)	26.116(6)
c (Å)	25.801(6)	14.953(3)	15.023(5)	25.396(6)
α (deg)	90.00	90.00	90.00	90.00
β (deg)	93.004(4)	115.309(4)	114.855(5)	94.002(5)
γ (deg)	90.00	90.00	90.00	90.00
V ($Å^3$)	13707	4380	4420	13434
Space group	$P2_1/n$	$P2_1/m$	$P2_1/m$	$P2_1/n$
Z	4	2	2	4
V/Z ($Å^3$)*	6854	4380	4420	6717
V_{sol} **	71.0%	54.5%	55.0%	70.4%

Table 3.2. Crystal Data of $CHCl_3$, CH_2Cl_2 and Mixed Solvates of $[P_3N_3(DMAP)_6]Cl_6$

* Volume of formula unit $[P_3N_3(DMAP)_6]Cl_6$·solvent

** Solvent accessible volume (calculated using PLATON)

The ionic arrangement of (B) is iso-structural to that of $[N_3P_3(DMAP)_6]Cl_6$·19 $CHCl_3$. Large parts of the solvent sphere are severely disordered, while eight chloroform molecules are not affected by disorder. The disordered part could not be modelled sufficiently, thus a reliable sum formula could not be obtained. In the absence of mother liquor the crystals rapidly degrade due to solvent loss prohibiting the accurate determination of solvent content by other methods of analysis. However the spatial arrangement of anions does not allow for bridging coordination modes. Despite this, the decrease in unit cell volume indicates contamination with dichloromethane. The reduction in volume amounts to 137 $Å^3$ per formula unit, which would equate to the replacement of 6-7 $CHCl_3$ molecules with CH_2Cl_2.

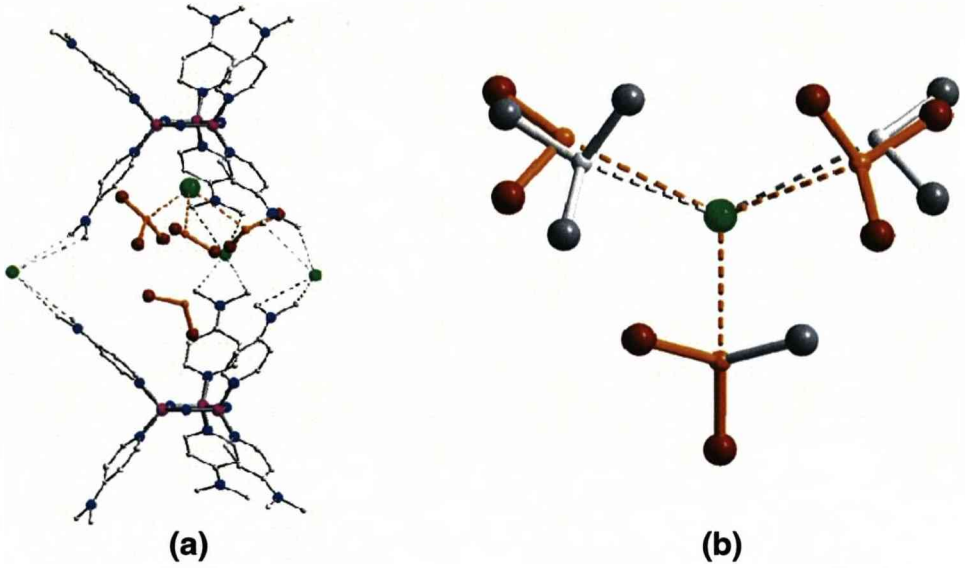

Figure 3.40. Crystal Structure of $[N_3P_3(DMAP)_6Cl_6 \cdot 10CH_2Cl_2 \cdot CHCl_3$

- showing the disorder of the inner-void arrangement consisting of one chloroform and two dichloromethane molecules coordinated to a chloride ion.

3.2.1.4. $[N_3P_3(DMAP)_6]Cl_6$ in 1,1,2,2-Tetrachloroethane

Other chlorohydrocarbon solvents that were tested included 1,1,2,2-tetrachloroethane (TCE), this is also used in the synthesis of $N_3P_3Cl_6$ from PCl_5 and NH_4Cl, as we discussed in Chapter 2. It was found that TCE dissolves $[N_3P_3(DMAP)_6]Cl_6 \cdot 5CHCl_3$ cleanly. When a mixture of $N_3P_3Cl_6$ and DMAP are dissolved in TCE an exothermic reaction occurs yielding a pale yellow solution. The $^{31}P\{^1H\}$ NMR taken from the reaction solution displays a single peak at δ = 10.3 ppm. The *ortho*-H nuclei of the hexacation display a characteristic low field shift of δ = 9.8 in the ^1H NMR indicative of the coordination of DMAP to electrophiles. Addition of chloroform to this solution followed by hexane leads to the precipitation of a colourless solid. Several washings with chloroform and subsequent treatment in vacuum produces $[N_3P_3(DMAP)_6]Cl_6$, as a white powder that melts at 200°C. It contains about five equivalents of chloroform per formula unit and traces of 1,1,2,2-tetrachloroethane as indicated by ^1H NMR. The $^{31}P\{^1H\}$ MAS NMR is

identical to that of $[N_3P_3(DMAP)_6]Cl_6 \cdot 5\ CHCl_3$ giving a chemical shift of δ = 6.7 ppm.

The hexacation decomposes very slowly in TCE at room temperature (> 1 week) and rapidly at elevated temperatures. The decomposition was accompanied by the formation of crystals, which formed at the surface of the solution upon cooling. These were identified as the salt [DMAPH]Cl·TCE. The decomposition reaction proved to be clean and quantitative. The $^{31}P\{^1H\}$ NMR spectrum of the heated solution consisted of a sole signal at δ = 21.3 indicating the formation of $N_3P_3Cl_6$, while its ^1H NMR spectrum showed a signal at δ = 6.4 due to the emergence of trichloroethylene. $N_3P_3Cl_6$ was extracted from the mixture with *n*-hexane, crystallised and structurally characterised. Hence, the formation of $[N_3P_3(DMAP)_6]Cl_6$ from $N_3P_3Cl_6$ and DMAP appears to be fully reversible. Evidently, HCl is eliminated from TCE and protonates the DMAP ligands, this then allows the chloride ions to re-connect to the phosphorus centres. This is summarised in the Figure 3.41 below showing the formation and decomposition of the hexacation in TCE.

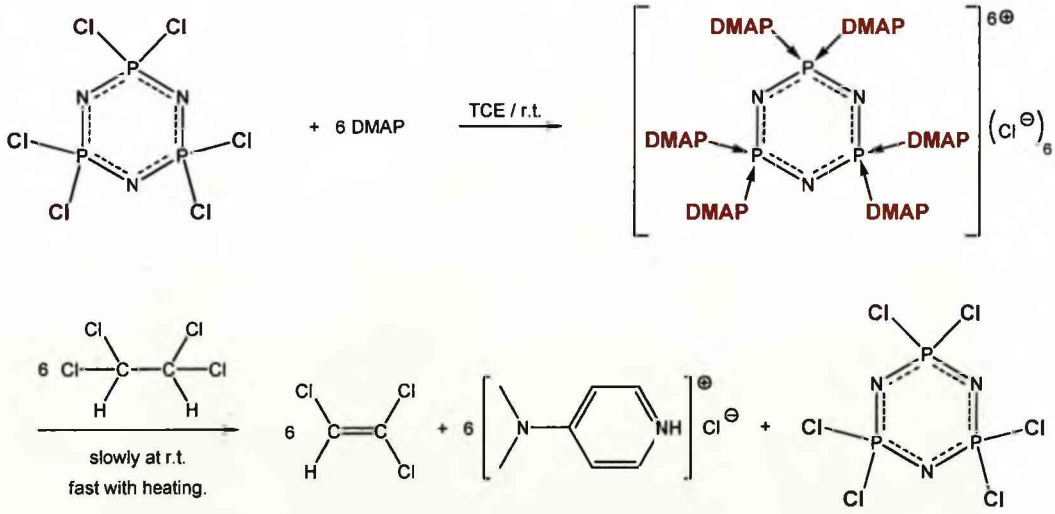

Figure 341.

Colourless single crystals of the product were obtained, prior to decomposition, by the addition of chloroform to the reaction solution followed

by gas phase diffusion of *n*-hexane into the mixture. The X-ray structure analysis showed that the crystals consist of the mixed solvate $[N_3P_3(DMAP)_6]Cl_6 \cdot (CHCl_3)_x \cdot (TCE)_y$. It was not possible to establish the exact solvent content due to the severe disorder of solvent molecules. A total of three chloroform and two TCE molecules per formula unit could be located in the solvent accessible regions. The remaining electron density could not be modelled adequately. The SQUEEZE routine in PLATON[75] was used for removing the contributions of the unaccounted disordered solvent from diffraction intensities in order to improve the refinement of ordered parts within the structure. As a result, the $[N_3P_3(DMAP)_6]^{6+}$ ion and the chloride ions refined well.

The compound crystallises in space group Cm; a crystallographic mirror plane bisects the hexacation perpendicular to the N_3P_3 ring. One $DMAP_3$ basket is occupied by a chloride ion, while the other basket accommodates a TCE molecule, which is disordered across the crystallographic mirror plane. Again, the *ortho*-H atoms of the DMAP ligands offer three tetradentate binding sites for chloride ions at equatorial positions. The two remaining chloride ions are hosted in the upper rim of one basket via *meta*-H atoms and methyl groups. Both ions interact with the TCE molecule hosted in the basket via CH...Cl contacts (Figure 3.42). In addition, there are close CH...Cl contacts from chloride ions, both from equatorial sites and the upper rim, towards methyl groups of neighbouring $[N_3P_3(DMAP)_6]Cl_6$ arrangements, which results in a 2D-network structure, see Figure 3.43.

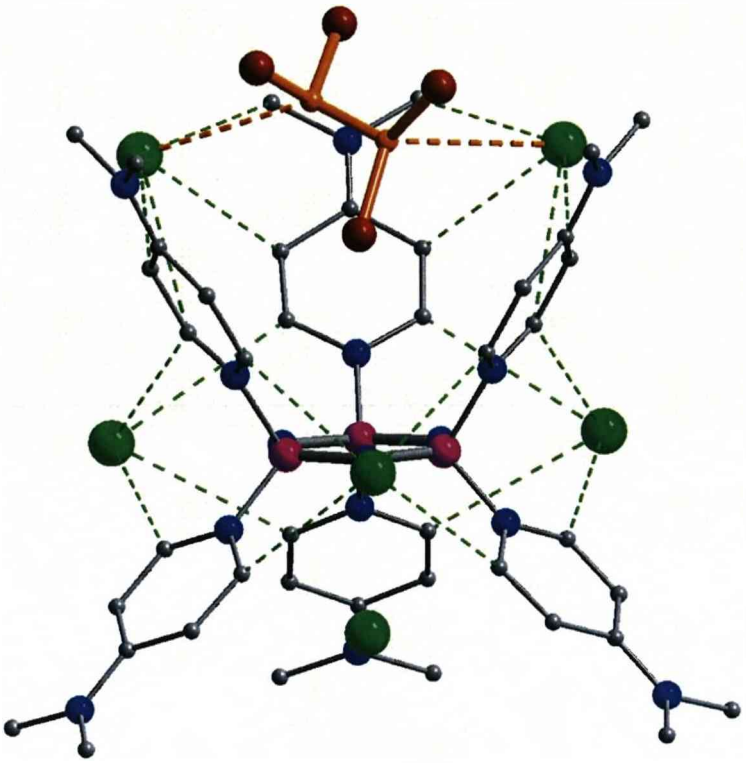

Figure 3.42. Crystal Structure of $[N_3P_3(DMAP)_6]Cl_6 \cdot (CHCl_3)_x \cdot (TCE)_y$.

- solvent molecules are omitted, except for the TCE molecule residing in one basket.

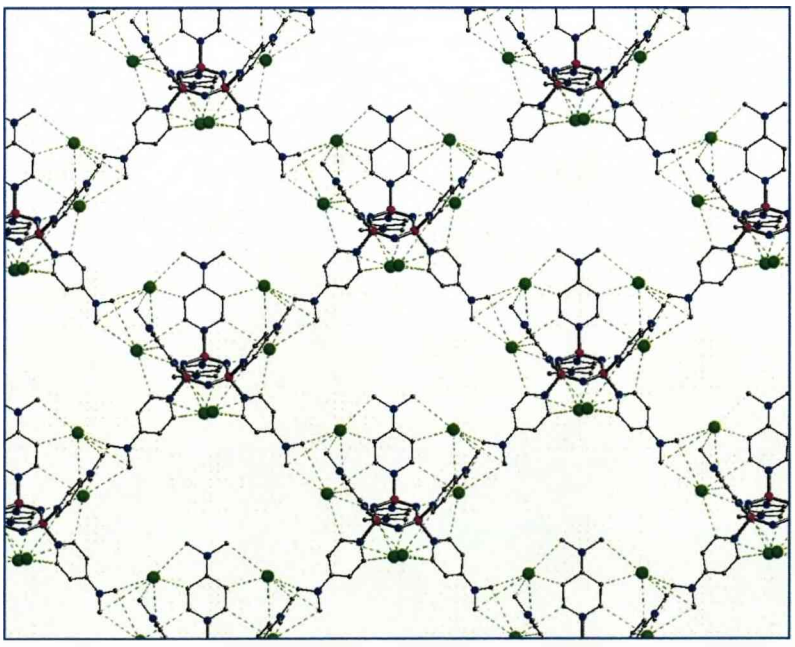

Figure 3.43. Crystal Structure of $[N_3P_3(DMAP)_6]Cl_6 \cdot (CHCl_3)_x(TCE)_y$.

- showing the network of hexacations and chloride ions. Solvent molecules are omitted.

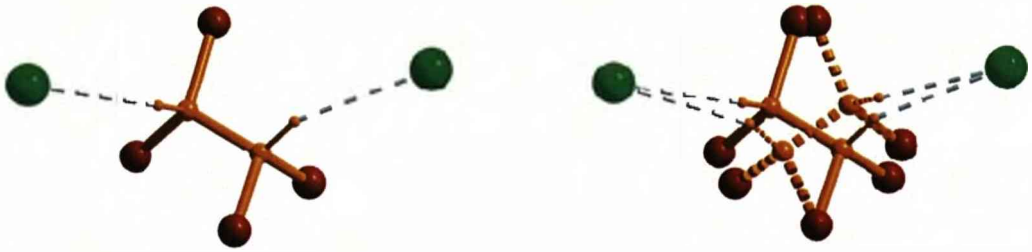

Figure 3.44. Bridging Mode of TCE Molecules and the Associated Disorder.

3.2.1.5. The Mixed Ion Derivative $[N_3P_3(DMAP)_6]Cl_4I_2$

The presence of other anions in the reaction of $P_3N_3Cl_6$ with DMAP was investigated. The iodide salt $[Bu_4N]I$ is well suited for this experiment due to its good solubility in chloroform. Crystals of $P_3N_3Cl_6$ and DMAP were covered with a solution of $[Bu_4N]I$ in chloroform. Within one day colourless crystals were growing at the glass wall of the container. Again, the crystals are prone to solvent loss in the absence of a solvent atmosphere. The X-ray structure determination revealed the formation of the mixed ion species $[N_3P_3(DMAP)_6]Cl_4I_2 \cdot 14CHCl_3$. The compound crystallises in space group P1 with two hexacations in the asymmetric unit. The familiar hexacation accommodates one chloride ion in one of the $DMAP_3$ baskets, while the other basket hosts a chlorofrom molecule. Again, three chloride molecules occupy the tetradentate ortho-H binding sites in equatorial positions. The two iodide ions occupy the upper rim of the $DMAP_3$ basket. This arrangement of ions resembles that of $[N_3P_3(DMAP)_6]Cl_6 \cdot (CHCl_3)_x \cdot (TCE)_y$. with the difference that the two upper rim positions are filled by iodide ions. Overall there are fourteen chloroform molecules per hexacation, which coordinate to both chloride and iodide ions, as shown in Figure 3.45.

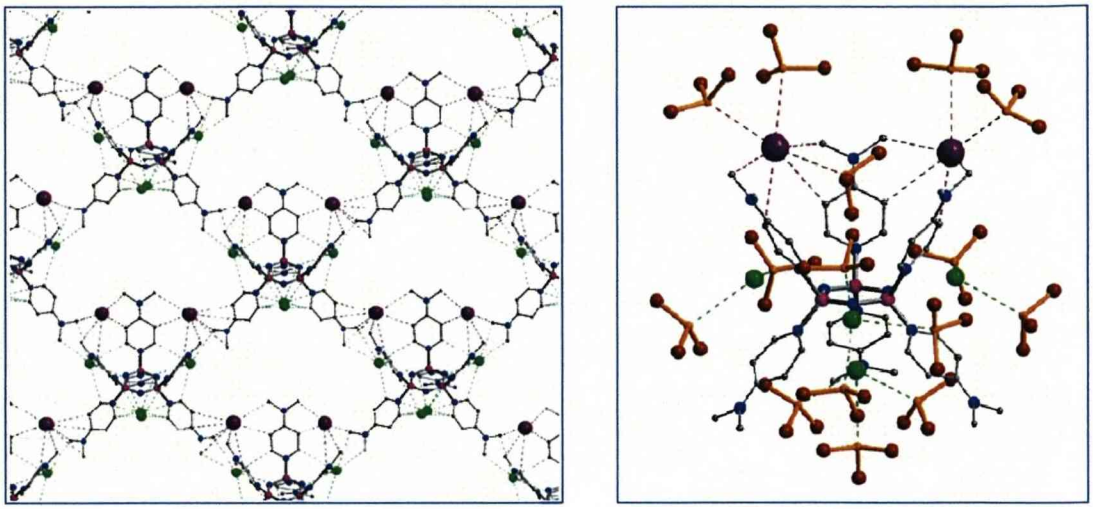

Figure 3.35. Crystal Structure of $[N_3P_3(DMAP)_6]Cl_4I_2 \cdot 14CHCl_3$.

Left: network of ions, right: Coordination of chlorofrom ligands to the $[N_3P_3(DMAP)_6]Cl_4I_2$ assembly.

3.2.1.6. The Hexacation with Silver Triflate

In order to exchange chloride for triflate ions in the coordination sphere of the hexacations, excess silver triflate was added to crystals of $[N_3P_3(DMAP)_6]Cl_6 \cdot 19\ CHCl_3$, whilst still in their chloroform mother liquor. After one hour stirring the crystals had vanished and the solution contained a white precipitate. After removal of this precipitate, single crystals formed in the solution. However upon X-ray analysis they were found to contain the salt $[DMAP_2Ag]OTf$; its cation consists of a linear silver complex. The $^{31}P\{^1H\}$ NMR spectrum of the remaining chloroform solution showed a single resonance at δ = 18.9 ppm, which remained stable after addition of methanol, see Figure 3.46. This species is likely to be $N_3P_3Cl_6$.

The presence of $N_3P_3Cl_6$ could originate from unreacted starting material or form by the removal of DMAP with silver. To clarify this situation the reaction was repeated, with removal of the chloroform mother liquor before the addition of silver triflate. The $^{31}P\{^1H\}$ NMR spectrum of the chloroform mother liquor had high signal to noise and showed little to no trace of $N_3P_3Cl_6$ still in solution. Instead signals were observed in the phosphazene

DMAP region of around δ = 8 ppm and in the negative region of the spectrum, indicating hydrolysed phosphazene species.

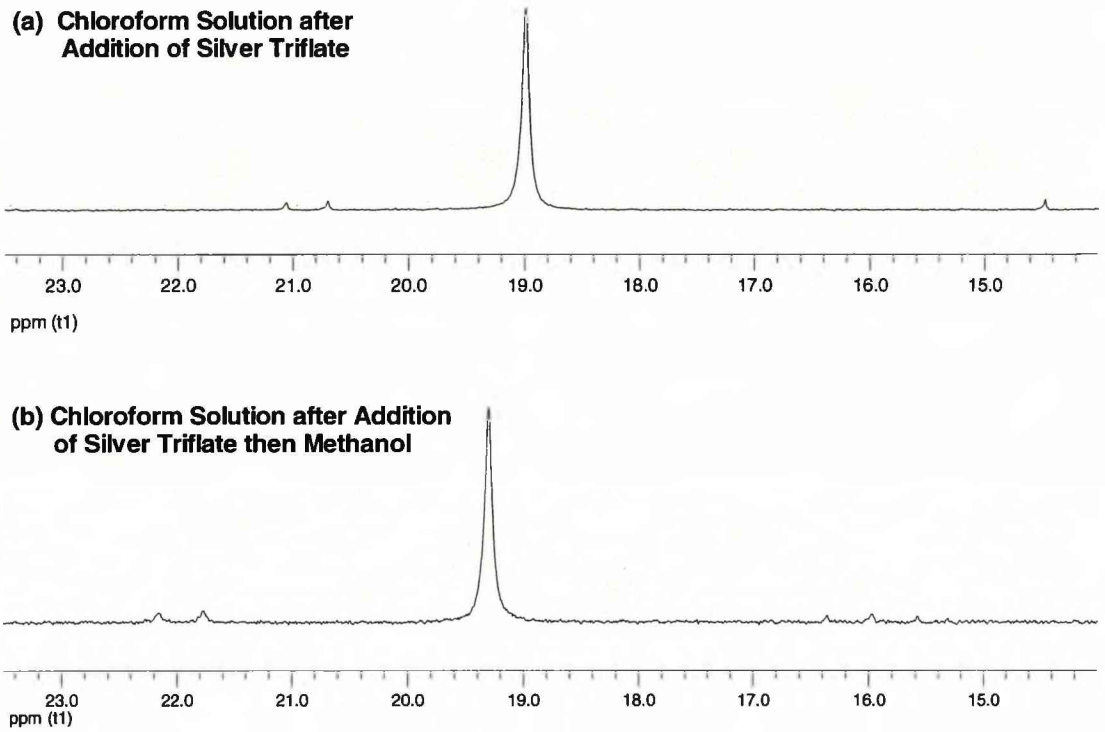

Figure 3.46. $^{31}P\{^1H\}$ **NMR Spectra of** $[N_3P_3(DMAP)_6]Cl_6$ **Reaction with Silver Triflate** (spectra recorded in $CHCl_3$ with d_6-acetone as external lock).

After the removal of chloroform, fresh solvent was added to the hexacation before the addition of silver triflate. Both chloroform and THF were used. The solutions were stirred for two hours then filtered. $^{31}P\{^1H\}$ NMR was run on both solutions. The chloroform solution showed no ^{31}P containing species where as the THF solution showed a major single resonance at δ = 8.4 ppm (spectrum was run in THF, with d_6-acetone as an external lock). This maybe due to the triflate salt of the hexacation, however structural analysis has not been possible.

3.2.1.7. Structure and Bonding in $[P_3N_3(DMAP)_6]^{6+}$

The X-ray data of the crystals of $[P_3N_3(DMAP)_6]Cl_6 \cdot 19CHCl_3$ that were obtained by slow diffusion gave the highest quality data for any of the structures containing the $[P_3N_3(DMAP)_6]^{6+}$ hexacation, with an R-value of 7.2%. It allowed the anisotropic refinement of all non-hydrogen atoms of the hexacation. Figure 3.47 shows that the thermal parameters are reasonably low. The following discussion is based on structural parameters from this set of data. The crystal structures of the other $[P_3N_3(DMAP)_6]^{6+}$ derivatives show comparable bonding parameters.

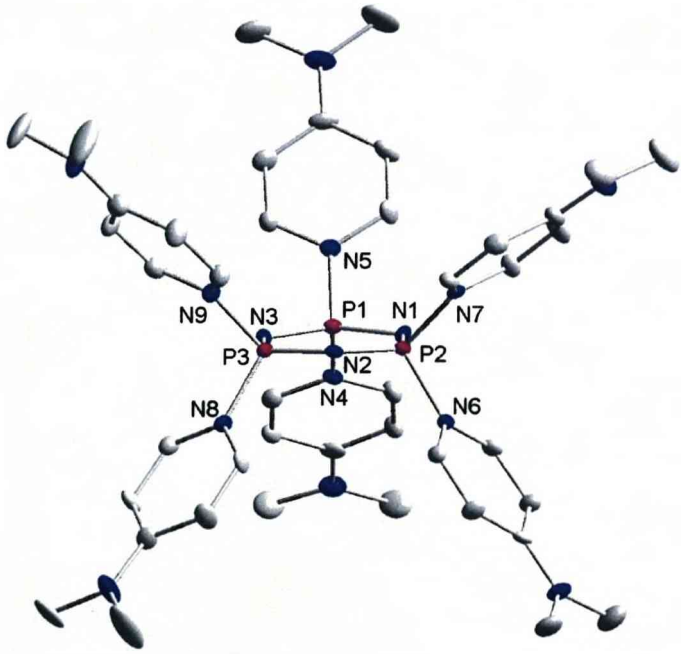

Figure 3.47. Crystals of $[N_3P_3(DMAP)_6]Cl_6 \cdot 19CHCl_3$ Showing the Hexacationic Unit.

Selected bond lengths [Å] and angles [deg]: P1 N1 1.573(6), P1 N4 1.705(6), P1 N5 1.714(6), P2 N2 1.568(6), P2 N1 1.570(6), P2 N7 1.706(6), P2 N6 1.707(6), P3 N2 1.566(6), P3 N3 1.575(6), P3 N8 1.575(6), P3 N9 1.707(6); N3 P1 N1 121.5(3), N2 P2 N1 121.2(3), N2 P3 N3 120.7(3), N4 P1 N5 100.1(3), N7 P2 N6 99.8(3), N8 P3 N9 100.2(3), P2 N1 P1 118.3(4), P3 N2 P2 118.9(4), P1 N3 P3 118.9(4).

The P-N bonds of the planar P_3N_3 ring measure on average 1.568 Å, which is at the short end of the spectrum of ring bond lengths in homoleptically substituted cyclotriphosphazenes.[41,76] The average P-N(DMAP) bond length

in **3.9** (av. 1.707 Å) is also at the short end of P-DMAP bonds (see Figure 3.49), but somewhat longer than the exocyclic P-N(amino) bonds in derivatives $(RNH)_6P_3N_3$ (1.66 Å).[77] The phosphazene ring describes almost a regular hexagon (av. N-P-N 121.1°, P-N-P 118.7°), while the exocyclic N-P-N angles towards DMAP ligands measure on average 100.0°.

Table 3.3 compares the internal bond lengths of DMAP ligands of the hexacation with those of the crystal structure of pure DMAP. The crystal structure determination of DMAP has been reported, but it shows a high R-value (7.5%) and is based on room temperature data.[78] Thus it was decided to re-determine the structure at 100 K to a high resolution in order to obtain an improved model. Large crystals of DMAP were obtained from a toluene solution, which gave good quality data to a resolution of 0.58 Å, while the refinement gave an R-factor of 4.5%.

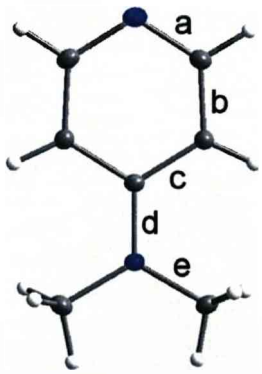

Å	DMAP	$[P_3N_3DMAP_6]^{6+}$
a	1.345	1.367
b	1.386	1.346
c	1.412	1.420
d	1.363	1.320
e	1.454	1.466

Table 3.3. Comparison of bond lengths in DMAP and $[N_3P_3(DMAP)_6]^{6+}$ (Å).
(Values are averaged)

A comparison of the bond lengths in both the free DMAP molecule and the DMAP ligands of the hexacation shows that bonds **a** and **c** are becoming longer (though by a small margin), while **b** and **d** shorten when DMAP is

attached to the phosphazene ring. This indicates that the contribution of the quinoidal resonance form **II** (Figure 3.48) increases upon adduct formation.

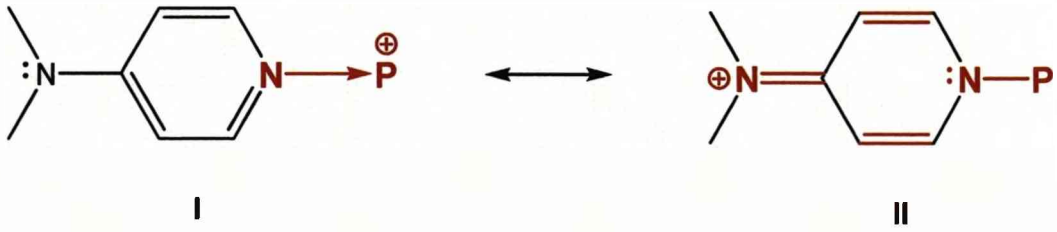

I II

Figure 4.48. Resonance Forms of DMAP.

In order to quantify the correlation between of the strength of adduct interaction and the quinoidal contribution, P-N(DMAP) bonds of various P-DMAP complexes were plotted against the bond **d** of the DMAP ligand.[79] The data were taken from 15 crystal structures with good agreement factors (<7.5%) and no major disorder. It shows that the P-N(DMAP) bond distances cover a wide range stretching from 1.70 to 1.88 Å, while the **d** bonds are more rigid ranging within a more narrow distribution. The plot (Figure 3.49) shows that the points are more or less scattered around a steep slope. However, the experimental errors of atom positions are simply too great to provide an accurate correlation of para-C-N bond lengths. Despite this, such diagrams present a useful tool to study correlations of structural parameters and assess the significance of those correlations. Figure 3.49 also shows that both the P-N(DMAP) and the para-C-N bonds of the hexacation $[P_3N_3(DMAP)_6]^{6+}$ are at the short end of the spectrum of bond distances in P-DMAP complexes, which indicates strong interactions between the DMAP ligands and the phosphorus centres of the phosphazene ring.

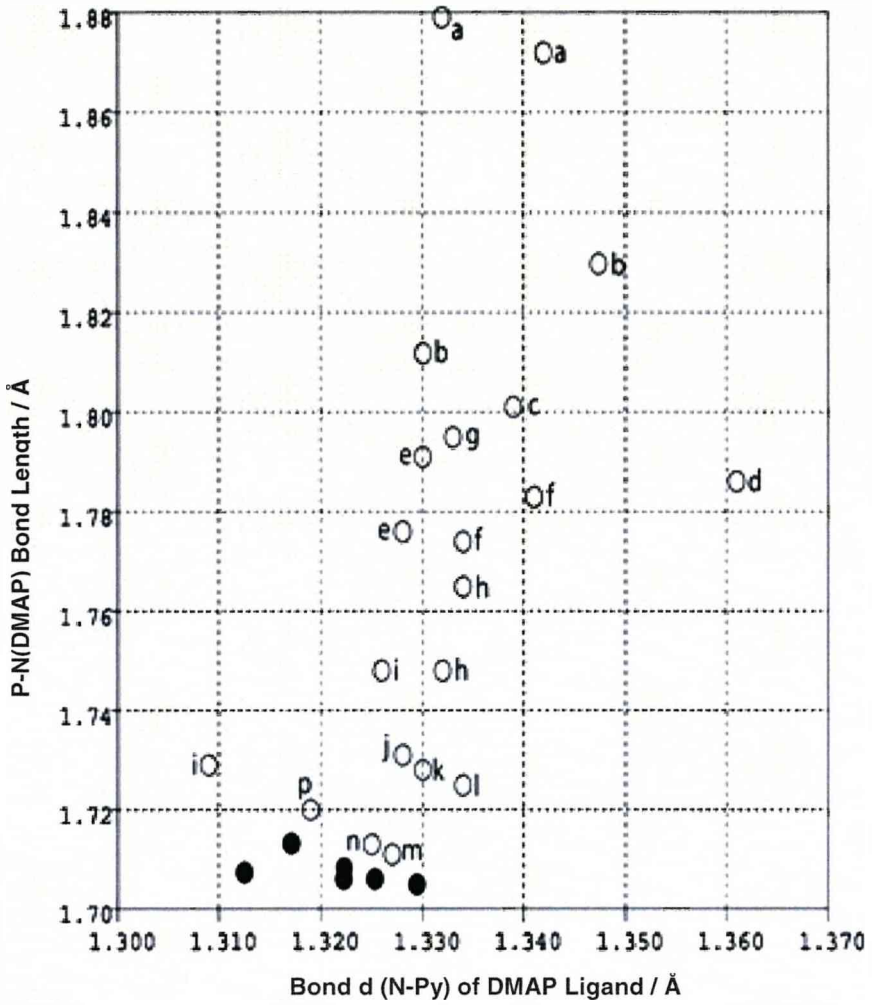

Figure 3.49. Scatterplot of Bond d vs P-N(DMAP) Bond for P-DMAP Complexes.

Spheres in black refer to the six pairs of parameters of the $[N_3P_3(DMAP)_6]^{6+}$ hexacation.

(Key given in box below)

a	$[(DMAP\rightarrow)_2P{\equiv}NR]OTf$	i	$[(DMAP\rightarrow)_2P\ (=O)_2]Br_3$
b	$[(DMAP\rightarrow)_2P\ (=NR)_2]Br$	j	$[DMAP\rightarrow P(OR')_2{=}NR]Cl$
c	$[DMAP\rightarrow PMe_2]OTf$	k	$[DMAP\rightarrow P(OR')_2{=}NR]OTf$
d	$[DMAP\rightarrow PPh_2]OTf$	l	$[DMAP\rightarrow P(OR')_2{=}NR]Br$
e	$[DMAP\rightarrow PNR]_2OTf_2$	m	$[DMAP\rightarrow P(OR')_2{=}NR]BF_4$
f	$[DMAP\rightarrow PSMe_2]OTf$	n	$[DMAP\rightarrow P(Cl)_2{=}NR]OTf$
g	$[DMAP\rightarrow P(Me)_2{=}NR]OTf$	p	$[DMAP\rightarrow PMe_3]OTf_2$
h	$[(DMAP\rightarrow)_2P\ (=O)_2]Cl$		

Table 3.4 compares the B3LYP/6-31G* Natural Population Analysis (NPA) charges of $[P_3N_3(DMAP)_6]^{6+}$ with that of other cyclotriphosphazenes.[22] It shows that the charge on phosphorus correlates with the electronegativity of the ligand, while the charge on nitrogen remains more or less constant. The computations gave an overall charge of 3.02 for the P_3N_3 ring of the hexacation as part of the $[N_3P_3(DMAP)_6]Cl_5^+$ assembly, which implies that the positive charge of the hexacation is equally shared between the phosphazene ring and the DMAP ligands.[22] However, while the substituents in neutral phosphazene derivatives carry a negative charge, the DMAP ligands must share the high positive charge of the hexacation. The electrostatic potential map, shown in Figure 3.50, illustrates the extent to which the positive charge is distributed onto the DMAP ligands. In particular, the *ortho*-H positions that interact with the equatorially arranged chloride ions exhibit a pronounced positive character.[22]

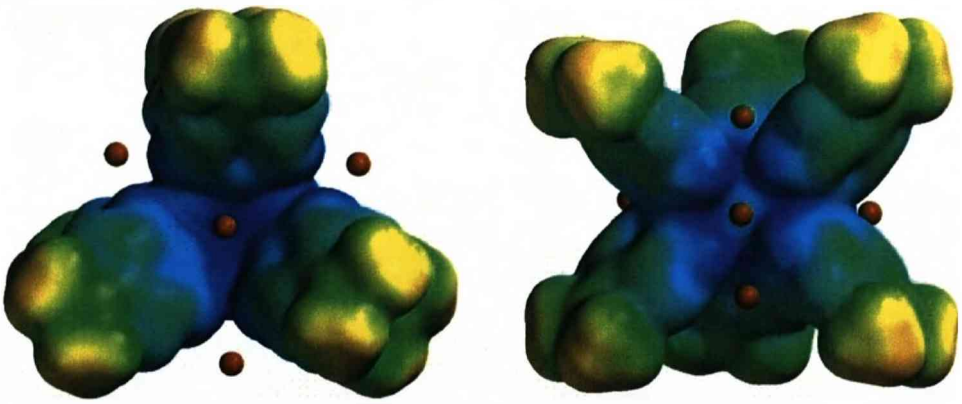

Figure 3.50. Electrostatic Potential Map of the $[N_3P_3(DMAP)_6]^{6+}$ Ion in the Presence of the Five Hosted Chloride Ions.[22]

(Blue represents the most positive regions, followed by green, then yellow with the most negative areas shown in red)

L in $P_3N_3L_6$	P	N	ring
F[80]	+2.57	-1.49	+3.24
DMAP *	+2.46	-1.45	+3.02
NH_2[81]	+2.30	-1.53	+2.31
Cl[82]	+1.88	-1.45	+1.29

Table 3.4. B3LYP/6-31G* NPA Charges at Experimental Geometries.[22]

* as part of the $([N_3P_3(DMAP)_6]Cl_5)^+$ assembly in **3.9**.

(Calculations carried out by Dr R. Bonar-Law)

The P-N bonds in cyclophosphazenes can be regarded as highly polar. In addition to covalent contributions there are strong electrostatic interactions between the positive P and the negative N centres. The result is a strong and short P-N bond. Various resonance forms can be envisaged for the hexacation $[P_3N_3(DMAP)_6]^{6+}$. Figure 3.51 displays two forms, which play a major part in the electronic structure as suggested by the B3LYP/6-31G* NPA charges of P (~2.5), N (~1.5) and DMAP ligands (~0.5).[22]

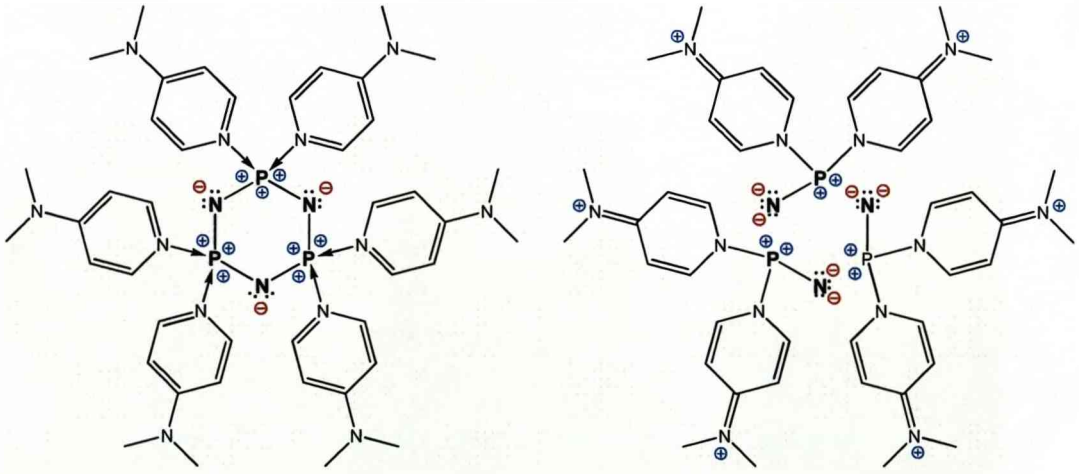

Figure 3.51. Major Resonance Forms of the Hexacation.[22]

3.2.2. Tetracations

3.2.2.1. The Tetracation $[(DMAP)_5N_3P_3O]^{4+}$ (3.10)

The salt $[N_3P_3(DMAP)_6]Cl_6$ slowly hydrolyses when water is added to the crystals in chloroform producing [DMAPH]Cl and an ill-defined mixture of hydrolysis products. In order to study the effect of water during the crystallisation of $[N_3P_3(DMAP)_6]Cl_6$, crystals of DMAP and $N_3P_3Cl_6$ were covered with standard solutions of water in chloroform, which were obtained by diluting saturated solutions (0.046 M at 20°C) with dry chloroform. It is interesting to note that crystals of $[N_3P_3(DMAP)_6]Cl_6 \cdot 19\ CHCl_3$ form if less than three equivalents of water were used. $N_3P_3Cl_6$ is known to be hydrolytically stable, but it hydrolyses in the presence of bases, for example pyridine, to form various chloro-oxo-phosphazene derivatives.[42] When more than six equivalents of water are added, a soluble compound is formed, which could only be analysed by NMR. The $^{31}P\ \{^1H\}$ NMR spectrum showed an AX_2 spin system with δ = - 8.9 and 21.0 ppm and $^2J_{PP}$ = 48.12 (t), 51.06 (t) and 48.06 (d) together with some minor signals of broad and undistinguishable multiplets.. These chemical shifts are indicative of phosphazenes carrying both chloro and oxo functions.

However, when crystals of $N_3P_3Cl_6$ and DMAP were covered with chloroform that contained three equivalents of water, single crystals were obtained after one day The X-ray structure analysis showed that the crystals contain the tetracation $[(DMAP)_5P_3N_3O]^{4+}$. One P centre of the P_3N_3 ring carries an oxo group and a DMAP ligand, while each of the other two are equipped with two DMAP ligands. Again, the crystals consist of a solvate containing nine chloroform molecules per formula unit. The reaction scheme for the synthesis of $[(DMAP)_5N_3P_3O]Cl_4 \cdot 9\ CHCl_3$ is shown below in Figure 3.52.

The crystal structure of $[(DMAP)_5N_3P_3O]Cl_4 \cdot 9CHCl_3$ exhibits some unusual features. Two tetracations are paired up in a dimeric arrangement. The oxo centre of one tetracation is located almost directly above the P_3N_3 ring of the other and vice versa (Figures 3.53 and 3.54).

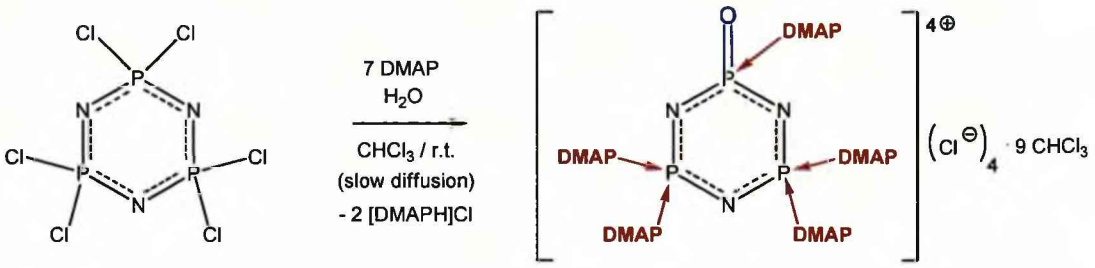

Figure 3.52.

The distance between the oxygen atom and the N_3P_3 ring centroid is 2.765 Å, while the three P...O distances range from 3.135 to 3.236 Å, which is below the sum of the Van-der-Waals radii {1.52 (O) + 1.80 (P) = 3.32 Å}.[83] A search of the CSD revealed that there are no other examples of cyclophosphazene structures, in which the ring is capped intermolecularly with short contacts to all three phosphorus atoms. However, the solvate $[N_3P_3(DMAP)_6]Cl_6 \cdot 11CH_2Cl_2$ discussed above features three P...Cl contacts (ranging from 3.468 to 3.481 Å) to the basket-hosted chloride ion that are below sum of the Van-der-Waals radii (3.55 Å). The short contacts in the latter example are the result of strong ion pairing between the hexacation and the chloride anions. The short P...O contacts between the two tetracations can be rationalised on the grounds of strong dipole-dipole interactions: The positively charged P_3N_3 ring interacts electrostatically with the negatively charged oxo-centre of the other tetracation. The two tetracations slot into each other very effectively; the oxo-centres are shielded by two of the DMAP ligands of the other tetracation.

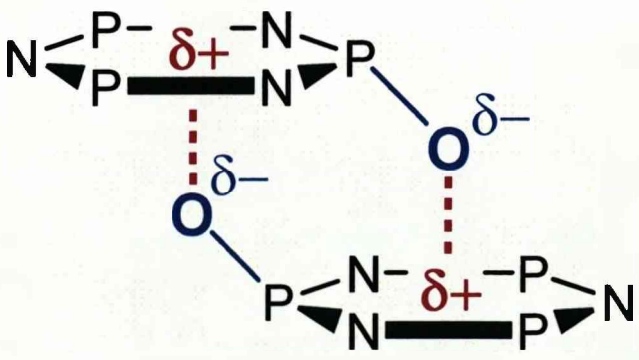

Figure 3.53.

The P=O bond length, measures 1.461(4) Å and is comparable to the P=O bond distance in the cationic complex $[(DMAP)_2PO_2]^+$ (1.4671(11) and 1.4626(12)[5]). The phosphazene ring is planar, with a twist angle of. The P-N ring bonds vary considerably: The two P-N bonds adjacent to the oxo unit are the longest averaging 1.624 Å, while the next two P-N bonds along the ring (P2-N2 and P3-N1, respectively) are shortest measuring 1.549 Å. The two ring bonds furthest away from the P=O unit are on average 1.572 Å long. The latter two bond lengths are comparable to the ring bond distances in the hexacation $[(DMAP)_6N_3P_3]^{6+}$. Cyclotriphosphazenes carrying substituents of different electronic properties commonly show alterations of P-N bond lengths around the ring. Here the presence of the strong P=O bond interaction reduces the bond strengths of the adjacent ring bonds. This effect then continues around the ring shortening the two ring bonds further along the ring. This behaviour is also reflected in the variation of N-P-N bond angles in the ring, which are wider at the $(DMAP)_2P$ centres, (N2-P2-N3 121.9(2) and N1-P3-N3 122.4(2) Å, respectively) and narrower at the DMAP→P=O unit (N2-P1-N1 113.7(2) Å).

The DMAP ligand that is attached to the P-O unit shows the longest P-DMAP bond (1.773(4) Å) within the tetracation, while the other four P-DMAP bond lengths range from 1.711(4) to 1.730(4) Å and resemble the P-DMAP bond distances of the hexacation. Also, the angle between the P-O bond and the plane of the P_3N_3 ring is large (145.2°), while the corresponding angle between the phosphazene ring and the associated P(O)-DMAP bond (P1-N4) is rather acute (109.0°). Thus the strong P=O bond tilts towards a co-planar arrangement with the phosphazene ring and in return the associated P-DMAP interaction becomes weaker and more dative in character. The tetracation can be regarded as a donor-stabilised derivative of the phosphazene oxide shown below, in which the phosphorus centre of the P=O bond features a trigonal planar environment (Figure 3.55). Such compounds, as well as other phosphazenes with trigonal planar P-centres, have not been isolated in the form of stable compounds, but are being discussed as intermediates in substitution reactions.[76,84]

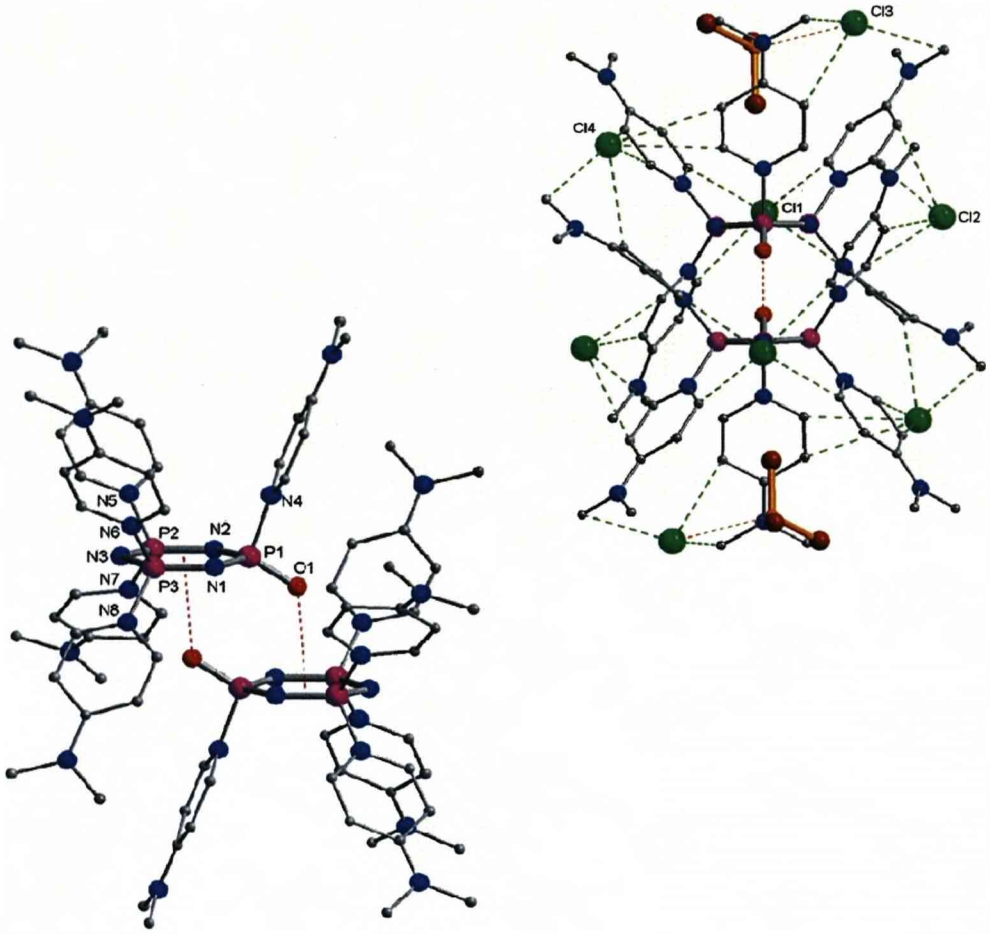

Figure 3.54. Crystal Structure of $[(DMAP)_5N_3P_3O]Cl_4 \cdot 9CHCl_3$;

left: dimeric arrangement of tetracations, right: coordination of chloride ions to the dimer (incl. $DMAP_3$-basket-hosted $CHCl_3$ molecules);

selected bond lengths [Å] and angles [deg]: P1 O1 1.461(4), P1 N4 1.773(4), P1 N2 1.622(4), P1 N1 1.626(4), P2 N2 1.549(4), P2 N3 1.567(4), P3 N1 1.549(4), P3 N3 1.578(4), P2 N7 1.711(4), P2 N5 1.730(4), P3 N6 1.722(4), P3 N8 1.725(4); O1 P1 N4 105.7(2), O1 P1 N2 116.9(2), O1 P1 N1 115.2(2), N2 P1 N1 113.7(2), N2 P2 N3 121.9(2), N1 P3 N3 122.4(2), N7 P2 N5 100.4(2), N6 P3 N8 101.6(2), P3 N1 P1

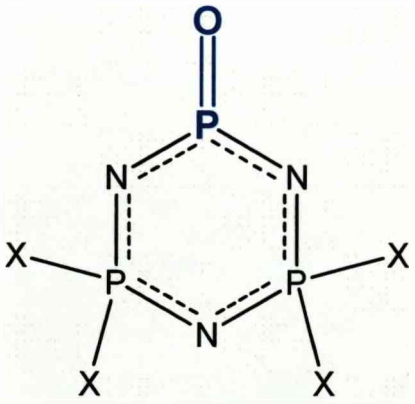

Figure 3.55

The dimeric arrangement of the two tetracations accommodates eight chloride ions in chelating pockets via aryl-H and methyl-H atoms of the DMAP ligands. In return all of the eight chloride ions interact with neighbouring tetracations. As a result the tetracations and chloride anions form a three dimensional open network structure with wide channels running along the a-axis. The eight chloride ions are coordinated by sixteen crystallographically well-defined chloroform molecules, coating the polar channel walls with a hydrophobic layer. The resultant hydrophobic channels are occupied by two non-coordinated disordered chloroform molecules per dimer see Figure 3.56.

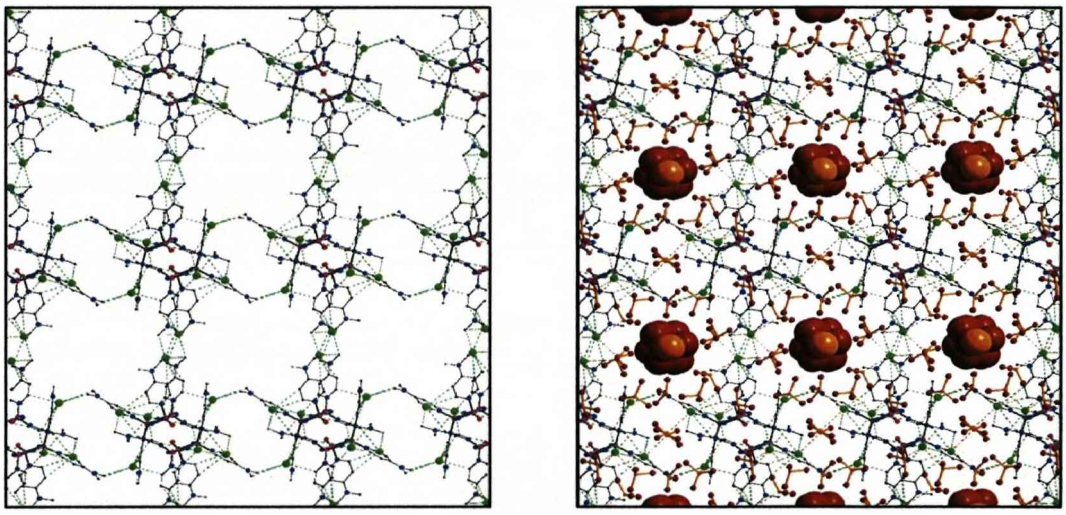

Figure 3.56. Left: Ionic Framework Consisting of Tetracation Dimers and Chloride Ions; Right: Ionic Framework Plus Chloroform Molecules

(the disordered non-coordinated solvent molecules occupying the hydrophobic channels are displayed as space filling spheres).

In the absence of chloroform vapour the crystals of $[(DMAP)_5P_3N_3O]Cl_4 \cdot 9\ CHCl_3$ loose solvent at atmospheric pressure. Treatment in vacuum at room temperature yields a white powder with a melting point of 101.5–103 °C. The TGA of this material shows a weight loss of 14.89% when heated to 100 °C that equates to the loss of three chloroform molecules.

The ^{31}P MAS NMR spectrum shows three ^{31}P resonances; the signal at -7.9 ppm corresponds to the phosphorus bound to oxygen while the other peaks at 6.2 and 7.8 ppm result from phosphorus bound only to DMAP (Figure 3.57). Their slight difference in chemical shift could be due to the asymmetric environment of chloride ions. The resonances at 6.2 and 7.8 ppm show 1:1 peak areas, while the P=O resonance is slightly lower in population, however this could be due to saturation of the signal.

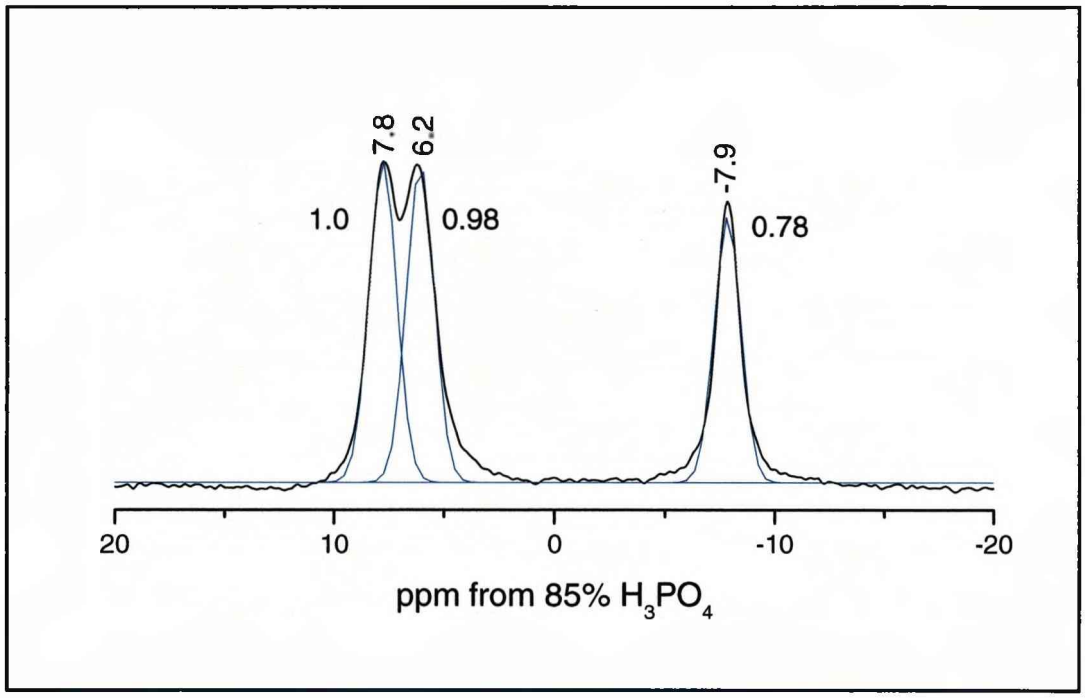

Figure 3.57. Solid State ^{31}P NMR Spectrum of $[N_3P_3(O)(DMAP)_5]Cl_4 \cdot CHCl_3$ (deconvoluted signals in blue).

3.2.2.2. The Tetracation $[(DMAP)_6N_4P_4O_2]^{4+}$ (3.11)

Attempts to generate crystals of the octacation $[(DMAP)_8N_4P_4]^{8+}$ from the cyclotetraphosphazene $N_4P_4Cl_8$ were unsuccessful. Both the slow diffusion method as well as microwave treatment only led to ill-defined product mixtures. However, when a mixture of $N_4P_4Cl_8$, DMAP and water in chloroform was reacted in the microwave at 100°C, colourless crystals were obtained that consisted of the solvate $[N_4P_4O_2(DMAP)_6]Cl_4 \cdot 14\ CHCl_3$ (Figure 3.58). This contains the tetracation $[(DMAP)_6N_4P_4O_2]^{4+}$, which features an

eight membered P_4N_4 ring; two formally dicationic $P(DMAP)_2$ units are located opposite to each other in the ring, while the other two consist of formally neutral DMAP→P=O units.

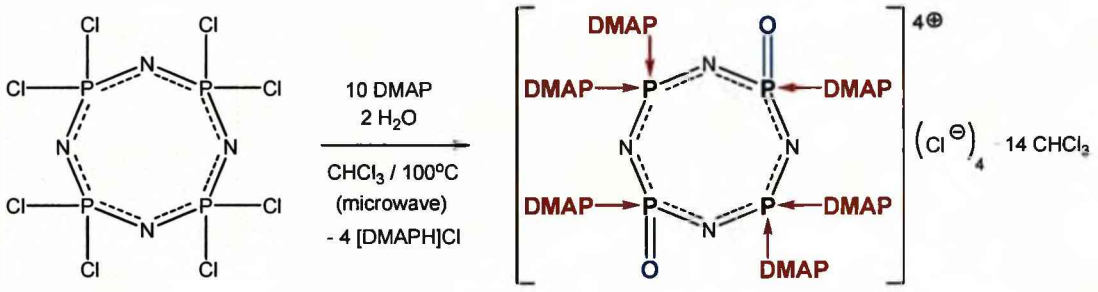

Figure 3.58

The tetracation $[(DMAP)_6N_4P_4O_2]^{4+}$ has inversion symmetry. The eight-membered phosphazene ring is puckered. The P-N(ring) bonds are only slightly shorter around the $P(DMAP)_2$ centres than at the DMAP→P=O units. The N-P-N angles of the P_4N_4 ring are similar to those of the six-membered ring of $[(DMAP)_4N_3P_3O]^{4+}$, while the angles at nitrogen are considerably wider. The P=O bond measures 1.454(9) Å, thus it is similar to the P=O bond in the six-membered ring derivative (Figure 3.59).

The tetracation interacts with chloride ions via CH...Cl contacts. The six DMAP ligands form pockets around the tetracation. These accommodate four chloride ions, two of which are chelated by three DMAP ligands while the other two interact with just two via aryl-H functions. The $[(DMAP)_6P_4N_4O_2]Cl_4$ units are connected via methyl-H...Cl bonds to form a 3D network (Figure 3.60). In contrast to the dimeric arrangement of $[(DMAP)_4P_3N_3O]^{4+}$, the tetracation $[(DMAP)_6P_4N_4O_2]^{4+}$ does not form close contacts with neighbouring tetracations. Overall the crystals contain fourteen chloroform molecules per formula unit. Ten chloroform molecules are coordinated to the chloride ions, two interact with oxo-units via CH...O contacts, while the remaining two are non-coordinated, see Figure 3.61.

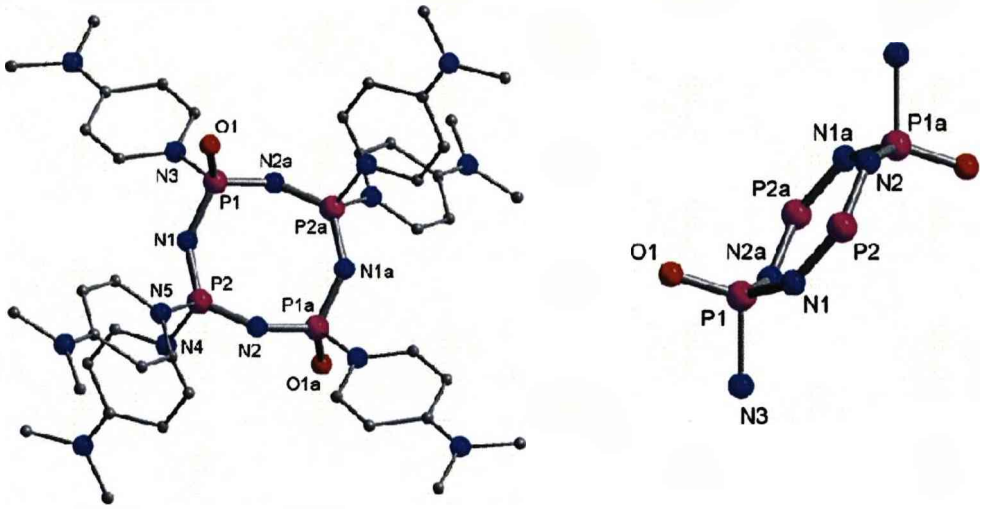

Figure 3.59. Crystal Structure of $[N_4P_4(O)_2(DMAP)_6]Cl_4 \cdot 14CHC_3$

- showing the tetracationic unit.

P1 O1 1.454(9), P1 N1 1.566(10), P1 N2a 1.588(10), P1 N3 1.758(10), P2 N1 1.551(10), P2 N2 1.553(10), P2 N5 1.719(9), P2 N4 1.731(10); O1 P1 N1 116.5(6), O1 P1 N2a 115.8(5), N1 P1 N2a 113.6(5), O1 P1 N3 107.1(5), N1 P2 N2 126.9(5), N5 P2 N4 100.2(5), P2 N1 P1 141.5(7), P2 N2 P1a 136.3(7).

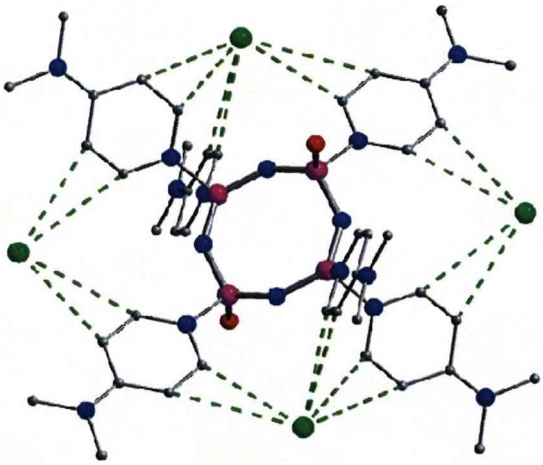

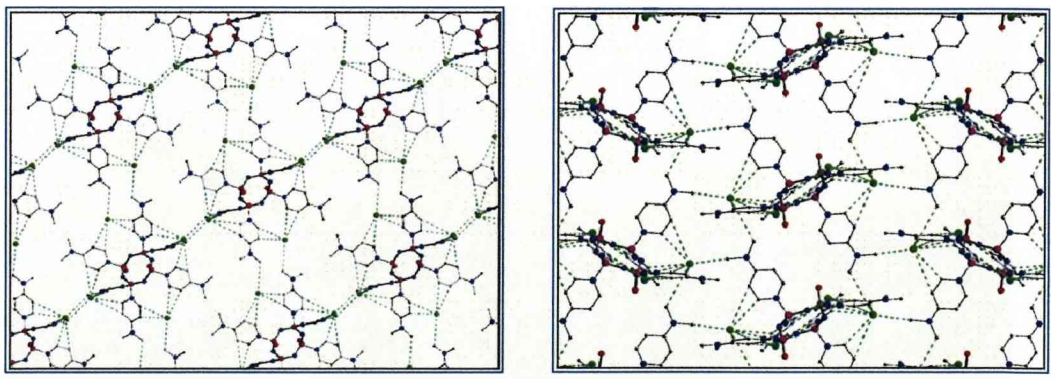

Figure 3.60. Crystal Structure of $[N_4P_4(O)_2(DMAP)_6]Cl_4 \cdot 14CHCl_3$

- showing the 3D network of tetracations and chloride ions.

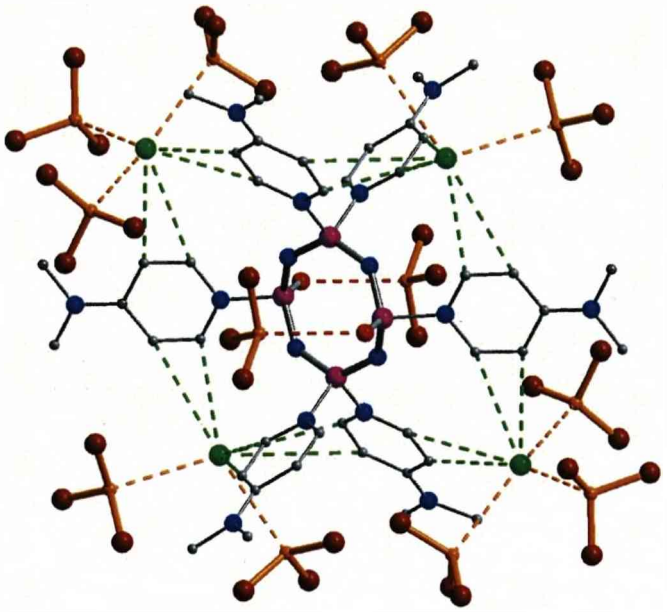

Figure 3.61. Crystal Structure of $[P_4N_4(O)_2(DMAP)_6]Cl_4 \cdot 14CHCl_3$
- showing the coordination of chloroform molecules.

3.2.3. Alternative N-Donor Ligands

Several reactions were investigated of $N_3P_3Cl_6$ with donor ligands other than DMAP (however, not as extensively). These include 2,2'-bipyridine (2,2'-BiPy), 4,4'-bipyridine (4,4'-BiPy), 1,4-diazabicyclo[2.2.2]octane (DABCO), N-methyl imidazole and the "linked-DMAP" pyridine piperazine species $N(CH)_2(CH)_2N(CH_2)_2(CH_2)_2N(CH)_2(CH)_2N$, **3.12** (Figure 3.62).

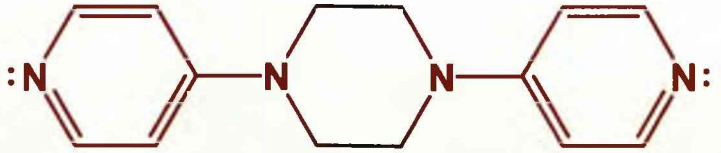

3.12

Figure 3.62

3.2.3.1. Bipyridine, DABCO and imidazole Ligands

Reactions of both 2,2'-BiPy and 4,4'-BiPy with $N_3P_3Cl_6$ were carried out in the microwave, using standard Schlenk techniques to reflux and by slow diffusion in chloroform. However none of these reactions led to the replacement of chloride at phosphorus. This was ascertained by $^{31}P\{^1H\}$ NMR of the reaction solutions as no solid material was formed during these reactions. This unreactive behaviour is not too surprising given the reduced donating power of bipyridines with respect to DMAP. However the supramolecular possibilities of forming linked-stabilized polycations mean it is worthwhile pursuing these studies further. One synthetic possibility arises from the reactions of silver triflate with [**3.9**]Cl_6. The preliminary investigations of this reaction appear to suggest that silver triflate removes DMAP from **3.9** by coordination of DMAP to silver (similar to the behaviour of **3.9** in TCE). However in the presence of chloride $N_3P_3Cl_6$ is simply reformed (Figure 3.63). If this reaction can be modified so that bipyridines are the only species able to coordinate to phosphorus after DMAP removal, then bipyridine stabilized cations may form.

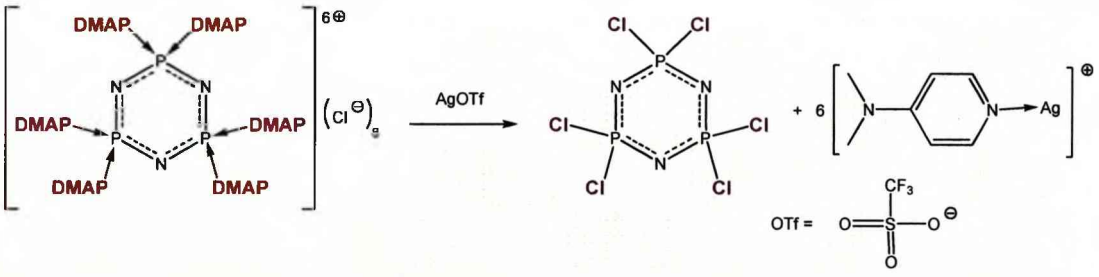

Figure 3.63

In contrast to this DABCO and methyl imidazole both react with $N_3P_3Cl_6$ in chloroform using both microwave and slow-diffusion methods. However, $^{31}P\{^1H\}$ NMR spectra of the reaction solutions indicated that only ill-defined product mixtures where obtained

3.2.3.2. The "Linked-DMAP" ligand (3.12)

Due to the low reactivity of bipyridines with cyclophosphazenes we decided to look for linking N-donor ligands with reactivity more comparable to that of DMAP. Louërat et al. had reported the synthesis of a piperazinyl pyridine species **3.12**, which is essentially two DMAP molecules with C-C bonds between the N-methyl substituents.[85] The reported synthesis involved the reaction of 4-chloropyridine hydrochloride with piperazine in DMF with di-*iso*-propylethylamine as a base.[85] After unsuccessful attempts to repeat the synthesis we modified the procedure: This involved heating two equivalents of 4-chloropyridine with piperazine in the melt. We were able to obtain **3.12** by this method although yields were low (13.3%) due to incomplete reaction forming a mixture of **3.12** and the mono-pyridine piperazine **3.13**, as shown in Figure 3.64. However these two compounds could be separated by recrystallisation from DCM and hexane.

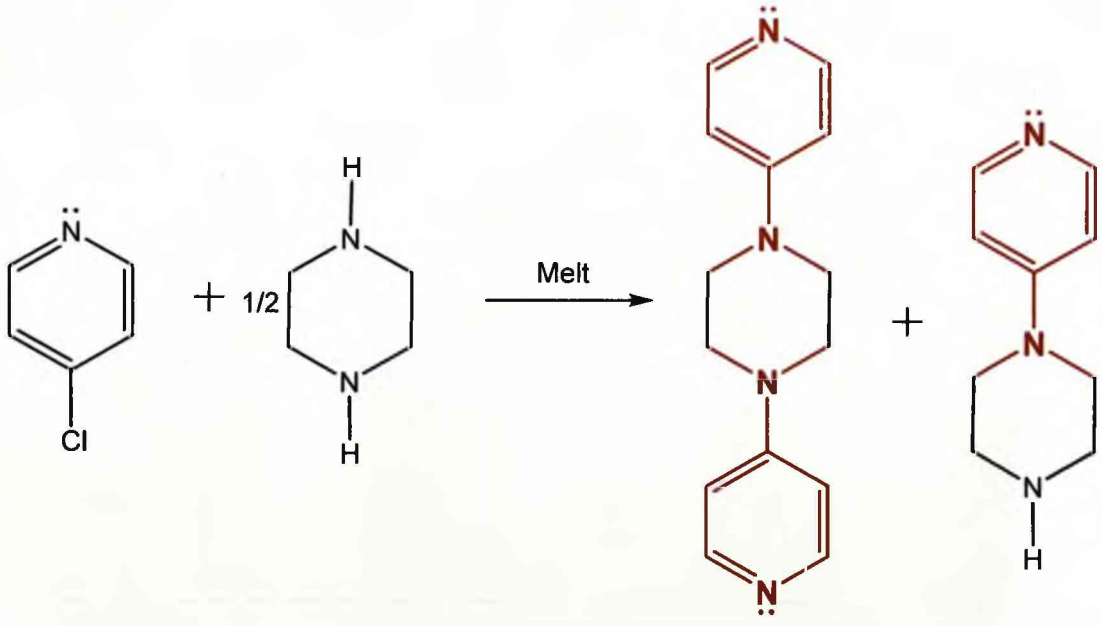

Figure 3.64

Slow diffusion and microwave reactions were carried out between $N_3P_3Cl_6$ and **3.12**. However no identifiable products were obtained from these reactions. **3.12** has a relatively low solubility in chloroform, DCM and TCE. Therefore sufficient diffusion of **3.12** into solution did not occur, even under microwave conditions. As a result complex formation with $N_3P_3Cl_6$ was not possible. However the coordination of DMAP to $N_3P_3Cl_6$ is heavily solvent dependant. Therefore more extensive studies of **3.12** in different solvent systems is likely to yield complexes with cyclotriphosphazenes.

3.3. Conclusions

The strong N-donor ligand DMAP reacts with $N_3P_3Cl_6$ in chlorinated solvents yielding salts that contain the hexacation $[P_3N_3(DMAP)_6]^{6+}$. Complete reactions are facilitated either under solvothermal conditions or using slow diffusion techniques. The former method ensures that all of the reactants are dissolved, while the latter method keeps the concentration of reactants to a minimum. The crystalline products exist as solvates, which contain large proportions of solvent molecules per formula unit. The chloride ions are situated in appropriate binding sites of the cations and are further coordinated to the chlorinated solvent molecules via CH...Cl interactions. The solvent has a structure-directing effect on the architecture of the salt lattice. While chloroform binds in a monodentate fashion, dichloromethane can also engage itself in a bridging manner. Addition of water prior to the reaction of chlorophosphazenes with DMAP generates tetracationic oxo derivatives, such as $[(DMAP)_4P_3N_3O]^{4+}$, which forms a dimer via dipole-dipole interactions between the negatively charged oxo-unit and the positively charged phosphazene ring.

The formation of the hexacation is reversible, which promises interesting applications for $[P_3N_3(DMAP)_6]^{6+}$ and related ions as intermediates in the synthesis of cyclo- and polyphosphazene derivatives. Moreover, the unique host qualities toward chloride ions, the ability to accommodate a large

amount of solvent in the crystal lattice and the suitability for solvothermal reaction conditions could pave the way for new main group based framework materials. For example, linearly bridging N-donor molecules could facilitate network architectures that are equipped with well-defined arrays of counter anions. These cationic systems stabilized by bridging N-donors should prove to be synthetically accessible simply by extending the synthetic methods we have presented here. In addition to this alternative donor molecules such as phosphines and carbenes could be used to stabilise polycationic phosphazenes.

References

(1) Boomishankar, R., Richards, P. I.; Steiner, A. *Angew. Chem., Int. Ed.* **2006**, *45*, 4632.

(2) Steiner, A., Zacchini, S.; Richards, P. I. *Coord. Chem. Rev.* **2002**, *227*, 193.

(3) Rivals, F.; Steiner, A. *Chem. Commun.* **2001**, 1426.

(4) Sulkowski, W. W. in Phosphazenes: A Worldwide Insight, (M. Gleria and R. De Jaeger), Nova Science Publishers, Inc., **2004**, 69.

(5) Rovnanik, P., Kapicka, L., Taraba, J.; Cernik, M. *Inorg. Chem.* **2004**, *43*, 2435.

(6) Meisel, M., Lonnecke, P., Grimmer, A. R.; WulffMolder, D. *Angew. Chem., Int. Ed. Engl.* **1997**, *36*, 1869.

(7) Bain, V. A., Killean, R. C. G.; Webster, M. *Acta Crystallogr., Sect. B: Struct. Sci.* **1969**, *B 25*, 156.

(8) Huynh, K., Rivard, E., Lough, A. J.; Manners, I. *Inorg. Chem.* **2007**, *46*, 9979.

(9) Hong, D. M., Wei, H. H., Gan, L. L., Lee, G. H.; Wang, Y. *Polyhedron* **1996**, *15*, 2335.

(10) Coles, M. P.; Hitchcock, P. B. *Chem. Commun.* **2007**, 5229.

(11) Cotton, F. A., Wilkinson, G., Murillo, C. A.; Bochmann, M., *Advanced Inorganic Chemistry*, 6th, Wiley and Sons, New York, **1999**.

(12) Greenwood, N. N., *Chemistry of the Elements*, Pergamon, Oxford, **1984**.

(13) Bechstein, O., Ziemer, B., Hass, D., Trojanov, S. I., Rybakov, V. B.; Maso, G. N. *Z. Naturforsch.* **1990**, *582*, 211.

(14) Adley, A. D., Bird, P. H., Fraser, A. R.; Onyszchu.M *Inorg. Chem.* **1972**, *11*, 1402.

(15) Hensen, K., Zengerly, T., Pickel, P.; Klebe, G. *Angew. Chem., Int. Ed. Engl.* **1983**, *22*, 725.

(16) Brotzel, F., Kempf, B., Singer, T., Zipse, H.; Mayr, H. *Chem. Eur. J.* **2007**, *13*, 336.

(17) Xu, S. J., Held, I., Kempf, B., Mayr, H., Steglich, W.; Zipse, H. *Chem. Eur. J.* **2005**, *11*, 4751.

(18) Ragnarsson, U.; Grehn, L. *Acc. Chem. Res.* **1998**, *31*, 494.

(19) Scriven, E. F. V. *Chem. Soc. Rev.* **1983**, *12*, 129.

(20) Hofle, G., Steglich, W.; Vorbruggen, H. *Angew. Chem., Int. Ed. Engl.* **1978**, *17*, 569.

(21) Burford, N.; Ragogna, P. J. *J. Chem. Soc., Dalton Trans.* **2002**, 4307.

(22) Boomishankar, R., Ledger, J., Guilbaud, J.-B., Campbell, N. L., Bacsa, J., Bonar-Law, R., Khimyak, Y. Z.; Steiner, A. *Chem. Commun.* **2007**, 5152.

(23) Huynh, K., Rivard, E., Lough, A. J.; Manners, I. *Chem. Eur. J.* **2007**, *13*, 3431.

(24) Burford, N., Spinney, H. A., Ferguson, M. J.; McDonald, R. *Chem. Commun.* **2004**, 2696.

(25) Weiss, R.; Engel, S. *Angew. Chem., Int. Ed. Engl.* **1992**, *31*, 216.

(26) Bouhadir, G., Reed, R. W., Reau, R.; Bertrand, G. *Heteroat. Chem.* **1995**, *6*, 371.

(27) Reed, R., Reau, R., Dahan, F.; Bertrand, G. *Angew. Chem., Int. Ed. Engl.* **1993**, *32*, 399.

(28) Meyer, B. N., Ishley, J. N., Fratini, A. V.; Knachel, H. C. *Inorg. Chem.* **1980**, *19*, 2324.

(29) Sheldrick, W. S. *J. Chem. Soc., Dalton Trans.* **1974**, 1402.

(30) Holmes, R. R., Gallagher, W. P.; Carter, R. P. *Inorg. Chem.* **1963**, *2*, 437.

(31) Muetterties, E. L., Bither, T. A., Farlow, M. W.; Coffman, D. D. *J. Inorg. Nucl. Chem.* **1960**, *16*, 52.

(32) Burford, N., Losier, P., Phillips, A. D., Ragogna, P. J.; Cameron, T. S. *Inorg. Chem.* **2003**, *42*, 1087.

(33) Burford, N., Cameron, T. S., Robertson, K. N., Phillips, A. D.; Jenkins, H. A. *Chem. Commun.* **2000**, 2087.

(34) Burford, N., Phillips, A. D., Spinney, H. A., Lumsden, M., Werner-Zwanziger, U., Ferguson, M. J.; McDonald, R. *J. Am. Chem. Soc.* **2005**, *127*, 3921.

(35) Burford, N., Cameron, T. S., Clyburne, J. A. C., Eichele, K., Robertson, K. N., Sereda, S., Wasylishen, R. E.; Whitla, W. A. *Inorg. Chem.* **1996**, *35*, 5460.

(36) Davidson, R. J., Weigand, J. J., Burford, N., Cameron, T. S., Decken, A.; Werner-Zwanziger, U. *Chem. Commun.* **2007**, 4671.

(37) Weigand, J. J., Burford, N., Decken, A.; Schulz, A. *Eur. J. Inorg. Chem.* **2007**, 4868.

(38) Blattner, M., Nieger, M., Ruban, A., Schoeller, W. W.; Niecke, E. *Angew. Chem., Int. Ed.* **2000**, *39*, 2768.

(39) Rivard, E., Huynh, K., Lough, A. J.; Manners, I. *J. Am. Chem. Soc.* **2004**, *126*, 2286.

(40) Huynh, K., Lough, A. J.; Manners, I. *J. Am. Chem. Soc.* **2006**, *128*, 14002.

(41) Allcock, H. R. *Chem. Rev.* **1972**, *72*, 315.

(42) Gabler, D. G.; Haw, J. F. *Inorg. Chem.* **1990**, *29*, 4018.

(43) Murchie, M. P., Passmore, J., Sutherland, G. W.; Kapoor, R. *J. Chem. Soc., Dalton Trans.* **1992**, 503.

(44) Burford, N., Cameron, T. S., LeBlanc, D. J., Phillips, A. D., Concolino, T. E., Lam, K. C.; Rheingold, A. L. *J. Am. Chem. Soc.* **2000**, *122*, 5413.

(45) Niecke, E., Nieger, M., Reichert, F.; Schoeller, W. W. *Angew. Chem., Int. Ed. Engl.* **1988**, *27*, 1713.

(46) Huynh, K., Rivard, E., LeBlanc, W., Blackstone, V., Lough, A. J.; Manners, I. *Inorg. Chem.* **2006**, *45*, 7922.

(47) Huynh, K., Lough, A. J., Forgeron, M. A. M., Bendle, M., Soto, A. P., Wasylishen, R. E.; Manners, I. *J. Am. Chem. Soc.* **2009**, *131*, 7905.

(48) Cameron, T. S., Chan, C.; Chute, W. J. *Acta Crystallogr. Sect. B-Struct. Commun.* **1980**, *36*, 2391.

(49) Smith, M. B.; March, J., *March's Advanced Organic Chemistry: Reactions Mechanisms and Structure*, 5th, Wiley Interscience, New York, **2001**.

(50) Dimagno, S. G., Waterman, K. C., Speer, D. V.; Streitwieser, A. *J. Am. Chem. Soc.* **1991**, *113*, 4679.

(51) Feng, A. S., Speer, D. V., Dimagno, S. G., Konings, M. S.; Streitwieser, A. *J. Org. Chem.* **1992**, *57*, 2902.

(52) Waterman, K. C., Speer, D. V., Streitwieser, A., Look, G. C., Nguyen, K. O.; Stack, J. G. *J. Org. Chem.* **1988**, *53*, 583.

(53) Waterman, K. C.; Streitwieser, A. *J. Am. Chem. Soc.* **1984**, *106*, 3874.

(54) Weiss, R., Pomrehn, B., Hampel, F.; Bauer, W. *Angew. Chem., Int. Ed. Engl.* **1995**, *34*, 1319.

(55) Koch, A. S., Feng, A. S., Hopkins, T. A.; Streitwieser, A. *J. Org. Chem.* **1993**, *58*, 1409.

(56) Weiss, R., May, R.; Pomrehn, B. *Angew. Chem., Int. Ed. Engl.* **1996**, *35*, 1232.

(57) Bock, H., Nick, S.; Bats, J. W. *Tetrahedron Lett.* **1992**, *33*, 5941.

(58) Weiss, R., Puhlhofer, F., Jux, N.; Merz, K. *Angew. Chem., Int. Ed.* **2002**, *41*, 3815.

(59) Rivals, F.; Steiner, A. *Chem. Commun.* **2001**, 2104.

(60) Brasselet, S., Cherioux, F., Audebert, P.; Zyss, J. *Chem. Mater.* **1999**, *11*, 1915.

(61) Cherioux, F., Audebert, P.; Hapiot, P. *Chem. Mater.* **1998**, *10*, 1984.

(62) Shumeiko, A. E., Titskii, G. D., Kurchenko, L. P.; Vapirov, V. V. *Zhurnal Obshchei Khimii* **1986**, *56*, 2275.

(63) Steiner, T. *Acta Crystallogr. Sect. B-Struct. Commun.* **1998**, *54*, 456.

(64) Steed, J. W. *Chem. Soc. Rev.* **2009**, *38*, 506.

(65) Kubik, S. *Chem. Soc. Rev.* **2009**, *38*, 585.

(66) Berryman, O. B.; Johnson, D. W. *Chem. Commun.* **2009**, 3143.

(67) Bowman-James, K. *Acc. Chem. Res.* **2005**, *38*, 671.

(68) Gale, P. A. *Coord. Chem. Rev.* **2003**, *240*, 191.

(69) Allen, F. H. *Acta Crystallogr. Sect. B-Struct. Commun.* **2002**, *58*, 380.

(70) Cambridge Structural Database (CSD) Cambridge Crystallographic Data Centre, 12 Union Road, Cambridge, CB2 1EZ

(71) *Entries in CSD version 5.30 (November 2008).*

(72) Xie, X. B.; McCarley, R. E. *Inorg. Chem.* **1997**, *36*, 4011.

(73) Kawaguch.T, Tanaka, K., Takeuchi, T.; Watanabe, T. *Bull. Chem. Soc. Jpn.* **1973**, *46*, 62.

(74) Fourme, R.; Renaud, M. *Comptes Rendus Hebdomadaires Des Seances De L Academie Des Sciences Serie B* **1966**, *263*, 69.

(75) Spek, A. L. *J. Appl. Crystallogr.* **2003**, *36*, 7.

(76) Chandrasekhar, V.; Krishnan, V. *Adv. Inorg. Chem.* **2002**, *53*, 159.

(77) Bickley, J. F., Bonar-Law, R., Lawson, G. T., Richards, P. I., Rivals, F., Steiner, A.; Zacchini, S. *Dalton Trans.* **2003**, 1235.

(78) Ohms, U.; Guth, H. *Zeitschrift Fur Kristallographie* **1984**, *166*, 213.

(79) *VISTA - A Program for the Analysis and Display of Data Retrieved from the CSD.*

(80) Singh, R. P., Vij, A., Kirchmeier, R. L.; Shreeve, J. M. *Inorg. Chem.* **2000**, *39*, 375.

(81) Golinski, F.; Jacobs, H. *Z. Naturforsch.* **1994**, *620*, 965.

(82) Bartlett, S. W., Coles, S. J., Davies, D. B., Hursthouse, M. B., Ibisoglu, H., Kilic, A., Shaw, R. A.; Un, I. *Acta Crystallogr. Sect. B-Struct. Commun.* **2006**, *62*, 321.

(83) Bondi, A. *J. Phys. Chem.* **1964**, *68*, 441.

(84) Allen, C. W. *Chem. Rev.* **1991**, *91*, 119.

(85) Louerat, F., Gros, P. C.; Fort, Y. *Synlett* **2006**, 1379.

Chapter 4:

Oxo-Functionalized Cyclophosphazenes

4.1. Introduction

This chapter will focus on the direct functionalization of the phosphazene ring to produce oxo-phosphazenes from geminal chlorides. This area of phosphazene chemistry has received little attention, in comparison to the modification of the molecular periphery of cyclophosphazenes. Herein, we present simple routes to cyclotriphosphazenes that feature oxo-functions at one ring phosphorus centre, while the other phosphorus atoms are protected with amino groups. Starting from di- and tetra-chlorides $Z_4P_3N_3Cl_2$ and $Z_2P_3N_3Cl_4$ (Z = NHR, NR_2) we have prepared the zwitterionic phosphate **D**, the pyrophosphate **E**, the phosphamide **F** and the phosphite **G** (Figure 4.1).

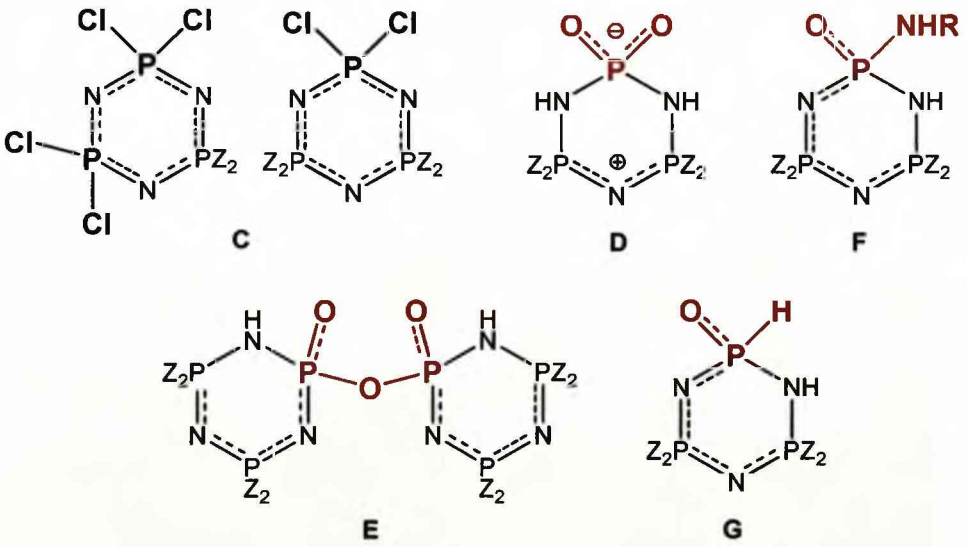

Figure 4.1.

There are very few reports of structurally characterized cyclotriphosphazenes containing oxo-functions. These are mainly limited to compounds containing ester (=P(O)OR) and phosphamide (=P(O)NHR)

units.[1-4] Their synthesis tends to be from lengthy manipulations of organic substituents or the fortuitous hydrolysis of chloro functions, which forms a P=O bond and protonates the adjacent ring nitrogen site.[1-11] As a result the P(O)-N(H) and N(H)-P(R) ring bonds become substantially elongated.[1-4] Therefore these compounds can be regarded as hybrids between formally unsaturated phosphaz*e*nes and saturated phosphaz*a*nes.

No accounts of pyrophosphates derived from cyclophosphazenes have been reported. However, there are limited examples of oxygen-bridged cyclotriphosphazenes in the literature. These include structural accounts of dimerised penta- and tri-chloro-hydroxyphosphazenes[12-14] and an oxygen bridged phosphamide derivative.[2] In addition, there is a cyclocarbophosphazene which contains P-O-P and P-O-Cu linkages.[15] The hydrolysis of $N_3P_3Cl_6$, has received extensive attention, particularly in view of the ring opening polymerisation.[16-20] The complete hydrolysis of $N_3P_3Cl_6$ yields the trimetaphosphimate ion $[N_3H_3P_3O_6]^{3-}$, **4.1** (Figure 4.5), which is the only structurally characterized phosphorus nitrogen ring system that contains dioxo phosphate centres $[=PO_2]^-$.[21-23] This trianionic ligand is a versatile building block for solid state compounds, but applications are limited to highly polar solvents.[22] A number of oxo-derivatives of saturated phosphorus nitrogen rings have been described. These include, trioxophosphazanes $(RNP(O)OR)_3$, which contain six-membered rings and are generated by the thermal rearrangement of $(RO)_6P_3N_3$[11,21,24,25] along with numerous compounds featuring four-membered P_2N_2 rings.[26-30]

4.1.1. The Hydrolysis of $N_3P_3Cl_6$

The hydrolysis of $N_3P_3Cl_6$ has been studied in great detail.[16-19] Incentives for these investigations include, the role of water in the ring-opening polymerization of the trimer, to give polyphosphazene $(Cl_2PN)_n$ and possible biomedical applications of phosphazenes.[18-20]

The ring-opening polymerisation of $N_3P_3Cl_6$ (Figure 4.2) has proved to be a complex and fickle reaction, where reaction times and quality of polymer produced can vary extensively by changing the batch of $N_3P_3Cl_6$ or even the glassware.[20] Therefore trace impurities were thought to have an important role in this polymerisation and this has lead to many catalytic and mechanistic studies. [18,20] These include the role of PCl_5 and in particular that of water, which is thought to have both a beneficial and detrimental role in the polymerization.[18]

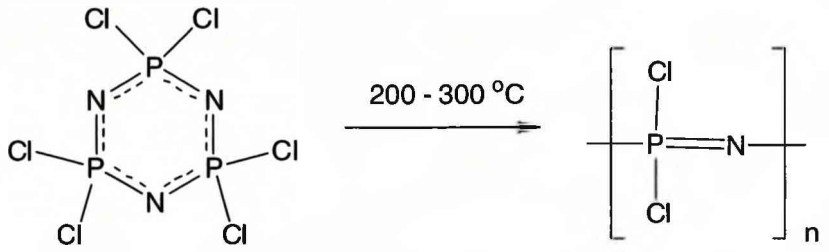

Figure 4.2. Ring Opening Polymerisation of $N_3P_3Cl_6$.

Studies by Allcock et al. and Haw et al. both suggest that the polymerization is initiated by hydrolyzed species, which ring open at elevated temperatures and that completely dry samples of $N_3P_3Cl_6$ may never undergo ring-opening polymerization.[18,20] These initiator species are thought to be the partially hydrolysed chloro derivatives, **4.2a – 4.2d**, in particular the mono-hydroxy derivative.[18,20,21]

Haw et al studied the hydrolysis of $N_3P_3Cl_6$ in THF with ^{31}P NMR spectroscopy and observed the stepwise formation of the hydroxy derivatives; mono-, gem-di-, non-gem-*cis*-di-, non-gem-*trans*-di- and the tri-hydroxy cyclotriphosphazene (Figure 4.3).[18] The existence of **4.2a** and ***4.2c-cis/trans*** have been further confirmed by reports of their crystal structures as salts with $[AsPh_4]^+$, $[KC_{12}H_{24}O_6]^+$ and $[N(C_4H_9)_4]^+$.[17,19] However, to our knowledge, **4.2b** and **4.2d** have not been structurally confirmed.

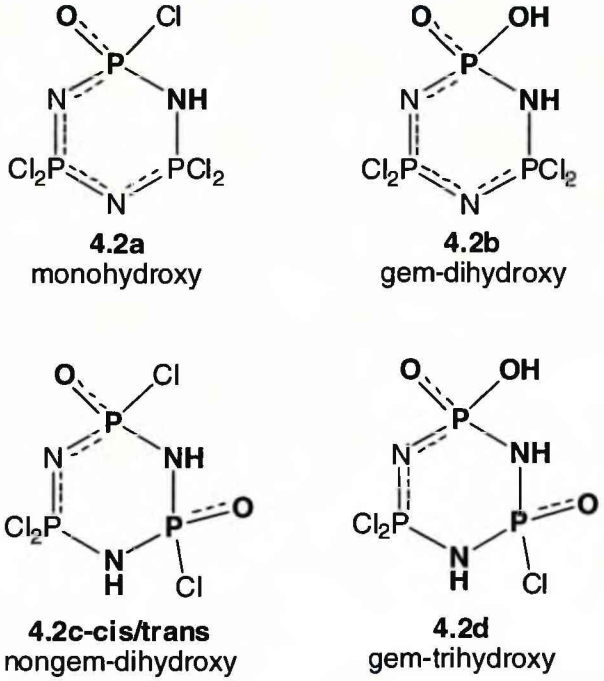

Figure 4.3

In contrast to this, more than one mol percent of water in the chloride trimer sample increases the formation of undesirable cross linked polymer.[18,20] Haw et al. reported the precursors of the cross linked polymer as the dimers **4.3a** and **4.3b**, which contain bridging oxygen moieties, see Figure 4.4.[18] These dimers were reportedly formed in solutions of $N_3P_3Cl_6$ in THF and water which had been reacting for several days, their formation was deduced by the appearance of A_2X and A_2M spin systems.[18] However, Van de Grampel has since disputed this as he claims that oxygen bridged phosphazenes of this form would cause an $A_2A'_2XX'$ pattern.[16] This assignment is taken from the structural determination of **4.3b** and ^{31}P NMR studies on the analogous **4.3c**, $(N_3P_3Ph_5)O(N_3P_3Ph_5)$ reported by Keats et al.[14,16,31]

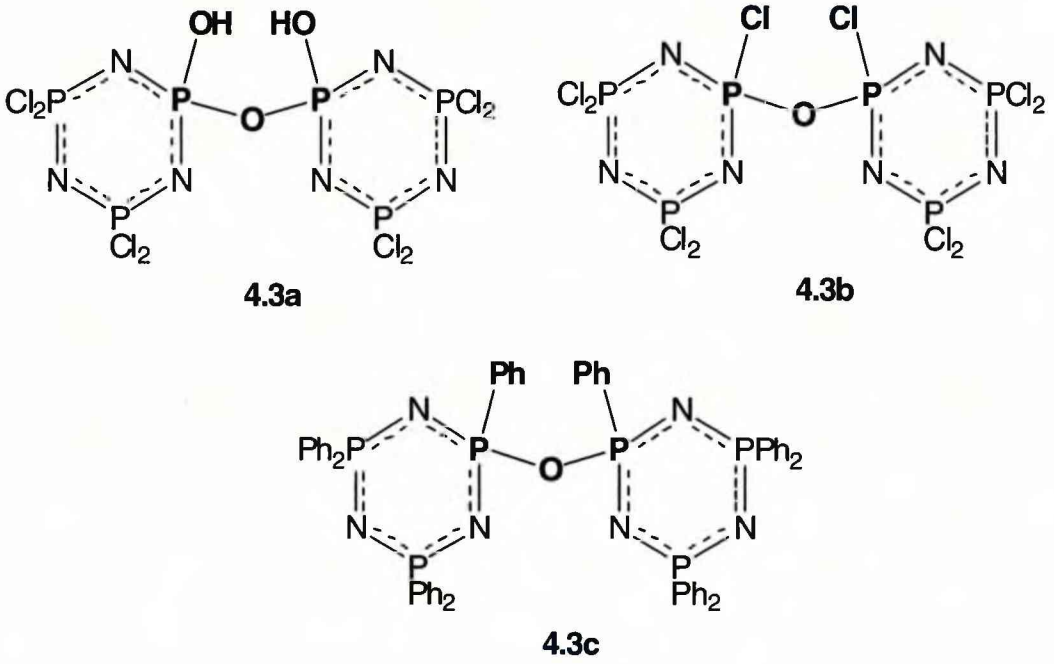

Figure 4.4. Oxygen Bridging Cyclotriphosphazene Dimers.

The complete hydrolysis of $N_3P_3Cl_6$ to $N_3H_3P_3O_6H_3$, **4.1**H_3 has also received extensive investigations (Figure 4.5).[21-23] $N_3P_3Cl_6$ has often been described as a hydrolytically unstable species, however its hydrolysis is actually slow compared to other phosphorus chloride compounds, although reaction times are greatly facilitated by the presence of an auxiliary base.[16,20] It has been well known for many years that **4.1**H_3 exists as its metaphosphimic acid form, which is susceptible to further hydrolysis resulting in phosphoric acid and ammoia.[23]

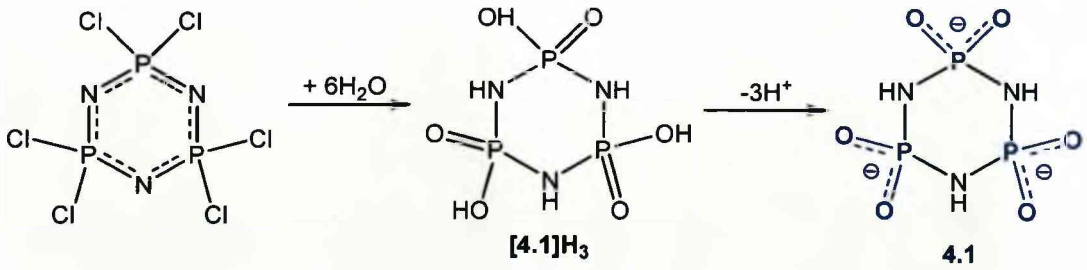

Figure 4.5. The Complete Hydrolysis of $N_3P_3Cl_6$ and Subsequent Deprotonation to the trimetaphosphimate ion 4.1.

Deprotonation of **4.1**H_3 yields the trimetaphosphimate ion **4.1** (Figure 4.5), which is the only structurally characterized phosphorus nitrogen ring system that contains dioxo phosphate centres $[=PO_2]^-$.[22] The trianionic ligand is a versatile building block for solid state compounds, but applications are limited to highly polar solvents.[22] Crystal structures of **4.1** containing monovalent cations have been obtained, these structures show that $[(PO_2NH)_3]^{3-}$ units tend to adopt a chair conformation and are connected via NH...O hydrogen bonds to form extended networks.[22] **4.1** can also coordinate as either a polydentate or bridging ligand to form phosphimatometallates and although theoretically this could occur either through oxygen or nitrogen it is predominately observed through oxygen.[22]

4.1.2. Oxo-Phosphazanes

Several oxo-derivatives of saturated phosphorus nitrogen rings have been described.[11,24,25] These include a series of trioxophosphazanes $(RNP(O)OR)_3$, **4.4**, which are analogues to **4.1**. They form by thermal rearrangement of $(RO)_6P_3N_3$ (Figure 4.6), which can be catalysed by the addition of alkyl halides.[21,24] The mechanism is thought to consist of nucleophilic attack by the ring nitrogen on the R group.[24] However it is not clear whether the attack is intra- or inter-molecular.[21,24] Ring nitrogen atoms of cyclophosphazenes undergoing nucleophilic attack is not unprecedented as quaternized amino cyclophosphazenes are known to form in this manner, as shown in Figure 4.7.[32]

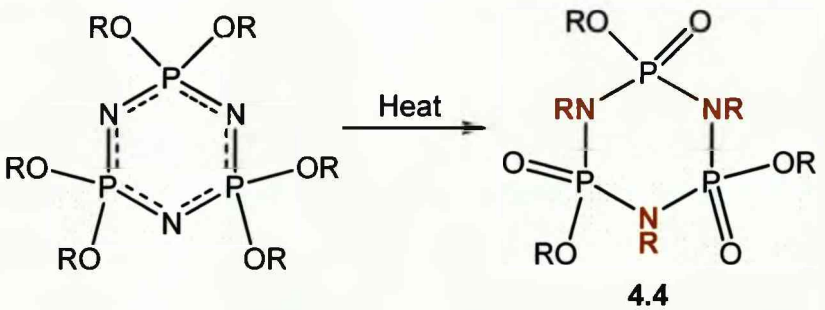

4.4

Figure 4.6

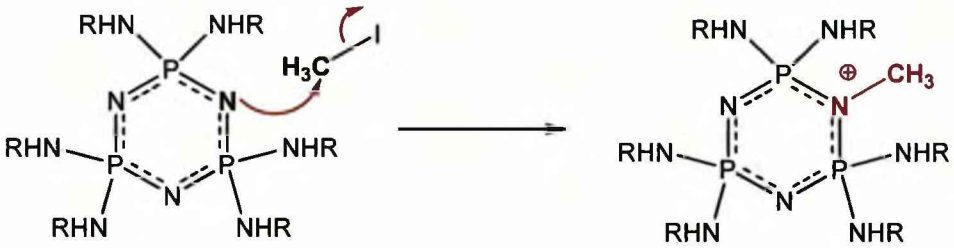

Figure 4.7. Quarternization of Amino Cyclophsphazenes.[32]

Shaw et al prepared a number of alkoxy derivatives of **4.4**, however aryloxy and fluoroalkoxy cyclophosphazenes would not rearrange.[24] The methyl derivatives **4.4a** and the **4.4b** have been structurally characterised, see Figure 4.8.[11,25] Both compounds adopt twisted boat conformations.[11] Other cyclic phosphazanes which carry oxo-functions at P feature four-membered P_2N_2 rings (Figure 4.9) and are obtained by either controlled oxidation or hydrolysis of P(III) centers.[26-30]

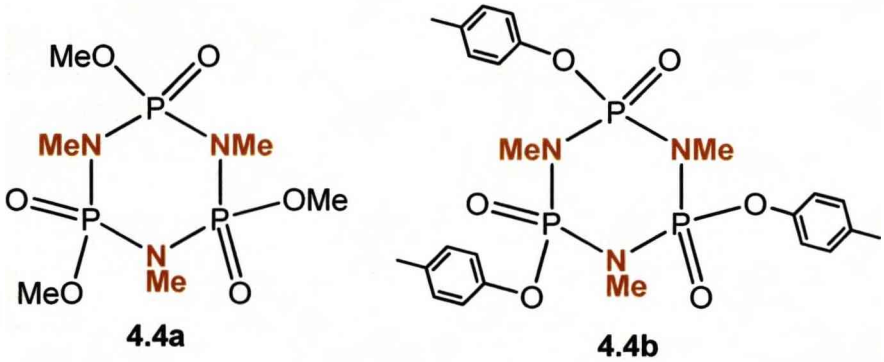

Figure 4.8

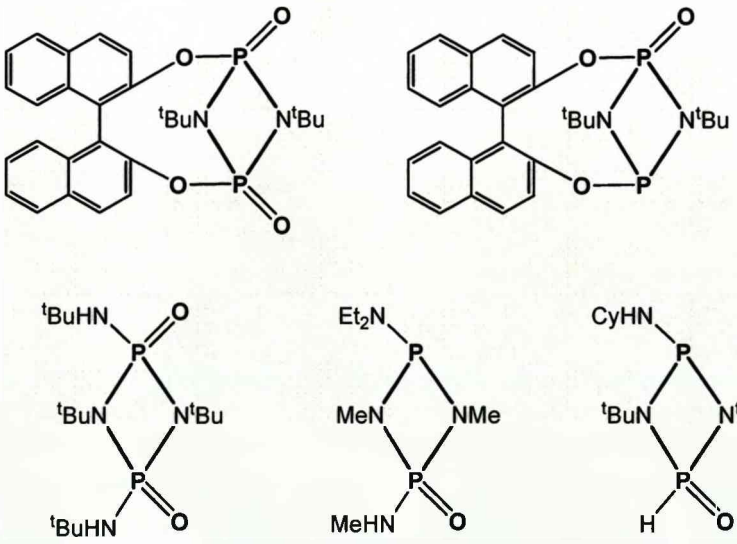

Figure 4.9. Examples of Four Membered Phosphazane Rings.

4.1.3. Synthesis and Structure of Oxo- functionalised Organophosphazenes

4.1.3.1. Hydrolysis of Organophosphazenes

There have been several accounts of the hydrolysis of organophosphazenes to produce phosphamide and ester derivatives of cyclotriphosphazenes.[2,5-8] These reports involve the hydrolysis of the organic substituents of cyclotriphosphazenes, rather than P-Cl bonds, to produce mono-hydroxy derivatives of the parent organophosphazene. Interest in this area has risen from possible biomedical applications of organophosphazenes, such as drug delivery, which require a detailed knowledge of their hydrolytic behaviour and stability.[6-8] When considering this method as a viable synthetic route to functionalising cyclotriphosphazenes it is clear that it can be applied to specific systems, but as a universal method it is limited. In particular, organoamino groups bind very strongly to the phosphazene ring, therefore hydrolysing the P-N bond to produce phosphamide derivatives can prove difficult.

In 1967 Shaw et al. presented the synthesis of several ester derivatives of cyclotriphosphazenes, **4.5 – 4.9** (Figure 4.10).[5] Compounds **4.6 – 4.9** were produced as by-products when substituting chloro groups with the relevant alcohol, as shown in Figure 4.11.[5] The report concluded that the oxo-phosphazenes were unlikely to have formed via the hydrolysis of P-Cl units either in the starting materials or in mono-chloride intermediate, since the reactions were carried out under anhydrous conditions.[5] However, they have stated that hydrolysis of the alkoxy group may have occurred during work up and under these conditions any mono-chloride intermediate would also be likely to hydrolyse.[5] Their conclusion was that **4.6 – 4.9** form mostly via attack of an alkoxide ion on P-Cl, followed by loss of alkyl halide.[5] This pathway is somewhat dubious, given more recent accounts of alkoxy-phosphazene synthesis. **4.5** was prepared separately from its mono-chloride (Figure 4.12) to aid in the structure determination of **4.6 – 4.9**.[5]

However its synthesis illustrates the ease of hydrolysing mono-chloride alkoxy phosphazenes.

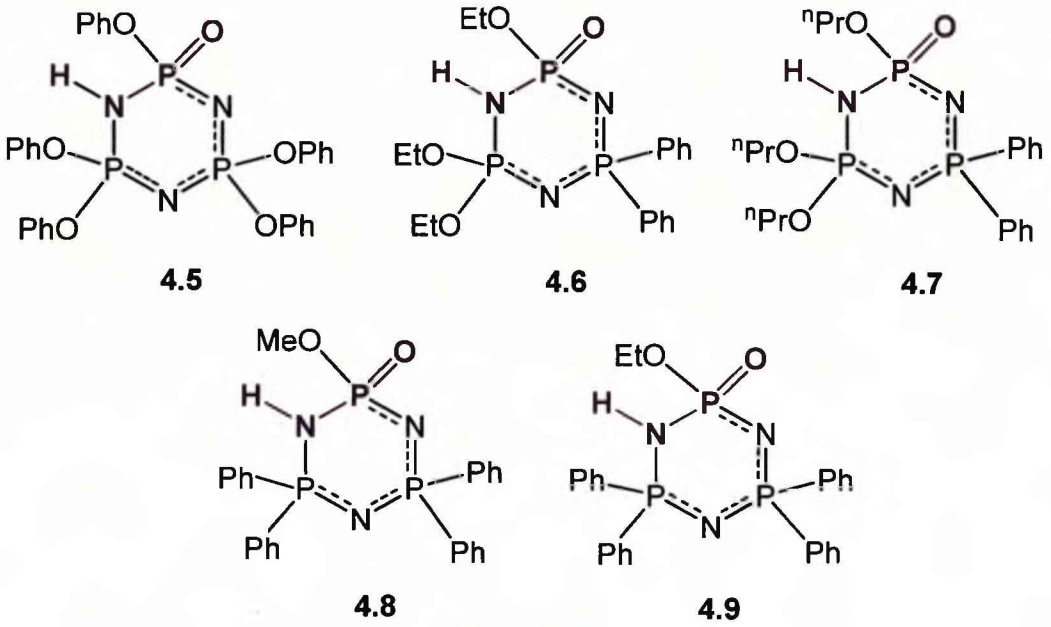

Figure 4.10

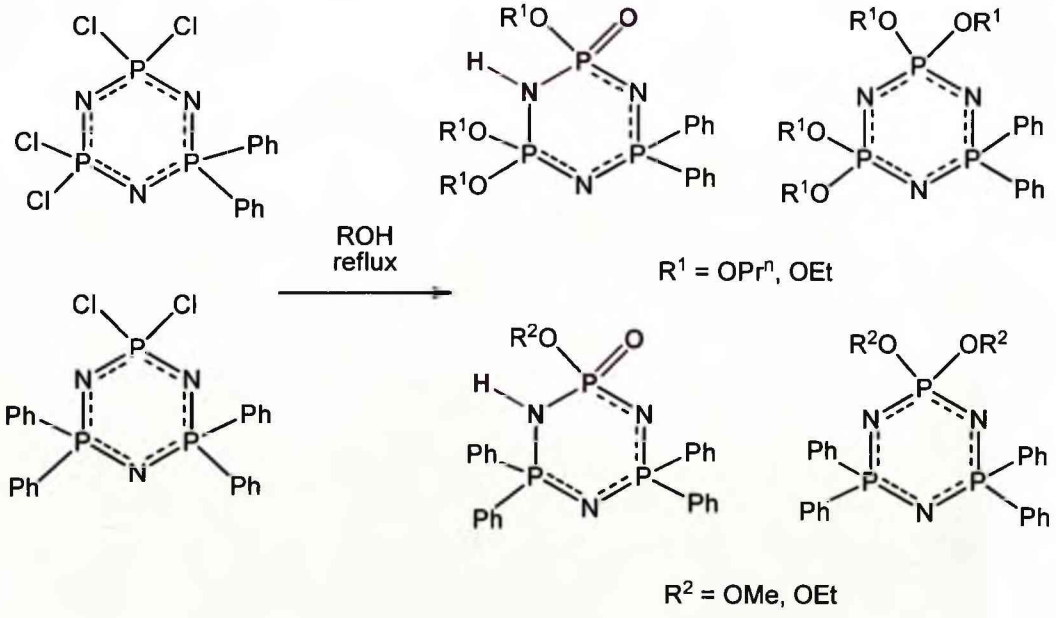

Figure 4.11.

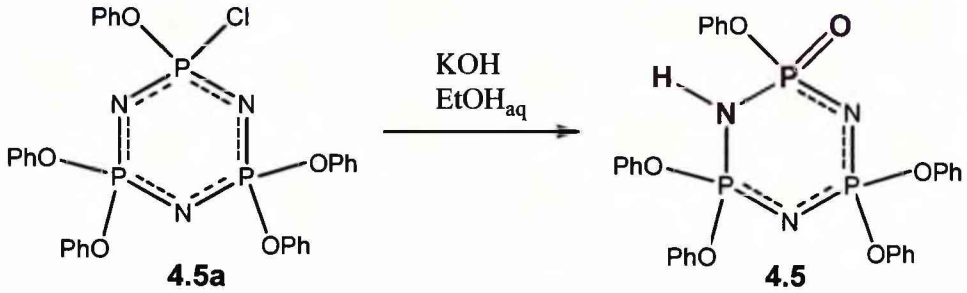

Figure 4.12.

In 1969 Allcock et al. reported the stepwise nongeminal hydrolysis of the hexa- trifluoroethoxy phosphazene, **4.10**.[6] This was achieved using sodium hydroxide in an aqueous methanol solution and the mono- and di- hydroxy derivatives, **4.10a** and **4.10b**, were isolated, see Figure 4.13.[6]

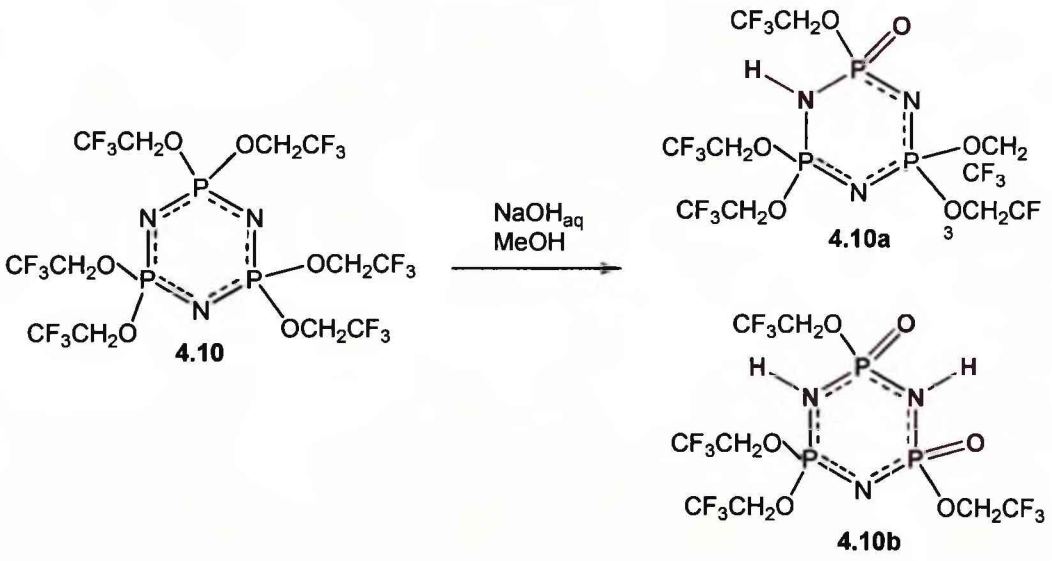

Figure 4.13.

Allcock et al. then went on to publish a detailed study into the hydrolytic behaviour of amino phosphazenes in the 1980s.[7,8] This study incorporated two routes for the synthesis of phosphamide derivatives of phosphazenes.[8] The first route was discussed for compounds **4.11** – **4.22** (Figure 4.15) and involved hydrolysing amino groups of the parent cyclotriphosphazene. The hydrolysis was studied in neutral, acidic and basic media by ^{31}P NMR spectroscopy.[8] **4.11** – **4.15** were all reported to hydrolyse in water at 100°C

(Figure 4.14) and decompose to phosphoric acid, ammonium ion and amine salts in acid media. Under basic conditions hydrolysis occurred at a reduced rate with **4.11**, **4.14** and **4.15** and was not observed for **4.12** and **4.13**.[8] Compounds **4.16 – 4.22** were reported to be hydrolytically stable in neutral and basic media but were not studied in acidic media due to solubility issues.[8] The second route was only mentioned for ammonia, methylamine, ethyl glycinate and imidazole derivatives, **4.11a - 4.13a** and **4.15a**.[8] Here mono-hydroxy phosphazene derivatives were synthesised via the hydrolysis of $N_3P_3Cl_6$ to produce the sodium salt of **4.2a**, followed by reaction with the relative amine, see Figure 4.14.[8]

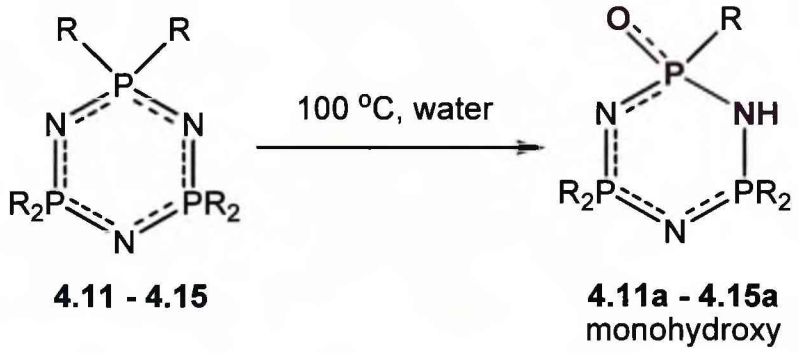

4.11 - 4.15

4.11a - 4.15a
monohydroxy

Figure 4.14. Hydrolysis of Amino Cyclophosphazenes as Reported by Allcock et al.[8]
Above: Reaction Scheme for Successful Hydrolysis using Route 1.
Below: Reaction Scheme for Hydrolysis by Route 2.

Figure 4.15 (below) shows compounds 4.11 - 4.22, which were used in the Study

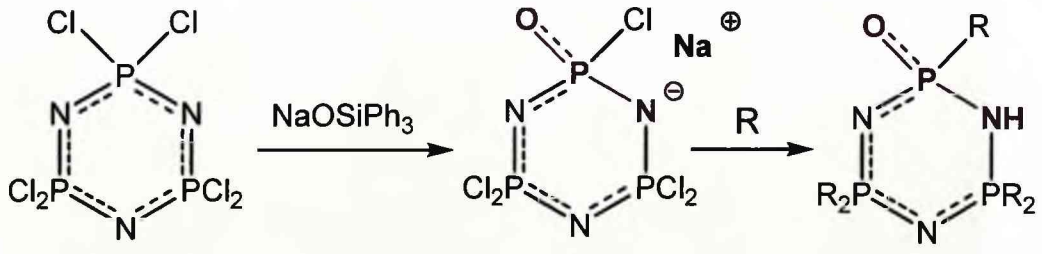

[4.2a]Na

4.11a - 4.13a, 4.15a
monohydroxy

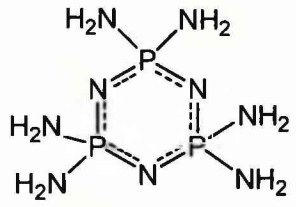

4.11

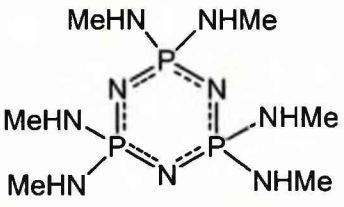

4.12

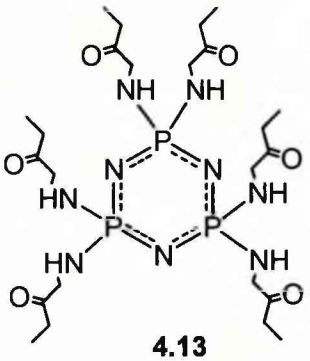

4.13

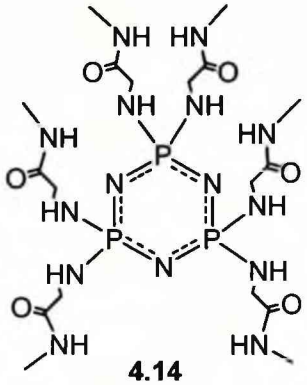

4.14

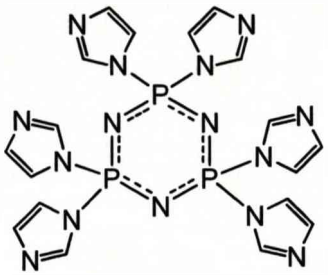

4.15

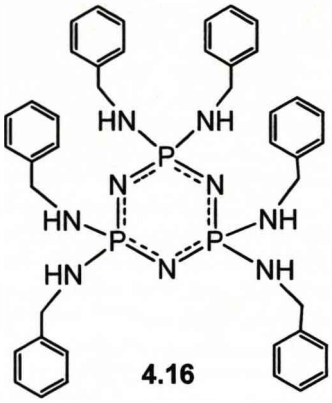

4.16

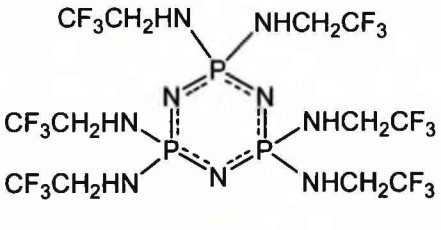

4.17

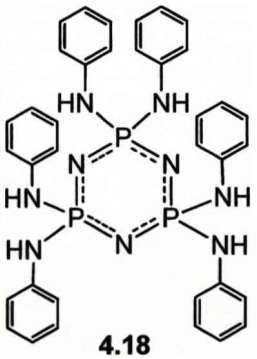

4.18

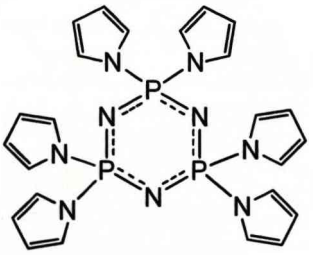

4.19

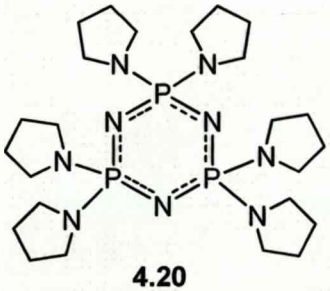

4.20

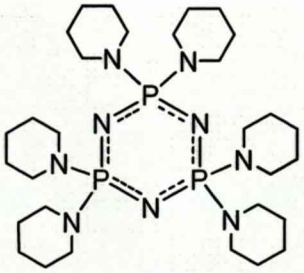

4.21

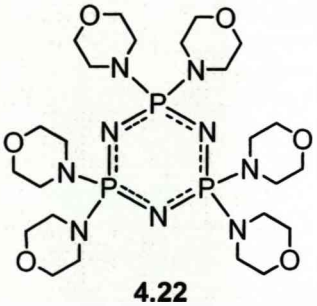

4.22

Figure 4.15.

A final example of phosphaminde synthesis was reported by Chandrasekaran et al. in 1994 (Figure 4.16).[2] The spirocyclic cyclotriphosphazene palladium complex **4.23** forms via cleavage of the P-N(amino) bond. This is facilitated by the coordination of N to the Pd centre, thus weakening the P-N bond.[2] This reaction yielded the mono metallic complex **4.23a** and the bimetallic dimer, **4.23b**; the mono- complex being the major species.[2] Both complexes were structurally characterised. **4.23a** adopts the expected P(O)-N(H) tautomer, whereas the dimer **4.23b** does not contain any ring NH functions.

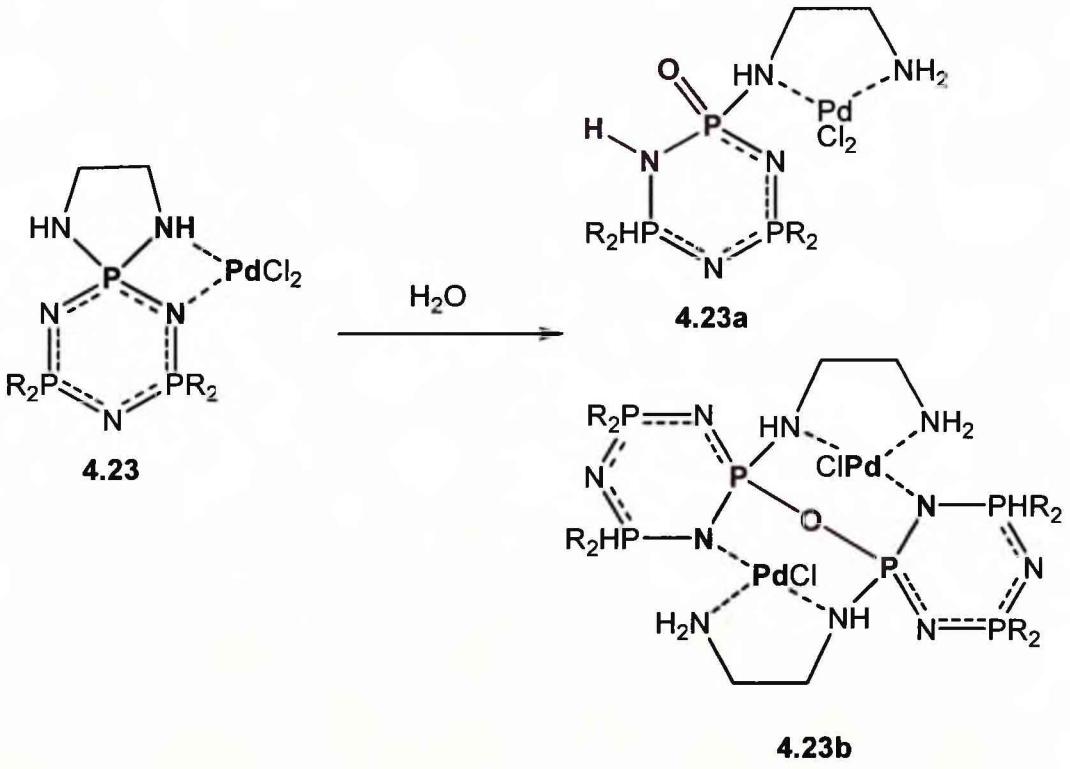

Figure 4.16.

4.1.3.2. Phosphamide Synthesis from Chlorophosphazenes.

Reports of phosphamide synthesis by hydrolysis of P-Cl units are limited. We have already mentioned the method reported by Allcock, in which one P-Cl bond of $N_3P_3Cl_6$ is hydrolysed to produce the intermediate **4.2a**, which then undergoes aminolysis.[8] However, accounts of hydrolysing P-Cl bonds

on aminophosphazenes are virtually non-existent and where they do occur it appears to be the result of fortuitous hydrolysis.[1] For example, Shaw et al. reported the hydrolysis of the ansa cyclophosphazene derivative **4.24** to **4.25**, while attempting to replace all P-Cl functions with aniline ($PhNH_2$), see Figure 4.17.[1] It is worth noting here that they only reported hydrolysis of the P(Cl)(NHR) function and the PCl_2 group was successfully replaced to $P(NHPh)_2$.[1] **4.25** was characterised structurally and in line with previous reports for oxo-phosphazenes it adopted the P(O)-N(H) tautomer, with a distorted P_3N_3 ring due to an elongated P-N(H)-P distance of 3.059 Å.[1]

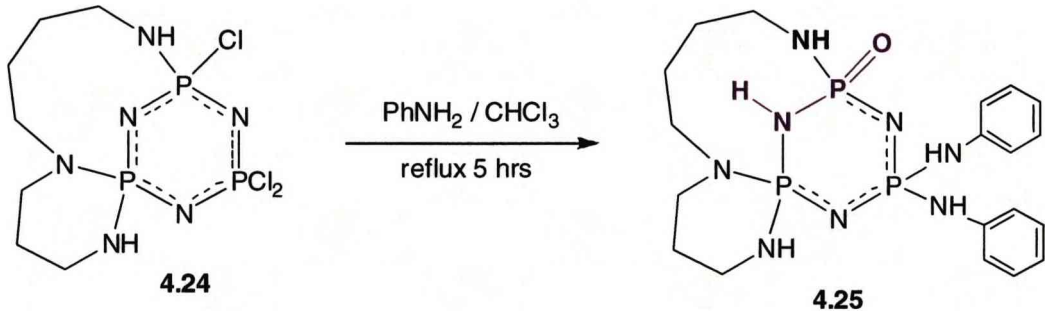

Figure 4.17.

4.1.3.3. Structural Determinations of Oxo-Phosphazenes

The structural characterization of ester and phosphamide phosphazene derivatives has been discussed in the literature.[1-10] However, these reports mainly focused on the possible tautomeric forms and the geometry of the phosphazene ring rather than their extended supramolecular structures. The tautomeric forms of oxo-cyclotriphosphazenes have been analysed with a variety of tools; from infra red spectra in the1960s,[5] to ^{31}P NMR studies in the 1980s[9,10] and more recently by x-ray crystallography.[1-4] These studies all considered the possible tautomeric forms **i** – **iv** (Figure 4.18) and have concluded that oxo-phosphazenes, of this type, exist as tautomers **ii** and **iii**. Species **i** and **iv** have never been observed and ^{31}P NMR studies indicate that dynamic exchange between **i** and (**ii-iii**) does not occur.[4,9,10]

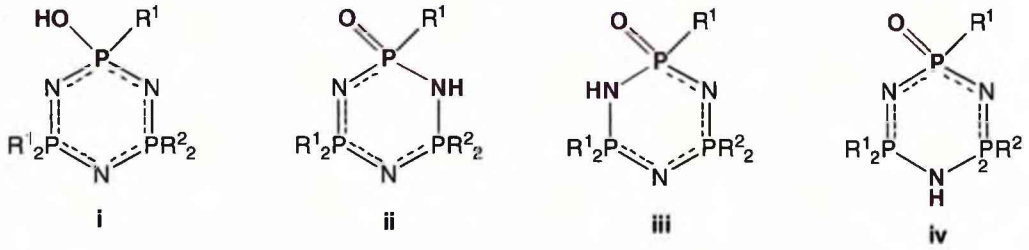

Figure 4.18. Possible Tautomeric Forms of Ester and Phosphamide Cyclophosphazenes.

When $R^1 = R^2$ conformations **ii** and **iii** are indistinguishable due to proton exchange between equivalent sites.[9] Where $R^1 \neq R^2$, ratios of **ii**:**iii** vary depending on the basictity of the protonation sites, as a result of the R substituents.[4,9] Examples of tautomer ratios are given below in Table 4.1.[4]

R^1	R^2	ii:iii
OMe	Ph	4:1
OPr^n	Ph	2:1
NEt_2	Cl	0:1
OMe	$NHBu^t$	1:0

Table 4.1. Ratios of Tautomers ii:iii when $R^1 \neq R^2$.[4]

X-ray crystallographic data shows that phosphamide and ester derivatives of cyclotriphosphazenes adopt distorted ring structures with elongated P-N(H)-P distances above 3.2 Å.[1-4] The exact ring conformations differ from molecule to molecule, however they all deviate from planarity usually observed in cyclotriphosphazene rings.[33] Ester and phosphamide derivatives of phosphazenes clearly display structural differences to non-functionalized cyclotriphosphazenes. This can be rationalized by considering them as hybrids between formally unsaturated phosphaz*e*nes and saturated phosphaz*a*nes. Table 4.2 illustrates this by comparing P-P non-bonded distances of functionalized and non-functionalized cyclotriphosphazenes, with those of cyclotriphosphazanes.

Compound	P-N(H)-P / Å	P-N-P / Å
4.23a[2]	3.328[2]	3.17[2*]
4.25[1]	3.059[1]	2.815[1*]
***gem*-$N_3P_3Ph_2(OMe)_3OH$**[4]	3.335[4]	3.1535[4*]
4.5[3]	3.292[3]	3.1315[3*]
$N_3P_3(NHR)_6$[33]		3.2[33*]
$N_3P_3(O_2C_6H_4)_3$[34]		3.144[34*]
$N_3P_3Cl_6$[35]		3.162[35*]
$N_3P_3(NH(CH_2)_3N(CH_2)_4NH)R_2$**[1]		2.734 - 2.819[1*]
4.4a[25]	3.326[25*]	
4.4b[11]	3.319[11*]	

Table 4.2. P-P Non-Bonding Distances of Cyclotriphosphazenes and Cyclotriphosphazanes.

*Values are averaged, **R = Cl, NHPh, OMe

4.1.3.4. P-O-P Bridged Cyclotriphosphazenes

We have already mentioned the oxygen bridged cyclotriphosphazenes **4.3a-4.3c** (Figure 4.4), as reported by Haw, Brandt and Keat.[14,18,31] **4.3a** and **4.3b** are reported hydrolysis products of $N_3P_3Cl_6$, however **4.3a** has only been identified by ^{31}P NMR and its identification has been disputed.[14,16,18] On the other hand, two polymorphs of **4.3b** have been structurally characterised.[13,14] Brandt et al reported the formation of **4.3b** as a hydrolysed side product in the polycondensation reaction of **1** with the monosodium salt of uracil and the phase transfer catalyst Bu_4NBr.[14] Brinek et al. again reported **4.3b** as a

by-product, however this was obtained via the reaction of the penta-fluoro-aminophosphazene, $N_3P_3F_5(NH_2)$, **4.26** with $SOCl_3$ (Figure 4.19).[13] **4.3b** was isolated from a mixture of the reactant **4.26** and its three products $P_3N_3Cl_5NSO$, **4.27**, $P_3N_3Cl_5NSNCl_5N_3P_3$, **4.28** and $P_3N_3Cl_5NSCl_2$ **4.29** after the removal of excess $SOCl_2$.[13] Structurally, these accounts indicate that **4.3b** contains a somewhat flexible central P-O-P angle, varying from 122.9 to 135.6 Å.[13,14]

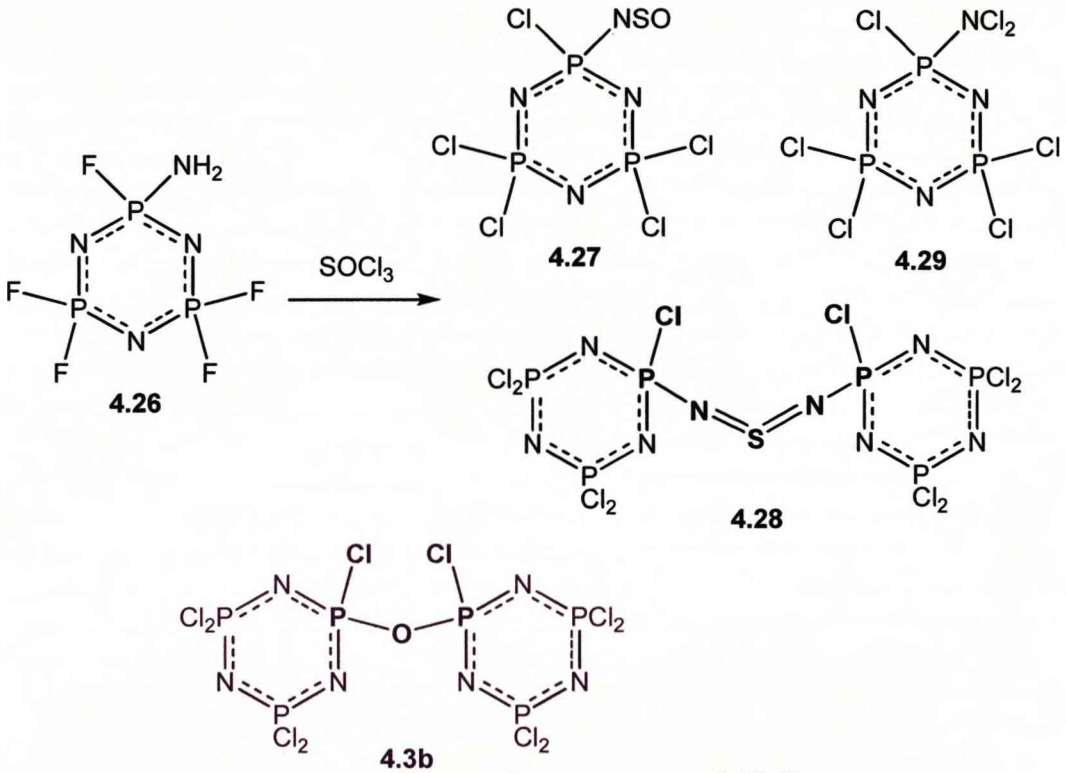

Isolated from the above reaction mixture after the removal of $SOCl_3$

Figure 4.19.

More recently, Panzner et al have reported the crystal structure of a hydrolysed dimeric tri-chloro phosphazene anion, $[(N_3P_3Cl_3O)_2O_2]^{2-}$, **[4.30]**$[Ag(C_6H_{10}N_2)_2]_2$.[12] The dianion **[4.30]**$^{2-}$ is a hydrolysed product of $N_3P_3Cl_6$ formed in the reaction of the silver carbene complex $[Ag(C_6H_{10}N_2)_2]Cl$ with $N_3P_3Cl_6$ and water, see Figure 4.20.[12] This dianion is a dimer of two partially hydrolysed phosphazene rings connected by two P-O-P bridging units.[12] The bridging P-O-P bonds are inequivalent (one

measuring 1.657(3) Å and the other 1.578(3) Å) and each P_3N_3 ring has two short P-N bonds (av. 1.555 Å).[12]

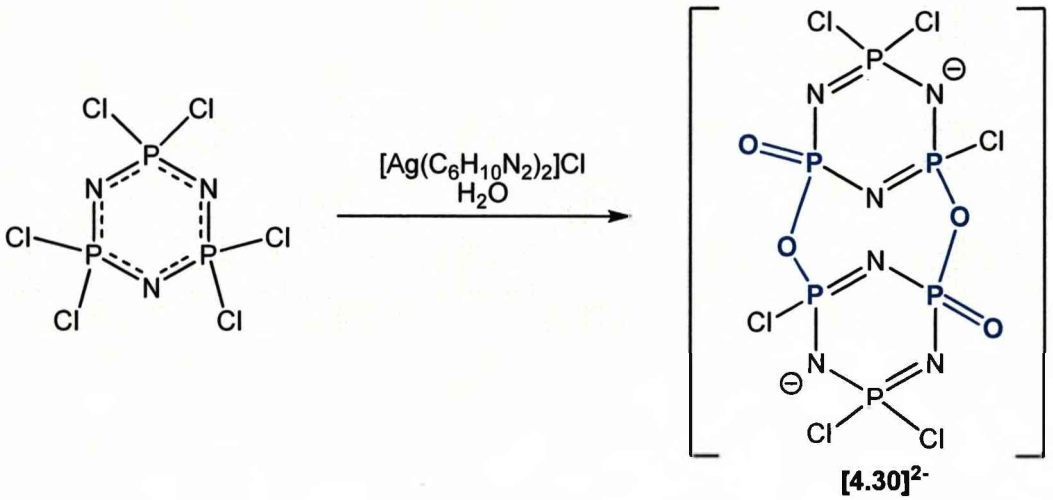

Figure 4.20.

A copper complex of a pyrophosphate compound derived from a cyclocarbaphosphazene has been structurally described. Complexes **4.31** and **4.32** contain a P-O-Cu linkage, in addition to the bridging pyrophosphate unit (O)P-O-P(O), see Figures 4.21 and 4,22.[15] They are formed by reaction of the hexakis-pyrazole cyclocarbophosphazene derivative, [(NP(3,5-$Me_2Pz)_2$)(NC(3,5-$Me_2Pz)_2)_2$], with copper chloride or copper bromide, in the presence of moisture.[15] The P_2O_3 chain of **4.31** and **4.32** adopts both cis-cis and trans-trans arrangements.[15]

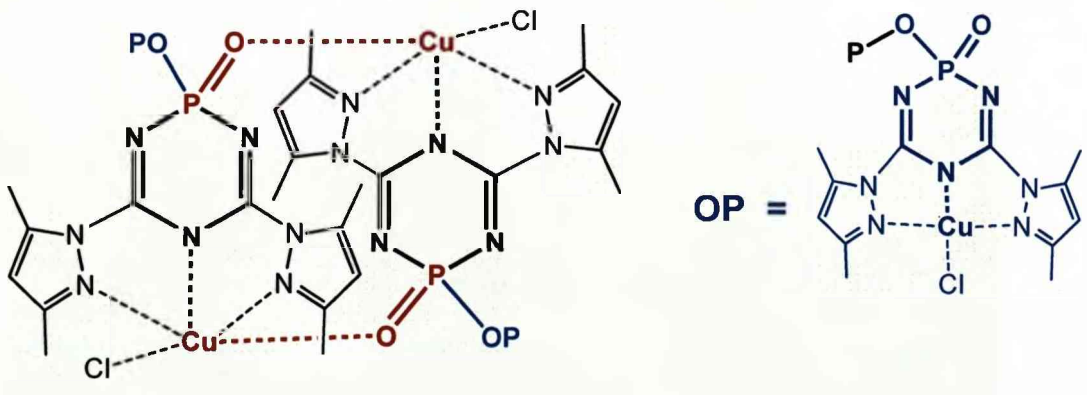

4.31

Figure 4.21. Schematic of Complex 4.31.

-Showing P-O-Cu linkage.

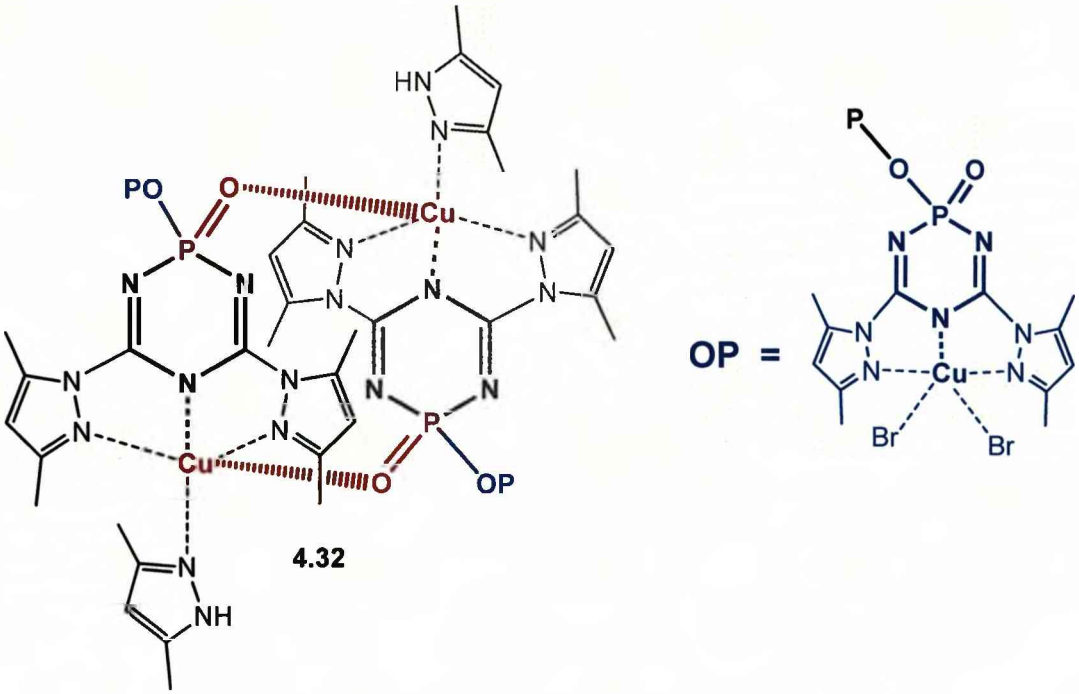

Figure 4.22. Schematic of Complex 4.32.

-Showing P-O-Cu linkage.

4.2. Results and Discussion

4.2.1. Synthesis of Di- and Tetra-Chlorides

Geminal di- and tetra-chloro phosphazenes **C** (Figures 4.1 and 4.23) are obtained by stoichiometric reactions of $N_3P_3Cl_6$ with either a primary, branched alkyl amine or ethylene and propylene diamines.[36-39] Here, our investigations have concentrated the di-chloro cyclohexyl amino derivative **4.33**, $N_3P_3(NHCy)_4Cl_2$ and the spirocyclic di- and tetra- chloro N,N'-diethyl propylene diamino derivatives **4.34**, $N_3P_3(N(Et)(CH_2)_3NEt)_2Cl_2$ and **4.35**, $N_3P_3(N(Et)(CH_2)_3NEt)Cl_4$, although some work has also been done on the di-chloro *tert*-butyl derivative **4.36**, $N_3P_3(NH^tBu)_4Cl_2$.

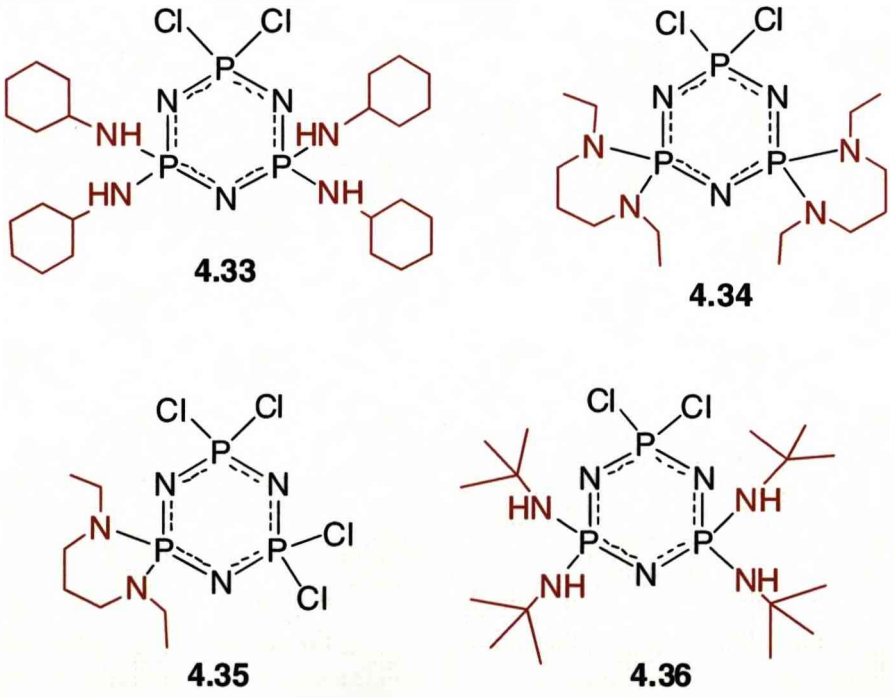

Figure 4.23. Geminal di- and tetra-Chloro Cyclotriphosphazenes (C).

Varying the amino function around the phosphazene ring was an important key to the synthetic approach of this investigation. It illustrates how the molecular periphery of a phosphazene ring governs not only the properties, both in molecular and supramolecular terms, but also the reactivity of the entire system resulting in different synthetic approaches being required for

varying amino derivatives. Our choices for amino derivatives were governed by several factors; the geminal substitution pathway of amines, the chemical inertness of amino phosphazenes and the ability to form supramolecular structures via N-H...N bonds, which aides crystal growth.

4.36 is the sole product when $P_3N_3Cl_6$ is reacted at elevated temperature with an excess of *tert*-butyl amine (Figure 4.24), as the hexakis- derivative, $N_3P_3(NHBu^t)_6$ only forms under autoclave conditions.[33,39,40] However, it turned out that **4.36** was a relatively unreactive geminal di-chlorophosphazene, due to the extreme bulk of *tert*-butyl amine.[33,40]

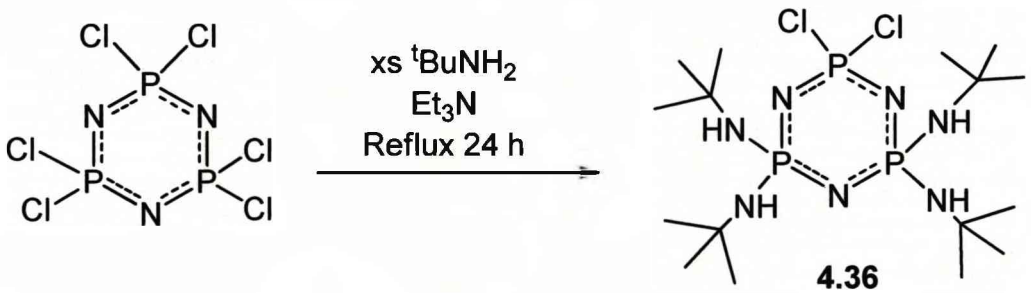

Figure 4.24.

Thus the less bulky cyclohexyl derivative **4.33** was chosen to be the main subject of this study as it is more reactive than **4.36**.[33] The substitution pattern of cyclohexyl amine on $N_3P_3Cl_6$ has been studied by Chandrasekaran et al.[36] They found that under reflux conditions full substitution occurs relatively slowly via the formation geminal isomers of the bis- and tetrakis-amino derivatives.[36] During the course of this project an improved method for the synthesis of **4.33** was found, see Figure 4.25. When slightly more than four equivalents of cylcohexylamine, and excess triethylamine used under reflux conditions, a product mix of **4.33** and **4.37** $N_3P_3(NHCy)_6$, was obtained at a 9:1 ratio. **4.33** was then easily isolated from **4.37** by column chromatography. Both **4.33** and **4.37** are crystalline solids[33,36] and a variety of crystal structures have been reported for metal complexes of **4.37**.[32,41,42] Thus, **4.33** was considered a good candidate for

investigating the supramolecular properties of oxo-functionalized cyclotriphosphazenes.

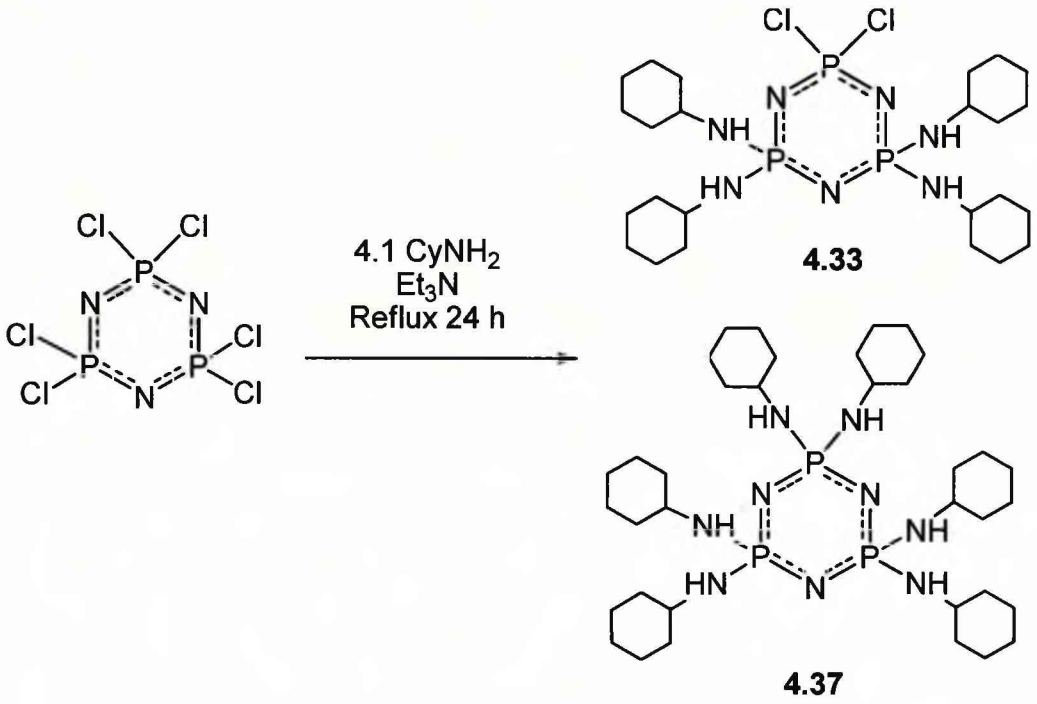

Figure 4.25. The Synthesis of 4.33.

4.34 and **4.35** are spirocyclic systems incorporating secondary amino substituents, while still maintaining reactive PCl_2 centres on the P_3N_3 ring.[37] **4.34** is expected to be less reactive than **4.33**, due to the more bulky secondary amine, whereas **4.35** is more reactive than **4.33,** as its molecular periphery is less sterically crowded. In addition to this **4.35** offers two reactive sites. This could lead to the formation of very interesting derivatives, where either one or two sites are functionalized. If just one PCl_2 unit reacts the resultant oxo-phosphazene will contain an active site for further reactions **4.34** was synthesised by refluxing $N_3P_3Cl_6$ in 8.2 equivalents N,N'-diethyl propylene diamine (Figure 4.26) and then isolated by recrystallisation.[38] The same reaction can be employed to synthesise **4.35** by using 4 equivalents of amine.[38,43]

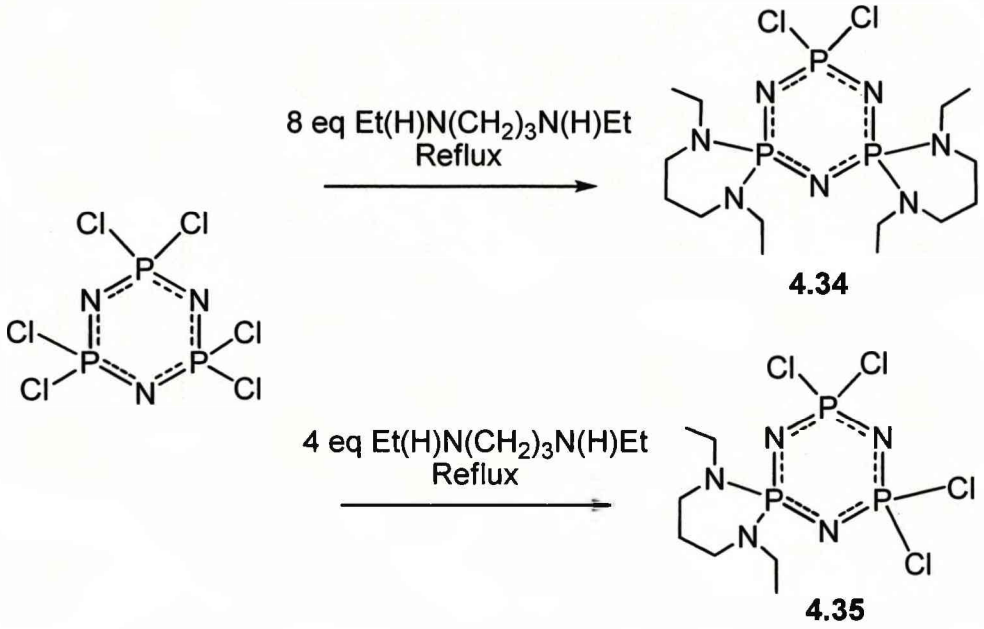

Figure 4.26. The Synthesis of 4.34 and 4.35.

4.2.2. Phosphate and Pyrophosphate

4.2.2.1. Cyclohexyl Phosphazene Derivatives

4.2.2.1.1. Phosphate Synthesis

We expected that the hydrolysis of the dichloride **4.33** would be a convenient route to phosphate **D**, see Figure 4.1. However, the PCl_2 unit remained unscathed when **4.33** had been refluxed in a biphasic mixture of THF and aqueous base for several days Figure 4.27. Also grinding of solid **4.33** with KOH had no effect. The reluctance of the P-Cl bonds to hydrolyze in the presence of hot hydroxide solution is surprising considering the moisture sensitivity of common phosphorus chlorides. To our knowledge there are no reports of P-Cl bonds that can withstand treatment with aqueous KOH at elevated temperature.

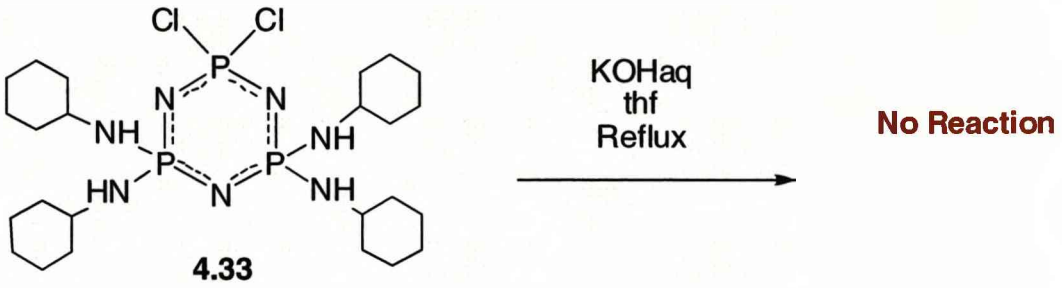

4.33

Figure 4.27

In search for a suitable catalyst for the hydrolysis of **4.33** we tested 4-dimethylamino pyridine (DMAP). Apart from being a strong nucleophile that catalyses a plethora of substitution reactions[44-47] it also forms stable adducts with a variety of phosphorus compounds.[48-52] For example as outlined in the previous chapter, $N_3P_3Cl_6$ reacts with six equivalents of DMAP in superheated chloroform to form a crystalline material that contains $[(DMAP)_6P_3N_3]^{6+}$ ions.[53] During the course of this study it was found that **4.33** reacts with two equivalents of DMAP, see Figure 4.28, when refluxed in chloroform for one day yielding the dicationic adduct $[(DMAP)_2(CyNH)_4P_3N_3]^{2+}$ **[4.38]**Cl_2. The ^{31}P NMR spectrum of **[4.38]**Cl_2 (Figure 4.29) shows the characteristic AX_2 signal pattern of cyclotriphosphazenes that contain two magnetically equivalent ^{31}P nuclei in the phosphazene ring. The chemical shift of the "triplet" signal resembles that of $[(DMAP)_6P_3N_3]Cl_6$.[53]

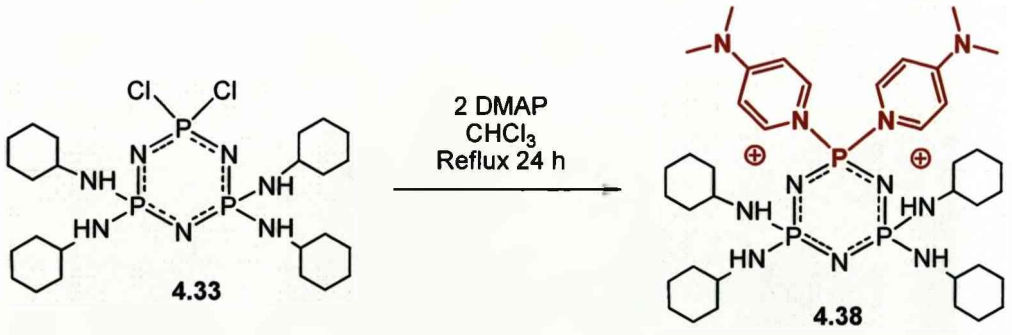

4.33 **4.38**

Figure 4.28. Formation of the DMAP Stabilised Dication **[4.38]**Cl_2.

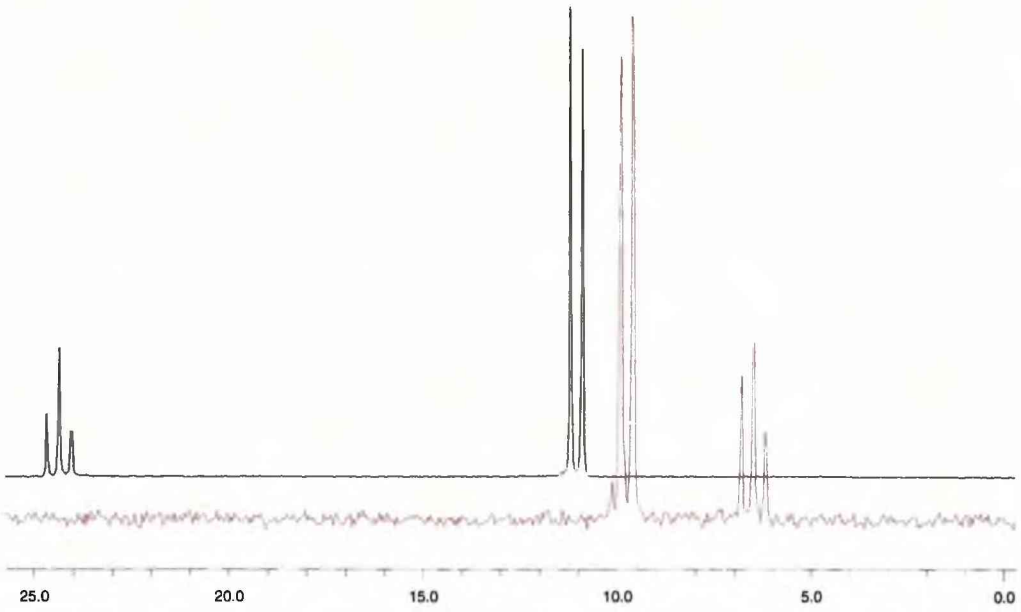

Figure 4.29. $^{31}P\{^{1}H\}$ NMR of 4.33 (black) and 4.38 (red).

(Recorded in $CDCl_3$)

We were able to grow crystals of [**4.38**]$Cl_2 \cdot 1½CHCl_3 \cdot 2H_2O$ from a solution in chloroform that was slowly infused by a THF atmosphere. The crystal structure of features a dicationic adduct complex, in which two DMAP ligands are coordinated to a phosphorus centre, see Figure 4.30. The P-N bonds towards the DMAP ligands are long measuring 1.737(7) and 1.747(7) Å, which reflect their more dative character, while the N5-P1-N4 angle towards both DMAP ligands is 95.8(3)°, this is small for a tetrahedral environment. The P_3N_3 ring is very slightly twisted along the P1-N3 axis. The ring angles are significantly wider at P1 (125.4(4)°) and N3 (127.4(4)°) than at the other ring atoms (P2: 114.1(3)°, P3: 114.7(3)°, N1: 118.3(4)°, N2: 118.9(4)°). There is also a marked deviation in the P-N ring bond lengths: The ring bonds at P1 measure 1.546(6) and 1.558(6) Å, thus are comparatively short. Similarly short bonds have been observed in the hexacation $[(DMAP)_6P_3N_3]^{6+}$.[53] The two adjacent P-N bonds are long (P2-N2: 1.632(7), P3-N1 1.645(7) Å), while the two P-N bonds furthest away from P1 are again short (P2-N3: 1.581(7), P3-N3 1.592(6) Å). This "ripple" effect (i.e. the alternation of P-N ring bond lengths) is characteristic of cyclophosphazenes that carry electron withdrawing groups at one P centre

and electron rich substituents at the other. The crystal structures of the dichloro derivatives **4.33**, **4.34** and **4.36** show a similar bonding pattern.[36,37,40,54]

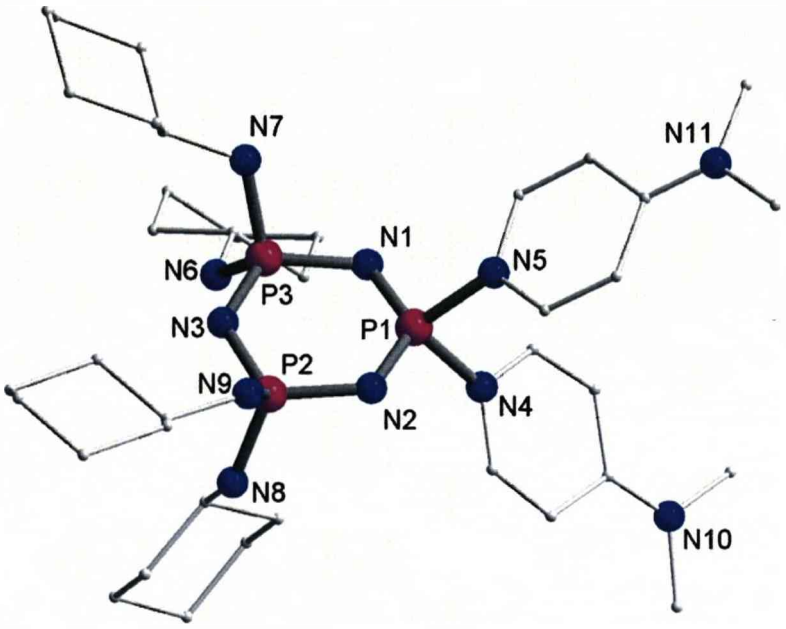

Figure 4.30. Crystal Structure of the Dication $[N_3P_3(NHCy)_4(DAMP)_2]^{2+}$ ([4.38]Cl_2).
(H-atoms are omitted for clarity).

The X-ray structure of [**4.38**]Cl_2 confirmed the existence of the dication. The presence of water in the crystal lattice suggests that phosphazene-DMAP adducts are to some extent stable towards hydrolysis. A partially hydrolysed by-product did appear to form in the reaction; however it was removed by washing [**4.38**]Cl_2 with THF. The impurity was identified by a ^{31}P NMR signal with a negative chemical shift.

The dichloride **4.33** was then refluxed in a mixture of aqueous KOH, THF and one equivalent of DMAP and a single product was formed after 24 hrs. This product was found to be the phosphate of **4.33**, which forms initially as the potassium salt $[N_3P_3(NHCy)_4O_2H]^- K^+$, **4.39** and can then be isolated in the form of the neutral zwitterion $N_3P_3(NHCy)_4O_2H_2$, **4.40** (Figure 4.31). The reaction was followed by ^{31}P NMR spectroscopy (Figure 4.32).

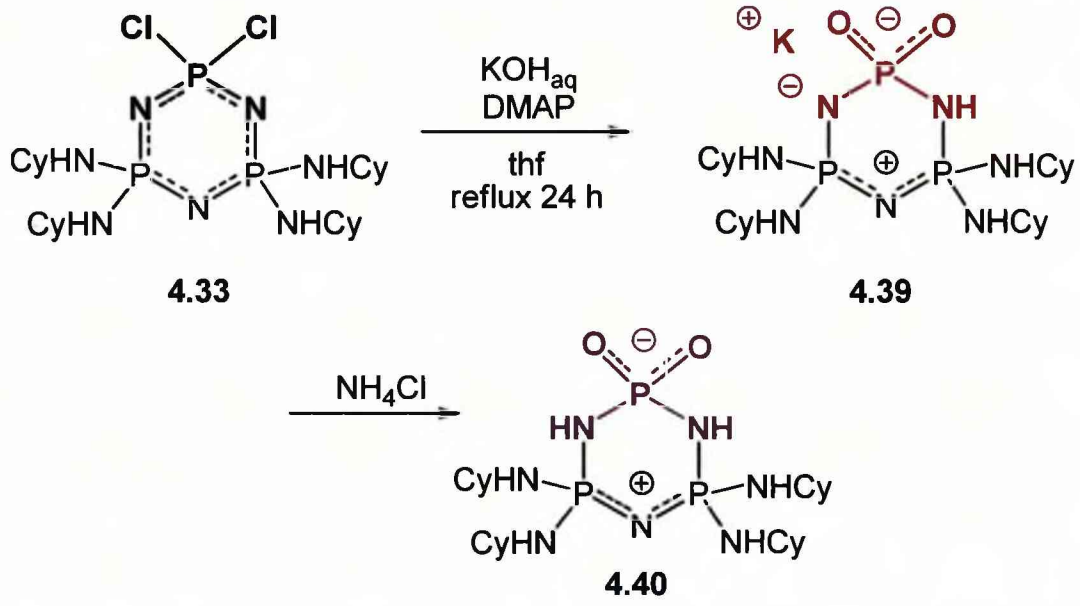

Figure 4.31. Synthesis of Phosphate 4.40.

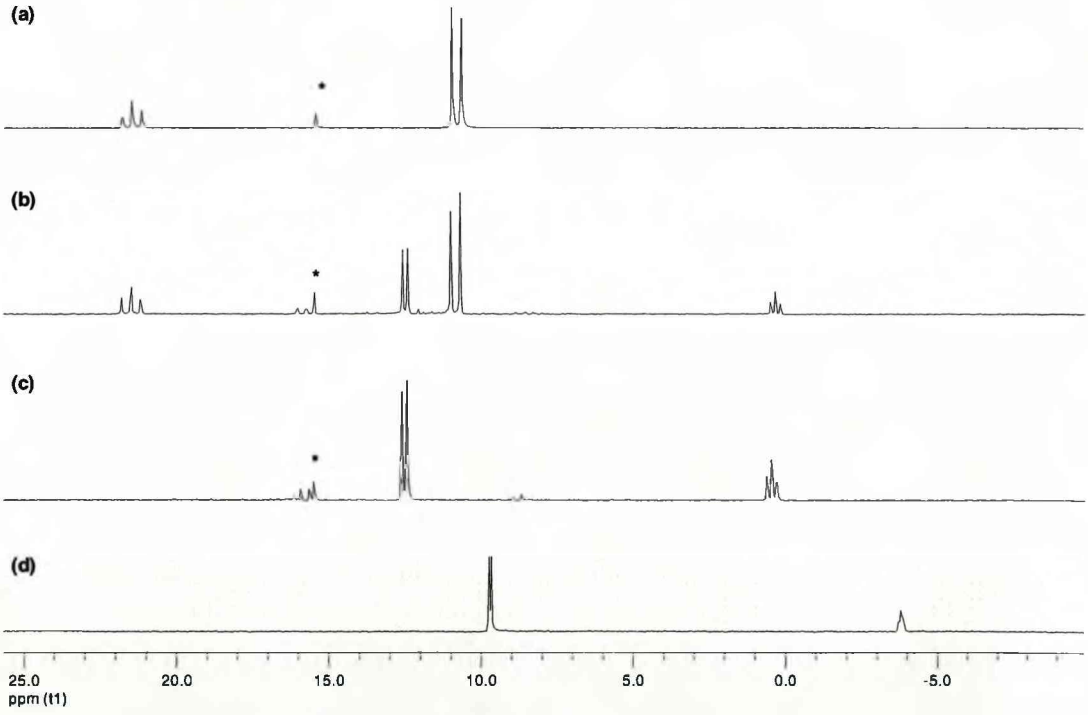

Figure 4.32. $^{31}P\{^{1}H\}$ NMR of the Formation of 4.39 and 4.40 from 4.33.

(Spectra a, b and c were recorded in d_6-acetone, d was recorded in MeOD)

(a) recorded after 24 h refluxing **4.33** in THF and KOH_{aq} – only shows **4.33**; (b) recorded after 2 h refluxing **4.33** in THF, KOH_{aq} and DMAP – shows **4.33** and **4.39**; (c) recorded after 24 h refluxing in THF, KOH_{aq} and DMAP – shows only **4.39** (**4.33** fully reacted); (d) recorded on ppt formed after addition of NH_4Cl – shows pure **4.40** (*indicates trace impurity of $N_3P_3(NHCy)_6$

The ^{31}P NMR spectrum, taken after ~ 2 h, indicates the formation of the phosphate by the appearance of a "triplet" at δ = 0.2 ppm. NMR spectra which were recorded at frequent intervals show signals due to **4.33** and **4.39** in a varying ratio. The absence of further signals suggests that the initial reaction of **4.33** with DMAP is slow compared to the hydrolysis of intermediate DMAP adducts. The potassium salt **4.39** was crystallized from the reaction solution. However, the crystals were highly mosaic and gave X-ray data of poor quality. Nonetheless, a crude structure model was obtained that verified the presence of one potassium ion per ligand anion. Treatment of the reaction solution with ammonium chloride yields the neutral zwitterion **4.40**, which is insoluble in toluene and chloroform, but soluble in methanol and sparingly soluble in thf. It crystallizes from thf in the form of the tetrahydrate **4.40**·$4H_2O$.

4.2.2.1.2. Crystal Structure of $N_3P_3(NHCy)_4O_2H_2$ (4.40·$4H_2O$)

The tetrahydrate **4.40**·$4H_2O$ crystallises in spacegroup $P2_12_12_1$. The asymmetric unit contains two molecules of **4.40** that exhibit very similar structural parameters. The P_3N_3 rings adopt a twist conformation: The two ring segments N11, P11, N12 and P12, N13, P13 are twisted with respect to each other along the P11-N13 axis by 18.8° (19.7° for the other crystallographically unique molecule). This "twist angle" gives an indication of planarity with in the N_3P_3 ring. A perfectly planar cyclotriphosphazene would have a twist angle of zero. There is a pronounced variation in the bond lengths of the N_3P_3 ring: Long P-N bonds are found adjacent to the protonated N-sites (av. $P(O_2)$-N(H) 1.665 Å, $P(Z'_2)$-N(H) 1.645 Å), while the P-N bonds involving the non-protonated N site are significantly shorter (av. 1.584 Å). In comparison the P-N bonds of $(RNH)_6P_3N_3$ derivatives are on average 1.60 Å long.[33] The P-O bonds of **4.40** measure on average 1.498 Å and the O-P-O bond angles 115.0°. These are similar to P=O bonds and O=P=O angles of dihydrogen phosphate ions of organic salts, phosphimate ions, **[4.4]**$^+$ and oxo-cyclotriphosphazanes **4.4a** and **4.4b**. Also the oxo-

phosphazene derivatives **4.5**, *gem*-$N_3P_3Ph_2(OMe)_3OH$ and **4.23a**, exhibit similar P=O distances (Table 4.3).

Compound	P=O / Å	O=P=O/ (deg) (O=P-O/N)
4.40	1.498*	115.0*
Organic salts**	1.505**	114.7**
[4.4]$^{+}$[55]	1.498[55]*	118.9[55]*
4.4a[25]	1.453[25]*	116.1[25]*
4.4b[11]	1.448[11]*	115.1[11]*
4.5[3]	1.470[3]*	105.81[3]*
gem-$N_3P_3Ph_2(OMe)_3OH$[4]	1.456[4]#	
4.23a[2]	1.469(5)[2]	105.9(3)[2]

Table 4.3. P=O Distances (Å) and O=P-(O/N) Angles of Oxo-Functionalised Phosphazenes and Phosphazanes.

(*Values are averaged, #Standard deviations not supplied in reference)

** The mean distance and angle of dihydrogen phosphate ions of organic salts (sample from 171 non-disordered crystal structures deposited in CSD with R < 5%).

The N-P-N ring angles are most acute at the PO_2 unit (av. N-P(O_2)-N 101.0°) and somewhat wider at the other P centres (av. 109.1°), which is in accordance with the bond orders of the relevant P-N bonds. It should be noted that **4.40** is valence-isoelectronic to the related zwitterion **4.41** (Figure 4.33), which shows a similar, albeit more pronounced, variation of P-N ring bond parameters.[56]

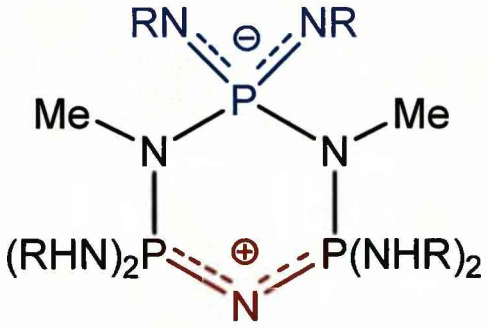

4.41

Figure 4.33.

The supramolecular structure of **4.40**·4H_2O displays a double helix. It consists of a helical chain of zwitterions, which is intertwined with a helical chain of water molecules, see Figure 4.34. The zwitterions are connected to each other via pairs of hydrogen bonds between N(ring)H and O functions with N...O distances ranging from 2.79 to 2.84 Å. The high quality of the X-ray data facilitated the location and refinement of all hydrogen atoms of the water molecules. The hydrogen bonding within the helical chain of water molecules follows the sequence [HOH...OH...O...HO...]. The water chain interacts as both a H-donor and a H-acceptor with N(exo)H functions and PO_2 units of the zwitterions. The double helix arrangement exhibits pseudo 4_1 symmetry containing four zwitterions and sixteen water molecules per turn. The result is a tightly knit network of hydrogen bonds that explains the low solubility of the tetrahydrate in aprotic solvents. The polar core of the double helix is covered effectively by a hydrophobic layer of cyclohexyl groups. The chains are packed via hydrophobic interactions in an orthorhombic, but overall chiral arrangement, shown in the Figure 4.34 below.

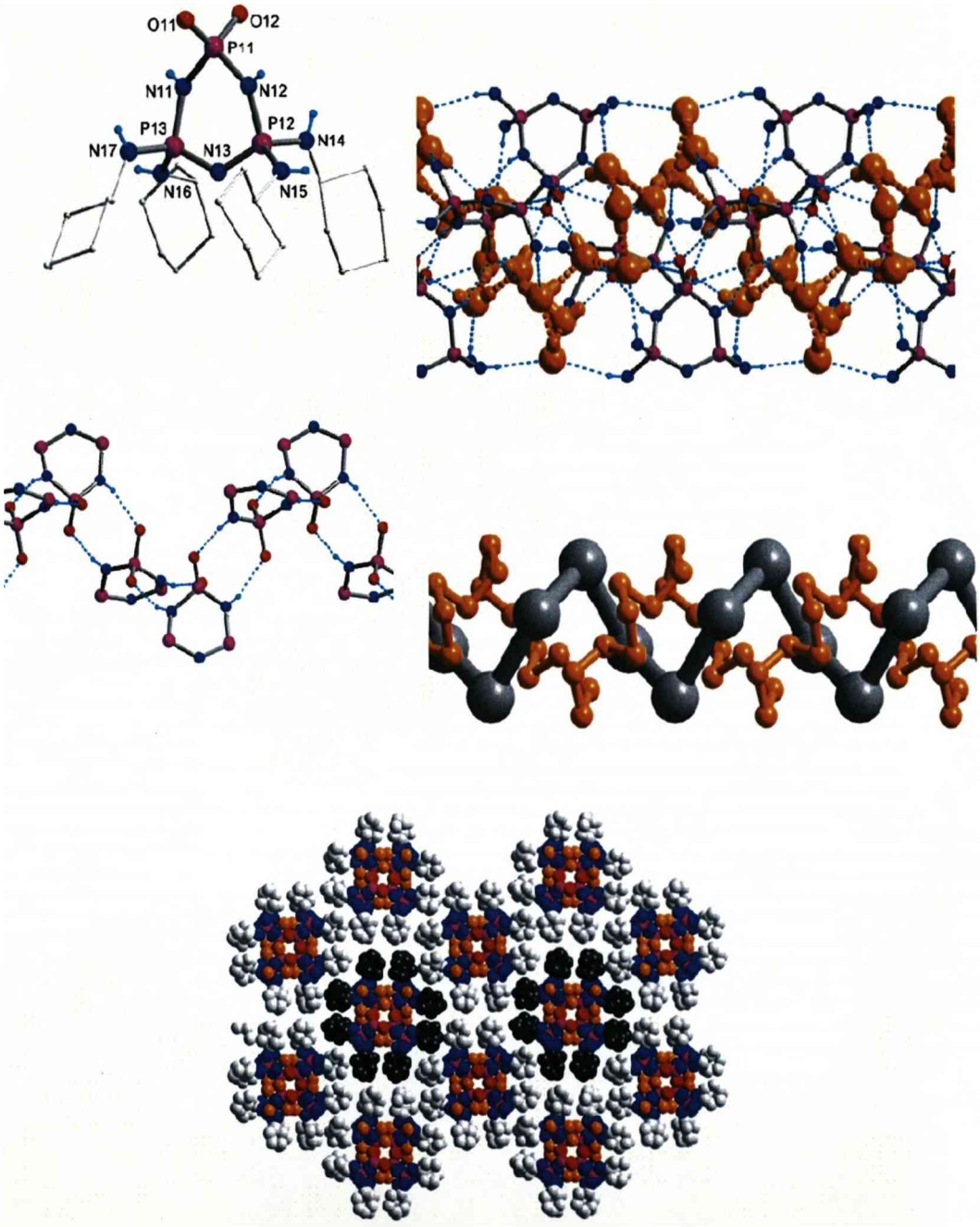

Figure 4.34. The crystal structure of the tetrahydrate of zwitterion 4.40

Top left: Molecular structure of zwitterion **4.40** (only one of two independent molecules is shown). Middle left: Hydrogen bonded helix of **4.40** (NHCy groups and water is not shown). Top right: Double helical assembly of **4.40** (water molecules – orange and hydrogen bonds- dashed lines). Middle right: Simplified illustration of the intertwined double helix (orange spheres: O atoms of water, grey spheres: centres of P_3N_3 rings). Bottom: Crystal packing viewed along the helical chains (cyclohexyl groups in grey).

4.2.2.1.3. Pyrophosphate Synthesis

Upon heating, **4.40**·4H_2O dehydrates and forms the pyrophosphate **4.42**, $(N_3P_3(NHCy)_4OH)_2O$. The thermogravimetrical analysis (TGA) of **4.40**·4H_2O shows a two-step weight loss upon heating to 180°C, which equates to the removal of 4.5 equivalents of water, see Figure 4.35.

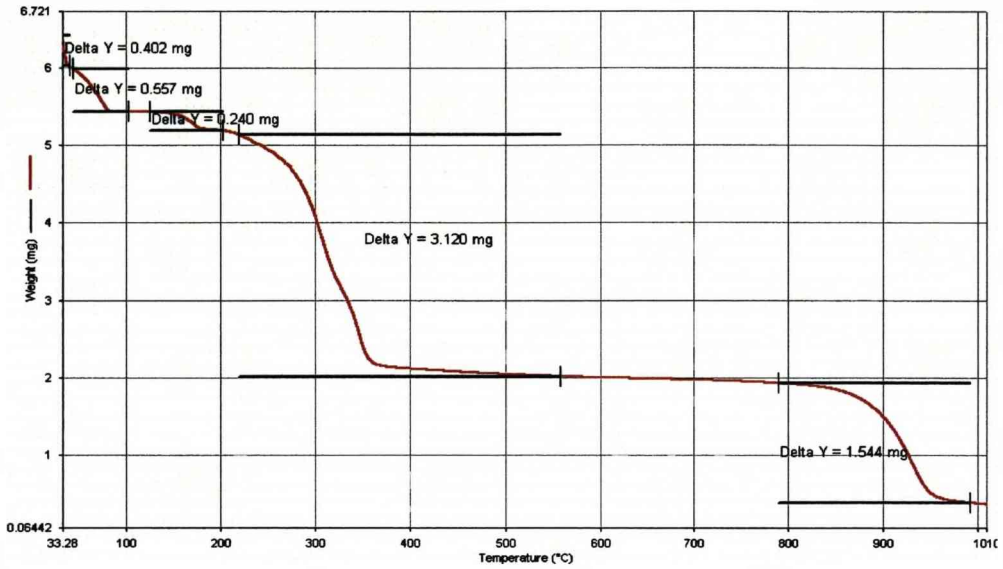

Figure 4.35. Thermogravimetric Analysis of 4.40•4H2O.

First loss (0.402 mg) = THF. Second and third losses (0.557 and 0.240 mg) = 4.5 equivalents of water (3 equiv. are lost between 50 to 80°C and a further 1.5 equiv. from 150 to 180°C), which dehydrates the crystal and also generates the pyrophosphate 9. Between 200°C and 360°C a further weight loss, which matches well with the elimination of four cyclohexane molecules.

Heating of **4.40**·4H_2O to 160°C under reduced pressure (0.1 torr) for four hours yields a colourless material that is soluble in various organic solvents including THF, chloroform and toluene. Its ^{31}P NMR spectrum consists of two broad signals, see Figure 4.36. MS-ESI exhibits a molecular ion peak M+ at 1105 Da, which corresponds to the pyrophosphate **4.42**. The formation of **4.42** can be followed by ^{31}P NMR (Figure 4.36), below we show two spectra recorded at intervals while heating **4.40**. The progressive formation of **4.42** is clearly observed with diminishing amounts of **4.40**. Figure 4.36(c) (showing only **4.42**) was recorded after 4 hrs heating and extraction with THF. The compound resisted crystallization forming glassy

beads from toluene. However, single crystals of the salt [**4.42**H]$_2$Cl$_2$·3H$_2$O·½HCl were obtained by gas-phase diffusion of conc. HCl into a solution of **4.42** in toluene. ^{31}P {^{1}H} NMR of [**4.42**H$_2$]Cl$_2$ in chloroform exhibits four signals, two "doublets" at δ = 8.2 and 6.4 and two "triplets" at δ = 0.0 and -8.5, indicating that the dication [**4.42**H$_2$]$^{2+}$ (Figure 4.37) contains two distinct phosphazene rings.

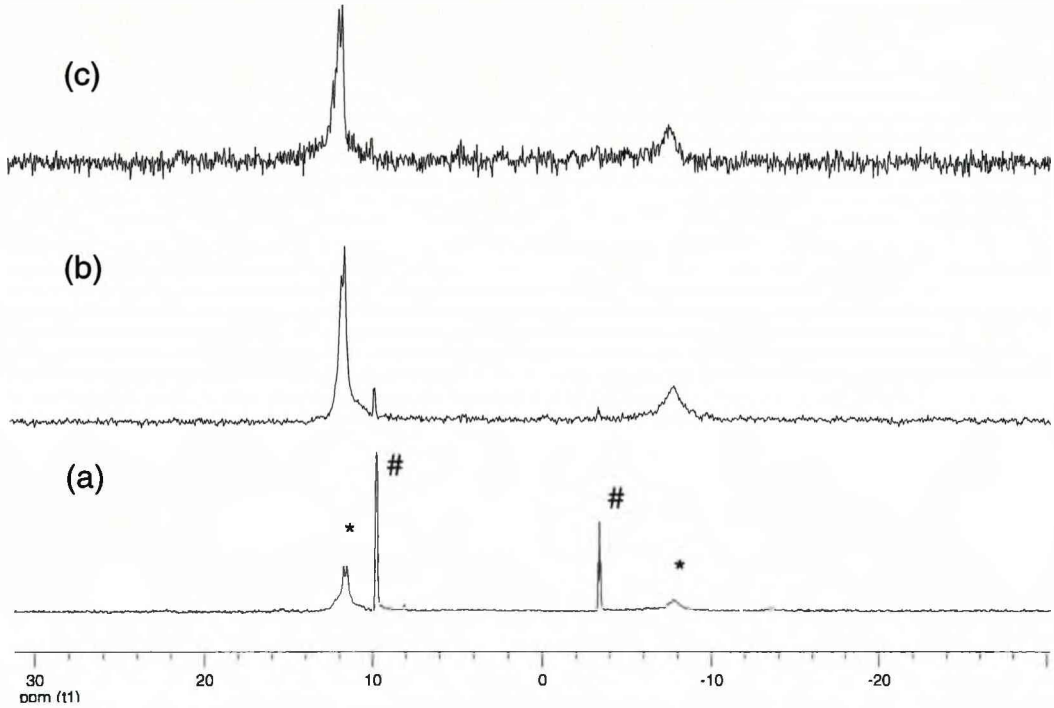

Figure 4.36. Formation of 4.42 on Heating 4.40 to 160 °C under Reduced Pressure for 4 h.

(# = **4.40**, * = **4.42**. Spectra recorded in MeOD)

(a) After 2 – shows only a small amount of **4.42** formation; (b) After 4 h – shows most **4.40** has condensed to **4.42**; (c) After 4 h and THF extraction – shows only **4.42**.

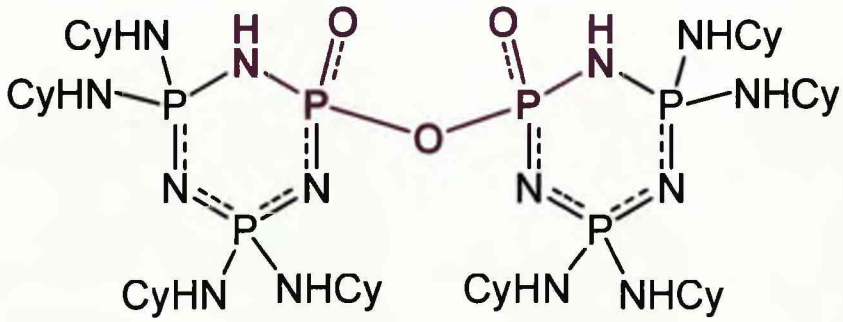

4.42

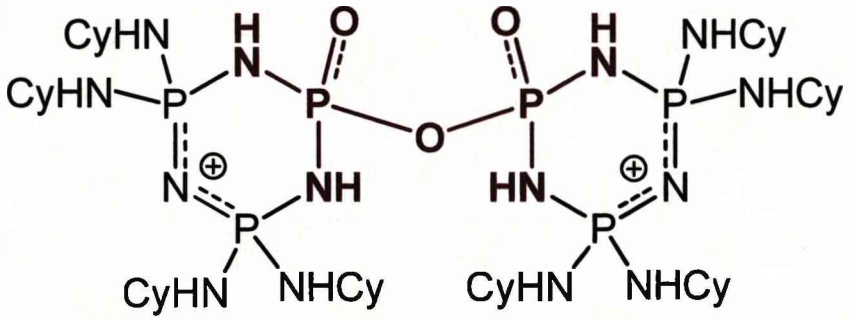

$[\mathbf{4.42}H_2]^{2+}$

Figure 4.37. Schematic of 4.42 and its Dication $[\mathbf{4.42}H_2]^{2+}$.

4.2.2.1.4. Crystal Structure of $(N_3P_3(NHCy)_4OH)_2O$ ($[\mathbf{4.42}H_2]Cl_2 \cdot 5H_2O \cdot ½HCl$)

The X-ray structure of $[\mathbf{4.42}H_2]Cl_2 \cdot 5H_2O \cdot ½HCl$ features a dication containing a pyrophosphate unit, which fuses the two phosphazene rings via the bridging oxygen atom (Figure 4.38). The four nitrogen ring sites adjacent to the pyrophosphate group are protonated. The P_2O_3 chain is almost planar with dihedral angles of 174° (O2-P1-O1-P4) and 8° (O3-P4-O1-P1). The chain shows a *cis-trans* arrangement and as a result the terminal oxygen atom O3 is situated directly above the phosphazene ring of P1. This arrangement is held in place by hydrogen bonds between two exocyclic NH groups and O3 displaying N...O distances of 2.934(9) and 2.968(10) Å, respectively. This accounts for two distinct AX_2 signal patterns observed in ^{31}P NMR spectrum of $[\mathbf{4.42}H_2]Cl_2$. As expected the terminal P-O bonds of the pyrophosphate group are short (P1-O2 1.474(6), P4-O3 1.444(6) Å), while the bridging P-O bonds are long (P1-O1 1.609(6), P4-O1 1.628(6) Å). The P-O-P angle at the bridging oxygen atom is 131.6(4)°. Analogous to the bonding pattern in the zwitterion **4.40**, the P-N ring bonds in $[\mathbf{4.42}H_2]^{2+}$ are long around the protonated ring nitrogen centres and short at the non-protonated N centre.

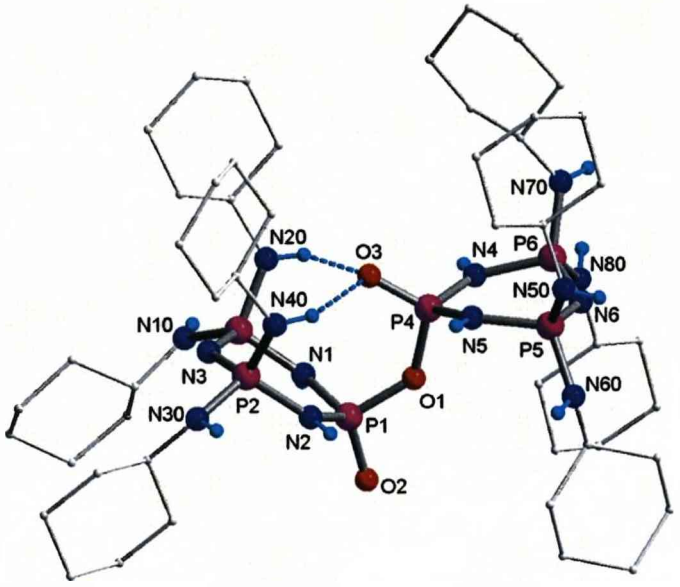

Figure 4.38. The crystal structure of the dication $[4.42H_2]_2^+$
(C-bound H-atoms are omitted for clarity).

Figure 4.39 shows the supramolecular structure of $[\mathbf{4.42}H_2]Cl_2 \cdot 5H_2O \cdot ½HCl$, which is governed by NH...O, NH...Cl, OH...O and OH...Cl bonds. The structure contains half an equivalent of HCl per formula unit. The proton, formally from HCl, is disordered across a chain of water molecules connecting two dications at their terminal PO sites (Figure 4.40). In one arrangement the proton is part of a H_3O^+ ion (Figure 4.40a). In the other arrangement the proton is situated on the terminal oxygen atom O2 to give the trication $[\mathbf{4.42}H_3]^{3+}$ (Figure 4.40b).

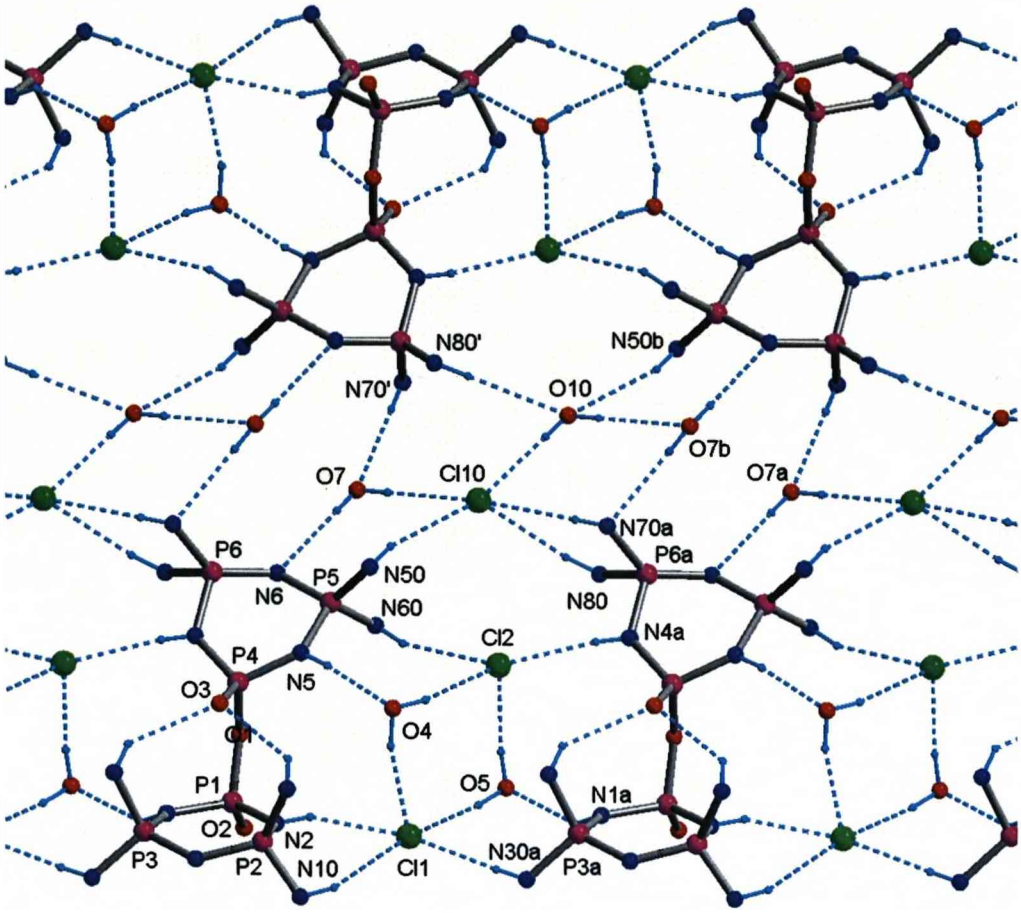

Figure 4.39. Supramolecular Structure of $[4.42H_2]Cl_2 \cdot 3.5H_2O \cdot 1/2HCl$.

-showing hydrogen bonded strands.

Atoms Cl10 and O10 share the same crystallographic site and are disordered across an inversion centre, which also affects the disorder of the amino groups bonded to P6 due to their involvement in hydrogen bonding to either the water molecule at O10 or the chloride ion Cl10. In this figure H-atoms have been added to O10 and O7 to illustrate H-bond donor and acceptor sites. Cyclohexyl groups and the water molecule O6 are omitted for clarity.

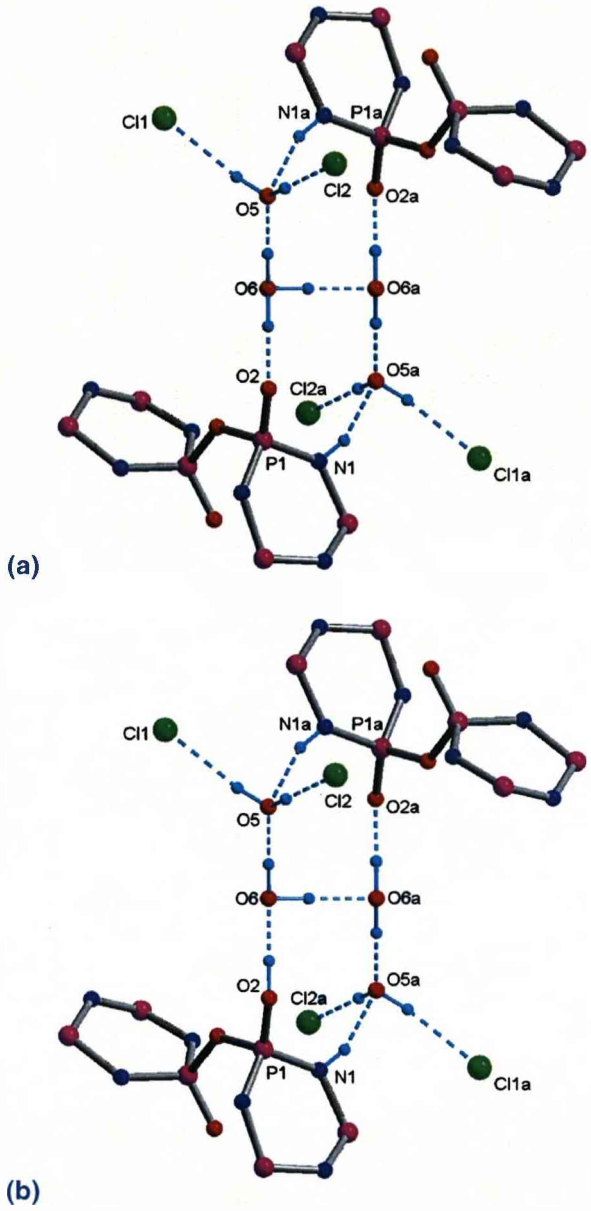

Figure 4.40. Supramolecular Structure of $[4.42H_2]Cl_2 \cdot 3.5H_2O \cdot 0.5HCl$.

-showing how the two strands are connected via water molecules O6 and O6a

(a) The proton is part of a H_3O^+ ion at O6 (and as such disordered across O6 and O6a, which are related by the crystallographic inversion centre; **(b)** The proton is bonded to the terminal oxygen atom O2 as part of the trication $[\mathbf{4.42}H_3]^{3+}$.

Note that H-atoms bonded to O2 and O6 were not located in difference maps and were not included in the refinement. They have been added here to illustrate the pattern of hydrogen bonding and the distribution of the extra proton.

4.2.2.2. N,N'-Diethyl Propylene Diamino and *tert*-Butyl Derivatives

The dichlorides **4.34** and **4.36** both reacted with two equivalents of DMAP to form the dications [**4.43**]Cl_2, $[N_3P_3(N(Et)(CH_2)_3NEt)_2(DMAP)_2]Cl_2$ and [**4.44**]Cl_2, $[N_3P_3(NH^tBu)_4(DMAP)_2]Cl_2$ in an analogous manner to **4.33** (Figure 4.41). However they required much longer reaction times due to their lower reactivity and showed no hydrolysed side products in their ^{31}P NMR spectra. [**4.43**]Cl_2 formed at 59 % conversion of **4.34** after 8 days reflux and the ^{31}P NMR spectrum showed an AX_2 system at δ = 7.2 and 21.0 ppm. [**4.44**]Cl_2 formed after 6 days refluxing giving an AB_2 signal pattern at δ = 5.0 - 6.1 ppm. Both compounds were isolated from their parent dichlorides by precipitation with dry hexane. However the samples were not pure, as some unreacted DMAP remained. Crystal structures were not obtained; therefore characterization was predominately due to NMR spectroscopy. The "triplet" resonance in at δ = 7.2 ppm for [**4.43**]Cl_2 is at a similar chemical shift as that of [**3.9**]Cl_6 and $[N_3P_3(DMAP)_6]^{6+}$ (discussed in Chapter 3), indicating that it arises from a $P(DMAP)_2$ centre. The second order spectrum of [**4.44**]Cl_2 arises as a result of the similar δ values for $P(DAMP)_2$ groups and $P(NH^tBu)_2$. In addition to this ^1H NMR spectra show two sets of patterns, these can be assigned to DMAP. One is clearly free DMAP, while the other is similar to the ^1H spectrum of [**3.9**]Cl_6.

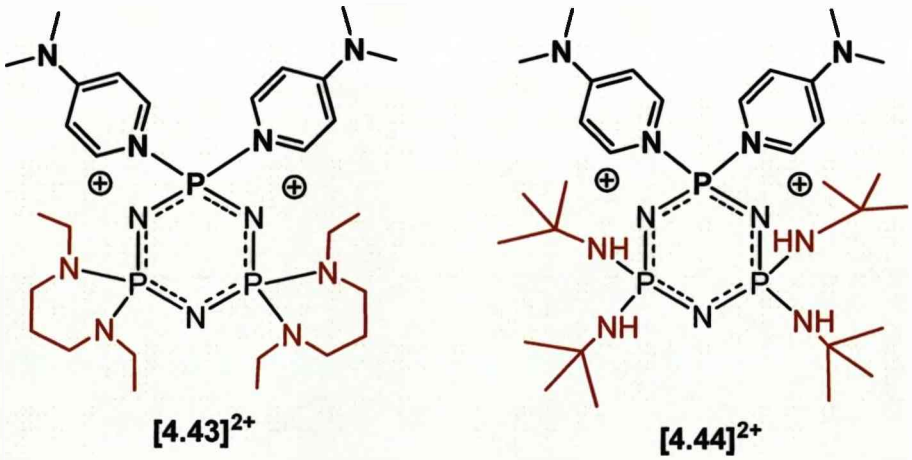

Figure 4.41

The hydrolysis of both the diamine and *tert*-butyl dichlorides, **4.34** and **4.36**, was then attempted using the same conditions as for the cyclohexyl species, **4.33** (one equivalent DMAP, Xs KOH_{aq} and thf). However after one week refluxing ^{31}P NMR spectra showed only 20 % conversion of **4.34** to the corresponding phosphate **4.45**, $N_3P_3(N(Et)(CH_2)_3NEt)_2O_2H_2$ (Figure 4.42), while **4.36** showed no reaction at all. Monitoring the reaction ^{31}P $\{^1H\}$ NMR spectroscopy showed that the reaction was analogous to that of the cyclohexyl derivative **4.33**; first showing an AX_2 system, which forms at δ = 1.3 (t) and 16.7 (d) and has been assigned as the potassium salt [**4.45**]K. Then neutralization occurs on addition of NH_4Cl causing the NMR signals to shift to δ = -4.6 and 10.9. The resulting neutral zwitterion **4.45** did not precipitate on addition of NH_4Cl. However, in solution it existed only as a minor species with the dichloride **4.34** and the di-substituted DMAP dication **4.43** and was therefore not isolated.

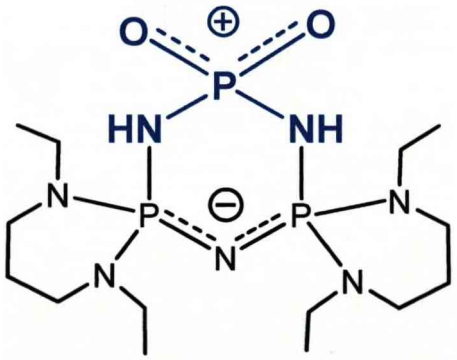

4.45

Figure 4.42.

Hydrolysis of the tetrachloride derivative $N_3P_3(EtN(CH_2)_3NEt)Cl_4$, **4.35** was also carried out under the same conditions. This compound was expected to show a higher reactivity than dichloride phosphazenes. Therefore, the reaction was first attempted with no DMAP and as with **4.33** no reaction was observed. A single product, **4.46** was then observed on addition of DMAP and overnight stirring. The ^{31}P NMR spectrum (Figure 4.43) of this species gives an AMX signal, which indicates that it is only partially hydrolysed and

that it still contains one unreacted PCl_2 centre, in addition to the phosphate moiety. However addition of NH_4Cl and 2 hrs stirring gives an AX_2 system with loss of coupling and chemical shifts at δ = -6.7 and 13.3 ppm. Unfortunately we were not able to isolate this product from solution therefore no other analysis was carried out.

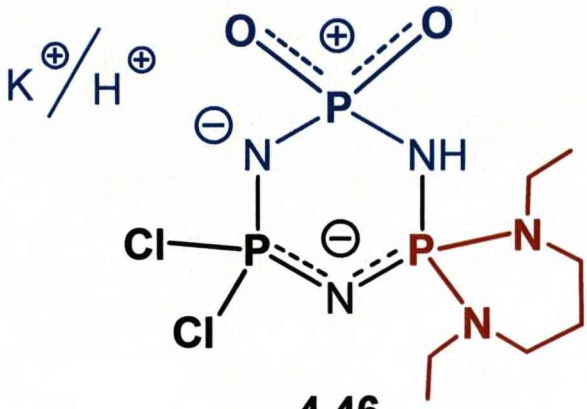

4.46

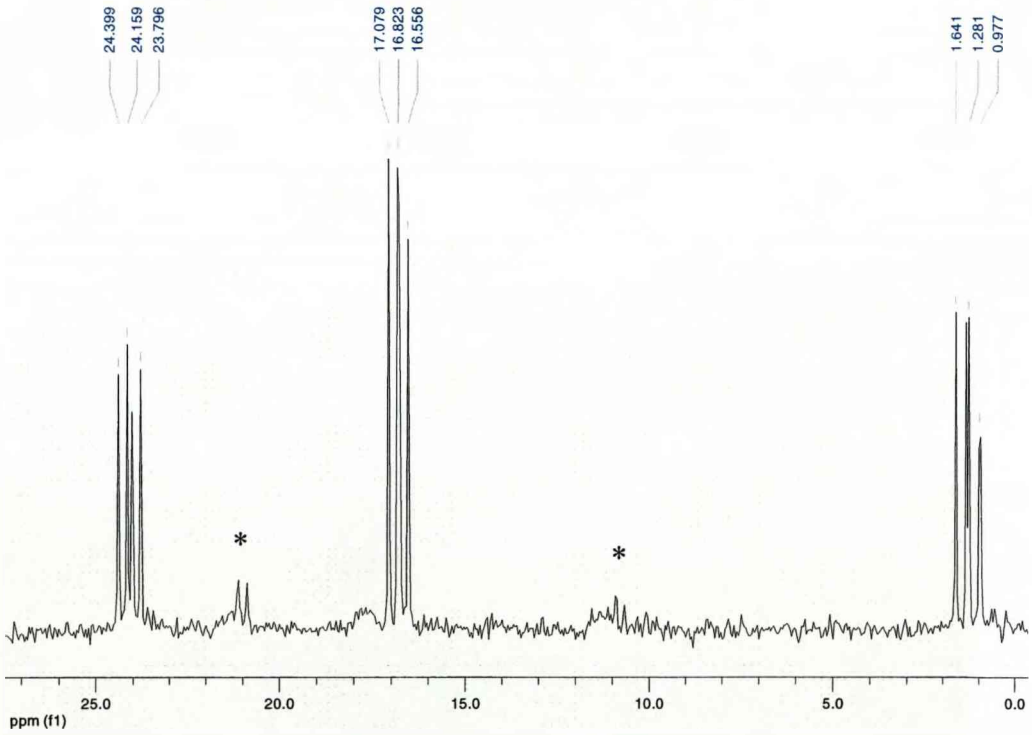

Figure 4.43. $^{31}P\{^{1}H\}$ **NMR Spectrum of 4.46.**

(* indicates 4.35)

4.2.2.3. Other Routes to Phosphates

Once we discovered that **4.40** could be formed with DMAP and KOH, other synthetic methods were analysed. Firstly, the dichloride **4.33** was refluxed in THF/water with DMAP and **4.40** precipitated out of solution. Using one equivalent of DMAP and 48 hrs reflux ~50% yield was obtained and three equivalents of DMAP with 24 hrs reflux gave a 37% yield. This clearly indicated that KOH was not necessary to form **4.40** however it increases the reaction rate needing just one equivalent of DMAP and shorter reflux times for the reaction to complete.

Secondly, we attempted to synthesise **4.40** under acidic conditions. However refluxing the dichloride **4.33** under aqueous acidic conditions yielded only [**4.33H**]Cl.

It is interesting to note that although the PCl_2 unit of geminal phosphazenes **4.33**, **4.34** and **4.36** is inert towards aqueous KOH and HCl, they are reactive towards alcohols, such as methanol. For example, refluxing **4.33** with aqueous HCl and methanol first forms [**4.33H**]Cl followed by the ester **4.47**. In the presence of HBr and methanol **4.47** slowly formed crystals of [**4.47H**]Br (Figure 4.44), which were analysed by X-ray diffraction. Thus water is either not sufficiently nucleophilic to attach the PCl_2 unit, or the attack is kinetically inhibited due to solvent effects, i.e. the highly polar hydroxide ion is prevented from penetrating the non-polar solvent cage surrounding the phosphazenes.

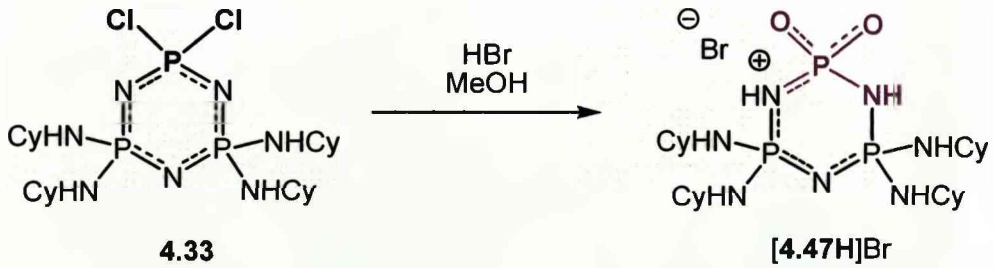

4.33 **[4.47H]Br**

Figure 4.44.

In order to probe this effect, the phase transfer catalyst, tetrabutyl ammonium iodide was used in place of DMAP. Indeed, we found that the reaction proceeds, however at a very slow pace, to give the potassium salt **4.39**. Following the reaction with $^{31}P\{^{1}H\}$ NMR showed that after one day only 4%, and after 72 hrs 10 % had reacted.

4.2.2.4. Crystal Structure of the Dichloro- HCl Adduct $[N_3P_3(NHCy)_4ClH]Cl$ ([4.33H]Cl·THF)

Single crystals of [**4.33**H]Cl·THF were obtained from a solution of THF containing [**4.33**H]Cl cooled to 2°C. The crystal structure shows that **4.33** is protonated at N(3) (Figure 4.44), opposite the PCl_2 centre, with a N(H)-Cl distance of 3.194(34) Å. The P_3N_3 ring has a slightly twisted conformation and contains two elongated P-N bonds either side of the protonated N(3), see Table 4.4. The remaining P-N(ring) bonds are similar to those reported for **4.33**, with shorter distances adjacent to the more electronegative chlorine substituent.[36] This structure is analogous to $[N_3P_3(NH^iPr)_4Cl_2H]Cl$, which was reported by Mani et al. in 1968 and also shows protonation of N(ring) opposite the PCl_2 center.[57]

Compound	P(2/3)-N(3)	P(2/3)-N(2/1)	P(1)-N(2/1)
[**4.33**H]Cl	1.667	1.6005	1.564
4.33[36]	1.585[36]	1.6215[36]	1.557[36]
$[N_3P_3(NH^iPr)_4Cl_2H]Cl$[57]	1.67[57]	1.58[57]	1.56[57]

Table 4.4. Comparison P-N (ring) Bond Lengths of [4.33H]Cl with the Parent Dichloro and the ^{i}Pr Analogue.

(Values are averaged)

The chloride ion, Cl(3) of each **[4.33H]Cl** units forms hydrogen bonds with four exocyclic NH functions, two each on a phosphorus centre of adjacent phosphazene rings. This creates a hydrogen bonded chain, which is sandwiched between layers of cyclohexyl groups, with chlorine substituents at the periphery, see Figure 4.4.

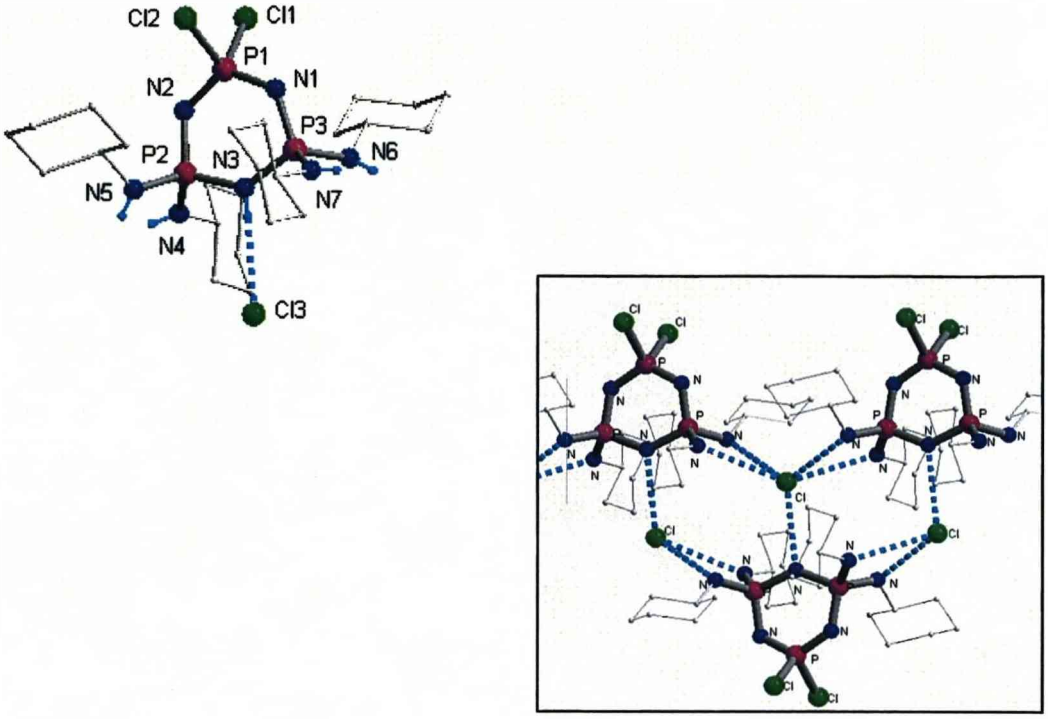

Figure 4.45. Crystal Structure [4.33H]Cl·THF

Top right: Molecular structure of [**4.33**H]Cl. Bottom left: A chain of interconnecting [**4.33**H]Cl units.

(Hydrogen bonds are shown as dashed lines and THF molecules are excluded).

4.2.3. Phosphamides

4.2.3.1. Phosphamide Synthesis

Phosphamides of type **F** (Figure 4.1) are formed by concurrent aminolysis-hydrolysis in a one-pot reaction. The reaction of the dichloride **4.33** with 1.5 equivalents of benzylamine in a biphasic mixture of THF and aqueous

potassium hydroxide solution (Figure 4.46) was followed by ^{31}P NMR. Upon completion of the reaction it showed two sets of AX_2 signals at δ = 15.3 and 10.5 and 18.8 and 15.9 ppm with relative intensities of 6.7:1. The signal of lower intensity was attributed to the mixed amino derivative $N_3P_3(NHCy)_4(NHBz)_2$. Work-up of the reaction mixture with aqueous NH_4Cl led to the precipitation of a pure colourless compound, which was identified as the phosphamide **4.48**, $N_3P_3(NHCy)_4(NHBz)OH$. The ^{31}P NMR exhibited an AX_2 signal at δ = 12.2 and 5.4 ppm. This mirrors the behaviour of **4.40**, which shows a similar up-field shift of the ^{31}P NMR signal upon treatment with NH_4Cl. The intermediate species has been assigned as the potassium salt [**4.48**]K.

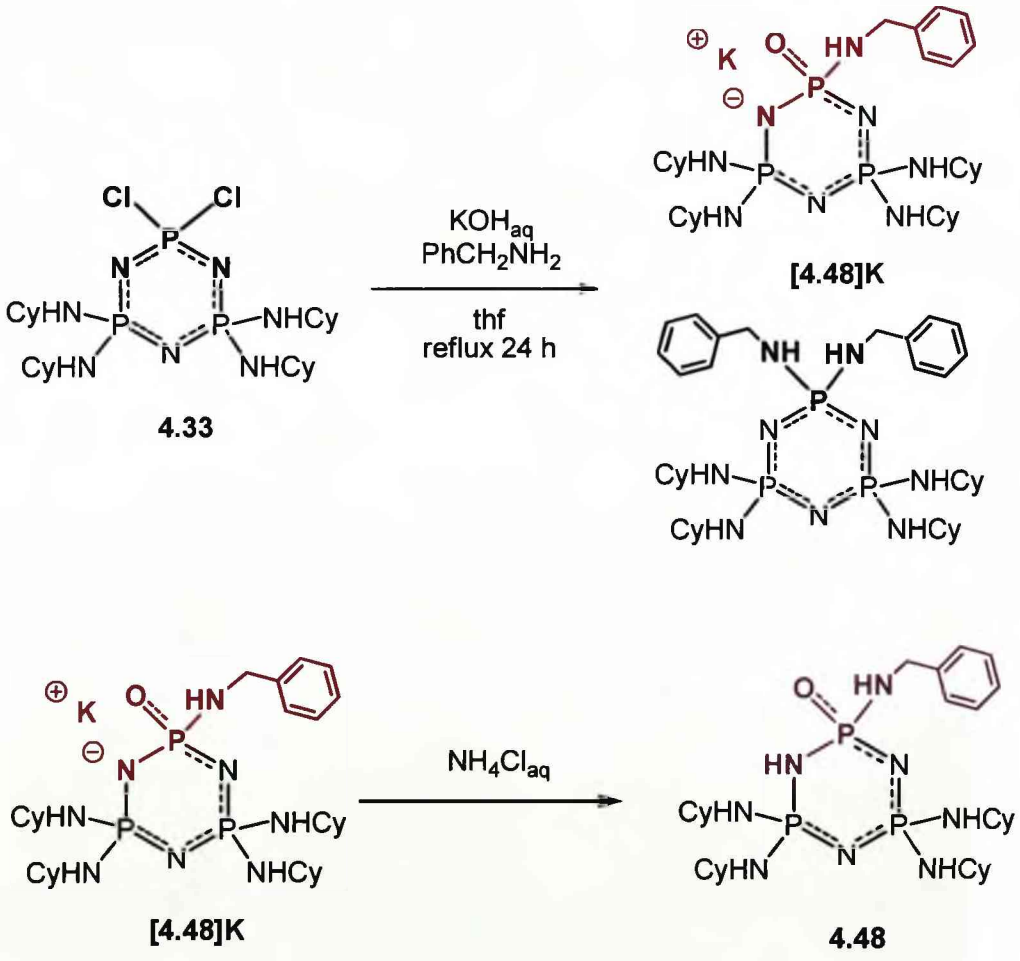

Figure 4.46. Synthesis of Phosphamide 4.48.

The compound co-crystallised with 2,5-dihydroxyterephthalic acid in a 2:3 ratio from methanol. **4.33** also reacts with iso-butyl amime to form **4.49**, $N_3P_3(NHCy)_4(NH^iBu)OH$. However the more sterically demanding *tert*-butyl amine showed no reaction at all. Also, **4.36** did not react correspondingly with isopropyl amine.

4.2.3.2. Crystal Structure of $[N_3P_3(NHCy)_4(NHBz)(O)H_2]^+$ ([4.48H][Hdhtp]·½ H_2dhtp)

Attempts to grow single crystals of the neutral phosphamide **4.48** remained unfruitful. However, addition of 1,4-dihydroxy terephthalic acid (H_2dhtp) to a solution of **4.48** in methanol yielded crystals of composition [**4.48**][Hdhtp]·½ H_2dhtp. The crystals contain two cations [**4.48**H]$^+$ in the asymmetric unit and both ring N centres adjacent to the phosphamide centre are shown to be protonated. The P-O bonds measure on average 1.487 Å resembling the P-O bond lengths of the zwitterion **4.48**. The exocylic P-N bond length of the phosphamide unit (av. 1.607 Å) is similar to the exocyclic P-N bonds of the $(CyNH)_2P$ units (av. 1.615 Å). The P-N ring bonds of [**4.48**H]$^+$ show a similar pattern as those of **4.40** and [**4.42**H_2]$^{2+}$ displaying long bonds around the protonated ring N sites and short bonds at the non-protonated site located opposite the oxo-P centre. The cations [**4.48**H]$^+$ form centrosymmetric hydrogen bonded dimers via pairs of NH...O bonds between the phosphamide units (Figure 4.47). The N...O distances of NH...O interactions are 2.92 Å on average. The dimers are embedded in a matrix of ions [Hdhtp]$^-$ and H_2dhtp molecules. The [Hdhtp]$^-$ ions form H-bonded chains that interact with the dimers via NH...O bonds. The resulting two-dimensional sheets are interlinked by H_2dhtp molecules that again are connected to the dimers via NH...O bonds.

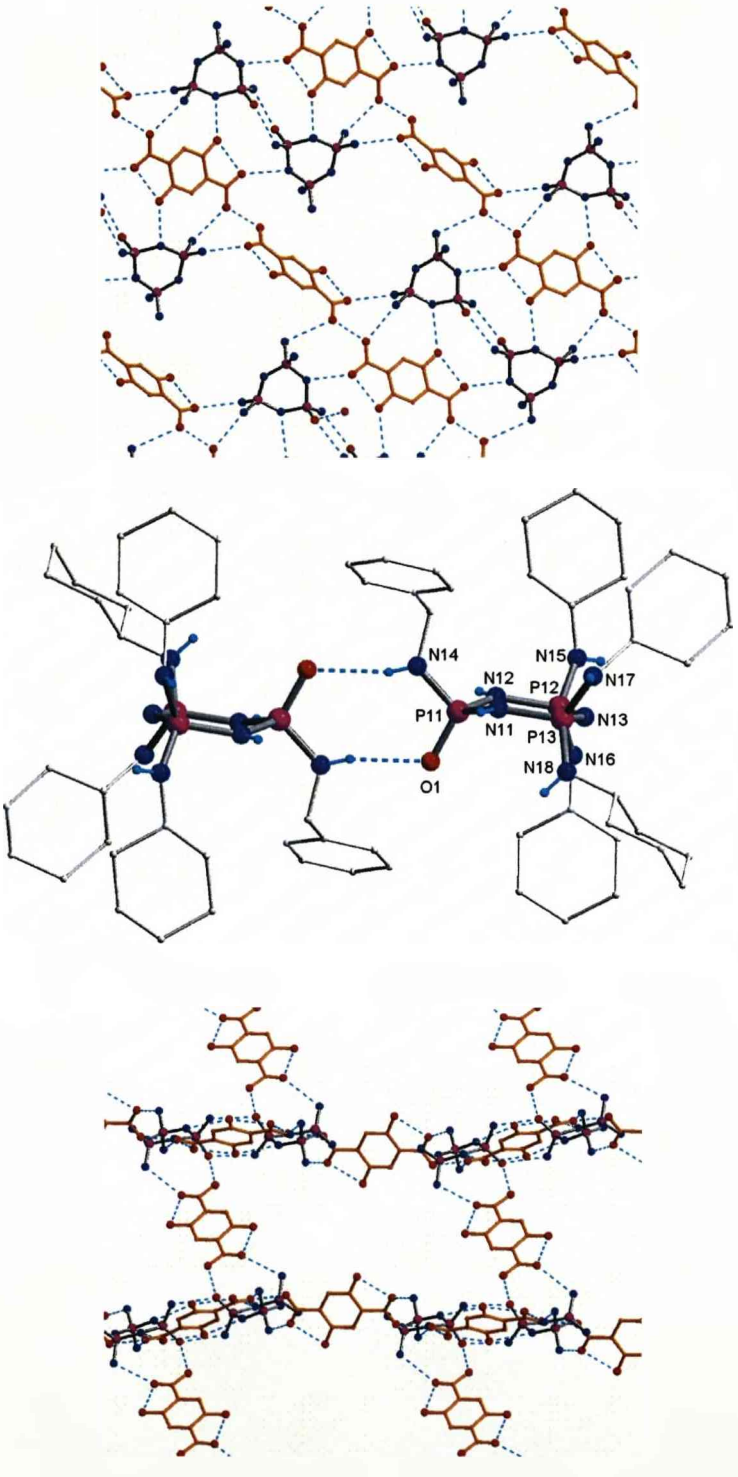

Figure 4.47. Crystal Structure of [4.48][Hdhtp]·½ H_2dhtp.

Top: A Layer of [**4.48**H]$^+$ [Hdhtp]$^-$ - connected by H_2dhtp molecules. Middle: Molecular structure of [**4.48**H]$^+$ - showing the hydrogen bonded dimeric arrangement (C bound H-atoms are omitted for clarity). Bottom: Layer assembly of [**4.48**H]$^+$ and [Hdhtp]$^-$ Ions.

4.2.3.3. Synthesis of Linked Phosphamides

The aminolysis-hydrolysis reaction presents a convenient route towards cyclophosphazene based phosphamides. This method is also applicable for the reaction with diamines, which then connects two phosphazene rings via a diamino linker. Hence, the extended linked species **4.50** $(N_3P_3(NHCy)_4(O)H)_2$(p-$(NHCH_2)_2$Ph and **4.51** $(N_3P_3(NHCy)_4(O)H)_2$(m-$(NHCH_2)_2$Ph (Figure 4.48) were obtained by heating a mixture of **4.33** and para-xylene diamine or meta-xylene diamine in a 2:1 ratio in the presence of aqueous KOH and a small amount of THF. The ^{31}P NMR spectra of the reaction solutions show only a single product, which alters its chemical shift on addition of NH_4Cl. These chemical shifts are very similar to those observed for **4.48**. The formation of linked phosphazene products was confirmed by MS-ESI. The MS-ESI of both the para- and meta- derivatives **4.50** and **4.51** both show a signal due to M^{2+} at 612 Da.

This reaction was also carried out with an excess of diamino xylene, resulting in the addition of just one phosphazene ring per xylene unit. Reacting **4.33** with an excess of meta-xylene diamine yielded compound **4.52**, which contains a dangling reactive amino function. This allows the possibility of linking together two different phosphazene ring systems. The ^{31}P $\{^1H\}$ NMR data for **4.51** and **4.52** are very similar, however they are clearly distinguishable by ^1H NMR and mass spectrometry. The mono substituted compound **4.52** gave an MS-ESI signal due to $[M+H]^+$ at 680 Da.

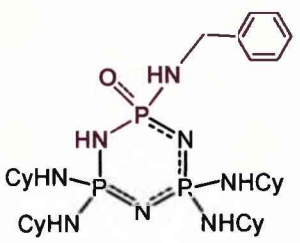

4.48

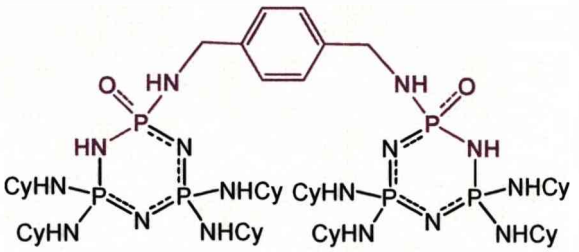

4.50

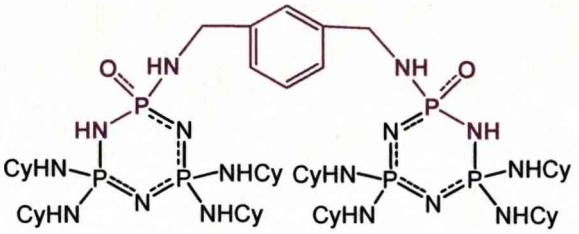

4.51

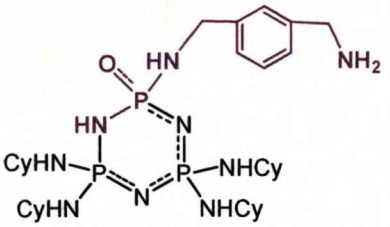

4.52

Figure 4.48.

4.2.4. Phosphites

4.2.4.1. Phosphite Synthesis and Variable Temperature NMR

Cyclophosphazenes of type **G** (Figure 4.1) containing phosphite units were prepared by reduction of a PCl_2 group followed by hydrolysis. The diamino dichloro derivative **4.34** was reacted with potassium in toluene followed by addition of finely ground KOH to the reaction solution. This yielded the phosphite derivative **4.53**, $[N_3P_3(N(Et)(CH_2)_3NEt)_2(O)(H)]K$, see Figure 4.49. The presence of the PH bond was confirmed by ^{31}P NMR. The $^{31}P\{^1H\}$ NMR spectrum of **4.53** shows the characteristic AX_2 signal pattern δ = 4.6 (t) and 24.6 (d) ppm, while the ^{31}P NMR displays the additional $^1J_{PH}$ coupling (536 Hz) of the "triplet". Crystals of the potassium salt **4.53** were obtained from toluene. The X-ray structure exhibits a hexameric complex. Addition of ammonium chloride to a solution of **4.53** in toluene yielded the neutral compound **4.54**, which crystallizes from a solution of THF.

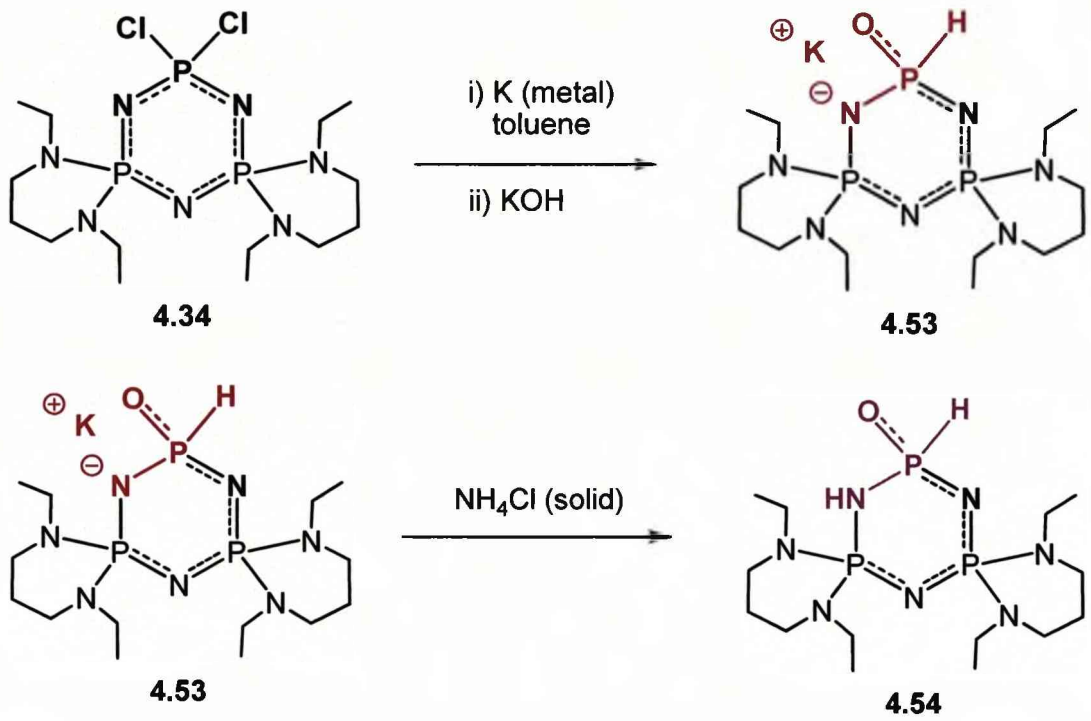

4.34 **4.53** **4.53** **4.54**

Figure 4.49. Synthesis of Phosphites 4.53 and 4.54.

Variable temperature ^{31}P NMR studies (Figures 4.50 and 4.51) show that **4.54** undergoes proton transfer between the two ring N sites adjacent to the PHO unit. At -40°C the ^{31}P $\{^{1}H\}$ NMR spectrum displays three signals with similar coupling constants, a "triplet" at δ = 20.0, and two "doublets" at δ = 13.6 and -5.0, respectively. Upon heating the two signals at δ = 20.0 and 13.6 broaden and coalesce at about 30°C. The signal at δ = -5.0 can be attributed to the PHO unit. It shows a characteristic $^{1}J_{PH}$ coupling of 580 Hz in the proton-coupled ^{31}P NMR spectrum. The "triplet" at δ = 20.0 can be assigned to the phosphorus centre bonded to two non-protonated ring nitrogen centres, while the P-P coupling across the protonated N-ring site with its long P-N bonds is too small to be observed. The rate of proton transfer is enhanced when a few drops of acetic acid are added to a solution of **4.54** in THF.

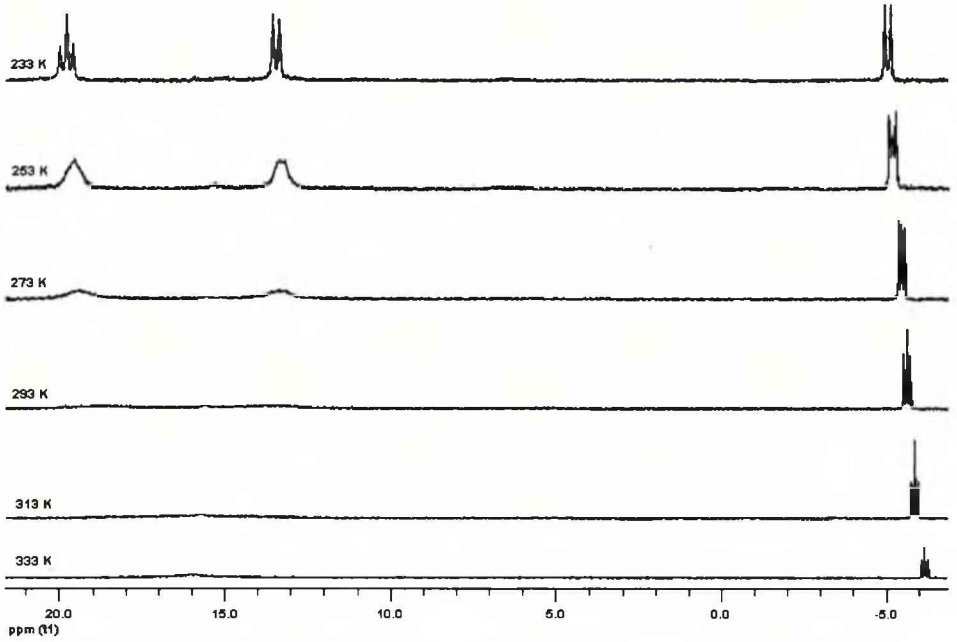

Figure 4.50. Variable Temperature ^{31}P {^{1}H} NMR Spectra of 4.54.

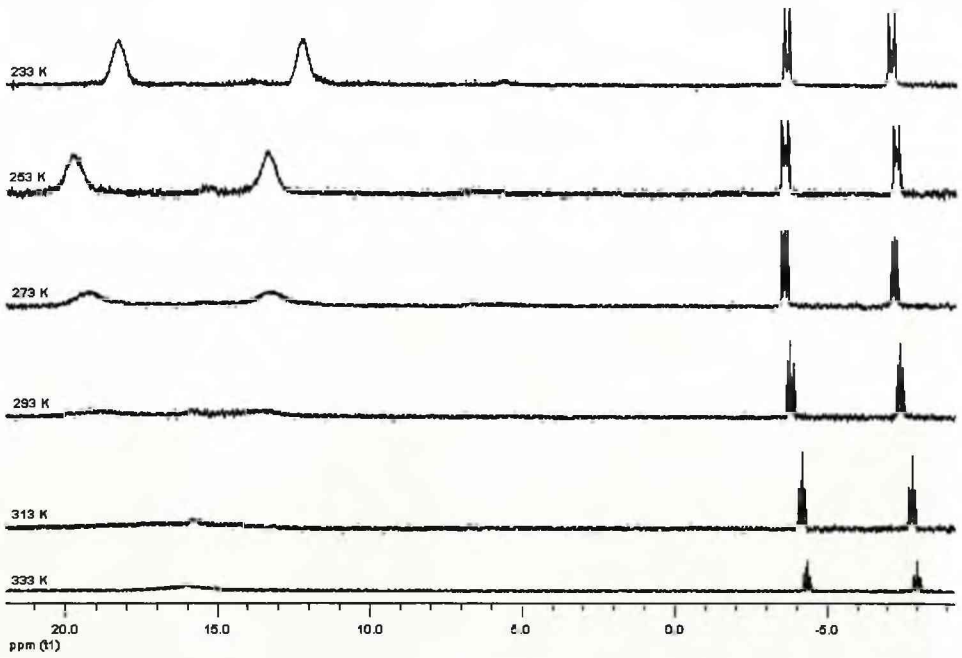

Figure 4.51. Variable Temperature ^{31}P NMR Spectra of 4.54.

4.2.4.2. Phosphite Crystal Structures

4.2.4.2.1. $[N_3P_3(N(Et)(CH_2)_3NEt)_2(O)(H)]K$ ($(4.53)_6$·3toluene)

Crystals of the potassium salt **4.53** were obtained after filtration and storage at -20 °C in the form of the solvate $(\mathbf{4.53})_6$·3 toluene. The crystal structure exhibits a hexameric potassium complex (Figure 4.52). The potassium ions and the O atoms of the monoanionic phosphite ligands form a K_6O_6 core structure that can be described as an arrangement of two face-sharing cubes. Alternatively, the structure can be portrayed as a stack of three K_2O_2 squares with K stacked above O and vice versa. Similar K_6O_6 arrangements are formed by some hexameric potassium aryloxide and amino oxide complexes, which contain additional donor ligands in the coordination sphere of the potassium ions.[58,59] To our knowledge, $(\mathbf{4.53})_6$ is the only homoleptic complex of a larger molecular K_nO_n aggregate ($n > 4$). The K-O distances range from 2.585(4) to 3.056(4) Å. The long contacts involve the O atoms of the central K_2O_2 square, which coordinate to four potassium ions, while shorter bonds are observed around the three coordinate O-atoms of the base squares. The centrosymmetric complex contains three crystallographically independent ligands (labelled *L1*, *L2* and *L3*). The ligands coordinate to the metal centres via the O-centres and both ring N-sites that are adjacent to the PHO unit. This unique arrangement of donor sites yields two bidentate N/O chelates. Thus the three independent ligands each chelate a pair of potassium ions, albeit at distinct sites of the central K_6O_6 core: *L1* chelates a pair located at opposite base squares, *L2* a pair occupying the same base square and *L3* a pair of potassium ions, one of which is part of a base and the other of the central square. The K-N bond lengths vary from 2.720(5) to 2.949(6) Å. In addition, *L2* forms a long K-N contact of 3.091(6) Å with an exocyclic nitrogen centre. The P-O bonds of the ligands are on average 1.501 Å long. The P-N(ring) bonds associated with the PHO unit measure on average 1.612 Å and are slightly longer than the P-N bonds further away from the PHO unit.

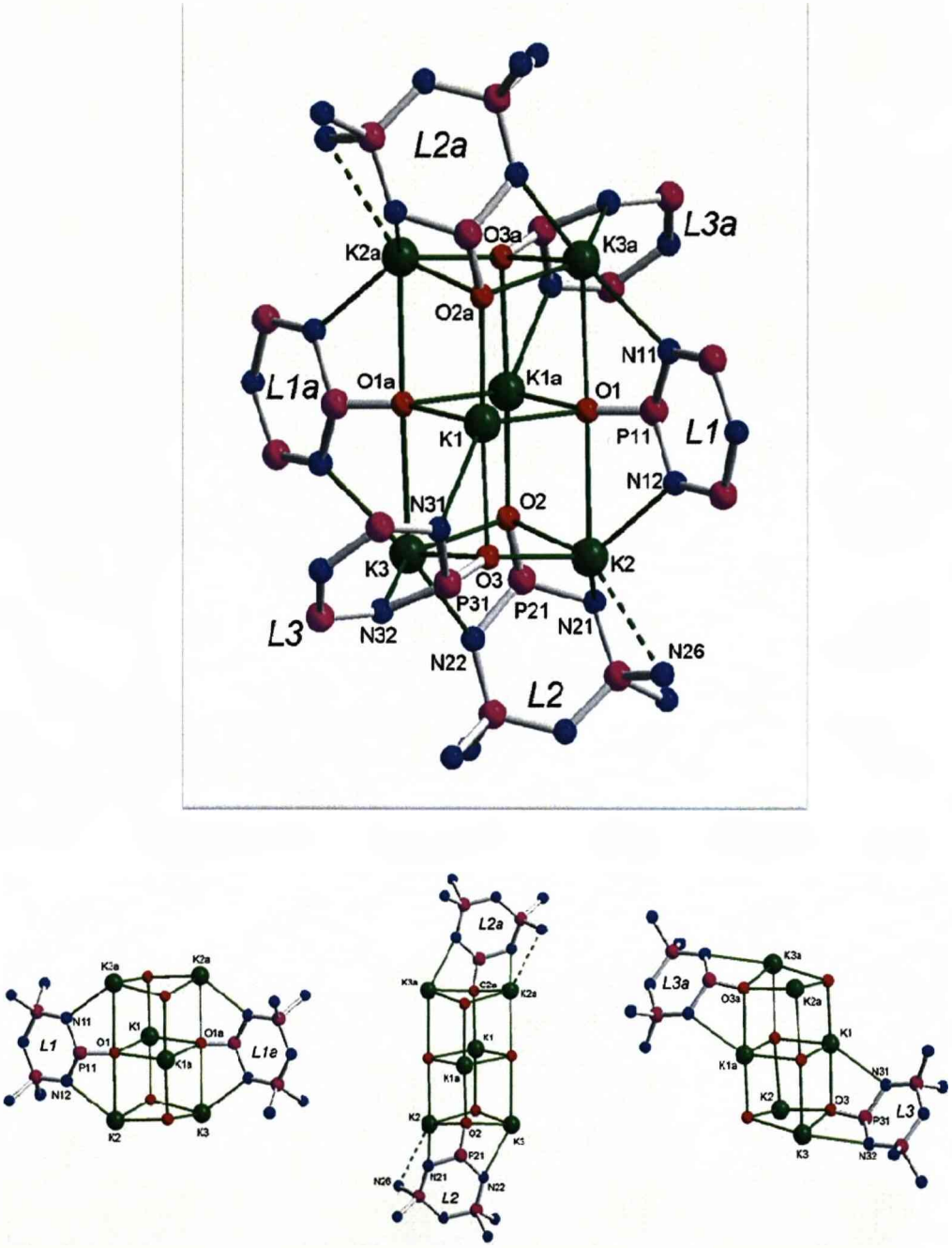

Figure 4.52. The Crystal Structure of the Hexameric Complex $(4.53)_6$.

Bottom: showing the K_6O_6 core and one set of ligands to illustrate the coordination mode of phosphite ligand.

(N(exo) atoms of L1 and L3 and C and H atoms are omitted for clarity)

4.2.4.2.2. $N_3P_3(N(Et)(CH_2)_3NEt)_2(O)(H)H$ (4.54)

The crystal structure of **4.54** shows a centrosymmetric hydrogen bonded dimer that is held together by two NH...O bridges with a N...O distance of 2.772(5) Å (Figure 4.53). The P-O bond measures 1.474(3) Å, which is slightly shorter than the P-O bond in the monoanionic ligand of **4.54**. The hydrogen atom at P1 was located in the difference fourier map. It was freely refined and shows a P-H distance of 1.39(5) Å. The P-N bonds at N2, the protonated N centre, (P1-N2 1.672(4), P2-N2 1.659(5) Å) are significantly longer than those of N1 and N3, which range between 1.565(4) and 1.602(4) Å. Both diamino substituents are affected by disorder indicating some conformational flexibility of the spirocyclic arrangement in the solid state.

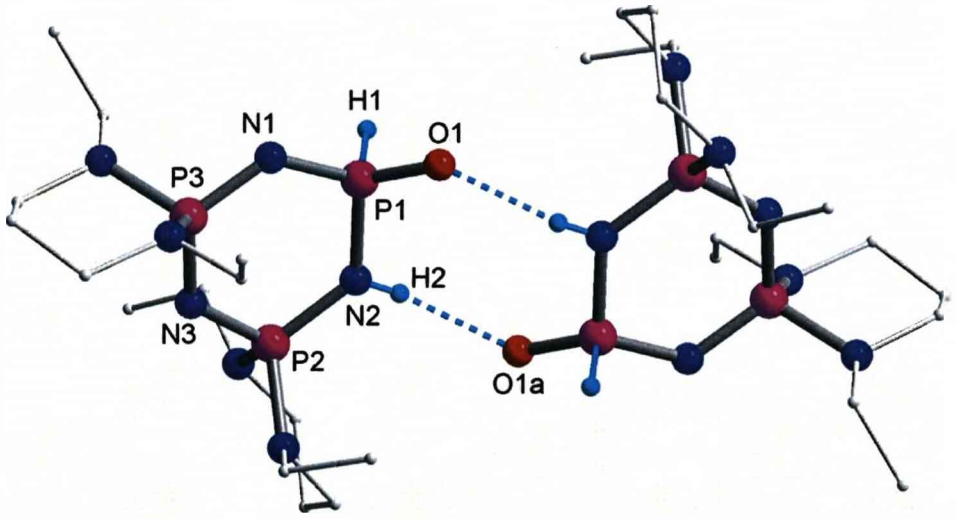

Figure 4.53. The Crystal Structure of 4.54

- showing dimeric H-bonded assembly. (H bound C atoms are omitted for clarity).

4.2.4.3. Synthesis of Cyclohexyl Phosphite Derivatives.

The phosphite synthesis was repeated for the cyclohexyl dichloride **4.33**. However after stirring **4.33** with potassium in toluene the ^{31}P $\{^1H\}$ NMR spectrum of the solution showed that no reaction had occurred. **4.33** was then treated with a THF solution of potassium and naphthalene (Figure 4.54), which contains the highly reductive radical anion $[C_{10}H_8]^{\cdot-}$. After 6 hrs stirring ^{31}P NMR spectroscopy showed that a reaction had occurred as the characteristic AX_2 spectrum of **4.33** had been replaced by a broad peak at δ = 15.1 ppm with a shoulder at δ = 6.1 ppm. It was, however, not possible to isolate this intermediate for further characterisation. Subsequently the reaction mixture was treated with finely ground KOH and then quenched with NH_4Cl upon which the ^{31}P $\{^1H\}$ NMR showed an AX_2 system with a "triplet" at δ = -8.5 and a "doublet" at δ = 9.5 ppm, ($^2J_{PP}$ = 24.0 Hz (t), 22.0 Hz (t) and 24.2 Hz (d)). The proton-coupled spectrum showed additional $^1J_{PH}$ coupling of 592.34 Hz, which verified the presence of the P-H bond. Prior to quenching with ammonium chloride the ^{31}P spectrum shows an AX_2 signal pattern with a "triplet" at δ = -2.2 and a "doublet" at δ = 13.2 ppm ($^2J_{PP}$ = 30.8 Hz), again PH coupling is observed in the proton-coupled spectrum at 547 Hz. These correlate well with ^{31}P NMR signals observed for **4.53** and **4.54**, suggesting that the cyclohexyl derivative forms an analogous compound **4.55**, $[N_3P_3(NHCy)_4(O)(H)]^- A^+$.

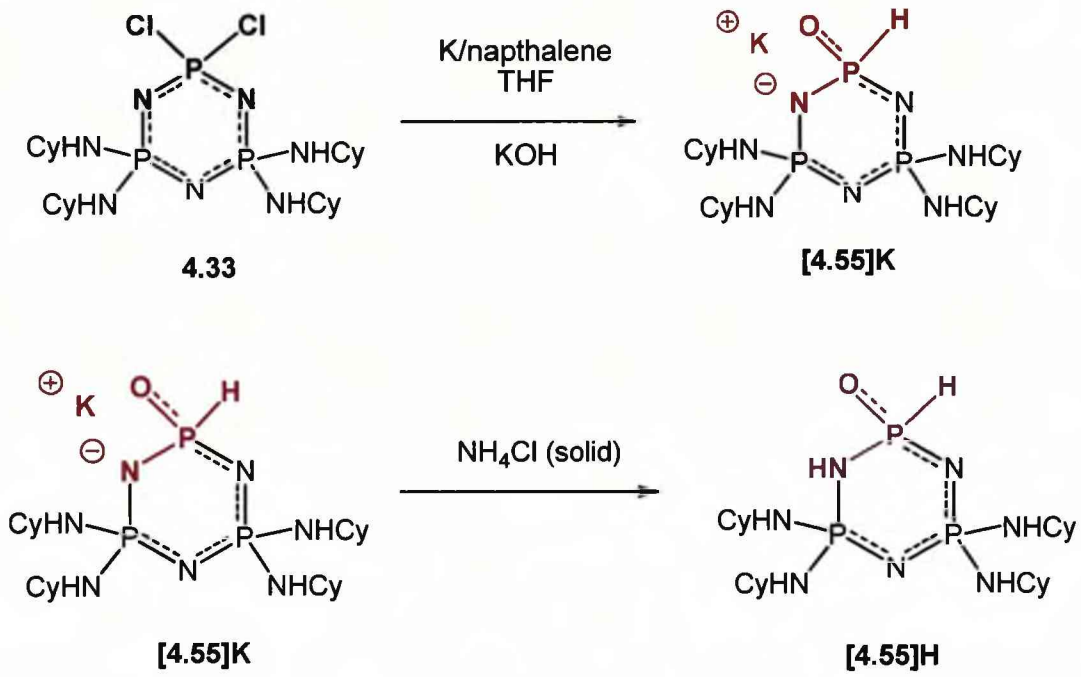

Figure 4.54.

4.3. Conclusions

Synthetic routes from geminal dichlorophosphazenes to a range of oxo-derivatives including phosphate, pyrophosphate, phosphamide and phosphite have been developed. The products are stable towards aqueous acids and bases. Although we have yet to determine pKa constants of these compounds, the above results show that they have amphiprotic properties undergoing protonation and deprotonation reactions at ring nitrogen sites adjacent to the PO unit. Hence, they can exist as anions and cations as well as neutral zwitterions. In addition, they can act as both H-bond donors, via NH sites, and H-bond acceptors, via N and O functions. The large number of potential H-bonding sites facilitates the formation of extended hydrogen bonded networks. While the phosphazene moiety headed by the P-oxo group can be regarded as the polar part of the structure, the four alkyl groups at the rear of the molecule provide a non-polar surface. This

amphiphilic behavior offers a variety of applications, for examples as surfactants, supramolecular building blocks and ligands for metal coordination and anion binding.

References

(1) Besli, S., Coles, S. J., Davies, D. B., Hursthouse, M. B., Ibisoglu, H., Kilic, A.; Shaw, R. A. *Chem. Eur. J.* **2004**, *10*, 4915.

(2) Chandrasekaran, A., Krishnamurthy, S. S.; Nethaji, M. *Inorg. Chem.* **1994**, *33*, 3085.

(3) Parvez, M., Kwon, S.; Allcock, H. R. *Acta Crystallogr., Sect. C: Cryst. Struct. Commun.* **1991**, *47*, 466.

(4) Dhathathreyan, K. S., Krishnamurthy, S. S., Murthy, A. R. V., Cameron, T. S., Chan, C., Shaw, R. A.; Woods, M. *J. Chem. Soc.-Chem. Commun.* **1980**, 231.

(5) Fitzsimm.Bw, Hewlett, C., Hills, K.; Shaw, R. A. *J. Chem. Soc. a Inorg. Phys. Theo.* **1967**, 679.

(6) Allcock, H. R.; Walsh, E. J. *J. Am. Chem. Soc.* **1969**, *91*, 3102.

(7) Allcock, H. R.; Fuller, T. J. *J. Am. Chem. Soc.* **1981**, *103*, 2250.

(8) Allcock, H. R., Fuller, T. J.; Matsumura, K. *Inorg. Chem.* **1982**, *21*, 515.

(9) Dhathathreyan, K. S., Krishnamurthy, S. S., Murthy, A. R. V., Shaw, R. A.; Woods, M. *J. Chem. Soc., Dalton Trans.* **1982**, 1549.

(10) Swamy, K. C. K.; Krishnamurthy, S. S. *J. Chem. Soc., Dalton Trans.* **1985**, 1431.

(11) Karthikeyan, S., Vyas, K., Krishnamurthy, S. S., Cameron, T. S.; Vincent, B. R. *J. Chem. Soc., Dalton Trans.* **1988**, 1371.

(12) Panzner, M. J., Youngs, W. J.; Tessier, C. A. *Acta Crystallogr., Sect. E: Struct. Rep. Online* **2009**, *65*, M105.

(13) Brinek, J., Alberti, M., Marek, J., Zak, Z.; Touzin, J. *Polyhedron* **1998**, *17*, 3235.

(14) Brandt, K., Vandegrampel, J. C., Meetsma, A.; Jekel, A. P. *Recueil Des Travaux Chimiques Des Pays-Bas-Journal of the Royal Netherlands Chemical Society* **1991**, *110*, 27.

(15) Chandrasekhar, V., Azhakar, R., Krishnan, V., Athimoolam, A.; Pandian, B. M. *J. Am. Chem. Soc.* **2006**, *128*, 6802.

(16) Vandegrampel, J. C. *Coord. Chem. Rev.* **1992**, *112*, 247.

(17) Meetsma, A., Vanderlee, A., Jekel, A. P., Vandegrampel, J. C.; Brandt, K. *Acta Crystallogr., Sect. C: Cryst. Struct. Commun.* **1990**, *46*, 909.

(18) Gabler, D. G.; Haw, J. F. *Inorg. Chem.* **1990**, *29*, 4018.

(19) Deruiter, B., Winter, H., Wilting, T.; Vandegrampel, J. C. *J. Chem. Soc., Dalton Trans.* **1984**, 1027.

(20) Allcock, H. R., Gardner, J. E.; Smeltz, K. M. *Macromolecules* **1975**, *8*, 36.

(21) Chandrasekhar, V.; Krishnan, V. *Adv. Inorg. Chem.* **2002**, *53*, 159.

(22) Marchand, R., Schnick, W.; Stock, N. *Adv. Inorg. Chem.* **2000**, *50*, 193.

(23) Allcock, H. R. *Chem. Rev.* **1972**, *72*, 315.

(24) Fitzsimmons, B. W., Hewlett, C.; Shaw, R. A. *J. Chem. Soc.* **1964**, 4459.

(25) Ansell, G. B.; Bullen, G. J. *J. Chem. Soc. a Inorg. Phys. Theo.* **1968**, 3026.

(26) Chakravarty, M., Suresh, R. R.; Swamy, K. C. K. *Inorg. Chem.* **2007**, *46*, 9819.

(27) Chakravarty, M., Kommana, P.; Swamy, K. C. K. *Chem. Commun.* **2005**, 5396.

(28) Doyle, E. L., Garcia, F., Humphrey, S. M., Kowenicki, R. A., Riera, L., Woods, A. D.; Wright, D. S. *Dalton Trans.* **2004**, 807.

(29) Briand, G. G., Chivers, T.; Krahn, M. *Coord. Chem. Rev.* **2002**, *233*, 237.

(30) Vijjulatha, M., Swamy, K. C. K., Vittal, J. J.; Koh, L. L. *Polyhedron* **1999**, *18*, 2249.

(31) Keat, R., Rycroft, D. S., Miller, V. R., Schmulbach, C. D.; Shaw, R. A. *Phosphorus, Sulfur Silicon Relat. Elem.* **1981**, *10*, 121.

(32) Benson, M. A., Zacchini, S., Boomishankar, R., Chan, Y.; Steiner, A. *Inorg. Chem.* **2007**, *46*, 7097.

(33) Bickley, J. F., Bonar-Law, R., Lawson, G. T., Richards, P. I., Rivals, F., Steiner, A.; Zacchini, S. *Dalton Trans.* **2003**, 1235.

(34) Allcock, H. R., Stein, M. T.; Stanko, J. A. *J. Chem. Soc.-Chem. Commun.* **1970**, 944.

(35) Bullen, G. J. *J. Chem. Soc. a Inorg. Phys. Theo.* **1971**, 1450.

(36) Chandrasekhar, V., Vivekanandan, K., Nagendran, S., Andavan, G. T. S., Weathers, N. R., Yarbrough, J. C.; Cordes, A. W. *Inorg. Chem.* **1998**, *37*, 6192.

(37) Chandrasekhar, V., Muralidhara, M. G. R.; Selvaraj, II *Heterocycles* **1990**, *31*, 2231.

(38) Chivers, T.; Hedgelan.R *Can. J. Chem.* **1972**, *50*, 1017.

(39) Das, S. K., Keat, R., Shaw, R. A.; Smith, B. C. *J. Chem. Soc.* **1965**, 5032.

(40) Bartlett, S. W., Coles, S. J., Davies, D. B., Hursthouse, M. B., Ibisoglu, H., Kilic, A., Shaw, R. A.; Un, I. *Acta Crystallogr. Sect. B-Struct. Commun.* **2006**, *62*, 321.

(41) Boomishankar, R., Richards, P. I.; Steiner, A. *Angew. Chem., Int. Ed.* **2006**, *45*, 4632.

(42) Richards, P. I.; Steiner, A. *Inorg. Chem.* **2004**, *43*, 2810.

(43) Boomishankar, R.; Steiner, A. Unpublished Work.

(44) Xu, S. J., Held, I., Kempf, B., Mayr, H., Steglich, W.; Zipse, H. *Chem. Eur. J.* **2005**, *11*, 4751.

(45) Ragnarsson, U.; Grehn, L. *Acc. Chem. Res.* **1998**, *31*, 494.

(46) Scriven, E. F. V. *Chem. Soc. Rev.* **1983**, *12*, 129.

(47) Hofle, G., Steglich, W.; Vorbruggen, H. *Angew. Chem., Int. Ed. Engl.* **1978**, *17*, 569.

(48) Huynh, K., Rivard, E., Lough, A. J.; Manners, I. *Chem. Eur. J.* **2007**, *13*, 3431.

(49) Davidson, R. J., Weigand, J. J., Burford, N., Cameron, T. S., Decken, A.; Werner-Zwanziger, U. *Chem. Commun.* **2007**, 4671.

(50) Rivard, E., Huynh, K., Lough, A. J.; Manners, I. *J. Am. Chem. Soc.* **2004**, *126*, 2286.

(51) Burford, N., Spinney, H. A., Ferguson, M. J.; McDonald, R. *Chem. Commun.* **2004**, 2696.

(52) Burford, N., Losier, P., Phillips, A. D., Ragogna, P. J.; Cameron, T. S. *Inorg. Chem.* **2003**, *42*, 1087.

(53) Boomishankar, R., Ledger, J., Guilbaud, J.-B., Campbell, N. L., Bacsa, J., Bonar-Law, R., Khimyak, Y. Z.; Steiner, A. *Chem. Commun.* **2007**, 5152.

(54) Begley, M. J., Sowerby, D. B.; Bamgboye, T. T. *J. Chem. Soc., Dalton Trans.* **1979**, 1401.

(55) Stock, N.; Schnick, W. *Acta Crystallogr., Sect. C: Cryst. Struct. Commun.* **1997**, *53*, 532.

(56) Benson, M. A., Ledger, J.; Steiner, A. *Chem. Commun.* **2007**, 3823.

(57) Mani, N. V.; Wagner, A. J. *Chem. Commun.* **1968**, 658.

(58) Venugopal, A., Berger, R. J. F., Willner, A., Pape, T.; Mitzel, N. W. *Inorg. Chem.* **2008**, *47*, 4506.

(59) Boyle, T. J., Andrews, N. L., Rodriguez, M. A., Campana, C.; Yiu, T. *Inorg. Chem.* **2003**, *42*, 5357.

Chapter 5:

Experimental

5.1. General Procedures

All air and moisture sensitive reactions were performed under an N_2 gas atmosphere using standard Schlenk techniques and a glove box. THF was distilled on demand over potassium. Hexane and toluene were distilled on demand over sodium. Chloroform and dichloromethane were purified in batches. They were pre-dried then distilled over phosphorus pentoxide, then distilled a second time over calcium hydride and stored over molecular sieves. Amines were distilled over KOH then stored with molecular sieves.

For all other reactions solvents were stored over KOH then used from the bottle. Chloroform and methanol were used as supplied. Amines were either used as supplied or stored over molecular sieves.

Standard solutions of aqueous KOH and NH_4Cl were prepared to a known molarity using deionised water.

$N_3P_3Cl_6$ was purchased from Aldrich or Avocado. The material from Aldrich was used as supplied. $N_3P_3Cl_6$ from Avocado contained ~10% $N_4P_4Cl_8$ by ^{31}P NMR. This mixture was separated by recrystallisation from hot hexane, which was also the source of $N_4P_4Cl_8$.

All chemicals were purchased from Aldrich, Acros, BDH or Avocado.

5.2. Instrumentation

FT-IR spectra were recorded on a Perkin-Elmer Paragon 1000 spectrometer in Nujol between NaCl plates or on a on an FT/IR-4000 type A instrument as the solid material.

NMR spectra were recorded on a Bruker AMX 400 spectrometer at room temperature (unless otherwise stated) using $SiMe_4$ (for ^1H and ^{13}C) and 85% H_3PO_4 (for ^{31}P) as external standards (^1H NMR. 400.14 MHz; $^{13}C\{^1H\}$ NMR. 100.62 MHz; $^{31}P\{^1H\}$ NMR. 161.97).

Solid-state NMR spectra were carried out on our behalf by Dr Y. Khimyak, Dr J. T. A. Jones and Dr J. B. Guilbard. The spectra were measured on a Bruker Avance DSX 400 spectrometer operating at 100.61 MHz for ^{13}C, 161.98 MHz for ^{31}P and 400.13 MHz for ^1H. All spectra were collected using a 4mm triple resonance probe and zirconia rotors. The values of ^{13}C and ^{31}P chemical shifts are referred to TMS and H_3PO_4 respectively. The $^1H \rightarrow ^{13}C$ cross-polarisation magic-angle spinning (CP/MAS) NMR spectra were measured at MAS rate of 10.0 kHz. The ^1H $\pi/2$ pulse was 3.0 µs. The two phase pulse modulation (TPPM) decoupling[1,2] was used during the acquisition at an *rf* field of *ca.* 83 kHz. The Hartmann-Hahn condition was set using glycine. The recycle delay was 10 s and the contact time was set to 2.0 ms. The ^{31}P MAS NMR spectra were measured at a MAS rate of 10 kHz with ^1H TPPM decoupling during acquisition at an *rf* field of *ca.* 83 kHz. A ^{31}P $\pi/3$ pulse length of 2.1 µs with a recycle delay of 120.0 s was used.

Mass spectra were recorded on VG analytical 7070E and Fisions Trio 1000 spectrometers using electrospray ionisation (ESI).

Elemental analysis (C, H, N and S) were recorded on Thermo-Flash EA1112 series CHNS analyser.

CHN analyses of compounds **4.39**, **4.43**, **4.42**, **[4.42]**Cl_2, **4.48**, **4.49**, **4.50**, **4.51**, **4.52** and **4.53** did not give consistent results. This is attributed to a large amount of solvent being contained in the bulk material.

Melting points were recorded using Stuart melting point apparatus SMP3.

5.3. ^{31}P NMR Spectroscopy of Hetero- Substituted Cyclotriphosphazenes

Hetero- substituted cyclotriphosphazenes generally give characteristic AX_2 signal patterns in their ^{31}P $\{^1H\}$ NMR spectra and their chemical shifts and coupling constants are reported as such through out phosphazene literature. However the phosphorus nuclei within hetero- substituted cyclotriphosphazenes are not true AX_2 systems. This is due to the nitrogen atoms within the phosphazene ring, which contain 0.37% ^{15}N. Thus, creating a slight inequivalence of phosphorus nuclei, which are otherwise equivalent. Conforming to the literature and for clarity in discussion all ^{31}P $\{^1H\}$ NMR data in this thesis is presented as if this effect is not present. However the terms triplet and doublet are used with inverted commas and a series of values are given for the coupling constants, as this effect causes a slight variation J values.

5.4. Synthesis

5.4.1. $[N_3P_3(DMAP)_6]^{6+}$ (3.9)

$[N_3P_3(DMAP)_6]Cl_6$ ([3.9]Cl_6)

Microwave reaction:

0.060 g of $P_3N_3Cl_6$ (0.173 mmol), 0.126 g of DMAP (1.031 mmol) and 3 ml of chloroform were placed in a 10ml CEM microwave reaction tube. The tube was then placed in the autosampler of a CEM Explorer™ microwave reactor and reacted at 100 °C at 300 W power with cooling (Max Power™) using compressed air to maximise energy input into the sample. The reaction was continued for 20 mins to produce a super saturated brown solution, which on cooling to room temperature yielded colourless needle like crystals, which were washed several times with chloroform and subsequently dried in vacuum.

Yield 0.190 g, 66.0%

M.p. = 200 °C (decomp.).

^{1}H NMR ($C_2D_2Cl_4$): δ = 3.24 (s, CH_3, 36H), 6.94 (d, *meta*-H, 12H, $^{3}J_{HH}$ = 7.2 Hz), 7.30, 9.80 ppm (m, *ortho*-H, 12H).

$^{13}C\{^{1}H\}$ NMR ($C_2D_2Cl_4$): δ = 41.6 (CH_3), 107.0 (*meta*-C), 141.0 (*ortho*-C), 157.9 ppm (*para*-C).

$^{31}P\{^{1}H\}$ NMR ($C_2D_2Cl_4$): δ = 10.3. ppm

Elemental analysis (%) for calcd. for $P_3N_{15}C_{42}H_{60}Cl_6 \cdot (CHCl_3)_5$: C, 33.65; H, 3.90; N, 12.52. Found: C, 32.04; H, 3.93; N, 12.74.

Single crystals of $[N_3P_3(DMAP)_6]Cl_6 \cdot 19CHCl_3$ suitable for X-ray structure analysis were obtained from a mixture of 0.030 g of $P_3N_3Cl_6$ (0.087 mmol), 0.063 g of DMAP (0.515 mmol) and 3 ml of chloroform using the same reaction protocol and after reaction the temperature was lowered at a steady ramp rate; 100 °C - 80 °C over 5 mins holding at 80 °C for 3 mins, then 80 °C - 60 °C over 5 mins holding at 60°C for 3mins followed by 60 °C - 40 °C over 5 mins holding at 40 °C for 3 mins to yield colourless plate like crystals. $^{31}P\{^{1}H\}$ NMR ($C_2D_2Cl_4$): δ = 10.3.

Synthesis from 1,1,2,2-tetrachloroethane:

0.60 g $N_3P_3Cl_6$ (1.73 mmol) and 1.268 g DMAP (10.38 mmol) were dissolved in 10 ml of 1,1,2,2-tetrachloroethane. The solution warmed up indicating an exothermic reaction and turned pale yellow in colour. After 30 minutes stirring the product was precipitated on addition of chloroform (2 ml) and hexane (15 ml). The product was isolated as a white solid after subsequent washing with chloroform (3 x 10 ml) and hexane (10 ml) to remove residues of trichloroethane and DMAP.

Yield 2.30 g, 79.9%

M.p. = 200°C (decomp.).

^{1}H NMR ($C_2D_2Cl_4$): δ = 3.25 (s, CH_3, 36H), 6.94 (d, *meta*-H, 12H, $^{3}J_{HH}$ = 7.2 Hz), 7.38 (s, $CHCl_3$, 5H), 9.80 ppm (m, *meta*-H, 12H).

$^{13}C\{^1H\}$ NMR ($C_2D_2Cl_4$): δ = 41.6 (CH_3), 78.3 ($CHCl_3$), 107.1 (*meta*-C), 140.9 (*ortho*-C), 157.9 ppm (*para*-C).

$^{31}P\{^1H\}$ NMR ($C_2D_2Cl_4$): δ = 10.3 ppm.

IR (nujol): $\nu(cm^{-1})$ = 1633, 1554, 1274, 1207, 1170($P\text{-}N_{ring}$), 1054 ($P\text{-}N_{ring}$), 940, 808.

Elemental analysis (%) for calcd. for $P_3N_{15}C_{42}H_{60}Cl_6\cdot(CHCl_3)_5$: C, 33.65; H, 3.91; N, 12.52. Found: C, 31.17; H, 4.04; N, 12.28.

Synthesis by Slow Diffusion

Single crystals of $[N_3P_3(DMAP)_6]Cl_6$ were grown from solutions containing $N_3P_3Cl_6$ (0.100 g, 0.288 mmol) and 6 equivalents of DMAP (0.211 g, 1.727 mmol) in 3 ml of $CHCl_3$ or DCM. Crystallisation occurred only when the solutions were left undisturbed, allowing the DMAP solids to dissolve slowly and therefore slowly diffuse into the solution of $N_3P_3Cl_6$, yielding $[N_3P_3(DMAP)_6]Cl_6\cdot 19CHCl_3$ and $P_3N_3(DMAP)_6]Cl_6\cdot 11\ CH_2Cl_2$, respectively.

Single crystals of $[P_3N_3(DMAP)_6]Cl_4I_2\cdot 14CHCl_3$ formed when $N_3P_3Cl_6$ (0.100 g, 0.288 mmol), 6 equivalents of DMAP (0.211 g, 1.727 mmol) and N^nBu_4I (0.638 g, 1.727 mmol) were slowly dissolved in 3 ml of $CHCl_3$.

5.4.2. $[N_3P_3(DMAP)_5(O)]Cl_4\cdot 9CHCl_3$ (3.10)

Single crystals were obtained from a solution of $P_3N_6Cl_6$ (0.100 g, 0.287 mmol) and six equivalents of (DMAP 0.211 g, 1.73 mmol) in 3 ml of a saturated solution of water in chloroform after 24 hrs.

Standard solutions of water in chloroform were obtained by diluting saturated solutions (0.046 M at 20°C) with dry chloroform.

Elemental analysis (%) calcd. for $P_3N_{13}C_{35}H_{50}OCl_4\cdot(CHCl_3)_9$: C, 26.72; H, 3.01; N, 9.21. Found: C, 25.88; H, 3.25; N, 9.44.

The chloroform solution was removed from the crystals and they were washed with dry chloroform (2 x 3 ml), then dried under vacuum.

Yield = 0.352 g, 62.0 %

M.p. = 101.5 – 103 °C

IR v(cm^{-1}): 3330, 3197, 3043, 2900 (C-H), 2811 (C-H), 2682, 1639, 1560, 1442, 1403, 1268, 1214, 1060 (P-N_{ring}), 991, 943, 809.956, 744.388.

Elemental analysis (%) calcd. for $P_3N_{13}C_{35}H_{50}OCl_4 \cdot (CHCl_3)_{1.5}$: C, 40.49; H, 4.79; N 16.81. Found: C, 40.80; H, 5.82; N, 16.22.

5.4.3. $[P_4N_4O_2(DMAP)_6]Cl_4 \cdot 14\ CHCl_3$ (3.11)

0.160 g of $P_4N_4Cl_8$ (0.2157 mmol), 0.211 g of DMAP (1.725 mmol) and 4 ml of chloroform were placed in a 10ml CEM microwave reaction tube. The tube was then placed in the autosampler of a CEM Explorer™ microwave reactor and reacted at 80 °C at 150 W power with cooling (Max Power™) using compressed air to maximise energy input into the sample. The reaction was continued for 20 mins, then cooled to 60 °C and held for 4 mins, then 40 °C for 4 mins and 20 °C for 4 mins. This produced a super saturated solution containing a brown solid. After standing overnight single crystals of $[P_4N_4O_2(DMAP)_6]Cl_4 \cdot 14\ CHCl_3$ had formed in the solution.

5.4.4. $PyN(CH_2)_2(CH_2)_2NPy$ (3.12)

4-Chloropyridine hydrochloride (2.341 g, 15.605 mmoles) was dissolved in distilled water. 30 ml, 2 M $KOH_{(aq)}$ was added and the solution was stirred for 10 mins. A pale orange oil formed in solution and was extracted with DCM. The DCM solution was dried over K_2CO_3 and the volatilities were removed under reduced pressure, to give 4-chloropyridine as a pale yellow oil.

Yield: 1.61 g, 91.0%

^1H NMR ($CDCl_3$): δ = 7.05 (d, 2H, CH, $^3J_{HH}$ = 6.17 Hz), 8.29 (d, 2H, NCH, $^3J_{HH}$ = 6.15 Hz)

Piperazine (0.601 g, 7.093 mmoles) was added to 4-Chloropyridine (1.61 g, 14.179 mmoles) and the mixture was heated until all the piperazine had melted (oil bath temperature = 140 °C). Heating was then maintained for 1 hr. After cooling ^{1}H NMR indicated that the reaction mixture contained $PyN(CH_2)_2(CH_2)_2NPy$ and $PyN(CH_2)_2(CH_2)_2NH$ as well as unreacted starting materials. The residue was washed with chloroform, this removed unreacted 4-chloropyridine and piperazine, then dissolved in water and treated with $KOH_{(aq)}$ (30 ml, 2 M). The crude product was then extracted with DCM. Crude Yield = 0.53 g, (31.5%). This was recrystallised from DCM and hexane to give pure $PyN(CH_2)_2(CH_2)_2NPy$.

Yield = 0.224 g (13.3%)

Single crystals of $PyN(CH_2)_2(CH_2)_2NPy$ were obtained from a methanol solution by slow evaporation.

M.p. = 210 °C (decomp.)

^{1}H NMR (CD_3OD): δ = 3.66 (s, 8H, CH_2), 6.92 (d, 4H, CH, $^3J_{HH}$ = 6.82 Hz), 8.17 ppm (d, 4H, NCH, $^3J_{HH}$ = 6.71 Hz).

^{13}C NMR (CD_3OD): δ = 46.2 (CH_2), 109.3 (CH), 146.8 (NCH), 158.0 ppm (NC).

IR ν(cm^{-1}): 3374, 3112, 3037, 2875 (C-H), 1629, 1527, 1446, 1396, 1292, 1224, 1195, 1056, 997, 948, 809, 744.

Elemental analysis (%) for calcd. for $N_4C_{14}H_{16}$: C, 69.97; H, 6.71; N, 23.22. Found: C, 65.25; H, 6.55; N, 19.09.

5.4.5. Dichlorides

The syntheses of **4.33**[3] and **4.34**[4] are modified literature procedures.

$N_3P_3(NHCy)_4Cl_2$ (4.33)

A solution of $N_3P_3Cl_6$ (22.71g, 65.32mmol) and triethylamine (80 ml), in 180 ml toluene was cooled to 0°C and cyclohexylamine (30.63 ml, 267.77 mmol, 4.1 eq) was added dropwise. The solution was stirred for 30 mins, then

allowed to warm to room temperature and refluxed for 24 hrs. After reflux a thick white precipitate of amine hydrochlorides and product had formed. The solution was allowed to cool to room temperature and then filtered under suction. The solids were washed twice with THF. Removal of the THF under vacuum yielded 17.94 g $N_3P_3(NHCy)_4Cl_2$ as a white, powdery solid. The volatilities were removed from the filtrate under vacuum leaving a sticky off-white solid containing 56.6% $N_3P_3(NHCy)_4Cl_2$, 22.3% $N_3P_3(NHCy)_6$, and 21.1% $N_3P_3(NHCy)_2Cl_4$ by $^{31}P\{^1H\}$ NMR. The crude product was purified by column chromatography using chloroform as the eluent to give 9.01 g $N_3P_3(NHCy)_4Cl_2$.

Yield: 26.95 g, 68.9%.

Mp: 181.0-181.5 °C.

^1H NMR ($CDCl_3$): δ = 1.11 - 1.20 (m, 40H, CH_2), 3.06 (m, 4H, CH).

$^{13}C\ \{^1H\}$ NMR ($CDCl_3$): δ = 25.6 (CH_2), 25.9 (CH_2), 36.4 (CH_2), 36.5 (CH_2), 50.5 ppm (CH).

$^{31}P\ \{^1H\}$ NMR ($CDCl_3$): δ = 11.1 (d, $^2J_{PP}$ = 49.6 Hz, 2P, P(NHCy)), 24.3 ppm (t, $^2J_{PP}$ = 48.4, 50.1 Hz, 1P, PCl_2).

IR v(cm^{-1}): 3409 (N-H), 3224 (N-H), 2923 (C-H), 2850 (C-H), 1446, 1403, 1292, 1218, 1170, (P-N_{ring}) 1099, 1006, 885, 846, 811.

Elemental analysis (%) for calcd. for $P_3N_7C_{24}H_{48}Cl_2$: C, 48.16; H, 8.08; N, 16.38. Found: C, 48.40; H, 8.13; N, 16.50.

$N_3P_3(N(Et)(CH_2)_3(Et))_2Cl_2$ (4.34)

To a solution of $P_3N_3Cl_6$ (8.00 g, 23 mmol) in 200 ml of diethyl ether, 30 ml of N,N'-diethylpropanediamine (24.48 g, 188 mmol) was slowly added and the mixture was heated to reflux. The progress of the reaction was monitored using ^{31}P-NMR. The reaction was complete after 7 days. The solvent and the excess amine were removed under vacuum. The residue obtained was dissolved in 15 ml of n-hexane and kept at -20 °C. Colourless crystals were

obtained after 2 days and collected by filtration. The filtrate was concentrated to 5 ml and kept for crystallization at -20 °C to obtain a further batch of crystals. The crystals were finally washed twice with 2 ml portions of cold pentane and dried.

Yield: 6.15 g, 57.8%.

M.p. = 71 °C.

^{1}H NMR ($CDCl_3$): δ = 1.11 (t, 12H, CH_3(Et)), 1.76-1.84 (m, 4H, $CH_2(CH_2)_2$), 2.95-3.00 (m, 8H, NCH_2(Et)), 3.10-3.15 ppm (m, 8H, NCH_2).

^{13}C {^{1}H} NMR ($CDCl_3$): δ = 13.9 (CH_3(Et)), 25.1 (CH_2(Pr)), 42.11 (NCH_2(Et)), 45.8 ppm (NCH_2(Pr)).

^{31}P{^{1}H} NMR ($CDCl_3$): δ = 18.9 (d, $^{2}J_{PP}$ = 39.6, 2P, P(N(Et)$(CH_2)_3$NEt)), 23.3 ppm (t, $^{2}J_{PP}$ = 39.6, 1P, PCl_2).

IR ν(cm^{-1}): 2969 (C-H), 2848 (C-H), 2005, 1544, 1465, 1380, 1313, 1228, 1205, 1159, (P-N_{ring}) 1120, 1056, 1022, 941, 891, 844, 755, 715.

Elemental analysis (%) for calcd. for $C_{14}H_{32}Cl_2N_7P_3$: C, 36.37; H, 6.98; N, 21.21. Found: C, 35.89; H, 6.90; N, 20.80.

5.4.6. DMAP Stabilised Dications

$[N_3P_3(NHCy)_4(DMAP)_2]Cl_2$ ([4.38]Cl_2)

$N_3P_3(NHCy)_4Cl_2$ (1.00 g, 1.671 mmol) was dissolved in chloroform (20 ml); to this a solution of DMAP (0.50 g, 4.093 mmol) in 10 ml chloroform was added. The solution was stirred for 15 mins then refluxed for 24 hrs after which it became dark orange. The chloroform was removed under vacuum and product was isolated as a white solid after washing with hexane and tetrahydrofuran to remove hydrolysed side products and excess DMAP.

Yield: 0.92 g, 64.8 %

Single crystals of $N_3P_3(NHCy)_4(DMAP)_2Cl_2$•1½$CHCl_3$·$2H_2O$ were obtained by slow diffusion of a THF atmosphere into a chloroform solution.

Mp = 130.5 – 131.0 °C

^{1}H NMR ($CDCl_3$): δ = 1.16-1.85 (m, 40H, CH_2(Cy) & 4H, CH(Cy)), 3.00 (br, 4H, NH(Cy)), 3.31 (s, 12H CH_3(DMAP)) 7.18-7.20 (m, 4H, meta-H(DMAP)), 9.03-9.06 ppm (m, 4H, ortho-H(DMAP)). (Impurity: Free DMAP: δ = 3.20, 6.71, 8.16 ppm, ratio 1:0.15).

^{13}C {^{1}H} NMR ($CDCl_3$): δ = 24.2 (CH_2(Cy)), 24.4 (CH_2(Cy)), 24.6 (CH_2(Cy)), 34.8 (CH_2(Cy)), 35.0 (CH_2(Cy)), 40.0 (CH_3(DMAP)), 49.4 (CH(Cy)) 108.0 (meta-C(DMAP)), 139.3 (ortho-C(DMAP)), 156.7 (para-C(DMAP)).

^{31}P {^{1}H} NMR ($CDCl_3$): δ = 6.5 (t, $^{2}J_{PP}$ = 49.0, 48.9 Hz, 1P, P(DMAP)$_2$), 9.7 ppm (d, $^{2}J_{PP}$ = 51.3 Hz, 2P, P(NHCy)$_2$).

IR ν(cm^{-1}): 3382, 3249, 3058 (N-H), 2925 (C-H), 2852 (C-H), 1633, 1563, 1504, 1446., 1403, 1321, 1290, 1243, 1170, (P-N_{ring}) 1076, (P-N_{ring}) 1049, 916, 889, 825, 765, 725, 642, 611.

Elemental analysis (%) for calcd. for $P_3N_{11}C_{38}H_{68}Cl_2{\cdot}2H_2O{\cdot}0.5CHCl_3$: C, 49.27; H, 7.79; N, 16.42. Found: C, 48.19; H, 7.89; N, 16.71.

MS-ESI: M^{2+} at 385.7 Da

$[N_3P_3(N(Et)(CH_2)_3NEt)_2(DMAP)_2]Cl_2$ ([4.43]Cl_2)

$N_3P_3(N(Et)(CH_2)_3NEt)_2Cl_2$ (0.288 g, 0.623 mmol) was dissolved in chloroform (5 ml), a solution of DMAP (0.170 g, 1.392 mmol) in 5 ml chloroform was added. The solution was stirred for 15 mins then refluxed for 8 days. The reaction was monitored by ^{31}P NMR after 8 days this showed 59% of $N_3P_3(N(Et)(CH_2)_3NEt)_2Cl_2$ had reacted to give a single product. The chloroform was removed under vac and the residue was stirred overnight in hexane.

This yielded a white solid containing $[N_3P_3(N(Et)(CH_2)_3NEt)_2(DMAP)_2]Cl_2$ and free DMAP after suction filtration.

Yield: 0.19 g, 43.2%.

Mp = 210 °C (Decomp.)

^{1}H NMR ($CDCl_3$): δ = 1.00 (t, 12H, CH_3(Et), $^3J_{HH}$ = 7.1 Hz), 1.80 - 1.97 (m, 4H, CH_2(Pr)), 2.80 - 3.26 (m, 8H, NCH_2(Et)), 3.15 - 3.4 (m, 8H, NCH_2(Pr)), 3.36 (s, 12H CH_3(DMAP)) 7.32 - 734. (m, 4H, meta-H(DMAP)), 9.04 – 9.08 ppm (m, 4H, ortho-H(DMAP)). (Impurity: Free DMAP: δ = 3.21, 6.74, 8.19 ppm, ratio 1:0.35).

^{13}C {^{1}H} NMR ($CDCl_3$): δ = 14.0 (CH_3(Et)), 24.2 (CH_2(Pr)), 41.8 (CH_3(DMAP)) 41.9 (NCH_2(Et)), 46.1 (NCH_2(Pr)), 109.7, 109.8 (meta-C(DMAP)), 140.6, 140.6 (ortho-C(DMAP)), 158.2 ppm (para-C(DMAP)).

^{31}P {^{1}H} NMR ($CDCl_3$): δ = 7.2 (t, $^2J_{PP}$ = 38.5, 38.5 Hz 1P, $P(DMAP)_2$), 21.0 ppm (d, $^2J_{PP}$ = 38.5 Hz, 2P, $P(NHCy)_2$,).

IR ν(cm^{-1}): 3330, 3045, 2965 (C-H), 2873 (C-H), 2815, 2680, 2107, 1637, 1562, 1442, 1332, 1267, 1243, 1214, 1168, ($P\text{-}N_{ring}$) 1051.01 ($P\text{-}N_{ring}$), 944, 894, 833, 784, 719, 667.

Elemental analysis (%) for calcd. for $P_3N_{11}C_{28}H_{52}Cl_2$: C, 47.59; H, 7.42; N, 21.81. Found: C, 42.71; H, 7.47; N, 19.64.

$[N_3P_3(NH^tBu)_4(DMAP)_2]Cl_2$ ([4.44]Cl_2)

$N_3P_3(NH^tBu)_4Cl_2$ (0.209 g, 0.423 mmol) was dissolved in chloroform (3 ml); a solution of DMAP (0.170 g, 1.392 mmol) in 5 ml chloroform was added. The solution was stirred for 15 mins then refluxed for 1 week. The reaction was monitored by ^{31}P NMR, after 1 week this showed a mixture of $[N_3P_3(NH^tBu)_4(DMAP)_2]Cl_2$ and $N_3P_3(NH^tBu)_4Cl_2$. The chloroform was removed under vac and the residue was stirred overnight in hexane then overnight in THF. This yielded a white solid containing $[N_3P_3(NH^tBu)_4(DMAP)_2]Cl_2$ and free DMAP after suction filtration.

Yield: 0.014 g, 4.5%

^{1}H NMR ($CDCl_3$): δ = 1.21 (s, 36H, $CH_3(^tBu)$), 3.07 (br, 4H, NH), 3.27 (s, 12H CH_3(DMAP)) 7.14 - 7.16 (m, 4H, meta-H(DMAP)), 9.03 – 9.06 ppm (m,

4H, ortho-H(DMAP)). (Impurity: Free DMAP: δ = 3.14, 6.68, 8.12 ppm, ratio 1:0.55).

^{13}C {^{1}H} NMR ($CDCl_3$): δ = 30.6 ($CH_3(^tBu)$), 41.3 (CH_3(DMAP)), 51.8 (NC), 109.2, 109.3 (meta-C(DMAP)), 141.2, 141.4 (ortho-C(DMAP)), 158.1 (para-C(DMAP)).

^{31}P {^{1}H} NMR ($CDCl_3$): δ = 5.0 – 6.1 (m, $P(DMAP)_2$ and $P(NH^tBu)$).

5.4.7. Phosphate and Pyrophosphate

$N_3P_3(NHCy)_4(OH)_2 \cdot 4H_2O$ (4.40)

$N_3P_3(NHCy)_4Cl_2$ (1.89 g, 3.16 mmol) was dissolved in THF (50 ml). DMAP (30 ml, 0.199 M in THF) was added, and the solution was heated to reflux for 30 minutes and KOH (12 ml, 1.5 M in water) was added. The reaction mixture was refluxed for 24 hrs. A yellow colour developed overnight. The solution was allowed to cool to room temperature and an NH_4Cl solution (20 ml, 1.46 M in H_2O) was added, crude product precipitated as a white solid.

Crude yield = 1.48 g, 74.0%.

Product was purified by recrystallisation from hot THF.

Yield = 1.345 g, 67.3%.

Single crystals of $N_3P_3(NHCy)_4O_2H_2 \bullet 4H_2O$ were obtained by slow evaporation from a THF solution.

Mp: 181.0 - 181.5 °C

^{1}H NMR (CD_3OD): δ = 1.10 - 2.05 (m, 40H, CH_2 (Cy)), 3.07 ppm (br, 4H, CH (Cy)).

^{13}C {^{1}H} NMR (CD_3OD): δ = 26.5 (2 x CH_2), 26.6 (CH_2), 37.2 (2 x CH_2), (CH_2), 52.1 ppm (CH(Cy)).

^{31}P {^{1}H} NMR (CD_3OD): -3.7 (t, $^{2}J_{PP}$ = 13.9 Hz, 1P, PO_2), 9.9 ppm (d, 2P, $^{2}J_{PP}$ = 13.9 Hz, $P(NHCy)_2$).

IR v(cm^{-1}): 3253 (N-H/O-H), 2925 (C-H), 2852 (C-H), 1681, 1446, 1332, 1213, 1166, (P-N_{ring}) 1124 (P-N_{ring}), 973, 931, 889, 844., 806, 725, 686.

Elemental analysis (%) for calcd. $P_3N_7C_{24}H_{58}O_6$: C, 45.49; H, 9.23; N, 15.47. Found: C, 45.11; H, 8.61; N, 14.32.

$[N_3P_3(NHCy)_4O_2H]K$ (4.39)

$N_3P_3(NHCy)_4(OH)_2 \cdot 4H_2O$ (1.00 g, 1.578 mmol) was stirred in THF. 8 ml, 4 M $KOH_{(aq)}$ was added and all the solid dissolved. The solution was stirred for 2 hrs. The water layer was separated off and washed with 3 x 5 ml THF. The volatilities were removed, under vac, from the THF washings and the organic layer. The remaining residue was washed with hexane and dried under vacuum at 50 °C for 1 hr.

Yield = 0.809 g, 85.5%

Single crystals obtained from a THF solution by slow evaporation.

Mp: 170.0-172.0 °C.

^{1}H NMR ($CDCl_3$): δ = 1.03 – 1.97 (m, 40H, CH_2(Cy)), 2.96 ppm (br, 4H, CH(Cy)).

^{13}C {^{1}H} NMR ($CDCl_3$): δ = 25.8 (2 x CH_2), 26.1 (CH_2) 36.5 (2 x CH_2), (CH_2), 50.4 ppm (CH).

^{31}P {^{1}H} NMR ($CDCl_3$): δ = -0.2 (m, 1P, $^2J_{PP}$ = 25.9 Hz, PO_2), 12.0 (m, 2P, $^2J_{PP}$ = 25.9 Hz, $P(NHCy)_2$).

IR v(cm^{-1}): 3255 (N-H/O-H), 2923 (C-H), 2852 (C-H), 1670, 1558, 1444, 1332, 1214, 1166, (P-N_{ring}) 1126 (P-N_{ring}), 973, 933, 889.023, 844.669, 806, 725.

Elemental analysis (%) for calcd. for $P_3N_7C_{24}H_{49}O_2K$: C, 48.80; H, 8.36; N, 16.60; found: C, 39.80; H, 7.64; N, 11.49.

$(N_3P_3(NHCy)_4(OH))_2O$ (4.42)

$N_3P_3(NHCy)_4O_2H_2 \bullet 4H_2O$ (1.00 g, 1.578 mmol) was heated slowly under reduced pressure (0.1 torr) until the oil bath reached 160°C. The temperature was then maintained for 2 h. After which, the reaction was allowed to cool to room temperature. The colourless solid was then washed with thf and the insoluble material was removed by suction filtration. The pure compound was then obtained on evaporation of thf from the washings. Yield 0.788g, 90.4 %

Mp: Decomp. 100 °C.

^1H NMR (CD_3OD): δ = 1.18 - 2.01 (m, 80H, CH_2(Cy)), 3.03 ppm (br, 8H, 8H, CH(Cy)).

^{13}C {^1H} NMR (CD_3OD): δ = 26.7 (3 x CH_2(Cy)), 37.1 (2 x CH_2(Cy)), 51.5 ppm (CH(Cy)).

^{31}P {^1H} NMR (CD_3OD): δ = -7.7 (br, 2P, PO_2), 11.6 ppm (br, 4P, $P(NHCy)_2$).

IR ν(cm^{-1}): 3604 (N-H), 3145, 2923 (C-H), 2850 (C-H), 2663, 1770, 1702, 1556, 1452, 1428, 1240, 1203, 1141, ($P\text{-}N_{ring}$) 1097, ($P\text{-}N_{ring}$), 964, 887, 848, 782, 719.

Elemental analysis (%) for calcd. for $P_6N_{14}C_{48}H_{98}O_3$: C, 52.16; H, 8.94; N, 17.74; found: C, 49.29; H, 8.58; N, 15.55

MS-ESI: M^+ at 1105 Da

$[(N_3P_3(NHCy)_4OH_2)_2O]Cl_2$ ($[\mathbf{4.42}H_2]Cl_2$)

Single crystals of $[\mathbf{4.42}H_2]Cl_2 \cdot 5H_2O \cdot ½HCl$ were obtained from a solution of $(N_3P_3(NHCy)_4OH)_2O$ in toluene exposed to a HCl atmosphere.

Mp: Decomp. 170 - 175 °C.

^1H NMR ($CDCl_3$): δ = 1.14 – 1.97 (m, 80H, CH_2(Cy)), 3.08 ppm (br, 8H, CH(Cy)).

^{13}C $\{^1H\}$ NMR ($CDCl_3$): δ = 26.1 (3 x CH_2(Cy)), 36.1 (2 x CH_2(Cy)), 52.2 ppm (CH(Cy)).

^{31}P $\{^1H\}$ NMR ($CDCl_3$): δ = -8.5 (t, 1P, $^2J_{PP}$ = 14.1 Hz), 0.0 (t, 1P, $^2J_{PP}$ = 14.1 Hz), 6.4 (d, 2P, $^2J_{PP}$ = 14.1 Hz), 8.2 (d, 2P, $^2J_{PP}$ = 14.1 Hz),

IR ν(cm^{-1}): 3164 (N-H), 2927 (C-H), 2852 (C-H), 1635, 1448, 1240, 1093 (P-N_{ring}), 916, 846, 667.

Elemental analysis (%) for calcd. for $P_6N_{14}C_{48}H_{100}O_3Cl_2 \cdot 5H_2O \cdot 0.5HCl$: C, 44.83; H, 8.62; N, 15.25. Found: C, 35.39; H, 8.55; N, 11.79

5.4.8. [4.33H]Cl and Ester 4.47

$[N_3P_3(NHCy)_4Cl_2H]Cl$ ([4.33H]Cl)

$N_3P_3(NHCy)_4Cl_2$ (0.34 g, 0.568 mmol) was dissolved in THF (10 ml) and distilled water (10 ml), concentrated HCl (0.75 ml) was added. The solution was refluxed for 2 days, with stirring. The volume of the solution was reduced under vacuum and single crystals of $N_3P_3(NHCy)_4Cl_2 \cdot HCl$ developed on cooling to ~ 2°C.

Mp = 215 - 220 °C

^1H NMR ($CDCl_3$): δ = 1.13 - 1.25 (m, 40H, CH_2(Cy)), 3.05 (br, 4H, CH(Cy)).

^{13}C $\{^1H\}$ NMR ($CDCl_3$): δ = 25.6 (3 x CH_2(Cy)), 35.6 (CH_2(Cy)), 35.8 (CH_2(Cy)), 51.7 ppm (CH(Cy)).

^{31}P $\{^1H\}$ NMR ($CDCl_3$): δ = 9.3 (d, $^2J_{PP}$ = 45.6 Hz, 2P, $P(NHCy)_2$), 20.2 ppm (t, $^2J_{PP}$ = 45.6 Hz 1P, PCl_2).

IR ν(cm^{-1}): 3183 (N-H), 2927 (C-H), 2850 (C-H), 1427, 1348, 1303, 1226, 1132. (P-N_{ring}), 1087 (P-N_{ring}), 1012, 844, 808, 738.

Elemental analysis (%) for calcd. for $P_3N_7C_{24}H_{49}Cl_3$: C, 45.40; H, 7.78; N, 15.44. Found: C, 44.22; H, 7.64; N, 15.05.

$N_3P_3(NHCy)_4(OMe)OH{\cdot}HBr$ (4.47)

Single crystals of $N_3P_3(NHCy)_4(OMe)OH{\cdot}HBr{\cdot}HOMe{\cdot}OH_2$ developed on slow evaporation of MeOH, from a solution of $N_3P_3(NHCy)_4Cl_2$ and aqueous HBr in MeOH.

Mp = 138 - 140 °C.

^1H NMR (CD_3OD): δ = 1.17-2.05 (m, 40H, CH_2(Cy)), 3.06 (b, 4H, CH(Cy)), 3.76 ppm (d, 3H, CH_3(Me), $^3J_{PH}$ = 12.53 Hz).

^{13}C {^1H} NMR (CD_3OD): δ = 26.8 – 27.0 (3 x CH_2(Cy)), 36.9 (CH_2(Cy)), 37.2 (CH_2(Cy)), 52.6 (CH(Cy)), 54.3 ppm (CH_3(Me)).

^{31}P {^1H} NMR (CD_3OD): δ = 5.8 (br, 2P, $P(NHCy)_2$), 6.6 ppm (br, 1P, P(OMe)O).

IR $\nu(cm^{-1})$: 3160 (N-H), 2925 (C-H), 2850 (C-H), 2674, 1623, 1444, 1367, 1299, 1230, 1108, ($P\text{-}N_{ring}$) 1027 ($P\text{-}N_{ring}$), 968, 835, 798, 765.

Elemental analysis (%) for calcd. for $P_3N_7C_{26}H_{59}O_4Br$: C, 44.19; H, 8.42; N, 13.88. Found: C, 44.51; H, 8.08; N, 14.22

5.4.9. Phosphamides

$N_3P_3(NHCy)_4(NHBz)OH$ (4.48)

$N_3P_3(NHCy)_4Cl_2$ (0.50 g, 0.835 mmol) was dissolved in 20 ml THF. 11 ml $KOH_{(aq)}$ (1.5 M) was added, with stirring, followed by 0.138 ml benzylamine (1.267 mmol). The solution was refluxed for 72 h. A pale yellow colour developed during reflux. The solution was allowed to cool to room temperature and a solution of NH_4Cl (18 ml, 2 M in H_2O) was added. The product precipitated as a white solid, which was isolated by suction filtration then washed with water, THF and hexane.

Yield = 0.493 g, 90.7%.

Mp = 209.5 – 211.0 °C

^{1}H NMR (CD_3OD): δ = 1.15 – 2.05 (m, 40H, CH_2(Cy)), 2.94 (br, & 4H, CH(Cy)), 3.96 (d, 2H, CH_2(Bz), $^{3}J_{HP}$ = 9.67 Hz), 7.18 - 7.39 (m, 5H, CH(Bz)). (Impurity: CH_2 of benzyl amine, may be due to a small amount of protonated product. δ = 4.13 ppm (d, J = 9.78 Hz)).

^{13}C {^{1}H} NMR (CD_3OD): δ = 26.9 (CH_2(Cy)), 27.0 (CH_2(Cy)), 27.2 (CH_2(Cy)), 37.5 (CH_2(Cy)), 47.0 (CH_2(Bz)), 51.7 (CH(Cy)), 128.2, 130.1 (ortho/meta-C(Bz)), 142.9 ppm (para-C(Bz)).

^{31}P {^{1}H} NMR (CD_3OD): δ = 5.4 (t, $^{2}J_{PP}$ = 31.8, 30.3 Hz, 1P, P(NHBz)O), 12.2 (d, 2P, $P(NHCy)_2$, $^{2}J_{PP}$ = 31.7 Hz,).

IR v(cm^{-1}): 3187 (N-H), 2923 (C-H), 2850 (C-H), 2690, 1448, 1403, 1294, 1226, 1199, 1149 (P-N_{ring}), 1097 (P-N_{ring}), 1022, 958, 925, 802, 730, 696.

Elemental analysis (%) for calcd. for $P_3N_8C_{31}H_{57}O_4$: C, 57.22; H, 8.83; N, 17.22. Found: C, 56.66; H, 8.85; N, 16.83.

$2N_3P_3(NHCy)_4(NHBz)OH_2 \cdot 3C_6H_4$-1,4$(COOH)_2$-2,5$(OH)_2$ ([4.48H][Hdhtp]·1/2H_2dhtp)

Single crystals were obtained by slow evaporation of a methanol solution containing $N_3P_3(NHCy)_4(NHBz)OH_2$ and C_6H_4-1,4$(COOH)_2$-2,5$(OH)_2$ in a 2:3 ratio, respectively.

Mp = 177-178 °C

^{1}H NMR ($CDCl_3$): δ = 1.15 - 1.88 (m, 40H, CH_2(Cy)), 3.02 (br, & 4H, CH(Cy)), 4.15 (m, 2H, CH_2(Bz), $^{2}J_{HP}$ = 10.50 Hz), 7.46 ppm (s, 6H, CH(acid)).

^{13}C {^{1}H} NMR ($CDCl_3$): δ = 25.5 (3 x CH_2(Cy)), 36.2 (2 x CH_2(Cy)), 47.0 (CH_2(Bz)), 51.1 (CH(Cy)), 128.2, 130.1 ppm (ortho/meta-C(Bz)).

^{31}P {^{1}H} NMR ($CDCl_3$): δ = 10.6 (s, 1.6P), 10.9 (d, $^{2}J_{PP}$ = 39.0 Hz, 2P, $P(NHCy)_2$), 14.2 ppm (t, $^{2}J_{PP}$ = 38.8, 39.7 Hz, 1P, P(O)(NHBz)).

IR v(cm^{-1}): 3243 (N-H/O-H), 2927 (C-H), 2854 (C-H), 1641, 1494, 1434, 1353, 1234, 1097 (P-N_{ring}), 944, 788, 744.

Elemental analysis (%) for calcd. for $P_6N_{16}C_{86}H_{132}O_{20}$: C, 54.48; H, 7.02; N, 11.82. Found: C, 53.83; H, 7.37; N, 11.22.

$N_3P_3(NHCy)_4(NH^iBu)OH$ (4.49)

$N_3P_3(NHCy)_4Cl_2$ (0.20 g, 0.334 mmol) was dissolved in THF (15 ml). $KOH_{(aq)}$ (5 ml, 1.5 M) and isobutyl amine (0.045 ml, 0.453 mmol) were added. The solution was refluxed for 48 hrs, with stirring, during reflux it became colourless. The solution was allowed to cool to room temperature and an NH_4Cl solution (20 ml, 2 M in H_2O) was added and the product precipitated as a white solid. This was filtered under suction and washed with water, THF then hexane.

Yield = 0.180 g, 87.37 %

Mp = 201.5 - 203.0 °C

^1H NMR (CD_3OD): δ = 0.91 (d, 6H, $CH_3(^iBu)$, $^3J_{HH}$ = 6.65 Hz) 1.15-2.05 (m, 40H, CH_2(Cy) & 1H $CH(^iBu)$), 2.62 - 2.66 (m, 2H, $CH_2(^iBu)$), 3.02 (br, 4H, CH(Cy)), (impurities: $^iBuNH_3Cl$ small signal at δ = 0.91 ppm (d, 6H, $CH_3(^iBu)$, $^3J_{HH}$ = 6.66 Hz).

^{13}C {^1H} NMR (CD_3OD): δ = 21.2 ($CH_3(^iBu)$), 27.1 (3 x CH_2(Cy)), 31.4 ($CH(^iBu)$), 37.5 (2 x CH_2(Cy)), 51.2 ($CH_2(^iBu)$), 51.7 ppm (CH(Cy)).

^{31}P {^1H} NMR (CD_3OD): δ = 5.7 (t, $^2J_{PP}$ = 29.7, 29.7 Hz 1P, P(NHBn)O), 11.9 ppm (d, $^2J_{PP}$ = 29.9 Hz 2P,$P(NHCy)_2$).

IR v(cm^{-1}): 3234 (N-H), 2923 (C-H), 2852 (C-H), 2669, 1643, 1448, 1295, 1216, 1095, (P-N_{ring}), 956, 927, 800, 705.

Elemental analysis (%) for calcd. for $P_3N_8C_{28}H_{60}O$: C, 54.44; H, 9.79; N, 18.14. Found: C, 48.88; H, 8.91; N, 13.68.

$(N_3P_3(NHCy)_4(O))_2p$-$(NH)_2Xy$ (4.50)

$N_3P_3(NHCy)_4Cl_2$ (0.50 g, 0.835 mmol) and p-diaminoxylene (0.057 g, 0.418 mmol) were heated into 5 ml THF. Once the solution was boiling 10 ml $KOH_{(aq)}$ (2 M) was added and all solids immediately dissolved. The solution was refluxed for 5 days then allowed to cool to room temperature. A solution of NH_4Cl (20 ml, 2 M in H_2O) was added and the product precipitated as a white solid. This was isolated by suction filtration and washed with water, thf and hexane then dried at room temperature under reduced pressure for 1hr.

Yield: 0.470g, 90.7 %

Mp = 218 – 220 °C

^1H NMR (CD_3OD): δ = 1.11 - 1.95 (m, 80H, CH_2(Cy)), 3.04 (br, 8H, CH(Cy)), 4.05 (m, 4H, CH_2(Xy)), 7.33 ppm (s, 4H, CH(Xy)).

^{13}C {^1H} NMR (CD_3OD): δ = 25.7 (3 x CH_2(Cy)), 36.6 (2 x CH_2(Cy)), 46.3 (CH_2(Xy)), 50.5 (CH(Cy)), 123.3 (ortho/meta-CH(Bz)), 145.9 ppm (para-C(Xy)).

^{31}P {^1H} NMR (CD_3OD): δ = 5.4 (t, $^2J_{PP}$ = 30.3, 29.9 Hz, 2P, P(NHXy)O), 12.2 (br, 4P, $P(NHCy)_2$).

IR v(cm^{-1}): 3205 (N-H), 2923 (C-H), 2852 (C-H), 2667, 1448, 1403, 1216, 1083 (P-N_{ring}), 956, 808.

Elemental analysis (%) for calcd. $P_3N_8C_{31}H_{57}O_4$: C, 54.98; H, 8.90; N, 18.32. Found: C, 44.24; H, 7.44; N, 14.93. MS-ESI:

M^{2+} at 612 Da

$(N_3P_3(NHCy)_4(O))_2m$-$(NH)_2Xy$ (4.51)

$N_3P_3(NHCy)_4Cl_2$ (0.600 g, 1.002 mmol) was dissolved in 5 ml THF. 4 ml $KOH_{(aq)}$ (4M) was added, followed by half an equivalent m-diaminoxylene (0.066 ml, 0.500 mmol). The solution was refluxed for 1 week then allowed to cool to room temperature. A solution of NH_4Cl (10ml, 2M in H_2O) was

added and the product precipitated as a white solid. This was isolated by suction filtration and washed with water, thf and hexane then dried at 50 °C under reduced pressure for 1hr.

Yield: 0.525g, 85.65%

Mp = 207 – 210 °C

^{1}H NMR ($CDCl_3$): δ = 1.05 - 2.01 (m, 80H, CH_2(Cy)), 3.01 (br, 8H, CH(Cy)), 4.01 (d, 4H, CH_2(Xy), $^{3}J_{HP}$ = 9.99 Hz), 7.16 - 7.44 ppm (m, 4H, 2 x meta-H(Xy), para-H(Xy), ipso-H(Xy) (impurity: δ = 3.87 ppm, s, 0.31H CH_2(Xy)-mono product).

^{13}C {^{1}H} NMR ($CDCl_3$): δ = 26.1 (3 x CH_2(Cy)), 44.0 (CH_2(Xy)), 50.5 (CH(Cy)), 123.5, 128.0 (ipso/meta/para-CH(Xy)), 142.6 ppm (C(Xy)).

^{31}P {^{1}H} NMR ($CDCl_3$): δ = 5.4 (t, $^{2}J_{PP}$ = 30.6, 30.7 Hz, 2P, P(NHXy)O) and 12.9 ppm (d, $^{2}J_{PP}$ = 30.9 Hz, 4P, $P(NHCy)_2$).

IR ν(cm^{-1}): 3266 (N-H), 2921 (C-H), 2850 (C-H), 2665, 1644, 1446, 1411.64, 1348, 1232, 1191, 1103 (P-N_{ring}), 1006 (P-N_{ring}), 925, 804.

Elemental analysis (%) for calcd. for $P_3N_8C_{31}H_{57}O_4$: C, 54.98; H, 8.90; N, 18.32. Found: C,53.03; H,8.56; N,15.44. MS-ESI:

M^{2+} at 612 Da

$N_3P_3(NHCy)_4$(O)m-NHXyNH_2 (4.52)

$N_3P_3(NHCy)_4Cl_2$ (0.500 g, 0.835 mmol) was dissolved in 5 ml THF. 10 ml $KOH_{(aq)}$ (2 M) was added, followed by excess m-diaminoxylene (0.55 ml, 4.168 mmol). The solution was refluxed for 22 hrs then allowed to cool to room temperature. A solution of NH_4Cl (10 ml, 2 M in H_2O) was added and the product precipitated as a white solid. This was isolated by suction filtration and washed with water, THF and hexane then dried at room temperature under reduced pressure for 1hr.

Yield: 0.453 g, 79.75%

Mp = 66 - 68 °C

^{1}H NMR (CD_3OD): δ = 1.15 – 2.05 (m, 40H, CH_2(Cy)), 3.03 (br, 4H, CH(Cy), 3.81 (s, 2H, CH_2(Xy)) 4.04 – 4.07 (m, 2H, CH_2(Bz)), 7.18 – 7.35 (m, 3H, 2 x meta-H, para-H(Xy)) 7.43 ppm (br, 1H, ipso-H(Bz).

^{13}C {^{1}H} NMR (CD_3OD): δ = 26.9 (CH_2(Cy)), 27.0 (CH_2(Cy)), 27.2 (CH_2(Cy)), 37.5 (2 x CH_2(Cy)), 47.0 (CH_2(Xy)), 47.1 (CH_2(Xy)), 51.8 (CH(Cy)), 127.43 (meta-C(Xy)), 127.7 (ipso-C(Xy)), 130.0 (para-C(Xy)), 143.2, 143.3 ppm (ortho-C(Xy)).

^{31}P {^{1}H} NMR (CD_3OD): δ = 4.2 (t, $^2J_{PP}$ = 31.1 Hz, 1P, P(NHXy)O) and 11.2 ppm (d, $^2J_{PP}$ = 31.1 Hz, 2P, $P(NHCy)_2$).

IR ν(cm^{-1}): 3185 (N-H), 2923 (C-H), 2850 (C-H), 1571, 1446, 1402, 1232, 1097 (P-N_{ring}), 887, 782.

Elemental analysis (%) for calcd. for $P_3N_8C_{31}H_{57}O_4$: C, 54.98; H, 8.90; N, 18.32. Found: C,51.12 ; H,8.13 ; N,12.95. MS-ESI:

M^+ at 680 Da

5.4.10. Phosphites

$[N_3P_3(N(Et)(CH_2)_3NEt)_2OH]K$ (4.53)

A solution of **4.34** (1.00 g, 2.163 mmol) in 10 ml of toluene was added drop-wise, with vigorous stirring, to a suspension of finely divided potassium metal (0.402 g, 10.282 mmol) in 10 ml of toluene. After 30 minutes crushed potassium hydroxide (1.00 g, 17.82 mmol) was added to the reaction vessel and the mixture was left stirring for 12 h. The solution was filtered and concentrated to 4 ml, then left for crystallization at -20 °C. Colourless crystals of $([N_3P_3(N(Et)(CH_2)_3NEt)_2OH]^- K^+)_6$.toluene were obtained after 7 days. The crystals were collected washed several times with cold pentane and dried.

Yield: 0.390 g, 40.65%.

M.p. = 200 °C (decomposition).

^{1}H NMR (THF-d_8): δ = 0.87 – 0.97 (m, 72H, CH_3(Et)), 1.51 - 1.61 (m, 24H, CH_2(Pr)), 2.60 – 3.10 ppm (m, 96H, NCH_2), 7.07 (d, 1H, PH, $^{1}J_{PH}$ = 536 Hz).

^{13}C{^{1}H} NMR (THF-d_8): δ = 13.1, 13.4 (CH_3(Et)), 40.8, (NCH_2(Et)), 45.4. ppm (NCH_2).

^{31}P{^{1}H} NMR (THF-d_8): δ = 4.6 (t, $^{2}J_{PP}$ = 27.5, 27.6, 6P, P(O)H), 24.6 ppm (d, $^{2}J_{PP}$ = 27.5). 12P, P(N(Et)(CH_2)$_3$NEt)).

^{31}P-^{1}H coupled NMR (THF-d_8): δ = 3.4 (dt, $^{1}J_{PH}$ = 536 Hz, (d) $^{2}J_{PP}$ = 27.5 (t), 23.3 ppm (br, 12P, P(N(Et)(CH_2)$_3$PrNEt)).

IR ν(cm^{-1}): 3423 (N-H/O-H), 2962 (C-H), 2852 (C-H), 2292, 1650, 1587, 1454, 1375, 1282, 1249, 1166 (P-N_{ring}), 1120 (P-N_{ring}), 1052 (P-N_{ring}), 1025, 979, 885, 842, 784, 746, 709, 663.

Elemental analysis (%) for calcd. For $C_{84}H_{198}N_{42}OP_{18}K_6$ (2684.88): C 37.58, H 7.43, N: 21.91. Found: C 32.40, H 6.70, N 15.40.

N_3P_3(N(Et)(CH_2)$_3$NEt)$_2$$OH_2$ (4.54)

Solid NH_4Cl was added to a solution of ([N_3P_3(N(Et)(CH_2)$_3$NEt)$_2$OH]K)$_6$ (0.200 g, 0.0745 mmol) in 10 ml of toluene, the resulting mixture was stirred for 6 hours. The solution was filtered and evaporated to dryness. Colourless crystals of [N_3P_3(N(Et)(CH_2)$_3$NEt)$_2$OH] were obtained from of solution of THF at -20 °C.

Yield: 0.150 g (83%).

M.p. = 230 °C (decomposition).

^{1}H NMR (THF-d_8,): δ = 0.93 - 0.97 (m, 12H, CH_3(Et)), 1.70 - 1.77 (m, 4H, CH_2(CH_2)$_2$), 2.81 - 3.13 ppm (m, 16H, NCH_2(Pr & Et)), 7.10 (d, 1H, P*H*, $^{1}J_{PH}$ = 580 Hz).

^{13}C{^{1}H} NMR (THF-d_8): δ = 123.1 (CH_3(Et)), 41.0 (NCH_2(Et)), 45.4 ppm (NCH_2))

$^{31}P\{^{1}H\}$ NMR (THF-d_8, -40 °C): -5.0 (d, 1P, P(O)H, $^{2}J_{PP}$ = 40.3), 13.6 (d, 1P, P(N(Et)$(CH_2)_3$NEt), $^{2}J_{PP}$ = 31.6), δ = 20.0 ppm (t, 1P, P(N(Et)$(CH_2)_3$)PrNEt), $^{2}J_{PP}$ = 31.5),

^{31}P-^{1}H coupled NMR (THF-d_8, -40 °C): δ = -5.0 (dd, $^{1}J_{PH}$ = 580 Hz (d), $^{2}J_{PP}$ = 31.6 (d) 1P, P(O)H,), 13.6 (br, 1P, P(N(Et)$(CH_2)_3$NEt)), 20.0 ppm (br, 1P, P(N(Et)$(CH_2)_3$NEt)).

IR v(cm^{-1}): 3369 (N-H/O-H), 2964 (C-H), 2927 (C-H), 2360, 1652, 1455, 1340, 1255, 1118 (P-N_{ring}), 1056. (P-N_{ring}), 887, 790, 715, 669, 613.

5.5. X-ray Crystallography

Crystallographic data were recorded on a Bruker Smart Apex Diffractometer using Mo Kα radiation (λ = 0.71073 Å) at T = 100 K. Empirical absorption corrections were applied (SADABS). Structures were solved by direct methods and refined by full-matrix least-squares against F^2 using all data (SHELXTL).[5] Non-hydrogen atoms that are not part of disordered groups were refined anisotropically with the exception of disordered atoms. H-atoms were placed in calculated positions. N- and O-bound H-atoms were refined freely when the quality of the data enabled this. Disordered groups were split on two positions and refined isotropically using similar-distance (SAME) and similar-U restraints (SIMU).

5.5.1. Crystallographic Data

Compound	$[3.9]Cl_6 \cdot 19CHCl_3$	$[3.9]Cl_6 \cdot xCHCl_3 \cdot yC_2H_2Cl_4$*
Chemical Formula	$C_{61}H_{79}N_{15}P_3Cl_{63}$	$C_{42}H_{60}N_{15}P_3Cl_6 \cdot x\ CHCl_3 \cdot y\ C_2H_2Cl_4$
M_r	3348.65	
T /K	100	100
Cryst. Syst.	monoclinic	monoclinic
Space group	$P2_1/n$	Cm
a, Å	20.056(8)	18.485(5)
b, Å	26.748(10)	23.980(6)
c, Å	25.940(10)	15.792(4)
α, deg	90	90
β, deg	92.836(6)	122.187(4)
γ, deg	90	90
V, Å^3	13899(9)	5924(3)
Z	4	2
μ(Mo Kα)/cm^{-1}	1.328	
ρ(calcd.)/g cm^{-1}	1.637	
R_{int}	17793/1326	
$2\theta_{max}$, deg	45	45
R1 (F> 4σ(F))	0.0712	0.0695
wR2 (all data)	0.1881	0.1885

* The SQUEEZE routine in PLATON[6] was used for removing the contributions of diffuse solvent from diffraction intensities (a total of 1027 electrons for a void volume of 2448 Å^3).

Compound	[3.9]$Cl_6 \cdot 11\ CH_2Cl_2$	[3.9] $Cl_6 \cdot 10CH_2Cl_2 \cdot CHCl_3$	[3.10]$Cl_4 \cdot 9CHCl_3$
Chemical Formula	$P_3N_{15}C_{53}H_{82}Cl_{28}$	$C_{61}H_{79}Cl_{63}N_{15}P_3$	$P_3N_{13}C_{44}H_{59}OCl_{31}$
M_r	2014.92	2042.23	1977.90
T /K	100	100	100
Cryst. Syst.	monoclinic	monoclinic	triclinic
Space group	$P2_1/m$	$P2_1/n$	P-1
a, Å	14.033(3)	13.972(4)	14.645(5)
b, Å	23.091(5)	23.297(7)	15.073(5)
c, Å	14.953(3)	15.023(5)	20.356(7)
α, deg	90	90	86.791(6)
β, deg	115.309(4)	114.856(5)	71.577(5)
γ, deg	90	90	82.290(5)
V, $Å^3$	4380.2(16)	4420(2)	4224(2)
Z	2	2	2
μ(Mo Kα)/cm^{-1}	0.997	0.988	1.093
ρ(calcd.)/g cm^{-1}	1.553	1.534	1.555
R_{int}	0.041	0.076	0.0641
$2\theta_{max}$, deg	45	45	50
R1 (F> 4σ(F))	0.092	0.073	0.0626
wR2 (all data)	0.262	0.199	0.1690

Compound	[3.11]Cl_4·14 $CHCl_3$	[4.38]Cl_2•1½$CHCl_3$·2H_2O
Chemical Formula	$C_{56}H_{74}N_{16}P_4Cl_{46}O_2$	$C_{39.5}H_{72.5}Cl_{6.5}N_{11}O_2P_3$
M_r	2758.02	1056.92
T / K	100	100
Cryst. Syst.	monoclinic	triclinic
Space group	$P2_1/n$	P-1
a, Å	17.835(15)	10.652(3)
b, Å	10.900(10)	12.295(4)
c, Å	29.44(3)	20.704(7)
α, deg	90	90.924(6)
β, deg	100.836(17)	101.061(5)
γ, deg	90	101.335(6)
V, $Å^3$	5621(6)	2605.0(15)
Z	2	2
μ(Mo Kα)/cm^{-1}	1.213	0.493
ρ(calcd.)/g cm^{-1}	1.618	1.347
R_{int}	0.092	0.041
$2\theta_{max}$, deg	45	45
R1 (F> 4σ(F))	0.109	0.094
wR2 (all data)	0.274	0.260

Compound	**4.40•4H_2O**	**[4.42H_2]Cl_2·3H_2O·½HCl**
Chemical Formula	$C_{24}H_{58}N_7O_6P_3$	$C_{48}H_{100.5}Cl_{2.5}N_{14}O_7P_6$
M_r	633.68	1260.37
T	100	100
Cryst. Syst.	orthorhombic	triclinic
Space group	$P2_12_12_1$	P-1
a, Å	11.251(2)	10.106(8)
b, Å	19.868(4)	17.588(14)
c, Å	29.263(6)	19.836(16)
α, deg	90	96.809(16)
β, deg	90	104.328(19)
γ, deg	90	100.413(16)
V, Å^3	6541(2)	3310(5)
Z	8	2
μ(Mo Kα)/cm^{-1}	0.229	0.319
ρ(calcd.)/g cm^{-1}	1.287	1.265
R_{Int}	0.0755	0.079
$2\theta_{max}$, deg	50	45
R1 (F> 4σ(F))	0.047	0.087
wR2 (all data)	0.082	0.201

Compound	[4.33H]Cl·THF	[4.48H][Hdhtp]·1/2H_2dhtp)
Chemical Formula	$C_{28}H_{57}Cl_3N_7OP_3$	$C_{43}H_{66}N_8O_{10}P_3$
M_r	707.07	947.95
T	100	100
Cryst. Syst.	triclinic	triclinic
Space group	*P*-1	*P*-1
a, Å	10.224(3)	11.4182(10)
b, Å	13.891(4)	20.1146(17)
c, Å	15.079(5)	23.768(2)
α, deg	108.653(6)	65.877(2)
β, deg	106.908(11)	80.423(2)
γ, deg	104.696(13)	89.878(2)
V, $Å^3$	1793.7(9)	4899.5(7)
Z	2	4
μ(Mo Kα)/cm^{-1}	0.423	0.183
ρ(calcd.)/g cm^{-1}	1.309	1.285
R_{int}	0.031	0.063
$2\theta_{max}$, deg	50	45
R1 (F> 4σ(F))	0.061	0.055
wR2 (all data)	0.132	0.101

Compound	$(4.53)_6 \cdot 3$toluene	4.54
Chemical Formula	$C_{105}H_{222}K_6N_{42}O_6P_{18}$	$C_{14}H_{34}N_7OP_3$
M_r	2961.31	409.39
T	100	100
Cryst. Syst.	monoclinic	triclinic
Space group	$P2_1/c$	P-1
a, Å	19.7445(18)	9.1235(12)
b, Å	15.9190(14)	9.4050(12)
c, Å	24.802(2)	12.2275(16)
α, deg	90	97.949(2)
β, deg	94.812(2)	98.822(2)
γ, deg	90	94.733(2)
V, Å^3	7768.0(12)	1021.0(2)
Z	2	2
μ(Mo Kα)/cm^{-1}	0.413	0.310
ρ(calcd.)/g cm^{-1}	1.266	1.332
R_{int}	0.076	0.018
$2\theta_{max}$, deg	45	50
R1 (F> 4σ(F))	0.081	0.069
wR2 (all data)	0.200	0.185

5.5.2. Crystal Structure Plots

(Showing 50% probability displacement ellipsoids for anisotropically refined atoms) (C-bound H atoms are omitted for clarity).

3.9

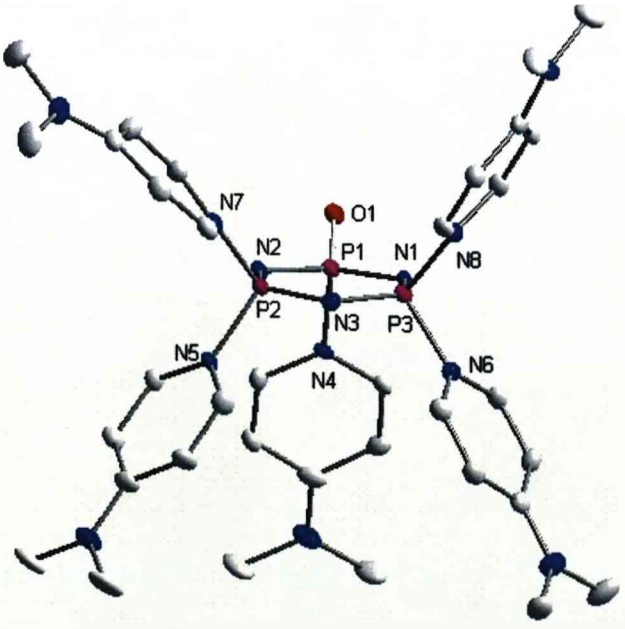

3.10

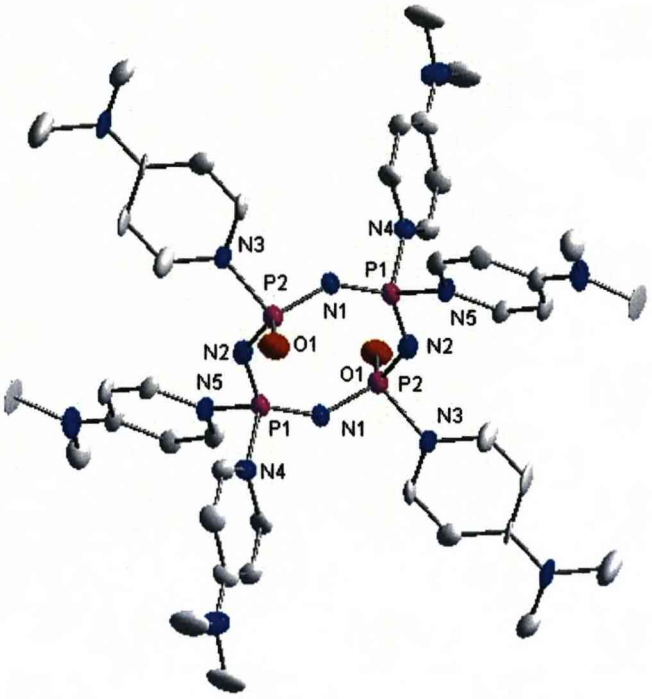
N3
N4
P2
P1
N1
N5
N2
O1
N2
O1
N5
P2
P1
N1
N3
N4

3.11

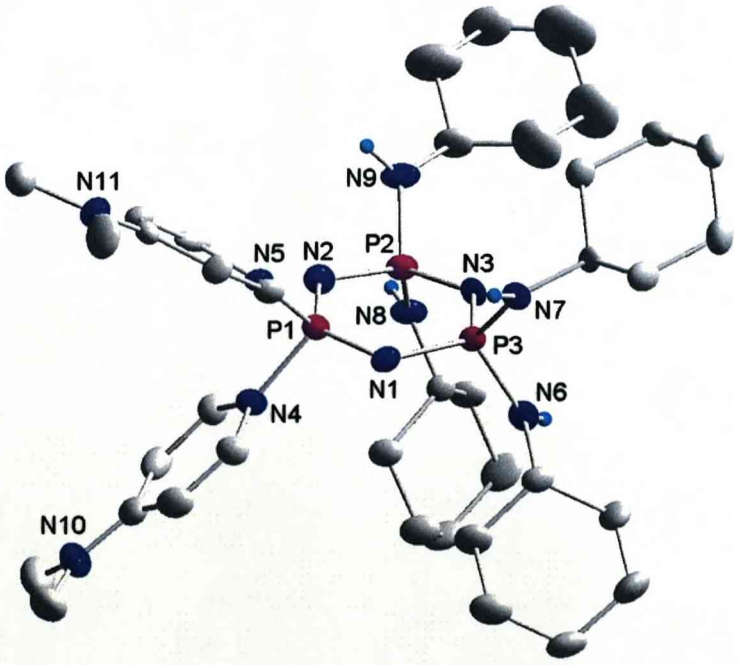
N11
N9
N5
N2
P2
N3
N8
N7
P1
P3
N1
N6
N4
N10

$[4.34]^{2+}$

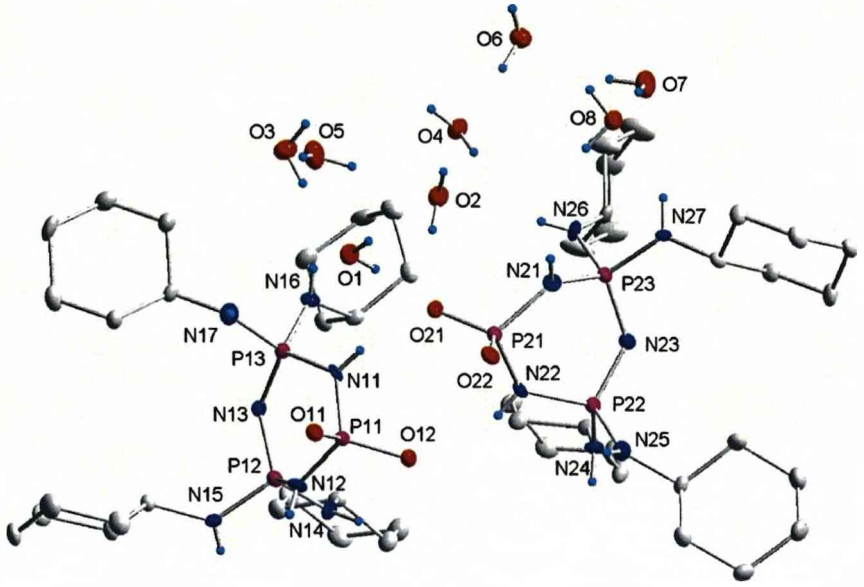

4.40·4H_2O

(Both crystallographically unique molecules shown)

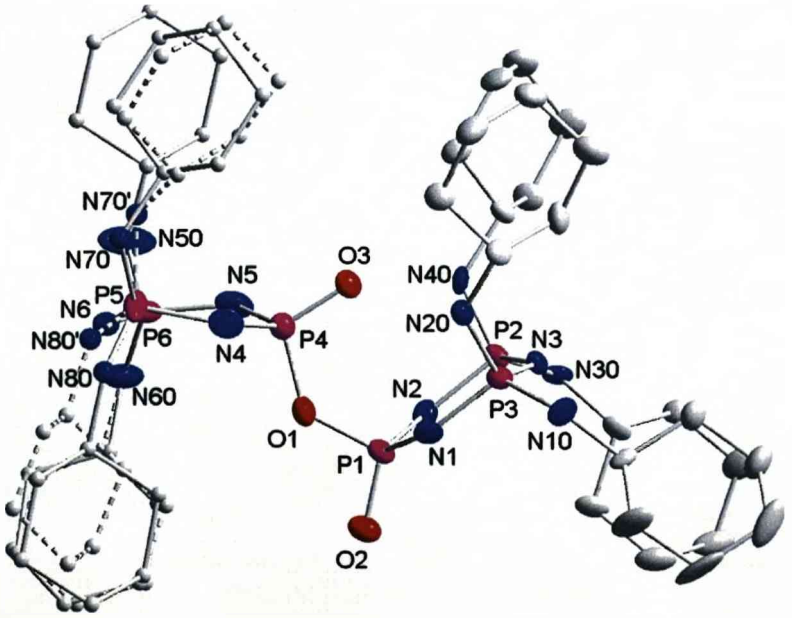

[4.42H_2]$^{2+}$

(Crystals of [**4.42**H_2]Cl_2·3.5H_2O·$^1/_2$HCl show non-merohedral twinning. The contribution of twin domains was treated with a batch scale factor, which refined to 0.39 (contribution of minor domain). Three of the cyclohexyl amino groups bonded to P5 and P6, respectively, are disordered. The chloride ion Cl10 and the oxygen atom O10 which is part of a water molecule share the same crystallographic site. Both were given site occupancies of 50%).

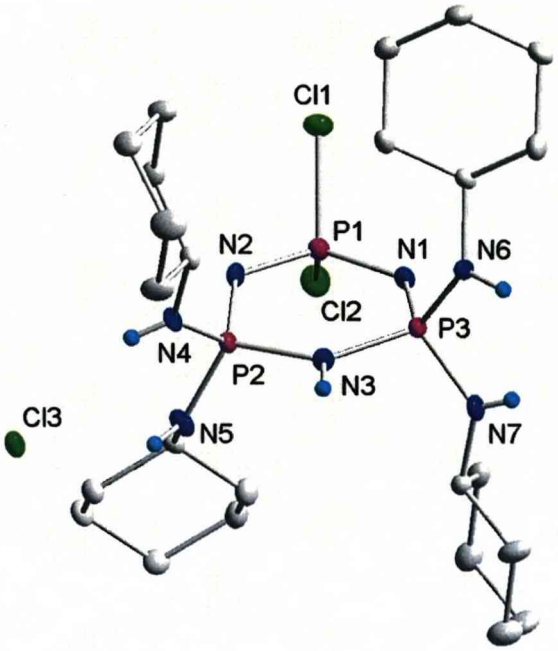

[4.33H]Cl

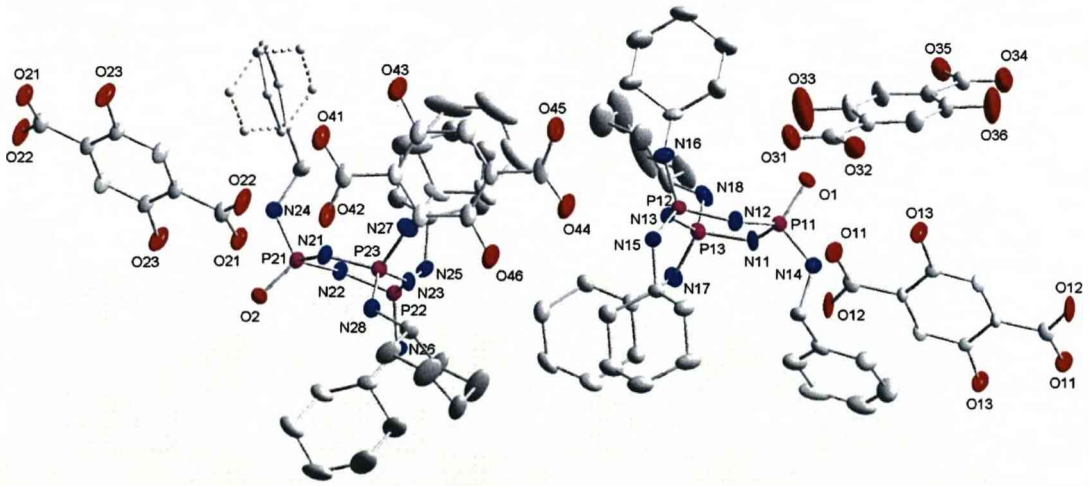

[4.48H][Hdhtp]·$^{1}/_{2}$H$_2$dhtp

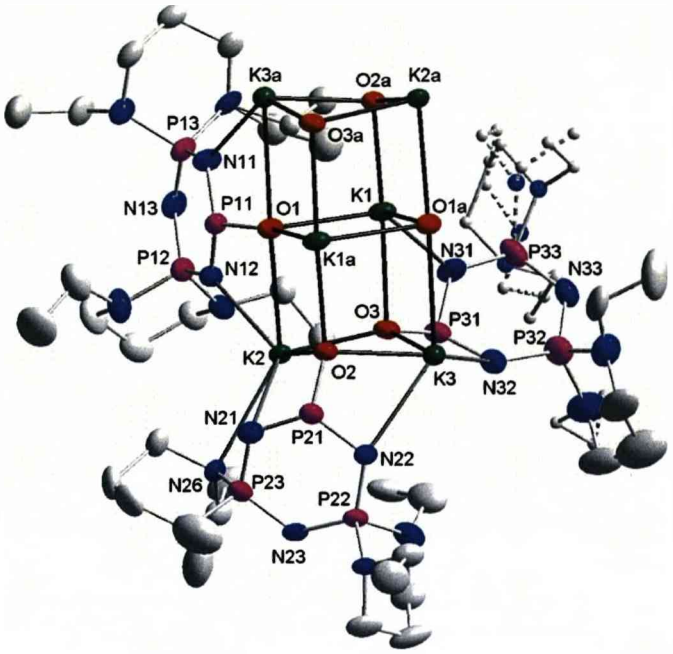

4.53

(The K_6O_6 core and the three crystallographically unique phosphite ligands)

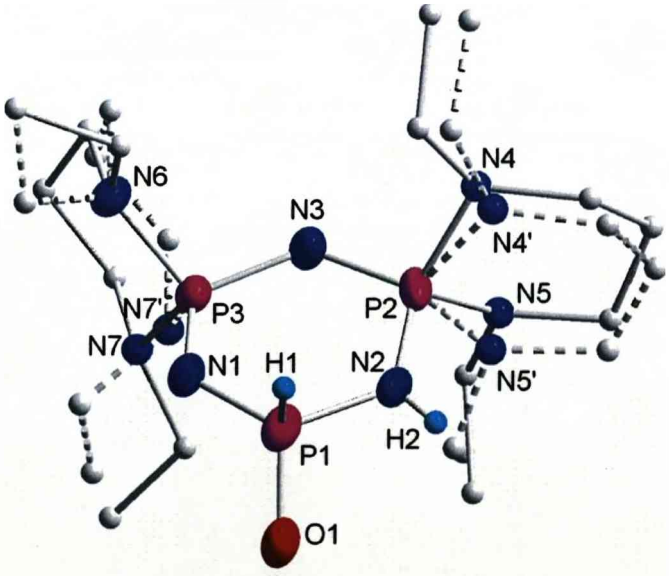

4.45

References

(1) Bennett, A. E., Rienstra, C. M., Auger, M., Lakshmi, K. V.; Griffin, R. G. J. *Chem. Phys.* **1995**, *103*, 695.

(2) Khitrin, K., Fujiwara, T.; Akutsu, H. *J. Magn. Reson.* **2003**, *162*, 46.

(3) Chandrasekhar, V., Vivekanandan, K., Nagendran, S., Andavan, G. T. S., Weathers, N. R., Yarbrough, J. C.; Cordes, A. W. *Inorg. Chem.* **1998**, *37*, 6192.

(4) Chivers, T.; Hedgelan.R *Can. J. Chem.* **1972**, *50*, 1017.

(5) Sheldrick, G. M., SHELX97, Program for X-ray crystal structure refinement, Universität Göttingen: Göttingen, Germany, **1997**

(6) Spek, A. L. *J. Appl. Crystallogr.* **2003**, *36*, 7.